AD-A148 109 RLE (RESEARCH LABORATORY OF ELECTRONICS) PROGRESS REPORT NUMBER 126(U) MASSACHUSETTS INST OF TECH CAMBRIDGE RESEARCH LAB OF ELECTRONICS J ALLEN ET AL. 1/3

UNCLASSIFIED JAN 84 DAAG29-83-K-0003 F/G 9/3 NL

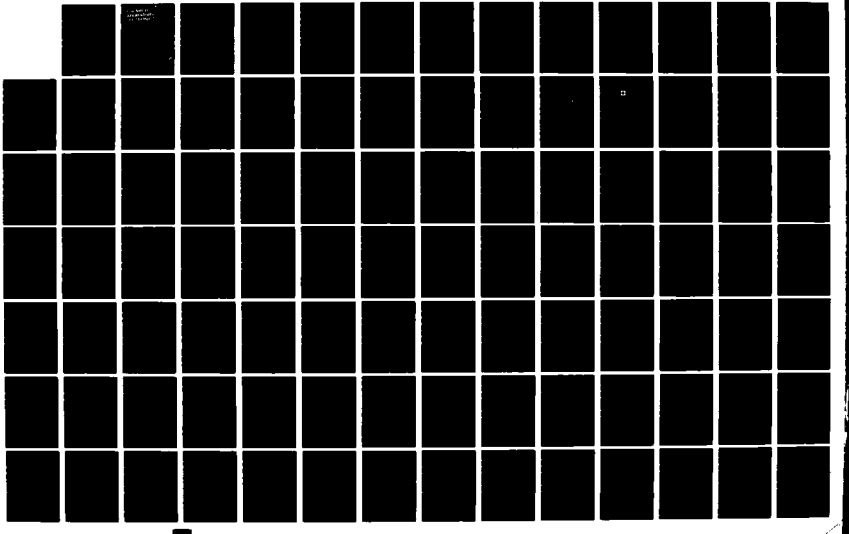

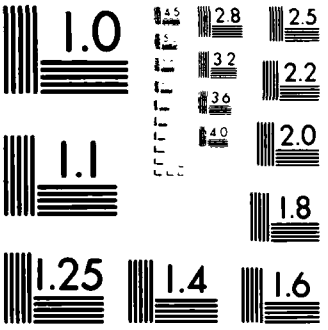

(16)

RESEARCH LABORATORY of ELECTRONICS

No. 126
Jan. 1984

PROGRESS REPORT

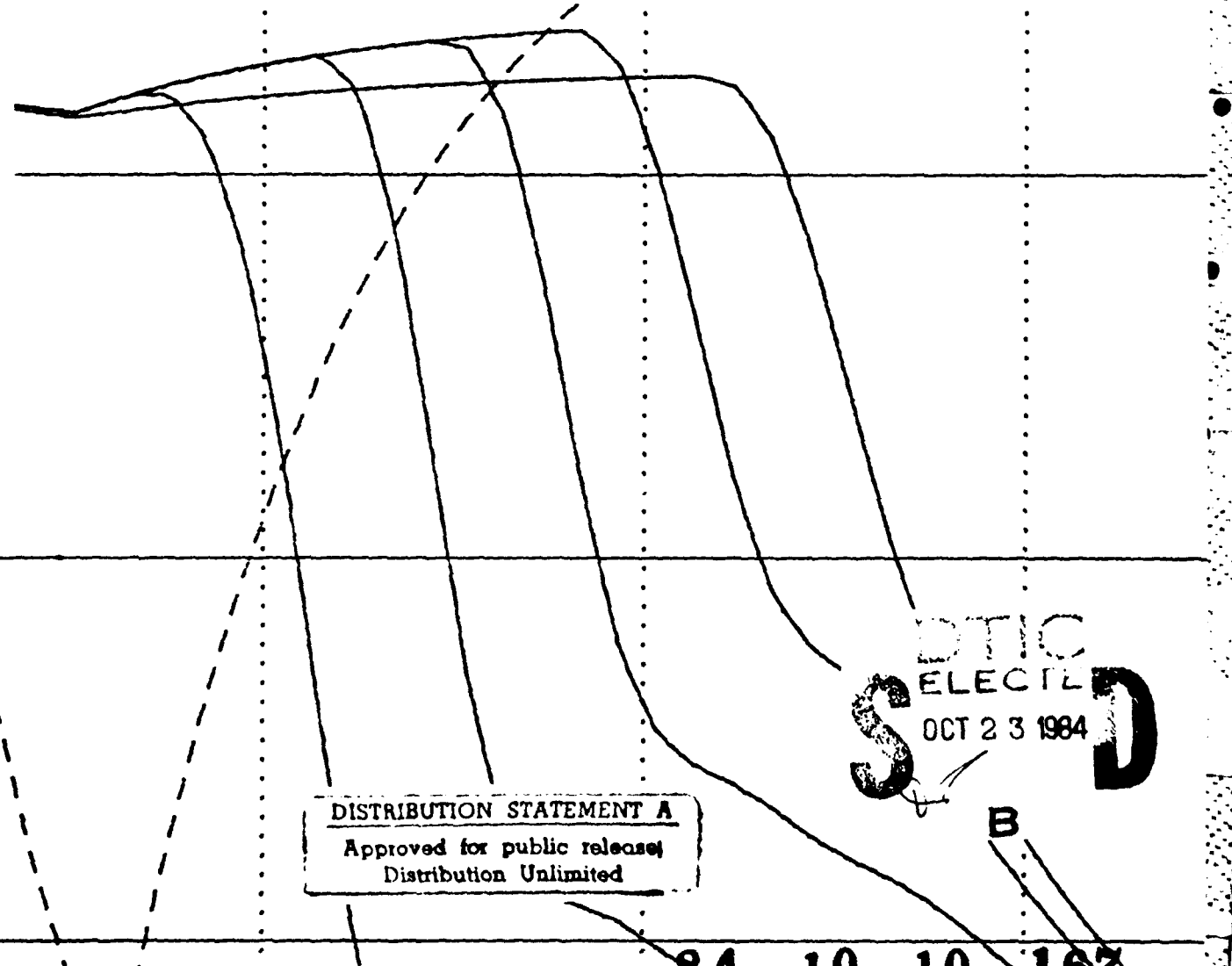

B

Massachusetts Institute of Technology • Cambridge, Massachusetts 02139

UNCLASSIFIED
SECURITY CLASSIFICATION OF THIS PAGE

REPORT DOCUMENTATION PAGE

1a. REPORT SECURITY CLASSIFICATION: Unclassified	1b. RESTRICTIVE MARKINGS
2a. SECURITY CLASSIFICATION AUTHORITY	3. DISTRIBUTION/AVAILABILITY OF REPORT: Approved for public release; distribution unlimited
2b. DECLASSIFICATION/DOWNGRADING SCHEDULE	
4. PERFORMING ORGANIZATION REPORT NUMBER(S)	5. MONITORING ORGANIZATION REPORT NUMBER(S)
6a. NAME OF PERFORMING ORGANIZATION: Research Laboratory of Electronics, Massachusetts Institute of Technology; 6b. OFFICE SYMBOL (If applicable):	7a. NAME OF MONITORING ORGANIZATION
6c. ADDRESS (City, State and ZIP Code): 77 Massachusetts Avenue, Cambridge, MA 02139	7b. ADDRESS (City, State and ZIP Code)
8a. NAME OF FUNDING/SPONSORING ORGANIZATION: U.S. Army Research Center; 8b. OFFICE SYMBOL (If applicable):	9. PROCUREMENT INSTRUMENT IDENTIFICATION NUMBER: DAAG 29-83-K-0003
8c. ADDRESS (City, State and ZIP Code): P.O. Box 12211, Research Triangle Park, North Carolina 27709	10. SOURCE OF FUNDING NOS.

PROGRAM ELEMENT NO.	PROJECT NO.	TASK NO.	WORK UNIT NO.
	P-19838-EL		

11. TITLE (Include Security Classification)

12. PERSONAL AUTHOR(S)

13a. TYPE OF REPORT	13b. TIME COVERED	14. DATE OF REPORT (Yr., Mo., Day)	15. PAGE COUNT
Progress Report	FROM 1/83 TO 12/83	Jan. 1984	270 pp.

16. SUPPLEMENTARY NOTATION

17. COSATI CODES			18. SUBJECT TERMS (Continue on reverse if necessary and identify by block number)
FIELD	GROUP	SUB. GR.	Electronics, Microwaves, Lasers, Optics, Plasma Physics, Signal Processing.

19. ABSTRACT (Continue on reverse if necessary and identify by block number)

This report, No. 126 in a series of Progress Reports issued by the Research Laboratory of Electronics, contains the customary annual statement of research objectives and summary of research for each group. The report covers the period Jan. 1 - Dec. 31, 1983, and the source of support is indicated for each project. The listing of personnel in the back of the book includes only members of the laboratory during 1983.

20. DISTRIBUTION/AVAILABILITY OF ABSTRACT	21. ABSTRACT SECURITY CLASSIFICATION
UNCLASSIFIED/UNLIMITED XX SAME AS RPT. ☐ DTIC USERS ☐	Unclassified

22a. NAME OF RESPONSIBLE INDIVIDUAL	22b. TELEPHONE NUMBER (Include Area Code)	22c. OFFICE SYMBOL
Janet E. Moore	(617) 253-2566	

DD FORM 1473, 83 APR EDITION OF 1 JAN 73 IS OBSOLETE.

SECURITY CLASSIFICATION OF THIS PAGE

Massachusetts Institute of Technology

RESEARCH LABORATORY OF ELECTRONICS

RLE PROGRESS REPORT No. 126

January 1984

Submitted by: J. Allen
R. Birgeneau

This report, No. 126 in a series of Progress Reports issued by the Research Laboratory of Electronics, contains the customary annual statement of research objectives and summary of research for each group. The report covers the period January 1, 1983–December 31, 1983, and the source of support is indicated for each project. On the masthead of each section are listed the academic and research staff and the graduate students who participated in the work of the group during the year. The listing of personnel in the back of the book includes only members of the laboratory during 1983.

Table of Contents

[28] As published in Association for Computing Machinery Special Interest Group on Automata and Computability Theory 15(1, Spring 1983.

List of Figures

stripes, with identical degrees of blur. The vertical line marks the center of the stripe

Figure 27-5: Plot of size of Snellen letters and the new letters as a function of visual acuity of subject

General Physics

1. Molecule Microscopy

Academic and Research Staff

Prof. J.G. King, Prof. A.P. French, Dr. A. Essig, Dr. J.A. Jarrell, Dr. S.J. Rosenthal

Whitaker Health Sciences Fund

John G. King, Joseph A. Jarrell

1.1 Desorption Studies

We are continuing the experiments begun by D. Lysy[1] and B. Silver[2] on the thermal and electron stimulated desorption of water and other small molecules from biological materials for four reasons. (1) To understand the contrast mechanism in molecule microscopy; (2) to measure the total water content of various samples; (3) to measure the binding energy of this water; and (4) to determine the order of the kinetics of the desorption process. The importance of these experiments comes from the central role of water in biological processes at the molecular level.

Progress

During 1983 we adapted the laser desorption apparatus of J. Yorker[3] for thermal desorption studies carried out in collaboration with Dr. D. Atkinson of the Biophysics Institute at Boston University. An essential part of the work was the development of sample holders that can be made cheaply in quantity so that many samples can be prepared at one time at Boston University for later study at M.I.T. The current design satisfies almost all requirements. It is cheap, has an inert, wettable surface, and can be installed easily in the apparatus along with the miniature thermocouple wires required for temperature monitoring. Improvements were made in the temperature control system, which includes LN_2 cooling and heating by current passing through a graphite rod.

Over 100 desorptions were made from a variety of samples, mostly cholesterol applied to the sample holder by micropipette from solutions with ethanol, methanol, and hexane. Reproducible results were obtained showing a dominant, anomalously narrow desorption peak at moderate temperature (60 C). We interpret this as associated with a phase change in the sample. Similar data were obtained with thymine, cytosine, and uracyl monohydrates. We believe that the sample is in the form of crystallites which undergo a phase change with the emission of water.

Rather than continue work with these imperfectly characterized samples, we decided to study monolayers of cholesterol and DPPC. Accordingly, a Langmuir trough with appropriate dipping mechanism was used, but two problems have appeared. First we find the cleaning procedure of the sample holder to be very critical and secondly its shape, essentially a cylinder, makes it difficult to coat only the end. We are planning further development of the sample holder, at the same time that we are analyzing the data that we have in terms of new theoretical models.

References

1. D.G. Lysy, "Measurement of the Activation Energy for Desorption and other Relevant Parameters by Thermal Desorption Techniques for Water Adsorbed on Biological Macromolecules," Ph.D. Thesis, Department of Physics, M.I.T., 1976.
2. B.R. Silver, "Scanning Desorption of Small Molecules from Model Biological Surfaces," Ph.D. Thesis, Department of Physics, M.I.T., 1976.
3. J.G. Yorker, "Thermal Desorption of Small Molecules from Biological Surfaces with Spatial Resolution," Ph.D. Thesis, Department of Physics, M.I.T., 1982.

1.2 Nanometer Resolution Scanning Desorption Molecule Microscopy

Francis L. Friedman Chair

John G. King, Joseph A. Jarrell

We are designing an SDMM capable of resolution between 1 and 10 nm. The pivotal invention is the use of a tungsten needle with a 1 μm radius tip maintained at low temperature which oscillates from 1 μm above the sample to the entrance of a time-of-flight mass spectrometer. When the needle is above the sample, molecules desorbed from the sample freeze on the tip — later when it is at the entrance of the mass spectrometer these molecules are field desorbed and field ionized by a short high voltage pulse. The molecules are desorbed from the sample by electron stimulated desorption using focused pulses of electron that can be scanned across the sample.

In this way we achieve good solid angle and high efficiency in the detection of neutral molecules whereas high spatial resolution is achieved by exploiting advanced scanning electron microscopy techniques. With this instrument we expect to determine the position and amounts of water and other desorbable molecules on biological samples, thus complementing data attainable in a limited number of cases by x-diffraction.

Progress

During 1983, we have set up experiments to confirm and extend our earlier measurements of ESD cross sections, to desorb molecules from tips with 200 – 400 kv pulses and to investigate ways of controlling and producing these pulses. The design of the instrument will thus be based on well-tested elements.

1.3 Scanning Micropipette Molecule Microscopy (SMMM)

National Institutes of Health (Grant AM-31546)
Joseph A. Jarrell, John G. King

The major goal of this research continues to be the study of water transport at the cellular level across hormonally responsive tissues that model the distal tubules of the mammalian kidney, specifically amphibian urinary bladder. The elucidation of these processes is basic to an understanding of the cellular and molecular mechanisms by which the kidney maintains salt and water balance in man.

This work is being carried out using the scanning micropipette molecule microscope.[1] This instrument uses a micropipette of about 1 μm tip radius sealed with a permeable plug and connected to a mass spectrometer to make concentration measurements of tracers such as labelled water. Thus spatial and temporal variations in the permeation of these tracers across epithelia can be monitored in vitro.

Progress

During the past year, we have continued our studies using microiontophoretic injection of the fluorescent dye, Lucifer Yellow. We have expanded this effort to address the long-standing issue of the role of the basal cells in cell-cell coupling in this epithelium. Our preliminary data suggest, contrary to the currently-held hypothesis, that the basal cells do not provide a major coupling pathway.

We have also initiated a collaboration with Dr. K. Zaner at the Massachusetts General Hospital to measure the diffusional water permeability of various cytoplasmic gel extracts from lung macrophages. The scientific objective is to determine to what extent cytoplasmic gels may restrict intracellular diffusional transport. Our initial measurements on water indicate that there is no significant long-range ordering of intracellular water as has been suggested by others.

Lastly, we have embarked on an effort to determine the feasibility of cryo-preserving amphibian urinary bladders. If this proves possible, it will allow us to use the technique of radiation inactivation to determine, in situ, the molecular weight of several important putative transport proteins.

References

1. J.A. Jarrell, J.G. King, and J.W. Mills, "A Scanning Micropipette Molecule Microscope," Science 211, 277 (1981).

Publications

Jarrell, J.A., "Reversible CO_2-induced Inhibition of Dye-Coupling in Necturus Gallbladder," Am. J. Physiol. 244, C419 (1983).

Jarrell, J.A., C.A. Rabito, and J.G. King, "Applications of Intracellular Dye Injection and Mass Spectrometry to the Study of Epithelial Transport," in M.A. Dinno, T. Rozzell, and A. Callahan

(Eds.), Physical Methods in the Study of Cellular Biophysics (A.R. Liss, New York, 1983).
Jarrell, J.A., "Dye Coupling in Amphibian Urinary Bladder," Abstract for the 1983 meeting of the American Society of Cell Biology.

1.4 Electrical Neutrality of Molecules

International Business Machines Corporation
Anthony P. French, John G. King

The present experimental upper limit on any departure from neutrality of molecules is approximately 10^{-21} of one elementary charge. This can be interpreted as a limit on the proton-electron charge difference, or on the charge on the neutron, or on some combination of these. The occurrence of innumerable transformations involving both leptons and baryons, and our long-standing belief in the conservation of electric charge as a fundamental law of nature, certainly support the assumption of exact equality of charges of either sign on all elementary particles. Nevertheless, the possibility that there might be some minute difference between electron and proton charges is something that cannot be ruled out on the basis of any existing experimental evidence or theoretical scheme, and its existence would have profound implications.

The fundamental interest of this question has led to a number of experiments by various investigators. These experiments have involved three different approaches: (1) direct tests for any net charge in a volume of gas released from a container; (2) tests for a charge on an isolated body (analogous to the Millikan oil-drop experiment); (3) molecular-beam deflection experiments.

In 1973 King and Dylla[1] pioneered a new technique based on the fact that an electric field, periodic in time, applied to a homogeneous medium will excite acoustic waves at the same frequency if the molecules of the medium are not completely neutral. (This is separable from any induced polarization effects, which will occur at doubled frequency).

Progress

We have designed and built a cylindrical resonant cavity in which an approximately uniform axial oscillating electric field can be established. One end of the cavity is a solid plug and the other end, adjustable in position, is a resonant diaphragm condenser microphone. We use the 5 MHz bridge technique developed by Linsay and Shoemaker[2] to measure vibration of the diaphragm near the thermal limit. The first runs will be in $CC1_4$ followed by LHe^4I and LH_2 and eventually LHe^3 and LD_2.

References

1. H. Dylla and J. King, Phys. Rev. A 7, 1224 (1973).
2. P.S. Sinsay and D.H. Shoemaker, Rev. Sci. Inst. 53, 1014 (1983).

2. Semiconductor Surface Studies

Academic and Research Staff

Prof. J.D. Joannopoulos, Dr. D.-H.T. Lee, Dr. A.D. Stone

Graduate Students

Y. Bar-Yam, K. Rabe, E. Kaxiras

2.1 Excitations at Surfaces and Interfaces of Solids

Joint Services Electronics Program (Contract DAAG29-83-K-0003)
John D. Joannopoulos, Dung-Hai T. Lee, Alfred D. Stone

Understanding the properties of surfaces of solids and the interactions of atoms and molecules with surfaces has been of extreme importance, both from technological and academic points of view. The recent advent of ultrahigh vacuum technology has made microscopic studies of well-characterized surface systems possible. The way the atoms move to reduce the energy of the surface, the number of layers of atoms involved in this reduction, the electronic and vibrational states that result from this movement, and the final symmetry of the surface layer are all of utmost importance in arriving at a fundamental and microscopic understanding of the nature of clean surfaces, chemisorption processes, and the initial stages of interface formation. Actually, one of the most difficult and fundamental problems in surface studies, both from the experimental and theoretical points of view, is simply the determination of the precise positions of the atoms on a surface. Currently, there are many surface geometries, even for elemental surfaces, that remain extremely controversial.

The theoretical problems associated with these systems are quite complex. We are, however, currently in the forefront of being able to solve for the properties of real surface systems (rather than simple mathematical models). In particular, we have recently developed a method of calculating the total ground-state energy of a surface system from "first principles" so that we may be able to provide accurate theoretical predictions of surface geometrics. Recent results of metal atoms deposited on a semiconductor surface look very promising. The first total energy map for an interacting atom-surface system has been obtained. The map clearly illustrates possible chemisorption sites as well as specific migration or diffusion channels.

Presently, we are attempting to combine the results of microscopic total energy calculations with the renormalization group techniques, developed in statistical mechanics, in order to study structural phase transitions at finite temperatures. If successful, this will provide an "ab-initio" framework for studying phase transitions and critical phenomena in solid systems.

3. Atomic Resonance and Scattering

Academic and Research Staff

Prof. D. Kleppner, Prof. D.E. Pritchard, Dr. R. Ahmad-Bitar, Dr. T. Ducas, Dr. D. Kelleher, Dr. M. Ligare, Dr. A.M. Lyyra, Dr. P. Moskowitz, Dr. K.L. Saenger, Dr. N. Smith, Dr. W.P. Spencer, Dr. G. Vaidyanathan, Dr. X. Zhong

Graduate Students

S. Atlas, V. Bagnato, L. Brewer, S.L. Dexheimer, R. Flanagan, T.R. Gentile, P.L. Gould, E. Hilfer, B.J. Hughey, R.G. Hulet, M.M. Kash, P.D. Magill, A.L. Migdall, W.P. Moskowitz, E. Raab, T.P. Scott, B.A. Stewart, R. Weisskoff, G.R. Welch

Undergraduate Students

I. Nir, K. Plonty, D. Sherman

3.1 Rydberg Atoms in a Magnetic Field

National Science Foundation (Grant PHY79-09743)

Michael M. Kash, Daniel Kleppner, Ishai Nir, George R. Welch

The general structure of atomic hydrogen in an arbitrarily strong magnetic field is still an unsolved problem of atomic physics. The diamagnetic Hamiltonian for hydrogen is known; the eigenstates are not. Highly excited, or Rydberg, atoms in a laboratory sized field (about 10 Tesla) exhibit strong principal quantum number "mixing". Even numerical solutions fail in this regime.

The experimental goal of our research is to map out the energy levels of a Rydberg lithium atom in a strong magnetic field in the vicinity of a crossing between levels from different principal quantum numbers. The scheme for producing the Rydberg atoms by optical excitation with lasers is 2s→3s via two photons (735 nm) and 3s→~40p via one photon (~620 nm). The atoms are detected by field ionization.

We have observed the two-photon transition by monitoring the cascade fluorescence to the ground state. Fig. 3-1 shows the two-photon transition in ^{7}Li, and Fig 3-2 shows the two-photon transition in ^{6}Li. The measurements are in an atomic beam of "natural" lithium in which only 7% is ^{6}Li. The markers are 300 MHz. Using the accurately known ground state hyperfine structure intervals, we have obtained the $3^2S_{1/2}$ hyperfine structure intervals: 190(20) MHz for ^{7}Li, and 50(20) MHz for ^{6}Li.

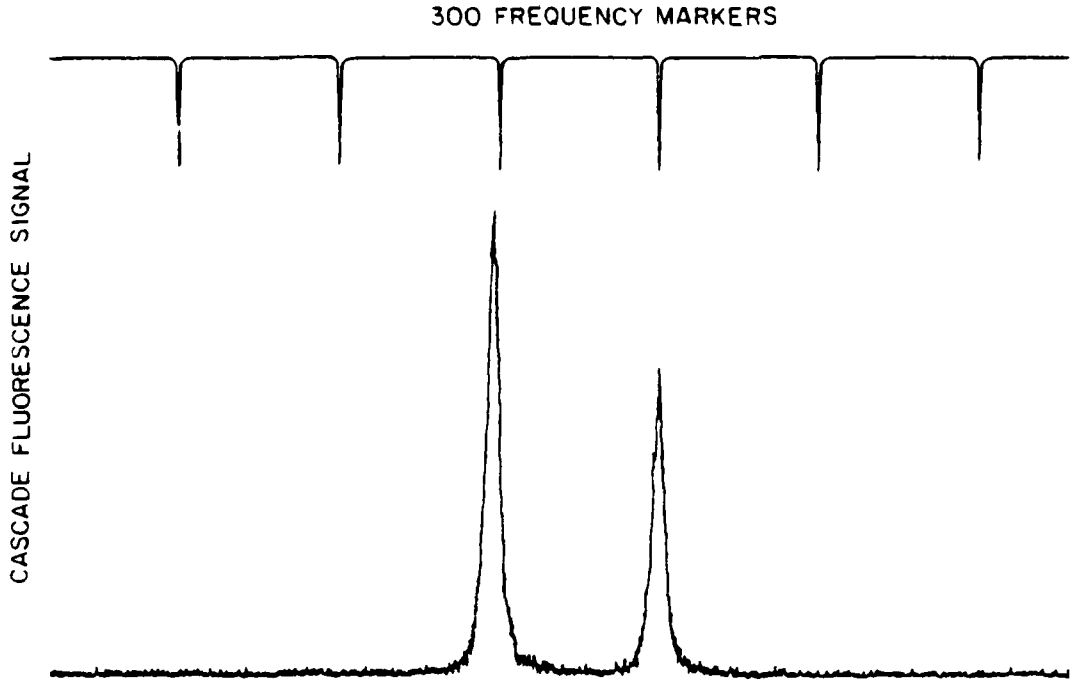

Figure 3-1: Two-Photon Absorption from 2s→3s in ^{7}Li

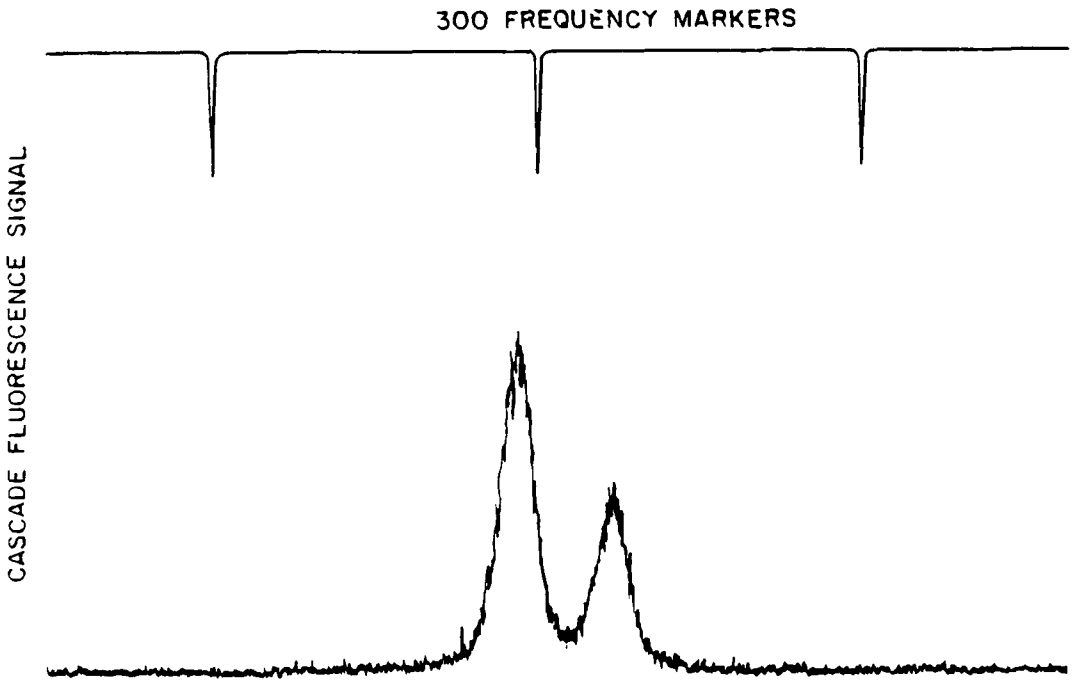

Figure 3-2: Two-Photon Absorption from 2s→3s in ^{6}Li

3.2 Electrodynamics in a Cavity

National Science Foundation (Grant PHY82-10486)
Joint Services Electronics Program (Contract DAAG29-83-K-0003)
U.S. Navy - Office of Naval Research (Contract N00014-79-C-0183)
Thomas R. Gentile, Barbara J. Hughey, Randall G. Hulet, Daniel Kleppner, William P. Spencer, A. Ganesh Vaidyanathan

Spontaneous emission of a photon by an excited atom depends on the nature of the space surrounding the atom. In free space, the photon can be emitted into the infinite number of modes of the radiation field which can support the photon. In a cavity, the number of modes is restricted, and this radically alters the way the atom emits radiation. With the cavity off resonance, spontaneous emission is inhibited. On resonance, the atom–cavity system oscillates between an excited atom with no photon, and a de–excited atom with a photon.

We are investigating these phenomena with our experiments on the electrodynamics of Rydberg atoms in a cavity. We also hope to study enhanced spontaneous emission, "super cooling" of the radiation field, and to observe the statistical behavior of small numbers of atoms interacting with small numbers of photons. In our initial experiments, we have observed a related phenomenon, enhanced absorption of blackbody radiation (see Fig. 3–3). These experiments enhance our understanding of atom–photon interactions at the single photon–single atom level as well as increasing our understanding of fundamental noise processes. The experimental methods have applications in the development of ultra sensitive far–infrared detectors.

The experiments are carried out in an atomic beam of sodium. The atoms are excited to a Rydberg state by pulsed dye lasers and then pass through a high Q ($\sim 10^7$) superconducting cavity. As the atoms leave the cavity, they are analyzed in a special detector which determines not only their final state but the time spent in the cavity. Much of the work over the past year has been devoted to perfecting the novel state selective detector and in developing the tunable super conducting cavity.

The Rydberg atom detector uses an inhomogeneous electric field to spatially resolve the state of the Rydberg atom (see Fig. 3–4). This has four advantages over the more commonly used time resolved pulsed field ionization: 1) Rydberg atoms can be individually counted; 2) The velocity of the Rydberg atoms can be directly measured; 3) All Rydberg atoms are collected; and 4) The detector may be used for detection of a continuous beam of Rydberg atoms.

A super conducting cavity with a Q of about 10^6 has been constructed. We are currently working to improve the Q cavity to 10^7, and to install a mechanism to tune the cavity. At 30 GHz, a cavity with a Q of 10^7 needs a tuning resolution of at least 1 kHz. Tuning is achieved by "squeezing" the cavity. We are using the TM_{010} mode of the cavity, which allows the cavity cylinder to be cut along its axis of symmetry. "Squeezing" is achieved by separating the two halves slightly and moving them together.

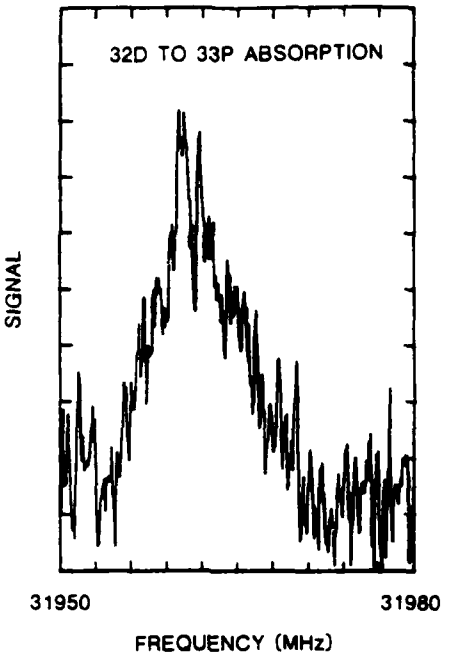

Figure 3-3: Enhanced absorption of blackbody radiation. Rydberg atoms are placed on the 32d state of sodium inside of a 77 K cavity. As the cavity is tuned on resonance, transfer of population from the 32d to the 33p state is observed. The transfer rate is increased on resonance by a factor of 10^4, the Q of the cavity. Total transfer is limited by collective atom effects inside the cavity.[2]

A motion of 10^{-7} cm corresponds to 1 KHz.

We are also working to observe inhibited spontaneous emission, using our recently developed techniques of populating Rydberg atoms in "circular" states.[1] These are Rydberg states with highest angular and orbital momentum. Because of selection rules, only one channel of spontaneous decay is available. If we place these atoms in a cavity beyond cutoff, no spontaneous emission can occur. The Rydberg state effectively becomes a new ground state for the atom.

References

1. R. Hulet and D. Kleppner, Phys. Rev. Lett. 51, 1430 (1983).
2. J.M. Raimond, P. Goy, M. Gross, C. Fabre, and S. Haroche, Phys. Rev. Lett. 49, 117 (1982).

3.3 Multiphoton Ionization

National Science Foundation (Grant PHY79-09743)
National Bureau of Standards (Grant NB83 NAHA-4058)
Lawrence Brewer, Daniel Kellcher, Daniel Kleppner, Martin Ligare

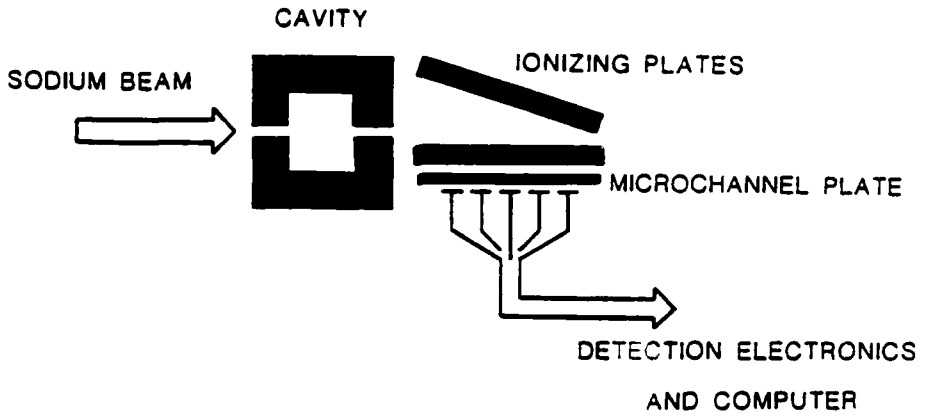

Figure 3-4: A novel detection scheme is employed for determining the final state of the Rydberg atom. A set of field plates are tipped with respect to one another by 5°. As the atom drifts into the detection region it experiences an increasing field until it ionizes. The position and time of the resulting electron is recorded by an array of collector strips. The position determines the final states of the atom and the time determines the velocity of the atom.

Multiphoton ionization of atoms and molecules is a non-linear phenomenon which can occur whenever matter interacts with intense optical fields such as those produced by high power lasers. Of particular interest to us is resonance enhanced multiphoton ionization. This occurs when the photon energy matches an allowed intermediate transition in the multiphoton absorption process. The multiphoton resonance absorption profile is affected by the shifts and ionization broadening of the intermediate energy levels due to the intense fields used to observe multi-photon ionization. Because multiphoton ionization is a non-linear process, the rate is sensitive to amplitude and phase fluctuations of the field. We have studied these processes in the four-photon ionization of atomic hydrogen. Three photon excitation is resonant with the 1s-2p transition of the atom, and the fourth photon ionizes the atom at threshold.

The experiment is carried out in a cooled atomic beam. Atomic hydrogen is generated from molecular hydrogen in an rf dissociator and then passed through an accomodator which can be cooled to liquid nitrogen or helium temperature. The multiphoton ionization requires photons near 364.6 nm. We use the frequency doubled output of a Nd:YAG laser to pump a dye laser-amplifier combination which produces tunable output near 554.6 nm. This is mixed in a non-linear crystal with the fundamental frequency of the ND:YAG laser at 1064 nm to give tunable light near 364.6 nm. This

produces 10 mJ pulses of 9 nsec duration. The photoions created by the laser pulse are swept out of the interaction region by a pair of field plates and are collected in an electron multiplier.

Fig. 3-5 shows a typical experimental lineshape for a 4.5 mJ pulse (about 15 GW/cm^2). The line profile is highly asymmetric, shifted to the blue from the zero field 1s-2p resonance, and very broad. As the laser power is increased the shift and width increase approximately linearly. The height of the peak of the profile grows with the third power of the laser intensity. Theory for a perfectly monochromatic light field indicates that the lineshape should be Lorentzian with a shift governed by the "A.C." Stark shift and with a width given by the ionization rate of the 2p state. The peak of the resonance profile should grow as the square of the laser intensity.[1]

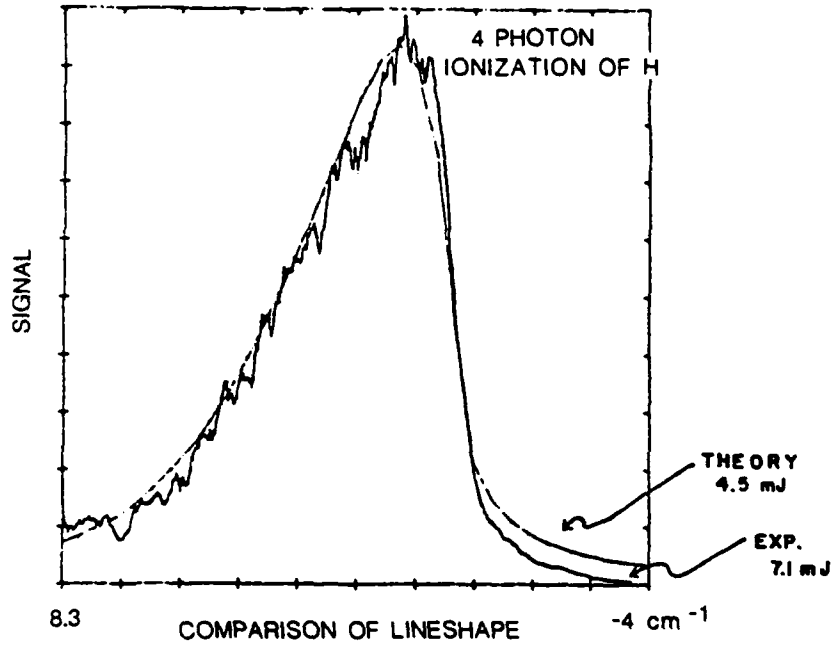

Figure 3-5: Comparison of the shape of experimental and theoretical resonance profiles for four photon multiphoton ionization of atomic hydrogen. Note that the power density used to generate the theoretical profile is not the same as the power density used for the experimental profile.

The experimentally observed effects can be understood qualitatively by averaging the Lorentzian lineshape (which is predicted for a constant amplitude monochromatic field) over the distribution of field amplitudes that occur in our finite bandwidth, multimode laser pulses. In addition, the theoretical results must be averaged over the spatial intensity distribution of a gaussian laser beam. This averaging yields profiles like that designated 'theory' in Fig. 3-5. The long "blue tail" of the profile is the result of contributions from the high intensity peak amplitudes produced by the mode beating in the pulse. It is these high intensities which are responsible for large A.C. Stark shifts and ionization

widths. The shape of the profile is well reproduced, but the power density predicted by the theory for a particular value of the shift and width is lower than that given by the experiment. In addition, the power dependence of the height of the peak is not correctly accounted for in such a simple theory.

We are currently constructing a single mode tunable dye laser system. The amplitude and phase fluctuations of this light should be much reduced compared to our present system. We are also working on a more complete theory in an attempt to understand all the features of the experimental profiles.

References

1. C.R. Holt, M.G. Raymer, and W.P. Reinhardt, Phys. Rev. A 27, 2791 (1983).

3.4 Velocity Dependence of Rotational Rainbow Structure in Na_2 – Ar

National Science Foundation (Grant CHE79-02967-A04)

Warren P. Moskowitz, Brian A. Stewart, J.L. Kinsey, David E. Pritchard

We have measured level-to-level differential cross sections for the rotationally inelastic process $Na_2(j_i = 7) + Ar \rightarrow Na_2(j_f = j_i + \Delta J) + Ar$ at center of mass energies 0.49 and 1.1 eV, with Na_2 in its lowest electronic and vibrational state. The angular momentum transfer Δj ranged from 2 to 40. The measurements were made in crossed molecular beams. The initial rotational level was selected using optical pumping, and the final rotational level was detected by laser induced fluorescence. The angular distribution was determined by a new Doppler technique, called PADDS, that gives good small angle resolution. In this technique, a single mode, c.w. dye laser beam intersects the collision region perpendicular to the relative velocity vector, and excites molecules which have been scattered into the final state with the correct Doppler—selected velocity component in the direction of the laser. The laser is tuned, and the resulting fluorescence signal yields the differential cross section through a deconvolution. A typical differential cross section is shown in Fig. 3–6.

3.5 High Precision Mass Measurement on Single Ions Using Cyclotron Resonance

National Science Foundation (Grant PHY83-07172)

Riyad Ahmad-Bitar, Robert W. Flanagan, Phillip L. Gould, David E. Pritchard, Robert M. Weisskoff

In the past few years powerful new techniques for study of resonances in trapped particles have been developed.[1,2] We plan to apply these techniques to precision mass measurement of single atomic and molecular ions using a novel, low-noise detection scheme. These measurements permit advances in mass and x-ray wavelength metrology, chemistry, and physics. Measurement of relative

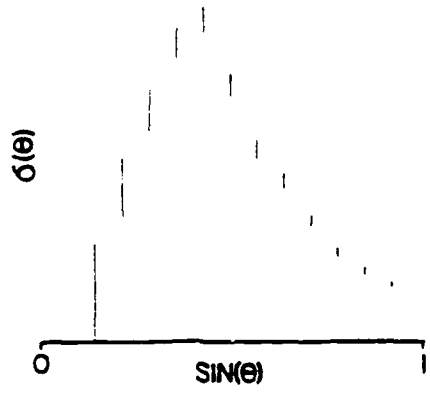

Figure 3-6: Differential cross section for $\Delta j = 16$, obtained by procedure described in paper submitted to J. Chem. Phys.

mass differences of one part in 10^{11} will permit the weighing of chemical bonds, ultra-precise measurement of energy differences in isomer nuclei, and improved knowledge of physical constants.

The experiments will involve capturing a single ion in a Penning trap and measuring the weak signals emitted as the ion oscillates. The small signals expected and the requirement for high precision demand the use of a SQUID (superconducting quantum interference device) detector, liquid helium-cooled coupling networks, and a high stability superconducting magnet. Single ion techniques are necessary since Van Dyck[2] has shown that space charge effects cause the cyclotron resonance to shift by about 1.2×10^{-10} per ion, even when using a compensated trap.

Currently, the cryogenic container, vacuum system and Penning trap are being designed. Modifications to commercial NMR magnet systems are being developed with assistance provided by several manufacturers. Some computer hardware has been purchased and some software has been developed. A stable voltage source (drift $\lesssim 10^{-8}$ per minute) has been constructed and our preliminary experiments with superconducting impedance matching circuits have been promising.

References

1. Robert S. Van Dyck, Jr., Paul B. Schwinberg, and Hans G. Dehmelt, in Daniel Kleppner and Francis Pipkin, (Eds.). Atomic Physics, Vol. 7 (Plenum Press, 1981) p. 340.
2. R.S. Van Dyck, Jr., and P.B. Schwinberg, Phys. Rev. Lett. 47, 395 (1981).

3.6 Intensity and Frequency Dependence of Atomic Beam Deflection by Transverse Standing Wave Radiation

National Science Foundation (Grant PHY83-07172)

Phillip E. Moskowitz, Phillip L. Gould, Susan Atlas, Eric Raab, David E. Pritchard

The deflection of an atomic beam by a standing wave laser field is a useful probe of the interaction of atoms with very intense optical radiation fields. We have studied this deflection as a function of laser intensity[1] and frequency by crossing a supersonic beam of sodium atoms with a perpendicularly oriented standing wave laser. The atomic beam is well collimated (4×10^{-5} rad) and has a narrow velocity distribution (10% FWHM). Total resolution of the apparatus is on the order of the momentum of a single photon ($p\gamma = hk$). The laser is tuned near the frequency of the $3S_{1/2} \rightarrow 3P_{3/2}$ transition and the interaction time is constrained to approximately one radiative lifetime (16 ns) in order to reduce the effects of spontaneous decay on the interactions.

Our results for the rms deflection as a function of laser power and frequency are shown in Figs. 3–7 and 3–8, respectively. The data are in rough agreement with semiclassical[2] and fully quantum mechanical[3] theories. Exact analysis is impossible due to the presence of multiple energy levels (hyperfine structure) in the sodium atom. However, the linear dependence of the deflection on electric field is evident at high fields and the frequency dependence is seen to have the predicted power–broadened resonance width.

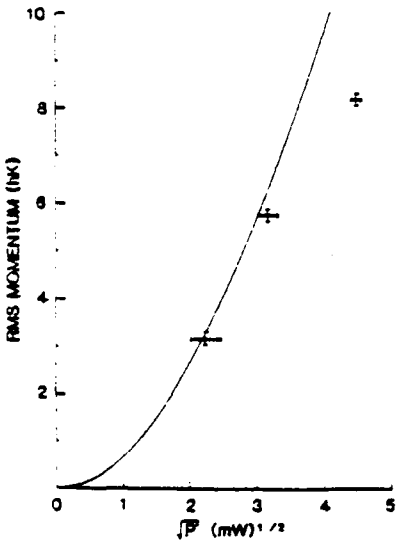

Figure 3-7:

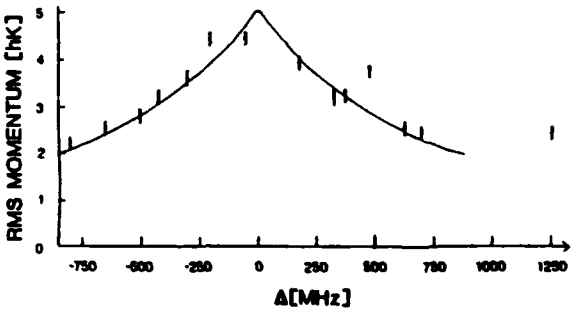

Figure 3-8:

References

1. P.E. Moskowitz, P.L. Gould, S. Atlas, and D.E. Pritchard, Phys. Rev. Lett. 61, 370 (1983).
2. A.P. Kazantsev, G.I. Surdutovich, and V.P. Yakovlev, JETP Lett. 31, 509 (1980).
3. A.F. Bernhardt and B.W. Shore, Phys. Rev. A 23, 1290 (1981).

3.7 Low Temperature Energy Transfer

Joint Services Electronics Program (Grant DAAG29-83-K-0003)
Alan L. Migdall, David E. Pritchard

We are investigating energy transfer collision processes at extremely low temperatures. Low temperatures were produced using a seeded supersonic beam source in which we have studied rotationally inelastic collisions for Li_2 – Ar at temperatures of 100°K and 250°K. Cross sections for these collisions were calculated from the data after accounting for the details of the expansion process. We are in the process of implementing a more accurate procedure to correct for the effects of multiple collisions.

We have fit our data to the ECS–EP law that has been used successfully on most of the existing rotationally inelastic data. We see some systematic deviation between our data and the fits, and we are testing to see if this deviation originates in our analysis or is an actual failure of the ECS theory.

We plan to make measurements using Li_2 – He. This system should dramatically show the effects of dynamical constraints due to the low mass of the collision partner, and hence the small amount of orbital angular momentum available to change j.

3.8 Trapping of Neutral Atoms

Vanderlei Bagnato, Riyad Ahman-Bitar, Phillip E. Moskowitz, David E. Pritchard, Eric Raab

Trapped atoms cooled below 10^{-7}K are an excellent system for studying collective phenomena (superradiance, Bose condensation, and phase transitions), studying collisions such as Na–Na or Na–Na*, and performing ultra-high resolution spectroscopy[1] with the possible objective of making a greatly improved frequency standard. Deceleration of a neutral atomic beam has been demonstrated recently by Phillips and Metcalf.[2,3] The next step is to trap the neutrals in a laboratory field and then cool them. Numerous schemes for such traps have been proposed including magnetic field traps,[1,4-7] electrostatic traps[8] and traps using near resonance radiation.[9,10] We have proposed schemes to cool the neutrals to 10^{-7}K in a magnetic field trap.

We are setting up an experimental apparatus to be used for decelerating and trapping atoms. Very briefly, the deceleration part is very much like Phillips et al.[3] The trapping of paramagnetic particles occurs in magnetic sublevels whose energy increases in proportion to the applied field. We are building such a trap whose well is 30 mK deep to trap the decelerated Na-beam.

References

1. D.E. Pritchard, Phys. Rev. Lett. 51, 1336 (1983).
2. W.D. Phillips and H. Metcalf, Phys. Rev. Lett. 48, 596 (1982).

3. J.V. Prodan, W.D. Phillips, and H.J. Metcalf, Phys. Rev. Lett. 49, 1149 (1982).
4. H. Friedberg and W. Paul, Naturwissenschaften 38, 159 (1951).
5. V.V. Vjadimirski, Zu. Eksp. Teor. Fiz. 39, 1062 (1960).
6. C.V. Heer, Rev. Sci. Instrum. 34, 532 (1963).
7. H.J. Metcalf, Nat. Bur. Stand. (U.S.) Spec. Publ. 653, 59 (1983).
8. W.H. Wing, Phys. Rev. Lett. 45, 631 (1980).
9. A. Ashkin, Phys. Rev. Lett. 40, 729 (1978).
10. A. Ashkin and J.P. Gordon, Opt. Lett. 4, 161 (1979).

3.9 Vibrationally Inelastic Collisions

National Science Foundation (Grant CHE79-02967-A04)

Thomas P. Scott, Neil Smith, Peter D. Magill, David E. Pritchard

In previous years we have exhaustively investigated Rotationally Inelastic (RI) collisions both theoretically and experimentally. We have shown the general applicability of scaling laws to these collisions and have illuminated general features of RI collisions using simple dynamical ideas.

We have now turned our attention to vibrationally–rotationally inelastic (VRI) processes for several major reasons. Firstly, it is now possible to study these collision processes with much greater detail than has been done previously. Secondly, no general theory exists for VRI collisions, inviting us to generalize the ideas which have developed for purely RI collisions to this more complicated situation. Finally, there is a need to reduce the thousands of vibrationally and rotationally level specific rate constants in order to model collision dynamics in many important regimes (e.g., planetary atmospheres, gas lasers, supersonic expansions).

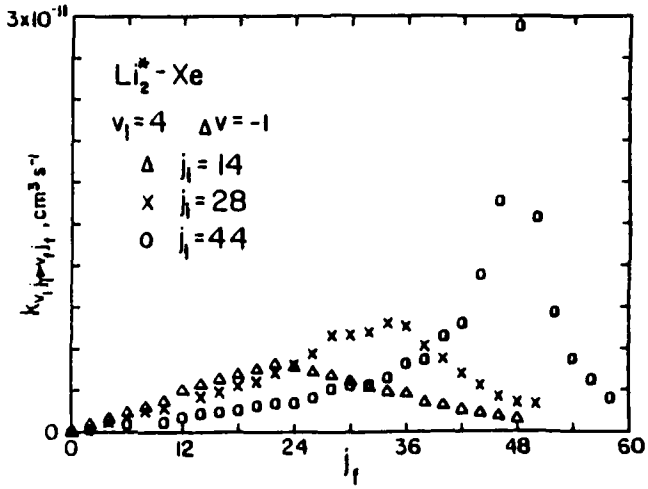

Figure 3-9:

Our initial measurements of VRI rate constants for $k_{v_i = 4, j_i \rightarrow v_f, j_f}$ for the system Li_2^*–Xe (SSD83), has demonstrated a significant role of initial rotation quantum number, j_i, in determining the magnitude of $k_{v_i, j_i \rightarrow v_f, j_f}$ and the specificity in the distribution of final rotational states for a given $\Delta v = v_{f v_i}$ (Fig. 3–9).

The peak of these distributions regardless of Δv is found to be given by the simple expression $(j_f)_{peak} = j_i - 4\Delta v$. This differs from the position of the peak given by energy resonance.

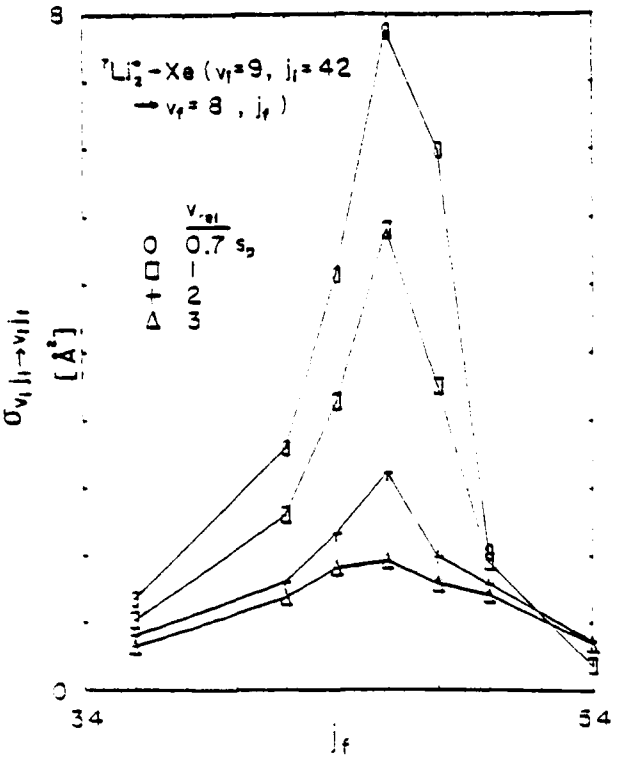

Figure 3-10:

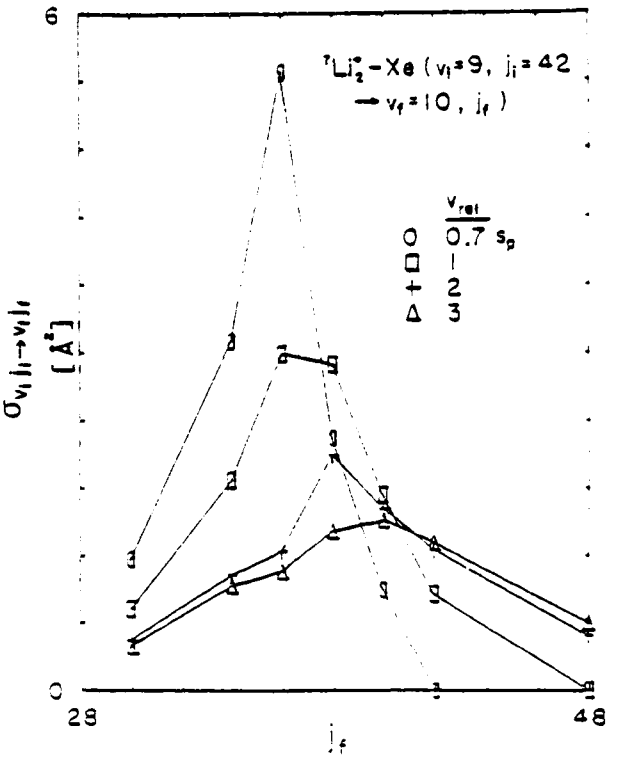

Figure 3-11:

Using our method of velocity selection by Doppler shift (VSDS) to measure the dependence of level to level specific cross sections on collisional velocity, we have measured the velocity dependence of these distributions for $Li_2^*(v_i = 9, j_i = 42 \to v_f, j_f) - Xe$ where $\Delta v = -1$ (Fig. 3–10) and $\Delta v = +1$ (Fig. 3–11). We find that the peak is reduced and the distribution is broadened as the collision velocity is increased. Further, while the peak of the $\Delta v = -1$ distribution is given by the $(j)_{fpeak} = j_i - 4\Delta v$ rule for all velocities, that for the $\Delta v = +1$ distribution moves toward higher j_f as the collision velocity is increased. For both values of Δv, the total VRI cross section (area under the peak) decreases monotonically with increasing collision velocity.

References

1. K.L. Saenger, N. Smith, S.L. Dexheimer, C. Engelke, and D.E. Pritchard, J. Chem. Phys. 79, 4076 (1983).

4. Chemical Reaction Dynamics at Surfaces

Academic and Research Staff

Prof. S.T. Ceyer

Graduate Students

J.D. Beckerle, D. Gladstone, M.B. Lee, M. McGonigal, R.J. Simonson, S.L. Tang

Undergraduate Students

M. Hines

4.1 Dynamics of Activated Dissociative Adsorption

National Science Foundation (Grant DMR81-19292)

Sylvia T. Ceyer, John D. Beckerle, Melissa Hines, Myung B. Lee, Sau Lan Tang

Our efforts this year have centered around the construction, assembly and testing of the molecular beam-EELS apparatus which will enable us to study the dynamics of molecule-surface interactions. In particular, we are interested in understanding why dissociative chemisorption does not occur on transition metal surfaces where the adsorption is known to be exoergic. In many of these cases it is likely that dissociative adsorption is activated and thus, is not observed when the adsorption is attempted by allowing ambient molecules, whose energies are characterized by a 300 K Maxwell-Boltzmann distribution to impinge on the surface. The existence of a barrier along the lowest energy pathway is the condition for activated dissociative chemisorption. On many metal surfaces, however, dissociative adsorption is observed when the surface has been modified with low coordination number sites or promoter atoms. Whether these modifications lower the barrier for dissociative adsorption, increase the atom-surface binding energy or affect both quantities is unknown. In short, the features of the potential energy surfaces which are modified to promote dissociation are simply not known experimentally.

Because activation energy barriers are extrema on the potential surface they are experimentally accessible. It is proposed to verify the existence of and to measure the magnitude of these dominant features in an experimental arrangement in which a beam of molecules that are to be adsorbed on a surface and high resolution electron energy loss spectroscopy are coupled. With this arrangement, the effect of the energy of the incoming molecule on its probability of dissociatively chemisorbing can be determined. If there exists a barrier to dissociation, there will be a sharp onset in intensity of the dissociated species at some incident beam energy. This beam energy then constitutes the appearance threshold or magnitude of the energy barrier to dissociation. The orientation of the barrier relative to the surface can be determined by variation of the incident beam angle. The effect

of lateral interactions on the height of the barrier can be investigated by variation of the surface coverage.

Carbon monoxide dissociation on Ni(111) is the rate limiting step in the methanation reaction, CO + $3H_2 \rightarrow CH_4 + H_2O$. This reaction occurs with measurable rates only at high surface temperatures (>500 K) and at high pressures (>1 atm). This observation suggests that CO dissociative adsorption is an activated process since the pressure must be high enough for the CO molecules to gain energy through multiple inelastic collisions with the hot surface prior to the collision which leads to dissociation. We have chosen to investigate this system on an apparatus which we have recently finished constructing. Preliminary results indicate that the dissociative adsorption of CO is indeed activated and that the barrier is at least 25 kcal. If we confirm this result, then the rate of the methanation reaction could be greatly increased by heating the reactants prior to their encounter with the nickel catalyst. We also have measured the decrease in the barrier height when a small quantity (<10% of a monolayer) of potassium is doped on the surface. It appears that this small amount of potassium decreases the barrier by two orders of magnitude. We are presently confirming these preliminary results.

4.2 Dynamics of Dissociative Adsorption

National Science Foundation (Grant CHE82-06422)
Research Corporation
Camille and Henry Dreyfus Foundation
Sylvia T. Ceyer, John D. Beckerle, Melissa Hines, Myung B. Lee, Sau Lan Tang

Investigations into the dynamics of the dissociative chemisorption process on transition metal surfaces are planned. The collision energy of the incident adsorbate is a convenient probe of the dominant features of the molecule-surface potential energy surface which governs the adsorption dynamics. High resolution electron energy loss spectroscopy and photon detection are sensitive detectors of the result of the dissociative adsorption event. The effect of translational energy and, where appropriate, internal energy on the extent of dissociative chemisorption will be studied for molecule-metal systems that are believed to dissociate via a precursor state, a direct, an activated and an electronic mechanism or are believed not to dissociate. The emphasis of these studies is on establishing a correlation between the nature of the potential energy surface for the molecule-surface interaction and the dynamics of dissociative adsorption.

4.3 Chemical Reaction Dynamics at Semiconductor Surfaces

Sylvia T. Ceyer, Marianne McGonigal, David Gladstone

An investigation into the reaction dynamics of atomic oxygen and atomic halogens with

semiconductor surfaces will be carried out with molecular beam-surface scattering techniques. These techniques enable the measurement of the mass distribution, the residence time distribution, the angular distribution, and the energy distribution of the product molecules. The goals of this research are to develop a kinetic model for the surface reaction, to determine the chemical identities of the reaction intermediates, to understand the mechanism of the desorption step and how it relates to the potential energy surface in the exit channel region and to investigate whether simple gas phase unimolecular decay theories may be applied to describe the angular and energy distributions of the desorbing molecule after chemical activation. The plans for this apparatus have been submitted to various machine shops.

4.4 Spectroscopic Studies of Small Molecule Adsorption on Rare Earth Single Crystal Metal and Metal Oxide Surfaces

Monsanto

Sylvia T. Ceyer, Robert J. Simonson

An investigation aimed at a spectroscopic study of the adsorption of small molecules on single crystal rare earth metal and metal oxide surfaces has begun. Such techniques as X-ray and ultraviolet photoelectron spectroscopy, Auger and high resolution electron energy loss spectroscopy, low energy electron diffraction and thermal desorption are being employed to determine the dissociative nature of the adsorption, the electronic structure and the binding site of the molecule, the kinetics of the desorption process and the binding energy of the molecule on the surface. These studies represent the first investigations into adsorption on single crystal rare earth metals even though these metals, their oxides and their intermetallics exhibit catalytic activity comparable to transition metal catalysts.

At the present time, we have temporarily side-tracked from these goals to investigate some interesting inner shell spectroscopy of the rare earths. We have observed and identified inner core to 4f transitions in an electron energy loss spectrum of a Gd single crystal. These resonances have been previously observed in X-ray absorption studies of polycrystalline rare earth metals. Since both these resonances and the Auger transitions can be observed in a single spectrum, we are attempting to identify the Auger transitions that can be attributed to direct recombination from the bound 4f excitations versus those that arise from continuum excitations.

Publications

Ceyer, S.T., W. Guthrie, T.H. Lin, and G.A. Somorjai, "D_2O Product Angular and Translational Energy Distributions from the Oxidation of Deuterium on Pt(111)," J. Chem. Phys. 78, 6982 (1983).

Ceyer, S.T. and J.T. Yates, J. Elect. Chem. 150, 17 (1983).

5. X-Ray Diffuse Scattering

Academic and Research Staff

Prof. R.J. Birgeneau, Dr. A.R. Kortan, Dr. M. Sutton

Graduate Students

K. Evans-Lutterodt, H. Hong, L.J. Martínez-Miranda, S.G.J. Mochrie, B.M. Ocko, E. Specht

Joint Services Electronics Program (Contract DAAG29-83-K-0003)

Robert J. Birgeneau

In this research program, modern x-ray scattering techniques are used to study the structures and phase transitions in novel states of condensed matter. We have two principal experimental facilities. At M.I.T. we have three high-resolution computer controlled x-ray spectrometers using either a conventional or high intensity rotating anode x-ray generator. The angular resolution can be made as fine as 1.8 seconds of arc; this enables one to probe the development of order from distances of the order of the x-ray wavelength, ~1 Å, up to 30,000 Å. The sample temperature may be varied between 2 K and 500 K with a relative accuracy of 2×10^{-3}K. We are currently installing a two spectrometer system at the National Synchrotron Light Source at Brookhaven National Laboratory. This makes possible high resolution scattering experiments with a flux more than three orders of magnitude larger than that from a rotating anode x-ray generator. This opens up a new generation of experiments. Synchrotron x-ray scattering experiments are also carried out on a wiggler beam line at the Stanford Synchrotron Radiation Laboratory.

As part of the JSEP program we have built an x-ray compatible high vacuum single crystal apparatus. This enables us to use synchrotron radiation to study the structure and transitions occurring at single surfaces; such experiments are now being initiated. Our current experiments in this program are concentrated in three areas: (i) the growth, structure, and phase transitions of intercalant materials, most especially bromine-intercalated graphite, (ii) the structure and phase transitions of smectic liquid crystals, (iii) the evolution from thin film to bulk structures of model systems.

5.1 Intercalation Compound Structures and Transitions

Intercalation compounds represent a family of materials in which a foreign species (e.g., Br_2) is inserted between the layers of a lamellar material such as graphite. If the intercalant enters every *n*th layer then the resultant material is referred to as a stage-*n* intercalation compound. In this program we study both the intercalation process itself and the structure and transitions of the intercalation compound as a function of temperature, concentration, and stage index. Our work to date has

concentrated on the systems bromine-intercalated graphite $C_{7n}Br_2$[1-3] and potassium-mercury intercalated graphite.

The intercalate plane is found to have three sublattices and each sublattice has a centered ($\sqrt{3}$ x 7) rectangular structure with four Br_2 molecules per 2D unit cell in the commensurate phase. The coherently ordered in-plane bromine regions exceed 10,000 Å in size. In the stage-4 material a commensurate-incommensurate (CIT) transition is observed at 342.20 ± 0.05°K. In the incommensurate phase, a stripe domain pattern becomes established in a single domain of a sublattice along the 7-fold direction. The incommensurability as a function of reduced temperature exhibits power law behavior with an exponent of 0.50 ± 0.02 confirming existing theories. The relative shifts observed for the various harmonics are accurately predicted by a sharp domain wall with $4\pi/7$ phase shifts. The intercalate layer exhibits a continuous melting transition from a two-dimensional solid phase to a smectic liquid crystal phase, occurring at 373.41 ± 0.10°K for a stage-4 compound. In the incommensurate phase it is predicted that the superlattic peaks should be power law singularities of the form $(Q - Q_n)^{-2 + x_n}$ where $x_n = \frac{2n^2}{49}$ and n is the order of the harmonic. To probe these line-shape effects we have carried out a high resolution synchrotron study of a sample of $C_{28}Br_2$ grown "*in situ*". Dramatic changes are indeed seen in the intensities and shapes of the successive harmonic peaks. Quantitative analysis is currently underway to compare the data critically with the theory.

We have synthesized and studied stage 1 KH_g - GIC.[2] From *in situ* x-ray studies we have learned that the compound forms by successive intercalation of K and then, after several hours, further intercalation of K and H_g to yield the final KH_g - GIC compound. We find a 2 x 2RO hexagonal network for the KH_g.

5.2 Smectic Liquid Crystals

Liquid crystals are made up of rod-like molecules. In the nematic phase the axes of the molecules align parallel to each other but the center of mass of the molecules are still randomly distributed so that one has a pure fluid structure factor. In the smectic A and C phases a one-dimensional sinusoidal density wave is set up either along (A) or at an angle (C) to the molecular axis. Thus, these smectics are like solids in one direction and fluids in the other two. These systems exhibit particularly interesting phase transitions which present an important challenge to modern theories of critical phenomena. At lower temperatures many liquid crystal materials exhibit more ordered phases such as smectic B, F, and G. These have well-developed in-plane triangular order. If the order is truly long range then the phase is a plastic crystal. Otherwise, the smectic may be a realization of a novel phase of matter labelled a "stacked hexatic" with long range order in the crystalline axes but only short range order in the positions of the molecules. We have recently studied in some detail the smectic phases and phase transitions in a number of materials.[4-6] Special emphasis has been given to multicritical behavior associated with the nematic-smectic A transition.

The nematic-smectic A transition was once thought to be always first order. However, a series of high resolution experiments, including our own, have shown that the opposite is the case and indeed the transition is usually continuous. However, thermodynamic data have suggested that if the temperature range over which the nematic phase is stable is sufficiently small then the nematic-smectic A transition is first order.

By studying the N-A transition in appropriate mixtures it is possible to monitor continuously this crossover from second to first order behavior. The crossover is believed to occur at a special point known as a "tricritical point". At the tricritical point, mean field theory should properly describe the critical behavior. We find that for concentrations near the tricritical point in the series alkoxycyanobiphenyl (NCB) and pentylbenzenethioalkoxybenzoate (n55) new critical behavior is indeed observed with exponents which are at least close to the mean field values; there are some subtle, but real, discrepancies which require an extension of the theory.

We have carried out an extensive high resolution x-ray scattering study of the nematic-smectic A(N-S_A) and reentrant nematic-smectic A(RN-S_A) phase transition behavior in mixtures of octyloxycyanobiphenyl (80CB) and hexyloxycyanobiphenyl (60CB). The smectic A phase boundary is found to be parabolic in the temperature-concentration plane with a median temperature T_M = 38.06°C and a critical concentration y_o = 0.427; here y is the 60CB:80CB molecular ratio. Detailed studies of the smectic fluctuations in the nematic phase are reported for y = 0.33, 0.413, 0.420, 0.429, 0.440 and 0.443. The first three concentrations exhibit N-S_A and RN-S_A transitions whereas in the latter three samples with decreasing temperature the smectic correlation lengths and susceptibility exhibit maxima at T_M and then decrease with a further decrease in temperature.

The data are analysed using an extension of the Pershan-Prost optimal density theory. All of the data are well-described by the phenomenological theory; the critical exponents so-obtained are $\nu_{\parallel}$ = 0.76 ± 0.03, $\nu_{\perp}$ = 0.62 ± 0.05 and γ = 1.49 ± 0.07. These agree quantitatively with values obtained in single layer materials with comparable nematic ranges; thus the N-S_A and RN-S_A transitions are identical in character to conventional N-S_A transitions provided that one includes the crossover effects inherent in the parabolic phase boundary. Studies of the in-plane fluid structure factor in the N, S_A and RN phases show that the mean molecular spacings and positional correlations are closely similar to those in single layer materials; in each phase the structure factor is well described by a circularly-averaged Lorentzian with a correlation length of 6.9 Å . These results argue strongly against pairing models for the reentrant behavior. Our current preference is for models based on competing order parameters which are required to describe the varied behavior observed in other polar materials.

5.3 Structures and Transitions of Ultra-Thin Rare Gas Crystals

For a number of years we have been studying the structure and transitions of rare gas monolayers on graphite.[7,8] This has yielded new information on the nature of melting in two dimensions and on two dimensional commensurate-incommensurate transitions. We have now begun studying the wetting characteristics of simple atoms and molecules on surfaces. Initial experiments on C_2H_4 on graphite show distinct layering transitions up to three layers and then a continuous evolution of the thickness to macroscopic values; the latter occurs in the liquid phase near the triple point. Initial studies of krypton on graphite indicate that in the solid phase the system grows layer by layer with the stacking of the layers in an fcc sequence even after three layers. Further, high resolution studies of this layer-by-layer growth are underway.

References

1. A. Erbil, A.R. Kortan, R.J. Birgeneau, and M.S. Dresselhaus, in M.S. Dresselhaus, G. Dresselhaus, J.E. Fisher, and M.J. Moran, (Eds.) Intercalated Graphite, Materials Research Society Symposia Proceedings, Vol. 20, (North-Holland Elsevier, New York 1982) p. 21.
2. A. Erbil, G. Timp, A.R. Kortan, R.J. Birgeneau, and M.S. Dresselhaus, Synthetic Metals 7, 273 (1983).
3. A. Erbil, A.R. Kortan, R.J. Birgeneau, and M.S. Dresselhaus, Phys. Rev. B 28, 6329 (1983).
4. B.M. Ocko, R.J. Birgeneau, J.D. Litster, and M.E. Neubert, Phys. Rev. Lett. 52, 208 (1984).
5. B.M. Ocko, A.R. Kortan, R.J. Birgeneau, and J.W. Goodby, J. Physique 45, 113 (1984).
6. A.R. Kortan, H. von Känel, R.J. Birgeneau, and J.D. Litster, J. Physique 45 (1984).
7. P.A. Heiney, P.W. Stephens, R.J. Birgeneau, P.M. Horn, and D.E. Moncton, Phys. Rev. B 28, 6416 (1983).
8. P.W. Stephens, P.A. Heiney, R.J. Birgeneau, P.M. Horn, D.E. Moncton, and G.S. Brown, Phys. Rev. B. 29, 3512 (1984).

6. Phase Transitions in Chemisorbed Systems

Academic and Research Staff

Prof. A.N. Berker, Dr. D. Blankschtein, Dr. J.O. Indekeu, Dr. M. Kardar, Dr. M. Kaufman

Graduate Students

D. Andelman, R.G. Caflisch, S.R. McKay

Undergraduate Students

R.E. Goldstein, R.J. Lenk

Microscopic theories are developed for condensed matter systems undergoing phase transitions. Phase diagrams and other macroscopic properties are deduced using renormalization-group techniques and other rigorous or approximate methods of statistical mechanics.

6.1 Phase Diagrams for Oxygen on Ni(100), SnTe, and Uranium Pnictides

Joint Services Electronics Program (Contract DAAG29-83-K-0003)

Robert G. Caflisch, A. Nihat Berker

We have completed[1] our renormalization-group theory of epitaxial adsorption onto a square substrate, with nearest-neighbor exclusion, second- and third-neighbor pair and trio interactions. Our global phase diagram study has led us to raise, for the first time, the possibility of two distinct 2x2 overlayer phases, characterized respectively by uniaxial and biaxial symmetry-breaking. The latter phase is novel, having four different sublattice coverages. Our phase diagrams exhibit 2x1, 2x2, and $\sqrt{2} \times \sqrt{2}$ ordered phases and a disordered phase. Thus, all three ordered structures observed with oxygen on nickel (100) are obtained within the same phase diagram in the coverage and temperature variables. One of these, the 2x1 phase, has a high entropy content, appears only at intermediate temperatures, and cannot be seen by classical theories. Other cross-sections of the global phase diagram, summing to six distinct topologies, may be applicable to chemisorbates such as oxygen, sulfur, selenium, or tellurium, on substrates such as nickel, copper, tungsten, or platinum (100). First- and second-order phase transition lines are punctuated by tricritical, critical-end, bicritical, and tetracritical points. Reentrant tricriticality, another new phenomenon, is found, yielding closed-loop coexistence regions.

To obtain the above results, we developed the renormalization-group treatment of competing atomic further-neighbor interactions. It now appears that our approach can yield the phase diagrams of a variety of other, bulk, condensed matter systems. Specifically, two such studies have been

initiated. First, the local structural degrees of freedom of the compound SnTe have been mapped onto an Ashkin-Teller model with thermal vacancies. This mapping already explains in simple energy-entropy terms the rhombohedral transition of this material. This project is pursued in collaboration with K. Rabe and J.D. Joannopoulos. *Ab initio* total energy calculations will be combined[2] with renormalization-group statistical mechanics. In another project, in collaboration with P. Erdös, the magnetic orderings of uranium pnictides are explored via our prefacing/renormalization-group mappings.

6.2 Metal-Insulator Transitions and the Spin-3/2 Ising Model

Joint Services Electronics Program (Contract DAAG29-83-K-0003)
Miron Kaufman, A. Nihat Berker

The metal-insulator transition has traditionally been described by the Hubbard Hamiltonian which includes a hopping term favoring the metal state and a Coulomb interaction. The solution of this model in $d>1$ dimension is quite difficult. We have initiated a study in which (1) the Hubbard Hamiltonian is mapped, approximately, onto a four-state classical model, and (2) the latter, which is a generalized spin-3/2 Ising model, is subjected to a position-space renormalization-group analysis. Our preliminary work indicates a phase diagram with metal, antiferromagnetic insulator, and paramagnetic insulator phases, in a critical end-point topology.

6.3 Phase Transitions in Potts Models with Broken Translational Invariance

Joint Services Electronics Program (Contract DAAG29-83-K-0003)
David Andelman, Daniel Blankschtein, Mehran Kardar, Miron Kaufman, A. Nihat Berker

We have established in our previous works that surface phase transitions can be modeled, in detail, by Potts models. During the last year, the critical amplitudes of the free energy of these models were studied[3,4] as a function of the number q of local states, in two dimensions and on the exactly solvable diamond hierarchical lattice.[5] Numerical renormalization-group and analytical duality-transformation techniques were employed. It was found that this amplitude diverges at an infinite number of values q_n, introducing logarithmic corrections to the critical singularities. In each interval (q_n, q_{n+1}), there is a value $\hat{q}_n$ where the amplitude vanishes, changing the quantitative nature of the singularity. Possible implications to the gelation and vulcanization of polymers were discussed. Other works on exactly solvable Hamiltonians have included the crossover to behavior imposed by long-range interactions, with interesting multicritical consequences,[6,12] and the construction of a sequence of hierarchical lattices which converge to ordinary Bravais lattices.[7]

We had also noted[8] that in adsorbed systems, substrate imperfections generate quenched random

fields, with strong effects on phase transition behavior. Thus, Potts models were studied[9] in the presence of random fields, which locally prefer alignment into any one of the q states. In d dimensions, the transition is expected to become first order for $q>q_c(d)$. As in the non-random case, mean-field theory gives $q_c(d) = 2$ for all d. Fluctuations are argued to shift the non-random value, $q_c^0(d)$, into a significantly higher value, $q_c(d)$. Accordingly, for $q_c^0(d)<q<q_c(d)$ quenched impurities are expected to turn the first-order transition into a second-order one. In three dimensions, this probably includes the experimentally realizable cases q = 3: diluted $SrTiO_3$ under a [111] uniaxial stress and q = 4: diluted NdSb, NdAs, CeAs, etc. under a [111] magnetic field.

We have also discovered[10] that the effective dimensional lowering caused by random fields can be simulated by another means of breaking translational invariance. In a rigorous statistical mechanical treatment,[10] the translational invariance of equivalent-neighbor Potts models was removed by introducing a Cayley-tree interaction K. For a range of K, the first-order transition persists, until a novel tricritical point, followed by continuously evolving second-order transitions. This is analogous to a continuous dimensional lowering.

6.4 Multicritical Phenomena in Cubic Symmetry Systems

Joint Services Electronics Program (Contract DAAG29-83-K-0003)
Robert G. Caflisch, Daniel Blankschtein

Phase transitions which are predicted to be first-order by the classical Landau theory can in fact be driven second-order by critical fluctuations. This fluctuation-induced criticality occurs in cubic systems which are almost tricritical. Application of symmetry-breaking perturbations suppresses fluctuations and may restore first-order behavior via new types of tricritical points. We are currently studying the effects of uniaxial quadratic symmetry-breaking perturbations on a three-component Hamiltonian with cubic symmetry present up to sixth order. We find that even at the mean-field level the competitions between the quadratic, fourth-order, and sixth-order anisotropies produce novel bicritical and tetracritical-like phase diagrams. Phases of the type [1,0,0], and [1,1,1], and [x,x,z] are encountered. Fluctuations are now analyzed with renormalization-group theory, and new multicritical phenomena are expected. The cubic phase diagrams are realizable experimentally by applying uniaxial stresses or magnetic fields to systems exhibiting structural or magnetic phase transitions, such as $KMnF_3$, $RbCaF_3$, $BaTiO_3$, MnO, TbP, etc.

6.5 Hydrogen-Bonding in Polymer Solutions: Reentrant Miscibility and Conformational Equilibria

Joint Services Electronics Program (Contract DAAG29-83-K-0003)
Raymond F. Goldstein

Phase Transitions in Chemisorbed Systems

A theory is presented[11] which describes reentrant miscibility transitions[13] in solutions of polar polymers. These transitions are driven by orientationally specific interactions such as hydrogen bonds. The theory is within the context of the Flory-Higgins approach to solubility transitions. Pair interactions are controlled by a two-level equilibrium (bonded and non-bonded states) with appropriate energy and entropy terms. The results are in qualitative agreement with experiments on systems such as polyethylene oxide + water.

Correspondences are shown[11] between the microscopics of polymer conformational transitions (e.g., helix-coil transitions of polypeptides) and solubility phase transitions. Experiments are proposed to elucidate the roles of hydrogen bonding in molecular and polymer mixtures, to investigate new types of solubility transitions in polymer solutions, and to determine the interplay of conformational and solubility equilibria.

References

1. R.G. Caflisch and A.N. Berker, "Oxygen Chemisorbed on Ni(100): Renormalization-Group Study of the Global Phase Diagram," Phys. Rev. B 29, 1279 (1984).
2. J. Ihm, D.H. Lee, J.D. Joannopoulos, and A.N. Berker, "Study of High Order Reconstructions of the Si(100) Surface," J. Vac. Sci. Technol. B 1, 705 (1983).
3. M. Kaufman and D. Andelman, "Critical Amplitude of the Potts Model: Zeroes and Divergences," Phys. Rev. B 29, 4010 (1984).
4. M. Kaufman, "Duality and Potts Critical Amplitudes in a Class of Hierarchical Lattices," Phys. Rev. B, accepted for publication.
5. A.N. Berker and S. Ostlund, J. Phys. C 12, 4961 (1979).
6. M. Kardar, "Crossover to Equivalent-Neighbor Multicritical Behavior in Arbitrary Dimensions," Phys. Rev. B 28, 244 (1983).
7. M. Kaufman and K.K. Mon, "Realizable Renormalization Group and Finite-Size Scaling," Phys. Rev. B 29, 1451 (1984).
8. R.J. Birgeneau and A.N. Berker, Phys. Rev. B 26, 3751 (1982).
9. D. Blankschtein, Y. Shapir, and A. Aharony, "Potts Models in Random Fields," Phys. Rev. B 29, 1263 (1984).
10. M. Kaufman and M. Kardar, "Pseudo-Dimensional -Variation and Tricriticality of Potts Models by Hierarchical Breaking of Translational Invariance," Phys. Rev. Lett., submitted for publication.
11. R.E. Goldstein, "Hydrogen Bonding in Polymer Solutions: Reentrant Miscibility and Conformational Equilibria," J. Chem. Phys., accepted for publication.
12. M. Kardar, "Ordering Phenomena under Competing Interactions in Adsorbed Layers and in Spin Systems," Ph.D. Thesis, Department of Phyics, M.I.T., 1983.
13. R.E. Goldstein, "Molecular Theory of Reentrant Phase Transitions in Binary Liquid Mixtures," S.B. Thesis, Department of Physics, M.I.T., 1983.

7. Optics and Quantum Electronics

A. Nonlinear Phenomena

Academic and Research Staff

Prof. C.G. Fonstad, Prof. H.A. Haus, Prof. E.P. Ippen, Prof. S. Kawakami[1], Dr. Y. Yamamoto, H. Stram, E. Wintner

Graduate Students

N. Dagli, J. Fujimoto, C. Gabriel, M.N. Islam, S.H. Kim, M. Kuznetsov, L. Molter-Orr, M. Stix, N. Whitaker, A.M. Weiner, G.E. Williams, J. Zayhowski

7.1 Picosecond Optical Signal-Sampling Device

National Science Foundation (Grants ECS82-11650 and ECS83-10718)
Hermann A. Haus

The goal of the research is to develop prototype optical waveguide devices that operate at rates of many tens of Gigahertz. A 20 GHz Mach-Zehnder waveguide interferometric sampler operating at λ = 6328 Å in $LiNbO_3$ has been built and tested.[1,2] Since the power throughput of the device was too small to permit direct detection of the output samples by Second Harmonic Generation, the operation of the device was monitored by observing the optical spectrum of the output. The observed spectrum was consistent with the conclusion that the sampler produced 19 ps FWHM pulses with a 97 percent depth of modulation.

Construction of Mach-Zehnder waveguide interferometers can be achieved either by the use of waveguide Y's or by means of sections of straight coupled waveguides.[3] To construct compact devices, the Y-section must be made as short as possible. A typical length is of the order of a few millimeters. Shortening of the structure leads to increased radiation loss. The optimization of a design requires knowledge of the radiation loss produced in the waveguide Y's. We have carried out such a study with a new approach, the socalled "Volume Current Method".[4,5] Previous analyses of radiation loss in bent fibers cannot be used because they require matching of the radiation field solution to the nearfield surrounding the structure over a coordinate surface separating the two regions. Only few systems have the requisite degree of symmetry.

Since much of our device work uses the Mach-Zehnder waveguide interferometer, ways of constructing it and fine-tuning it after fabrication are of special interest. Kogelnik and Schmidt have

[1] Visiting Professor

shown that a coupled waveguide structure can be adjusted after fabrication via $\Delta\beta$ coupler principle. It is of interest to extend this principle to waveguide structures containing more than two waveguides, such as the waveguide Y constructed of three coupled waveguides.[3] We have shown that the principle is extendable and a $\Delta\beta$-type three-waveguide coupler is currently in the testing stage.

References

1. H.A. Haus and L. Molter-Orr, "Picosecond Optical Waveguide Devices," Proceedings of the Fifteenth National Science Foundation Grantee-User Meeting, M.I.T., Cambridge, Massachusetts, June 1-3, 1983.
2. H.A. Haus and L. Molter-Orr, "Coupled Multiple Waveguide Systems," IEEE J. Quantum Electron. QE-19, 5, 840-844, (1983).
3. H.A. Haus and C.G. Fonstad, "Three-Waveguide Couplers for Improved Sampling and Filtering," IEEE J. Quantum Electron. QE-17, 12, 2321-2325 (1981).
4. M. Kuznetsov and H.A. Haus, "Radiation Loss in Dielectric Waveguide Structures by the Volume Current Method," IEEE. J. Quantum Electron., accepted for publication.
5. H.A. Haus and M. Kuznetsov, "Radiation Loss of Coupled Waveguide Structures," IOOC'83, Tokyo, Japan, June 27-30, 1983.

7.2 Devices for High-Rate Optical Communications

National Science Foundation (Grant ECS83-05448)

Clifton G. Fonstad, Hermann A. Haus

(c) The Waveguide Lens

Recently, a great deal of attention has been devoted to laser diode arrays that emit coherently, so that their entire output power can be focused into a diffraction limited spot.[1-3] One may ask the question whether it is possible to devise a passive, coupled waveguide system that would be capable of combining the power of the array into one "output" waveguide. Our theory of coupled waveguides is well adapted to provide the answer to such a question. We found that it is possible to combine all the power entering a N-th order planar coupled waveguide array (N is odd) into the center waveguide using axially uniform guides by proper choice of waveguide coupling and detuning in the following two cases.[4]

(a) The input excitations are all equal in magnitude and in phase.

(b) The input excitations are all equal in magnitude and alternate in phase by π.

The latter case is of most interest because diode arrays prefer this mode of operation. We plan to test the idea in a waveguide array fabricated in $LiNbO_3$.

References

1. D.R. Scifres, R.D. Burnham, and W. Streifer, "Phase Locked Semiconductor Laser Array," Appl. Phys. Lett. 33, 1015-1017 (1978).
2. D.R. Scifres, W. Streifer, and R.D. Burnham, "Experimental and Analytic Studies of Coupled

Multiple Strip Diode Lasers," IEEE J. Quantum Electron. QE-15, 917-922 (1979).
3. W.T. Tsang, R.A. Logan, and R.P. Salathe, "A Densely Packed Monolithic Linear Array of GaAs-$Al_xGa_{1-x}As$ Strip Buried Heterostructure Laser," Appl. Phys. Lett. 34, 162-165 (1979).
4. H.A. Haus, L. Molter-Orr, and F.J. Leonberger, "A Multiple Waveguide Lens," CLEO'84, Anaheim, California, June 19-22, 1984, submitted for presentation.

7.3 Picosecond Optics

Joint Services Electronics Program (Contract DAAG29-83-K-0003)
Hermann A. Haus

All Optical Logic Gates

Waveguide optics, or the more ambitiously named Integrated Optics, will not compete seriously with integrated electronics in all those functions that can be performed electronically. Optical devices have a more demanding topology (e.g., optical waveguides have transverse dimensions of several optical wavelengths and do not permit sharp bends) and higher power requirements. However, waveguide optics can perform certain signal processing functions at greater speeds than electronic circuits. High speed signal processing is one application in which waveguide optics can seriously compete with electronics. Another function of integrated optics may become the direct processing of optical signals, obviating the need for conversion to an electrical signal, if the signal processing function can be performed conveniently and at low optical power levels.

In the last progress report we described a universal optical logic gate which was fabricated in $LiNbO_3$ to demonstrate its operation as an all-optical logic gate. The optical nonlinearity in $LiNbO_3$, the n_2 coefficient, was measured in our experiment[1] and was found to be about two orders of magnitude smaller than the values quoted for GaAs. The optical power available in the experiment was too small to demonstrate logic operation of the device; instead we demonstrated the operation of the device as an all-optical waveguide modulator operating on a picosecond time scale.

This experience shifted our interest to the fabrication of GaAs, GaAlAs waveguides. In cooperation with Dr. F.J. Leonberger of Lincoln Laboratory we succeeded in fabricating high quality waveguides with a ridge on top of a guiding layer providing transverse optical confinement.

The waveguides are presently used in an experiment which will determine $\chi^{(3)}$ in a waveguide structure. The value of $\chi^{(3)}$ in GaAs has been quoted differently by three different researchers.[2-4] It is possible that the discrepancy between these reports is due to different background doping and thus different free-carrier contributions to the nonlinearity. Our waveguides are constructed in material with well determined doping characteristics.

Another intriguing possibility for the design of fast logic gates with low-power drives has emerged recently. The quantum well, room temperature exciton absorption line has been modulated with

fields of the order of $6 \times 10^4 V/cm$.[5] The excitons were not destroyed with fields of this magnitude. This raises the possibility of removing by fast drift the carriers generated in nonlinear optical interactions and thus speeding up device operation into the 100 Gbit range. The exciton nonlinearity is enormous, so that the logic gate could be operated at power levels available from laser diodes. We are currently investigating the feasibility of such a device.

References

1. A. Lattes, H.A. Haus, F.J. Leonberger, and E.P. Ippen, "An Ultrafast All-Optical Gate," IEEE J. Quantum Electron., November 1983.
2. S.Y. Yuen, "Fast Relaxing Absorptive Nonlinear Refraction in Superlattices," Appl. Phys. Lett. 43, 813 (1983).
3. Y.J. Chen and G.M. Carter, "Measurement of Third Order Nonlinear Susceptibilities by Surface Plasmons," Appl. Phys. Lett. 41, 307 (1982).
4. J.J. Wynne, "Optical Third-Order Mixing in GaAs, Ge, Si, and InAs," Phys. Rev. 178, 1295 (1969).
5. T.H. Wood, C.A. Burns, D.A.B. Miller, D.S. Chemla, T.C. Damen, A.C. Gossard, and W. Wiegman, "High-Speed Optical Modulation with GaAs GaAlAs Quantum Wells," to be published.

Theory of the Soliton Laser

Recently, Dr. Mollenauer and Dr. Stolen at Bell Laboratories succeeded in operating a soliton laser.[1] This laser contains a synchronously pumped laser as its gain section and a nonlinear fiber as the pulse-forming section. The novel feature of this structure is that the pulse width is governed by the width of the characteristic soliton formed in the fiber and less by the shaping of the pulse in the laser section as is the case in conventional modelocked lasers. In this way pulse-widths can be achieved (0.29 ps) that are much shorter than the pulsewidths achievable with the synchronously modelocked laser by itself.

We have been encouraged by Dr. Mollenauer and Dr. Stolen to develop the theory of the soliton laser because our previous work on modelocking bears on the problem. Indeed, the system can be described as a modelocked laser locked in turn to an injection signal consisting of a stream of pulses. We have succeeded in developing the steady state theory of the laser. One puzzling feature of the laser, namely its tendency of operating in the higher order, N = 2, soliton is well explained by the theory.

The temporal shape of the output pulse is predicted and the relation between fiber length and pulsewidth is established. The predictions of the theory will be tested at Bell Laboratories.

References

1. H.A. Haus and M.N. Islam, "Theory of the Soliton Laser," IQEC'84, Anaheim, California, June 18-21, 1984.

7.4 Ultrashort Pulse Formation

National Science Foundation (Grant ECS80-20639)
Joint Services Electronics Program (Contract DAAG 29-83-K-0003)
Erich P. Ippen

Considerable progress is still being made in the generation of ultrashort pulses. This year we report the production and measurement of pulses as short as 16 femtoseconds. These pulses, with a center wavelength of about 620 nm, are comprised of only 8 optical periods and are the shortest pulses ever generated.[1]

Initially, in our experiments, pulses of 55 fsec duration are generated by a colliding-pulse-modelocked (CPM) ring dye oscillator. Single pulses from this oscillator are selected and amplified at a 10 Hz rate by the first two stages of a high-power femtosecond dye amplifier chain. After spatial filtering and compensation of dispersion with a grating-pair, the amplified pulses of about 65 fsec are coupled into an 8 mm length of optical fiber. Following spectral broadening in the fiber, the pulses are compressed by the final factor of four with a second grating pair. Measurement is performed by noncollinear autocorrelation in a 0.1 mm crystal of KDP.

During this period we have also achieved cw and modelocked operation of a syncronously-pumped ZnCdSe platelet laser. Pulses of 10 psec duration are generated at a wavelength of 482 nm, the shortest wavelength operation achieved to data with a semiconductor laser.[2]

Work has also continued on improving our theoretical understanding of pulse generation[3] and propagation, especially in the presence of dielectric mirror and material group velocity dispersion. Investigations of fiber pulse compression for the wavelength range 800-900 nm and of semiconductor diode laser modelocking at 1.3 μm have been initiated.

References

1. J.G. Fujimoto, A.M. Weiner, and E.P. Ippen, "Generation and Measurement of Optical Pulses as Short as 16 Femtoseconds," Appl. Phys. Lett., to be published.
2. J. Yorsz, S.G. Shevel, and E.P. Ippen," Optically Pumped $Zn_xCd_{1-x}S$ Platelet Lasers," Opt. Commun. 48, 2 (1983).
3. M. Stix and E.P. Ippen, "Pulse Shaping in Passively Mode-Locked Ring Dye Lasers," IEEE J. of Quantum Electron. QE-19, 520 (1983).

7.5 Femtosecond Laser System

Joint Services Electronics Program (Contract DAAG29-83-K-0003)
Erich P. Ippen

Work continues on the development of femtosecond optical techniques for broadband

time-resolved spectroscopy and on their application to specific problems.

Our femtosecond oscillator-amplifier system, the construction of which was described in last year's report, has been further improved by optimizing the pumping configuration and dye concentration in each stage and by improving the temporal stability of the Q-switched Nd:YAG pump laser. Present characteristics are: 2nd stage — 5 μJ, 65 fsec; 3rd stage — 50 μJ, 65 fsec; 4th stage — 250 μJ, 70 fsec. New, in-house developed software routines for data recording and analysis have increased sensitivity and accuracy in spectroscopic applications.

An especially interesting area of application is the study of relaxation processes in optically excited semiconductors. This year we investigated the phenomenon of exciton screening by free carriers in the direct-gap II-VI semiconductor CdSe.[1,2] Our experiments show that, following above band-gap excitation of free carriers, the free-exciton resonance, which occurs about 15 meV below the bandgap at 77 K, broadens and loses amplitude without shifting wavelength. This screening, which was observed by dynamic spectral changes of sample reflectivity, occurred on a time-scale of 100 fsec and was effectively complete for excitation densities greater than $2 \times 10^{17}/cm^3$. Recovery of the exciton peak was also studied on the longer time-scale of several hundred picoseconds.

Preliminary results have also been obtained (in collaboration with N. Bloembergen of Harvard and J.-M. Liu of GTE) from experiments designed to study electron-photon coupling in metals. Electron heating by intense femtosecond optical pulses is being observed by multi-photon photoelectron emission.

References

1. J.G. Fujimoto, S.G. Shevel, and E.P. Ippen, "Femtosecond Time-Resolved Exciton Dynamics in CdSe," Sol. St. Commun. 49, 605 (1984).
2. E. Wintner, J.G. Fujimoto, and E.P. Ippen, "Picosecond and Femtosecond Diagnostics of Semiconductors," Proc. S.P.I.E., 452, 142 (1984).

7.6 Parametric Scattering with Femtosecond Pulses

Joint Services Electronics Program (Contract DAAG29-83-K-0003)
Erich P. Ippen

Transient four-wave mixing is being investigated as a means for generating shorter pulses and as a means for studying polarization dephasing in liquids and solids. Several important advances have been made within the past year.

By focusing two intense pulses into a solution of the dye malachite green we have obtained relatively high-power, parametrically scattered pulses with durations as short as 37 fsec.[1] The durations of the scattered pulses are observed to depend strongly on the time delay between the two incident pulses; and we have shown theoretically that this dependence can be used to obtain

information about the actual pulse shapes as well as the medium response time.

For studies of femtosecond dephasing, we have introduced a novel, multiple-pulse scattering technique[2] that offers several important advantages over previous two-pulse methods. These include i) separation of transverse relaxation (T_2) effects from those due to longitudinal (T_1) relaxation; ii) ready availability of an experimentally determinable ($T_2 = 0$) reference curve for accurate deconvolution of data; and iii) a clear distinction between scattering from homogeneously and inhomogeneously broadened transitions. With the first experiments using this technique we have observed dephasing of the electronic polarization in the dye nile blue to occur in less than 20 fsec.

References

1. J.G. Fujimoto and E.P. Ippen, "Transient Four-Wave Mixing and Optical Pulse Compression in the Femtosecond Regime," Opt. Lett. 8, 446 (1983).
2. A.M. Weiner and E.P. Ippen, "Novel Transient Scattering Technique for Femtosecond Dephasing Measurements," Opt. Lett. 9, 53 (1984).

7.7 Near-IR Diagnostics

National Science Foundation (Grant ECS80-20639)
Joint Services Electronics Program (Contract DAAG29-83-K-0003)
Erich P. Ippen

A cavity-dumped, synchronously-pumped dye laser has been developed for tunable operation in the range 760-900 nm. Picosecond pulses from this system are being used for pump-probe studies of active, semiconductor diode laser devices. Effort is also presently directed at achieving sub-picosecond pulse durations in this wavelength regime by compression techniques using polarization preserving optical fibers. For pump-probe studies in optical waveguides, we have demonstrated an experimental technique for separating, and temporally resolving, the collinear pump and probe beams following transmission through a guide. The method utilizes a synchronized, third pulse to gate the desired probe pulse by sum-frequency up-conversion. In preliminary experiments we have resolved and monitored multiple reflections occuring in an uncoated diode. Gain saturation by successive pulses and group velocity delays are easily observed.

7.8 Quaternary (InGaAsP) Diagnostics

National Science Foundation (Grant ECS80-20639)
Joint Services Electronics Program (Contract DAAG29-83-K-0003)
Erich P. Ippen

Under high excitation densities, carrier lifetimes in semiconductors can be shortened dramatically by Auger recombination processes. Loss of carriers by such processes is now thought to be a

contributing factor to the high threshold current densities (relative to GaAlAs) and strong temperature dependence of long wavelength (InGaAsP/InP) laser diodes. Improved understanding of Auger recombination is therefore important to future device development.

Most of the existing experimental data on the Auger coefficients of interest have been derived from characteristics of existing laser devices. In our experiments this year we have used a direct, picosecond pump-probe technique to both excite carriers and monitor their recovery dynamics. Thin film samples of three different compositions (bandgaps: 1.3, 1.55, and 1.65 μm) were studied with 80 psec pulses from a cw modelocked Nd:YAG laser. Accurate evaluation of the data was achieved by developing a computer model which relates the observed absorption bleaching to carrier density and takes into account spatial averaging effects as well as temporal convolution of the nonlinear response with the laser pulses. The effective Auger coefficients, determined as curve fitting parameters, were found to be A(1.3 μm) = $1.5 \times 10^{-29} cm^6/s$, A (1.55 μm) = $7.5 \times 10^{-29} cm^6/s$ and A(1.65 μm) = 9.8×10^{-29} cm^6/s. These experimental values are lower than those calculated theoretically by previous authors and exhibit a wavelength dependence that is stronger than that observed by device threshold measurements.

Our present efforts are directed at trying to separate nonlinear radiative effects from the nonradiative effects by time-resolved fluorescence and photo-acoustic spectroscopy. Development of a TI-defect color center laser for extending our probing capability to shorter pulses and longer wavelengths is also underway.

References

1. E. Wintner and E.P. Ippen, "Nonlinear Carrier Dynamics in $Ga_xIn_{1-x}As_yP_{1-y}$ Compounds," Appl. Phys. Lett., to be published.

B. Grating Structures

Academic and Research Staff

Prof. H.A. Haus, Dr. J. Melngailis, D.-P. Chen

Graduate Students

E.M. Garber, M.N. Islam

7.9 Surface Acoustic Wave Grating Structures

National Science Foundation (Grant ECS82-11650)

Hermann A. Haus, John Melngailis

The goal of this research is to develop a better understanding of SAW grating structures for mode control, suppression of spurious and improved transducer design.

In the design of a unidirectional SAW transducer, C. Hartmann and P. V. Wright discovered[1] that the wave excited by the transducer traveled in a direction opposite to the one predicted by theory.[2,3] This prompted us to look into the theory of SAW excitation by metal strips. It became clear in the course of the investigation that a reliable theory could be used to design reflection-free metal strips. This in turn would obviate the necessity of splitting the metal fingers, a current practice to reduce reflection with an attendant doubling of the demand on fabrication tolerances and an increase in finger loss.

We have developed a comprehensive theory of metal strip gratings and transducers based solely on a previously utilized variational principle. The theory shows the possibility of constructing metal strips with zero reflectivity by proper balancing of the mass-loading, stress- and piezoelectric effects of the metal strip. The theory derives all pertinent grating- and transducer-parameters in terms of the material constants and geometry. The mistake in the previous theory was corrected so that the behavior of unidirectional transducers is now predicted correctly.

The design of SAW filters with low sidelobes in their transfer characteristics is difficult to implement with apodization and uniform spacing. The constraint of uniform spacing leads to small tap weights which in turn produces undesirable effects. We have developed a filter design that maintains uniform overlap. The spectral weighting is accomplished with variation of the finger spacing. The parameters are selected by a quasi-Newton optimization technique.[4]

Many years ago we published a theory of transverse modes in grating structures.[5] The predicted mode structure was rather peculiar in that the mode pattern of a particular mode could acquire, with increasing frequency, additional maxima and minima. The experimental evidence on higher order transverse modes is very limited[6,7] and none of the published experiments followed the mode pattern

over a sufficient frequency range to confirm the theoretical predictions. We have made measurements with a laser probe on the mode patterns of a SAW resonator with a large spacing between the grating reflectors so that many resonant modes occurred within the stopband (reflection-band) of the grating. The experiments confirmed the predicted mode pattern behavior.

References

1. C. Hartmann and P.V. Wright, private communication.
2. S. Datta and B.J. Hunsinger, "First Order Reflection Coefficient of Surface Acoustic Waves from Thin-Strip Overlays," J. Appl. Phys. 50, 9, 5661-5665 (1979).
3. S. Datta and B.J. Hunsinger, "An Analytical Theory for the Scattering of Surface Acoustic Waves by a Single Electrode in a Periodic Array on a Piezoelectric Substrate," J. Appl. Phys. 51, 9, 4817-4823 (1980).
4. E. Garber and H.A. Haus, "Synthesis of High Performance Compact SAW Filters with Nonuniformly Spaced Fingers," 1983 IEEE Ultrasonics Symposium, Atlanta, Georgia, October 31-November 2, 1983.
5. H.A. Haus and K.L. Wang, "Modes of Grating Waveguide," J. Appl. Phys. 49, 3, 1061-1069 (1978).
6. L.A. Coldren, H.A. Haus, and K.L. Wang, "Experimental Verification of Mode Shape in SAW Grating Resonators," Electron. Lett. 13, 642-644, October 1977.
7. W.J. Tanski and N.D. Wittels, "SEM Observations of SAW Resonator Transverse Modes," Appl. Phys. Lett. 34, 156-157, May 1979.

8. Quantum Optics and Photonics

Academic and Research Staff

Prof. S. Ezekiel, Prof. B.R. Mollow, J. Kierstead

Graduate Students

J.-M. Chanty, D. DiFillipo, P.R. Hemmer, S.H. Jain, R.E. Meyer, B.W. Peuse, D.R. Ponikvar, M.G. Prentiss, G.A. Sanders, R.E. Tench, F. Zarinetchi

8.1 Measurement of Fresnel-Drag in Moving Media Using a Ring Resonator Technique

U.S. Air Force Geophysics Laboratory (Contract F19628-70-C-0082)
Joint Services Electronics Program (Contract DAAG29-83-K-0003)
Glen A. Sanders, John Kierstead, Shaoul Ezekiel

It has been known for many years that the observed velocity of light in a moving medium differs from that in a stationary medium. This effect, namely the Fresnel-drag, was explained by the special theory of relativity. While special relativity has been very accurately tested, no tests of comparable precision can be claimed regarding the theory's predictions for light propagation in moving media.

We have performed careful measurements of the Fresnel-drag in various moving glass media and tested the dependence of the drag coefficient on refractive index and dispersion. A solid medium was used in our experiments to provide a precisely known velocity and index.

Our technique is based on moving a glass plate of known index and dispersion back and forth inside a ring resonator. In this way, any nonreciprocal phase shift induced by the motion of the glass manifests itself as a difference in the resonance frequencies of the cavity for oppositely propagating field directions. The precision measurement of small resonance frequency differences in a ring cavity is described in detail elsewhere in connection with the measurement of nonreciprocal phase shift due to the Sagnac effect.[1]

In order to distinguish the drag effect from various sources of noise, the glass plate was moved sinusoidally at a rate of 5 Hz to enable the use of AC detection techniques. To avoid the effects of multiple reflections inside the glass, the normal of the glass sample was tilted by an angle O with respect to the optical axis of the cavity. In addition the glass plate was anti-reflection coated to reduce cavity losses. The velocity of the glass was determined interferometrically using a stabilized HeNe laser.

Measurements of the Fresnel-drag were repeated for glass samples of different index n and

dispersion $\partial n/\partial\lambda$. In addition, the dependence of the drag on the glass thickness ℓ, the velocity $\vec{v}$, and θ was also measured. Variations of the above parameters provided for fifteen different sets of measurements of the effective Fresnel-drag coefficient α. In each case, the experimental drag coefficient α_e was compared to that predicted by theory α_{th}. Weighting each measurement by its respective error bar gave an average agreement with theory for the fifteen measurements of

$$\frac{\alpha_e - \alpha_{th}}{\alpha_{th}} = 6 \times 10^{-5} + 2.4 \times 10^{-4},$$

which constitutes the most accurate verification of the Fresnel-drag effect thus far.[2] In addition, the confidence of including the dispersion dependence of the drag was improved to approximately 1 part in 130.

References

1. G.A. Sanders, M.G. Prentiss, and S. Ezekiel, Opt. Lett. 6, 569 (1981).
2. H.R. Bilger and W.K. Stowell, Phys. Rev. A 16, 313 (1977).

8.2 Observation of Lineshape Distortion by Raman Induced Focusing

National Science Foundation (Grant PHY82-10369)
Joint Services Electronics Program (Contract DAAG29-83-K-0003)
Robert E. Tench, Shaoul Ezekiel

We have observed strong, spatially dependent lineshape distortion while studying the interaction of two copropagating monochromatic laser fields with a folded, Doppler broadened three level system in I_2 vapor. In our experiment, the pump field is generated by a single mode CW argon laser operating at 5145 Å and the probe field at 5828 Å is generated by a single mode CW dye laser. The pump is resonant with a hyperfine component of the B-X, 43-0 R(15) transition in I_2, while the probe is resonant with the corresponding hyperfine component of the B-X, 43-11 R(15) transition. Copropagating pump and probe fields are ensured by coupling both the pump and the probe beams into a single mode fiber. The combined beams which emerge from the fiber are collimated before passing through a cell containing a few mTorr of I_2 vapor. After the cell, the pump and probe beams are separated by a dielectric filter. Raman induced gain at the probe frequency is measured by amplitude modulating the pump field and synchronously demodulating the detected probe beam. Lineshapes are recorded by holding the pump frequency fixed and scanning the probe frequency.

Figure 8-1(a) shows the observed probe lineshape for a strong pump field (4 W/cm^2) and for a detector size that is large compared to the probe beam diameter. However, when the detector is apertured so that only part of the probe is detected, an asymmetric lineshape is observed; the magnitude and sign of the asymmetry depend on the spatial position of the detector. We attribute this

lineshape distortion to the focusing of the probe beam induced by the nonlinear refractive index generated by the Gaussian pump field in the I_2 vapor. Preliminary calculations are in reasonable agreement with the data.

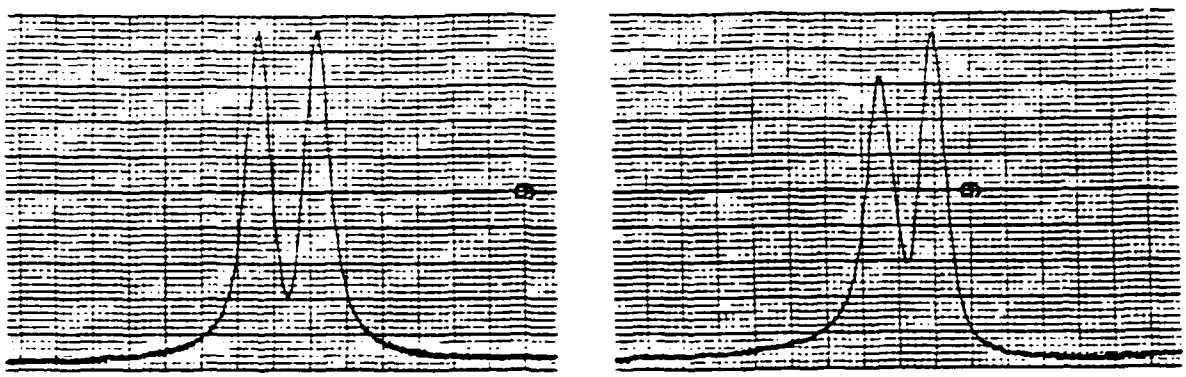

a b

Figure 8-1: Probe Lineshape as a Function of Frequency for a Pump Intensity of 4 W/cm^2:
(a) detector size large than probe beam diameter
(b) detector size smaller than probe beam diameter

Frequency Scale: 560 kHz per large box

This lineshape asymmetry can be eliminated by using a large detector with uniform sensitivity over the detector surface; a highly symmetric laser beam profile; and a uniform number density. In practice, however, it is difficult to satisfy the above conditions, particularly with regard to detector uniformity. Therefore, such lineshape distortion must be considered in precision studies and applications of resonance Raman interactions.

8.3 Performance of a Microwave Clock Based on a Laser Induced Stimulated Raman Interaction

U.S. Air Force - Rome Air Development Center (in collaboration with C.C. Leiby, Jr.)
U.S. Air Force - Rome Air Development Center (Contract F19628-80-C-0077)
National Science Foundation (Grant PHY82-10369)
Philip R. Hemmer, Shaoul Ezekiel

Recent experimental work[1-4] has demonstrated that a microwave oscillator can be stabilized using a

stimulated resonance Raman transition in a sodium atomic beam. This Raman technique is of interest because optical lasers rather than microwaves are used in the interaction and, aside from fundamental interest, the greater flexibility of optical systems may make it possible to eventually develop more stable and more portable atomic clocks.

The experimental setup consists primarily of a single mode dye laser, an acousto optic frequency shifter and a sodium atomic beam. The dye laser is used to generate the pump laser field and is locked to the sodium $3^2S_{1_2}(F = 1) \leftrightarrow 3^2P_{1_2}(F = 2)$ transition, near 5896 Å, via fluorescence induced in the atomic beam. The probe laser field is obtained by shifting a portion of the dye laser output by 1772 MHz using an acousto optic frequency shifter driven with a quartz controlled microwave oscillator. This technique reduces the effects of laser jitter by generating one laser frequency directly from the other so as to correlate the jitters in the two laser fields. To reduce transit time linewidth, Ramsey's method of separated oscillatory fields is employed with interaction region separations up to L = 30 cm producing Ramsey fringes as narrow as 1.3 kHz (FWHM).

To demonstrate the applicability of the stimulated resonance Raman technique to clock development, a microwave oscillator at 1772 MHz was stabilized using a Ramsey fringe of width 2.6 kHz (FWHM), corresponding to L = 15 cm. The measured short term stability of 5.6×10^{-11} for τ = 100 sec compared well with conventional microwave C_s clocks when differences in transition frequency and transit time were taken into consideration.

Present research is concerned primarily with an experimental as well as a theoretical study of error sources and level shifts in this Raman stabilization scheme. An extension of the Raman region to 150 cm will be incorporated in the near future.

In addition, we are setting up a Raman clock based on a simple beam of Cesium and employing semiconductor lasers and fiberoptics technology. Such a Cesium clock may provide a low cost alternative to the present portable cesium clocks using microwave cavities and magnetic state selectors.

References

1. J.E. Thomas, S. Ezekiel, C.C. Leiby, Jr., R.H. Picard, and C.R. Willis, Opt. Lett. 6, 298 (1981).
2. J.E. Thomas, P.R. Hemmer, S. Ezekiel, C.C. Leiby, Jr., R.H. Picard, and C.R. Willis, "Observation of Ramsey Fringes Using a Stimulated Resonance Raman Transition in a Sodium Atomic Beam," Phys. Rev. Lett. 4, 867 (1982).
3. P.R. Hemmer, S. Ezekiel, and C.C. Leiby, Jr., "Stabilization of a Microwave Oscillator Using a Resonance Raman Transition in a Sodium Beam," in W.D. Phillips (Ed.), Laser-Cooled and Trapped Atoms, Nat. Bur. Stand. (U.S.), Special Publication 653, June 1983, p. 47.
4. P.R. Hemmer, S. Ezekiel, and C.C. Leiby, Jr., "Stabilization of a Microwave Oscillation Using a Resonance Raman Transition in a Sodium Beam," Opt. Lett. 8, 440 (1983).

8.4 Fiberoptic Ring Resonator "Gyroscope"

U.S. Air Force - Office of Scientific Research (Contract F49620-82-C-0091)
Joint Services Electronics Program (Contract DAAG29-83-K-0003)
Raymond E. Meyer, John Kierstead, Farhad Zarinetchi, Shaoul Ezekiel

We are investigating the use of an all-fiber ring resonator as a sensor of absolute rotation. The principle here is similar to that of the discrete mirror resonator method that has been under development in our laboratory for several years. In brief, the mirror resonator is simply replaced with a single mode fiber resonator and the input-output coupling is accomplished by means of a fused evanescent wave fiber coupler.[1-2] At present the finesse of the 3 meter fiber resonator is 140. Preliminary data on short-term noise is about 0.5°/hr (r = 1 second) (rms) which is 10 times greater than the shot noise limit in our present setup.

There are a number of problems that are being investigated. These include the backscattering in the fiber, the stability of the polarization alignment and nonlinear phenomena such as the optical Kerr effect.

References

1. R.E. Meyer and S. Ezekiel, "Fiberoptic Resonator Gyroscope," presented at First International Conference on Optical Fiber Sensors, IEE, London, England, April 1983.
2. R.E. Meyer, S. Ezekiel, D.W. Stowe, and V.J. Tekippe, "Passive Fiberoptic Ring Resonator for Rotation Sensing," Opt. Lett. 8, 644 (1983).

8.5 Precision Atomic Beam Studies of Atom-Field Interactions

National Science Foundation (Grant PHY82-10369)
Joint Services Electronics Program (Contract DAAG29-83-K-0003)
Bruce W. Peuse, Mara G. Prentiss, Shaoul Ezekiel

The interaction of radiation with two and three level quantum mechanical systems is of much interest because it involves basic processes. So far we have studied the interaction of 2-level and 3-level sodium atoms with one and also with two monochromatic fields provided by stable, single frequency dye lasers. One laser acts as the pump and interacts primarily with two of the levels. The second laser then probes the absorption between either one of these levels to a third level. In this way we have studied a cascade system, a Vee system, and also an inverted Vee system. In the case of a weak pump field, our probe data was in very good agreement with theoretical calculations. However, when the pump was made very intense the probe data could not be explained by the a.c. stark effect alone. Atomic recoil had to be included in the calculations in order to explain the peculiarities observed.[1-6]

The research at present is primarily concerned with reducing atomic recoil effects and the study of atom–field interaction in non-uniform fields.

References

1. R.E. Tench, B.W. Peuse, P.R. Hemmer, J.E. Thomas, and S. Ezekiel, "Two Laser Raman Difference Techniques Applied to High Precision Spectroscopy," Journal de Physique, Colloque C8, Supplement au n°12, December 1981.
2. P.R. Hemmer, B.W. Peuse, F.Y. Wu, J.E. Thomas, and S. Ezekiel, "Precision Atomic-Beam Studies of Atom-Field Interactions," Opt. Lett. 6, 531 (1981).
3. B.W. Peuse, R.E. Tench, P.R. Hemmer, J.E. Thomas, and S. Ezekiel, "Precision Studies in 3-Level Systems," in A.R.W. McKellar, T. Oka, and B.P. Stoicheff (Eds.), Laser Spectroscopy V (Springer-Verlag 1981) p. 251.
4. B.W. Peuse, M.G. Prentiss, and S. Ezekiel, "Distortion in Atomic Beam Absorption Lineshapes," Journal de Physique, Colloque C8, Supplement au n°12, Tome 42, C8-53, December 1981.
5. B.W. Peuse, M.G. Prentiss, and S. Ezekiel, "Observation of Resonant Light Diffraction by an Atomic Beam," Phys. Rev. Lett. 49, 269 (1982).
6. B.W. Peuse, M.G. Prentiss, and S. Ezekiel, "Elimination of Lineshape Distortion in Laser Absorption Spectroscopy in Atomic Beams," Opt. Lett. 8, 154 (1983).

8.6 Fiber Interferometer "Gyroscope"

U.S. Air Force - Office of Scientific Research (Contract F49620-82-C-0091)
Joint Services Electronics Program (Contract DAAG29-83-K-0003)
David DiFillipo, John Kierstead, Shaoul Ezekiel

The fiberoptic gyroscope has been receiving considerable attention for the past several years. A number of different approaches have been studied, and as these studies progress a number of problems were uncovered.

Our approach employs a 200 m long fiber wound around a 19 cm diameter spool and operated in a closed loop mode. Our measurement technique is based on the use of two acousto-optic frequency shifters placed within the fiber interferometer for providing nonreciprocal phase modulation as well as nonreciprocal frequency offsets needed in closed loop operation. Short-term random drift is about 0.03°/hr for averaging times of 30 seconds which is close to that predicted by the photon shot noise limit in our setup. The long-term performance departs from the photon noise limit and considerable effort is at present directed into the sources of long-term drift. In this connection, we have predicted and observed an intensity-induced nonreciprocity in the fiberoptic gyro. We found that a nonreciprocal phase shift of 1.4×10^{-6} radians can be generated by a one microwatt power difference between the oppositely propagating light beams. Our fiber is 200 m long with a core diameter of 4.5 microns, and wound on a 19 cm diameter spool. The intensity dependent nonreciprocal phase shift, which is attributed to a four wave mixing process in the quartz medium, is equivalent to a rotation rate of 0.2°/hr in the present geometry, and therefore stresses the need for a strict intensity control in precision fiber rotation sensors.[1-3]

Our present effort is in the study of noise sources in a 1 km long interferometer gyro setup that employs evanescent wave fiber couplers. In addition, we are developing techniques of light frequency shifting that would be suitable for fiber gyro application.

References

1. J.L. Davis and S. Ezekiel, "Closed Loop, Low Noise Fiberoptic Rotation Sensor," Opt. Lett. 6, 505 (1981).
2. M.G. Prentiss, J.L. Davis, and S. Ezekiel, "Closed Loop, High Sensitivity Fiber Gyroscope," in S. Ezekiel and H.J. Arditty (Eds.), Fiberoptic Rotation Sensors (Springer-Verlag 1982).
3. S. Ezekiel, J.L. Davis, and R.W. Hellwarth, "Observation of Intensity-Induced Nonreciprocity in a Fiberoptic Gyroscope," Opt. Lett. 7, 457 (1982).

8.7 Long Term Frequency Stabilization of Semiconductor Lasers

U.S. Air Force - Rome Air Development Center (Contract F19628-80-C-0077)

Sudhanshu K. Jain, Shaoul Ezekiel

We are interested in developing techniques for the long term frequency stabilization of semiconductor lasers. This area of research is becoming very important for communication, frequency standards, as well as for sensor applications. We are considering both narrow band and broadband lasers in the wavelength range 0.8 μ–1.5 μ.

9. Optical Spectroscopy of Disordered Materials and X-Ray Scattering from Surfaces

Academic and Research Staff

Prof. J.D. Litster, Dr. Satyendra Kumar

Graduate Students

J. Brock, B.D. Larson, J. Samseth, L.E. Solomon, S. Sprunt

Joint Services Electronics Program (Contract DAAG29-83-K-0003)

Brent D. Larson, James D. Litster, Lorraine E. Solomon

A. Studies of Micellar Liquid Crystals

In this program, we are studying the structure of ordered phases of surfactants. We use three experimental techniques. To study orientational long range ordering, we use quasielastic light scattering, while time-resolved spectroscopy gives us information on orientational short range order and dynamics. Finally, x-ray scattering is used to study positional order of the molecules.

In last year's report, we explained the theory behind the time-resolved method and how our data showed that dye probe molecules were oriented on average by the surfactant, but that dynamical information was difficult to obtain from probes whose fluorescence lifetime was only 2 to 2.5 ns. We have since tested dyes with significant triplet conversion and found one, rose bengal, whose fluorescence lifetime exceeds 12 ns. We have not yet used it to study the rotational diffusion of micelles. We have used birefringence measurements to study the average orientational order parameter in aqueous solution of the soap cesium perfluoro-octonate (CsPFO) and found a very weakly first order transition; it is not yet understood why this should be so weak.

B. Study of Surfaces

Our eventual plan is to study surfaces by x-ray scattering. Some of these will use an x-ray compatible high vacuum apparatus which is described in more detail in R. Birgeneau's report (see Chapter 5). This apparatus has recently been tested and obtained a vacuum of 10^{-11} Torr. Other surface experiments involve the spreading and ordering of organic molecules on liquid metal (e.g., mercury) substrates. We expect to use a combination of x-ray scattering and optical second harmonic generation to study the structure of these films. Preliminary experiments have been carried out where cyano biphenyl liquid crystals have been spread on mercury. These molecules are expected to lie flat on the surface and should provide a realization of a two-dimensional smectic material where only short range order is permitted according to current statistical mechanical concepts.

We have just spent a week studying CsPFO using an 8 pole wiggler beam line at the Stanford Synchrotron Radiation Laboratory. This has provided us with preliminary data while we await the commissioning of our beam line at the Brookhaven National Synchrotron Light Source.

10. Infrared Nonlinear Optics

Academic and Research Staff

Prof. P.A. Wolff, Dr. R.L. Aggarwal, Dr. Piotr Becla, Dr. C. Jagannath, Dr. L.R. Ram-Mohan, Dr. Y.C.S. Yuen

Graduate Students

G. Boebinger, J. Warnock, S. Wong, E. Youngdale

10.1 Infrared Nonlinear Processes in Semiconductors

U.S. Air Force - Office of Scientific Research (Contract F49620-80-C-0008)

Roshan L. Aggarwal, Peter A. Wolff, Chiravurri Jagannath, L.R. Ram-Mohan, Y.C. Sunny Yuen, Gregory Boebinger, Stephen Wong, Eric P. Youngdale

Four wave mixing spectroscopy[1] has been used to study the stress dependence of the ground state multiplet of phosphorus donors in silicon at 1.8 K, using a quantitative stress cryostat. For compressive force, F, along [100] or [110], the 1s(E) level splits into two singlet levels. These measurements determine the stress deformation potential constants, Ξ_u, characterizing the 1s — ground state multiplet. A direct measurement of the effect of uniaxial stress on the size of the envelope function should be possible via diamagnetic techniques.

Saturation behavior of the band-gap resonant optical nonlinearity at 10.6 μ in HgCdTe was studied[2] by degenerate four-wave mixing experiments over a wide range of laser intensities. The reflectivity saturates when the laser power density reaches 100 W/cm^2, and the third-order nonlinear susceptibility drops as the inverse of the laser intensity, thereafter. A theory of interband absorption at the pump frequency, due to state blocking, is in good agreement with the experiments.

Four wave mixing experiments were used to study[3] the variation of the third order nonlinear susceptibility, $\chi^{(3)}$, with difference frequency $\Delta\omega$ and laser intensity I in low carrier concentration HgCdTe crystals. At small $\Delta\omega$, $\chi^{(3)}$ is caused by nonparabolicity of free electrons generated by two photon absorption, with $\chi^{(3)}$ scaling as $(\Delta\omega)^{-1}$ and $I^{2/3}$. The $\Delta\omega$ variation of $\chi^{(3)}$ indicates that the electron thermalization time is longer than 8 psec. At large $\Delta\omega$, $\chi^{(3)} \simeq 3 \times 10^{-8}$ esu and is mainly due to valence electrons.

Three wave mixing, to generate far infrared radiation in the 100 μ range, has been investigated[4] in uniaxially-strained n-InSb. This work was stimulated by a recent observation of stress-enhanced, electron dipole spin resonance absorption in n-InSb. In the current work, two CO_2 laser beams, with difference frequency $\Delta\omega$ near the electron spin resonance frequency, were combined in a cold

n-InSb crystal. The FIR signal at $\Delta\omega$ was enhanced by a factor of 10 with uniaxial stress; at the same time the spin resonance broadened substantially. Overall, the effect is smaller than anticipated and probably not useful for tunable FIR generation.

Measurements of the difference frequency dependence of $\chi^{(3)}$ have been used to determine[5] the light to heavy hole scattering rate in p-type GaAs. At 300 K the scattering time is $T = 1 \times 10^{-13}$ sec; it increases to 2×10^{-13} sec at 77 K. These values are in good agreement with those calculated for polar optic phonon scattering.

References

1. C. Jagannath and D.M. Larsen, Bull. APS 28, No. 3, 534 (1983).
2. S.Y. Yuen and P. Becla, Opt. Lett. 8, 356 (1983).
3. S.Y. Yuen, Appl. Phys. Lett. 41, 590 (1983).
4. R.L. Aggarwal, C. Jagannath, and P.A.Wolff, to be published.
5. S.Y. Yuen, to be published.

11. Quantum Transport in Low Dimensional Disordered Systems

Academic and Research Staff

Prof. P.A. Lee

11.1 Quantized Hall Effect

Joint Services Electronics Program (Contract DAAG29-83-K-0003)

Patrick A. Lee

In the past year, important progress was made in understanding the anomalous quantized Hall effect. It was discovered experimentally that when a two dimensional electron gas (realized in GaAs–GaAlAs heterojunctions) is subject to a large magnetic field so that the lowest Landau level is partially occupied, steps appear in the Hall conductance at $Re^2/\hbar$ where R are simple fractions like 1/3, 2/3, 2/5, etc. This phenomenon is referred to as the anomalous quantized Hall effect where R are integers) which can be understood based on noninteracting electrons, a theory of the anomalous Hall effect must take full account of the interaction between electrons. In collaboration with D. Yoshioka (University of Tokyo) and B. Halperin (Harvard), numerical calculations of the eigenstates of a few (4 to 6) particles subject to periodic boundary conditions were performed.[1] The ground state is found to exhibit downward cusps at $\nu = 1/3$ and $\nu = 2/5$, where ν is the fractional filling of the Landau level. By studying the density-density correlation function, we found that the ground state is not a Wigner solid, but instead is best described as a liquid. We speculate that the liquid state at $\nu = 1/3$ is separated by an energy gap from a variety of excited states. By going to a moving frame, it is clear that at $\nu = 1/3$, a Hall current will flow without dissipation, even in the presence of impurities. The state of ν close to 1/3 can be considered as the $\nu = 1/3$ state plus a small density of quasi-particles. The Hall step at $\sigma_{xy} = 1/3e^2/\hbar$ can then be explained if the quasi-particles are localized by impurities and do not contribute to the Hall current, which is carried by the underlying $\nu = 1/3$ state.

At about the same time, R.B. Laughlin wrote down a trial wavefunction in which correlation between pairs of electrons are included. The variational energy and the nature of Laughlin's state compares favorably with our numerical solution. While much work remains in elucidating the nature of this new state, we can be confident that the theory is proceeding in the right direction.

11.2 Resonance Tunnelling in Narrow MOSFET's

The conductivity of narrow MOSFET's exhibits oscillations as a function of gate voltage at low temperatures. These observations were interpreted in terms of resonance tunnelling through localized states in barriers along the MOSFET channel.[2] (See Prof. Kastner's report for greater

details). Further theoretical work is in progress towards understanding the effect of time dependent fluctuations on the resonance tunnelling phenomenon.

References

1. D. Yoshioka, B.I. Halperin, and P.A. Lee, Phys. Rev. Lett. 50, 1219 (1983).
2. R.F. Kwasnick, M.A. Kastner, J. Melngailis, and P.A. Lee, Phys. Rev. Lett. 52, 224 (194).

12. Microwave and Quantum Magnetics

Academic and Research Staff

Prof. F.R. Morgenthaler, Prof. R.L. Kyhl[2], Dr. T. Bhattacharjee, D.A. Zeskind

Graduate Students

M. Borgeaud, L. Hegi, C.M. Rappaport, N.P. Vlannes

Objective

Our objective is to develop an understanding of electromagnetic, magnetostatic, and magnetoelastic wave phenomena and to employ them to create novel device concepts useful for microwave signal-processing applications. We are especially interested in developing novel device concepts for the millimeter wavelength portion of the electromagnetic spectrum.

12.1 Millimeter Wave Magnetics

Frederic R. Morgenthaler, Robert L. Kyhl, Dale A. Zeskind

The Microwave and Quantum Magnetics Group within the M.I.T. Department of Electrical Engineering and Computer Science and the Research Laboratory of Electronics recently began a research program aimed at developing coherent magnetic wave signal processing techniques for microwave energy which may form either the primary signal or else the intermediate frequency (IF) modulation of modulation of millimeter wavelength signals.

We are currently waiting for renewed Army support so that we can reactivate and continue this research program.

12.2 New Techniques to Guide and Control Magnetostatic Waves

National Science Foundation (Grant 8008628-DAR)
Joint Services Electronics Program (Contract DAAG29-83-K-0003)
U.S. Army Research Office (Contract DAAG29-81-K-0126)
Frederic R. Morgenthaler, Dale A. Zeskind, Larry Hegi

We have recently reviewed[1,2] our early interest and work[3-5] in controlling magnetostatic waves and modes in thin ferrite films by means of spatial gradients in the effective dc bias that depends upon

[2]Emeritus

applied field, magnetic anisotropy and saturation magnetization.

Special emphasis has been given to a bias that varies in magnitude and/or direction while maintaining an orientation transverse to the propagation direction. Both rectangular and circular film geometries have been studied when the bias is either normal (forward-volume wave) or parallel (surface-wave) to the film.

An especially interesting case exists when the orientation of an in-plane bias is changed so as to alter the propagation direction of magnetostatic surface waves. Experimental confirmation of the basic idea has previously been reported by Stancil and Morgenthaler[6] and has very recently been extended by Stancil[7] to the case of a high Q surface wave ring-resonator that shows considerable device promise.

The analysis of mode propagation in bias gradient environments is complicated by the fact that even weak gradients can cause large changes in the rf susceptibility tensor whenever the components of the latter are very near resonance. Therefore, although there are regimes in which perturbation theory is very valid, there are those in which it is decidedly not.

In an invited paper to be published in Circuits, Systems and Signal Processing, Morgenthaler first develops a very general mathematical formulation applicable to ferrite films of both cartesian and circular geometries when the effective bias is normal to the film plane and conducting ground-planes may be present. All of the special cases, previously studied,[8] are embraced by the new theory.

Next, we consider the comparatively simple case of modes or waves without thickness variations and review how weak gradients can control the basic frequency dispersion and how larger gradients can sometimes create what are in effect "microwave domains" of the rf magnetization residing in a single domain environment of the static-equilibriummagnetization. Such "virtual-surface" modes[5] are predicted to have very large microwave energy densities associated with their "microwave-domain walls".

Continuing, we separate the ground planes, that were used to justify the consideration of modes without thickness variation, and discuss the three-dimensional modes of both a rectangular strip with finite width and a circular disk of finite radius. At first, the bias is kept uniform but then width (or radial) variations are added to reveal (through numerical solutions of the differential equations) how even weak gradients can sometimes cause major adjustments in the transverse mode patterns. Such gradient-induced field displacement effects are shown to be highly nonreciprocal and may have important ramifications for developing new types of microwave MSW devices.

An effective particle density $\hat{n}$ is defined (that includes the effects of fringing fields) such that its integration over the ferrite volume yields the total magnetostatic mode energy. Plots of $\hat{n}$ as a function of transverse coordinate provide valuable insight into the mode properties.

Finally, we show how the new analysis complements and extends our coupled-integral equation approach to solving boundary value problems when the in-plane bias (surface wave geometry) is a function of the width coordinate. This is done by simply interchanging width and thickness parameters in the new theory which then allows one to consider surface-wave propagation when there are thickness (but not width) variations in the effective bias. For a thin film such variation would come from thickness gradients in either the saturation magnetization or magnetic anisotropy (or both) and thus the modified theory can also treat the case of multiple graded layers with or without dielectric spaces between them.

References

1. F.R. Morgenthaler, "Novel Devices Based upon Field Gradient Control of Magnetostatic Modes and Waves." FERRITES: Proceedings of the International Conference, Japan, September-October 1980, pp. 839-846.
2. F.R. Morgenthaler, "Field Gradient Control of Magnetostatic Waves for Microwave Signal Processing Applications," Proceedings of the 1981 RADC Microwave Magnetics Technology Workship, June 10-11, 1981; F.R. Morgenthaler, "Workshop on Application of Garnet and Ferrite Thin Films to Microwave Devices," Session FC, Third Joint Intermag — Magnetism and Magnetic Materials Conference, Montreal, Canada, July 1982; N.P. Vlannes, "Investigation of Magnetostatic Waves in Uniform and Nonuniform Magnetic Bias Fields with a New Induction Probe," Third Joint Intermag — Magnetism and Magnetic Materials Conference, Montreal, Canada, July 1982.
3. D.A. Zeskind and F.R. Morgenthaler, "Localized High-Q Ferromagnetic Resonance in Nonuniform Magnetic Fields," IEEE Trans. Magn. MAG-13, 5, 1249-1251, September 1977.
4. F.R. Morgenthaler, "Magnetostatic Waves Bound to a DC Field Gradient," IEEE Trans. Magn. MAG-13, 5, 1252-1254, September 1977.
5. F.R. Morgenthaler, "Bound Magnetostatic Waves Controlled by Field Gradients in YIG Single Crystal and Epitaxial Films," IEEE Trans. Magn. MAG-14, 5, 806-810, September 1978.
6. D.D. Stancil and F.R. Morgenthaler, "Guiding Magnetostatic Surface Waves with Nonuniform In-plane Fields," J. Appl. Phys. 54, 3, 1613-1618 (1983).
7. D.D. Stancil, private communication paper presented at the 1983 Conference on Magnetism and Magnetic Materials, Pittsburgh, Pennsylvania, November 1983.
8. F.R. Morgenthaler, "Nondispersive Magnetostatic Forward Volume Waves under Field Gradient Control," J. Appl. Phys. 53, 3, 2652-2654 (1982).

12.3 Optical and Inductive Probing of Magnetostatic Resonances

Joint Services Electronics Program (Contract DAAG29-83-K-0003)

Frederic R. Morgenthaler, Nickolas P. Vlannes, Robert L. Khyl

Having finished development of the new induction probe that measures microwave magnetic field patterns of magnetostatic waves in LPE-YIG thin films, Nickolas Vlannes turned to making operative the optical probe based upon a Spectra Physics 125 laser tuned to the 1150 nonometer wavelength.

12.4 Magnetostatic Wave Dispersion Theory

Joint Services Electronics Program (Contract DAAG29-83-K-0003)
Frederic R. Morgenthaler

Larry Hegi has been carrying out theoretical and experimental determinations of the frequency dispersion of magnetostatic wave guides in the form of thin film rectangular strips of various width to thickness ratios when the external magnetic bias is either uniform of spatially nonuniform. He has written a report that includes sections on

- Measuring Dispersion The Antenna Finite Width Technology Fabrication Procedures

A paper based upon the S.M. Thesis of D.A. Fishman was published in the Journal of Applied Physics, June 1983. The abstract follows:

The velocity of energy circulation associated with the uniform precession mode in a ferrite sphere is studied. Specifically, the effect of the boundary conditions imposed by a concentric conducting spherical cavity is considered for the uniform precession magnetic resonance mode of a yttrium-iron-garent (YIG) sphere. Theoretical analyses show that there is a critical ratio between the radius of the ferrite sphere and the conducting cavity where the energy velocity of the uniform precession mode approaches zero. Spin wave instabilities, as a result of the nonlinear coupling of the uniform precession mode to spin wave excitations are brought on if the rf-energy density expected to decrease the amount of incident power required for the onset of spin wave instability have been observed as a function of the cavity radius. The experimental cavity consists of two conducting partial hemispheres, one on each side of the YIG sphere.

References

1. D.A. Fishman and F.R. Morgenthaler, "Investigation of the Velocity of Energy Circulation of Magnetostatic Modes in Ferrites," J. Appl. Phys. 54, 6 (1983).

12.5 Magnetoelastic Waves and Devices

Joint Services Electronics Program (Contract DAAG29-83-K-0003)
National Science Foundation (Grant 8008628-DAR)
Frederic R. Morgenthaler, Maurice Borgeaud

The evolution of the magnetoelastic delay line has progressed gradually over a period of the last twenty years. In 1961, Schlömann[4] first proposed the possibility of spin wave excitation in nonuniform magnetic fields. In 1963, this effect was experimentally verified by Eschbach.[5,6] He showed that the excited spin waves propagated in the direction of decreasing magnetic field until their wavelengths matched those of elastic waves. As that value of wavelength (or corresponding magnetic field), most of the spin waves appeared to convert to elastic waves. This connection between conversion point and magnetic field, also verified by Strauss[7] in 1965, led both Strauss and

Schlömann[8,9] to propose the magnetically tunable delay line.

Since the proposal in 1965, a variety of magnetically tunable delay lines have been designed with limited success. To electromagnetically excite the spin waves in the YIG rod, designs utilizing thin wire coupling antennas,[1,10] stripline cavity resonators,[11] and more recently thin film antennas[2,3] have all been tried. Most designs have also had specific nonuniform field shapes imposed by either ferrimagnetic geometry[12,13] or auxiliary pole pieces designed into the housing.[1-3] In almost all of the previous attempts at producing linear delay with frequency in YIG delay lines, the focus has been on synthetizing a linear axial magnetic field.[1,2] However, no reason exists why a nonlinear axial magnetic field cannot also be used to obtain the desired delay function. Wadsworth[3] proved it by achieving insertion losses of 30 dB over a bandwidth of 500 MHz. The advantage of removing the unnecessary constraint of linearity from the axial magnetic field profile gives an extra degree of freedom which can be used to attempt to lower insertion loss and increase bandwidth.

Delay lines which were built by Itano[2] and Wadsworth[3] used a highly polished surface of the rod to get a reflection in the elastic region. These devices suffered because the input and output antennas lay in the same plane and were not very well electrically isolated.

References

1. F.R. Morgenthaler and A. Platzker, "Magnetic Field Synthesis Procedures for Magnetostatic and Magnetoelastic Devices," Proceedings of the 1978 International Symposium on Circuits and Systems, New York, May 1978, pp. 574–578.
2. L.M. Itano, "Microwave Delay Line with Thin Film Antennas," Technical Report 43, S.M. Thesis, Microwave and Quantum Magnetics Group, Massachusetts Institute of Technology, August 1981.
3. A.K. Wadsworth, "Improvements in the Design of Microwave Magnetoelastic Delay Lines," Technical Report 46, S.M. Thesis, Microwave and Quantum Magnetics Group, Massachusetts Institute of Technology, January 1982.
4. E. Schlömann, "Advances in Quantum Electronics," (Columbia University Press, New York, 1961) p. 437.
5. J.R. Eschbach, "Spin Wave Propagation and the Magnetoelastic Interaction In Yttrium Iron Garnet," Phys. Rev. Lett. 8. 9, 357–359, May 1962.
6. J.R. Eschbach, "Spin Wave Propagation and the Magnetoelastic Interaction in Yttrium Iron Garnet," J. Appl. Phys. 34, 4, 1298–1304 (1963).
7. W. Strauss. "Elastic and Magnetoelastic Waves in Yttrium Iron Garnet," Proc. IEEE 53, 10, 1485–1495 (1965).
8. E. Schlömann, "Generation of Spin Waves in Nonuniform DC Magnetic Fields. I. Conversion of Electromagnetic Power Into Spin Wave Power and Vice Versa," J. Appl. Phys. 35, 1, 159–166 (1964).
9. E. Schlömann, "Generation of Spin Waves in Nonuniform DC Magnetic Fields. II. Calculation of the Coupling Length," J. Appl. Phys. 35, 1, 167–170 (1964).
10. E. Schlömann, R.I. Joseph, and T. Kohane,"Generation of Spin Waves in Nonuniform Magnetic Fields with Applications to Magnetic Delay Lines," Proc. IEEE 53, 10. 1495–1507 (1965).
11. B.A. Auld, J.H. Collins, and D.C. Webb, "Excitation of Magnetoelastic Waves in YIG Delay Lines," J. Appl. Phys. 39, 3, 1598–1602 (1968).
12. H. Dotsch, "Magnetoelastic Delay Lines with Linear Dispersion," J. Appl. Phys. 43, 4, 1923 (1972).

13. R.W. Kedzie, "Magnctostatic Mode Propagation in Axially Magnetized YIG Rod Containing a Turning Point," J. Appl. Phys. 39, 6, 2731–2734 (1968).

12.6 On the Electrodynamics of a Deformable Ferromagnet Undergoing Magnetic Resonance

National Science Foundation (Grant 8008628-DAR)
Joint Services Electronics Program (Contract DAAG29-83-K-0003)
Frederic R. Morgenthaler

The energy–momentum tensor of a deformable ferromagnet is developed using the Chu formulation of electrodynamics which we reviewed in an invited paper presented in Paris during July 1983 at the Mechanical Behavior of Electromagnetic Solid Continua Symposium. It is shown that when the magnetization is undergoing ferromagnetic resonance, the new tensor differs from that of conventional theory, principally because large–signal linear momentum due to spin precession can appear in the rest–frame of the solid. Under transient conditions, the time rate of change of that momentum leads to predictions of an altered net force even when the ferromagnet is acting as a rigid body.

12.7 Microwave Hyperthermia

Frederic R. Morgenthaler, Tushar Bhattacharjee, Carey M. Rappaport

Our understanding of both physics and physiology is challenged in trying to optimize techniques for heat production and for the thermometry associated with Hyperthermia modalities used in connection with cancer therapy.

Fundamental considerations are based on designing proper microwave applicators which must be able to handle the microwave power required to raise the temperature of the tumor. They must also minimize the amounts of microwave power being delivered to the healthy tissue or being radiated into free space.

12.8 Synthesis of Microwave Applicators

National Institutes of Health (Grant 1 P01 CA31303-01)
Frederic R. Morgenthaler, Carey M. Rappaport, Tushar Bhattacharjee

We have recently given consideration to radiating trough waveguides as a possible microwave applicator for the delivery of hyperthermia. The asymmetric geometry shown in Fig. 12–1 was first discussed in 1958 by Rotman and Naumann.[1]

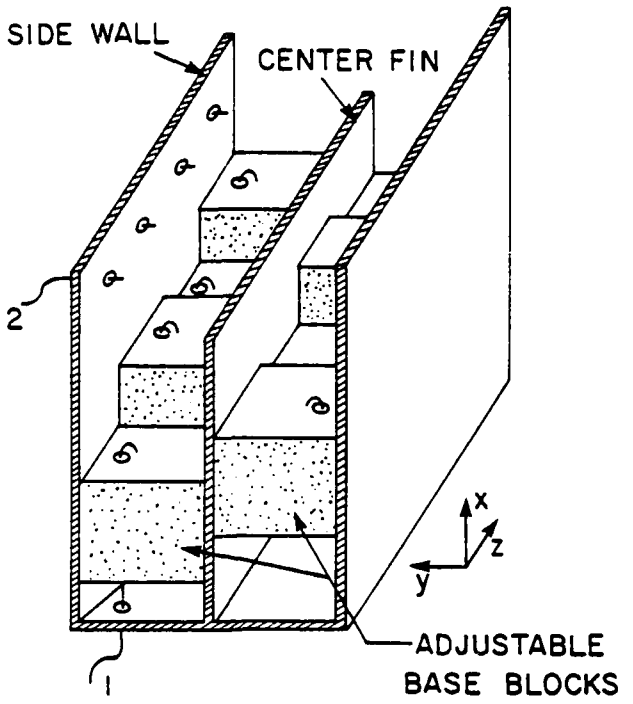

Figure 12-1: Trough Waveguide with alternating base asymmetry and field sampling probes (1 → H field, 2 → E field).

Being a leaky wave transmission line, it radiates in the x-direction as it guides waves in the z-direction. It can be derived either from a symmetric bisection of a strip line carrying the 1st higher order TE mode or from the folding of a slotted rectangular waveguide carrying TE_{01} mode. The base asymmetry supports an asymmetric radiating mode. The complex transcendental equation solution has been derived from the equivalent circuit for the asymmetric trough waveguide using the transverse resonance technique. The derivation includes the reflection due to the finite length of the guide and also the effect of the finite thickness of the fin in the trough guide geometry. Programs have been written which solve such geometries from both analysis and synthesis points of view. For example, one can calculate the dimensions of a troughguide with a specified complex propagation constant γ or the γ can be determined from a particular known geometry.

An experimental model has been designed and built to investigate the trough waveguide performance. Intended for use at 915–2450 MHz, this applicator will focus power in synthetic muscle phantom material. As a single unit with an aperture of 2½" by 8½", it is a building block for either a planar array — where several troughs are placed next to one another; or for a cylindrical array — where axial troughs would radiate into a phantom in the center.

The asymmetry of the test model is adjustable. The base is formed by blocks which can be finely displaced vertically. Note the alternating block heights in Fig. 12–1. This provides for 180° phase

reversals, allowing configurations of aperture as a Fresnel lens. The Fresnel zone width was chosen to maximize power in muscle phantom at a depth of one wavelength at 915 MHz.

A major concern of this applicator is monitoring radiated power. Electric and magnetic field probes sample the total forward and backward waves at each block section. Combining the outputs from these probes gives power guided by the trough waveguide.

To investigate the cylindrical applicator configuration, software has been written which calculates the radial ($\hat{r}$) and axial ($\hat{z}$) field distribution produced by E-field sources on a finite cylindrical section. Given the dielectric characteristics of a medium and the frequency, field intensity is plotted as a function of radius or length. The radial impedance (Z_r) can also be calculated. Typical results for an infinitely long cylindrical aperture are shown in Fig. 12-2 for muscle tissue and frequencies 433, 915, 2450 MHz.

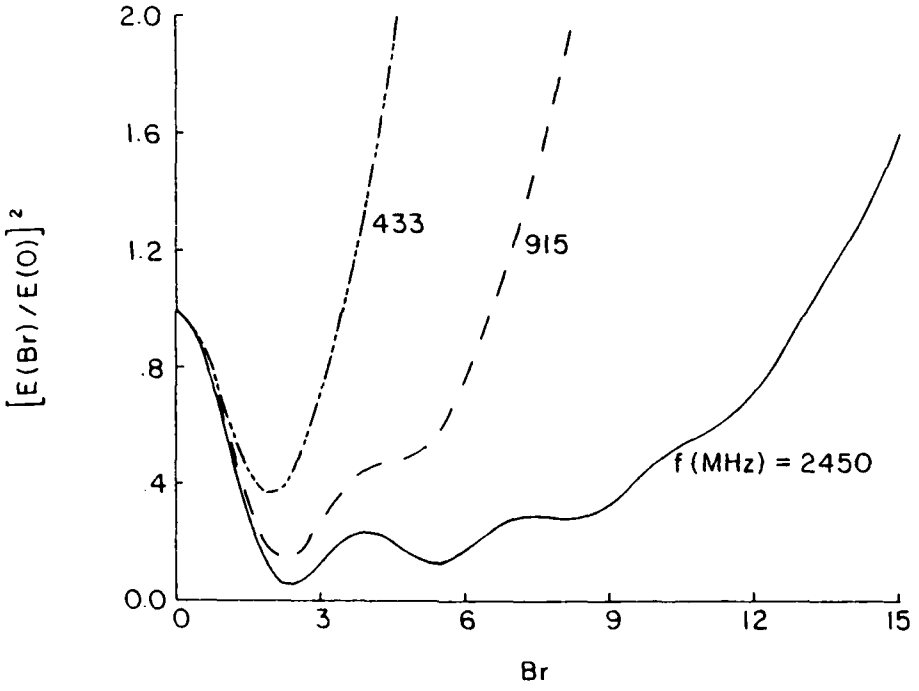

Figure 12-2: Relative power absorption for an infinite cylinder of muscle tissue

References

1. W. Rotman and S.J. Naumann, "The Design of Trough Waveguide Antenna Arrays," AFCRC-TR-58-154, June 1958.

Publications

Borgeaud, M., "An Improved Two-port Magnetoelastic Delay Line," S.M. Thesis, Department of Electrical Engineering and Computer Science, M.I.T., January 1984.

Morgenthaler, F., "On the Electrodynamics of a Deformable Ferromagnet Undergoing Magnetic Resonance," Proceedings of the IUTAM-IUPAP Symposium on Mechanical Behavior of Electromagnetic Solid Continua.

Morgenthaler, F. and T. Bhattacharjee, "Design of Annual Arrays to Contol Microwave Power Deposition in Biological Tissues," poster paper presented at the Hyperthermia Workshop at IEEE MTT-S International Microwave Symposium, May 31-June 3, 1983.

Fishman, D.A. and F.R. Morgenthaler, "Investigation of the Velocity of Energy Circulation of Magnetostatic Modes in Ferrites," J. Appl. Phys. 54, 6 (1983).

Melcher, J.R., "Analytic Solutions to the Bioheat Equation in a Cylindrical Geometry," S.B. Thesis, Department of Electrical Engineering and Computer Science, M.I.T., May 1983.

Stancil, D.D. and F.R. Morgenthaler, "Guiding Magnetostatic Surface Waves with Nonuniform In-plane Fields," J. Appl. Phys. 54, 3 (1983).

Morgenthaler, F.R., "Field Gradient Control of Magnetostatic Waves for Microwave Signal Processing Applications," Proceedings of the 1981 RADC Microwave Magnetics Technology Workshop, June 10-11, 1981, RADC In-house Report, January 1983.

Morgenthaler, F.R., "Control of Magnetostatic Waves in Thin Films by Means of Spatially Nonuniform Bias Fields," Circ. Syst. Sig. Proc., to be published.

13. Radio Astronomy

Academic and Research Staff

Prof. A.H. Barrett, Prof. B.F. Burke, Prof. J.W. Dreher, Prof. R.L. Kyhl, Prof. J.H. Lang, Prof. D.H. Staelin, Dr. D.H. Roberts, Dr. P.W. Rosenkranz, Dr. M. Shao, J.W. Barrett, J.G. Kang, D.C. Papa

Graduate Students

A.D. Ali, B.R. Allen, J.T. Armstrong, C.L. Bennett, P.J. Benson, A.C. Briançon, M.M. Colavita, V. Dhawan, S.B. Dynes, P.M. Garnavich, J.N. Hewitt, J.M. Jackson, C.R. Lawrence, J.H. Mahoney, H.S. Mulvar, D.C. Murphy, K.S. Nathan, S.-M. Shih, J.M. Sulecki, W. Williams, Y. Yam

National Science Foundation (Grant AST 81-21416)

Alan H. Barrett

During 1983 the following programs of research on the interstellar medium and star formation were pursued:

1. We conducted a brief survey of molecular clouds in the $5_{05} \rightarrow 4_{04}$ and $4_{04} \rightarrow 3_{03}$ transitions of HNCO at 109.9 and 87.9 GHz, respectively. The lines were detected in seven clouds with typical ΔT_A^* of a few tenths of a degree, with one notable exception. In the Sgr A molecular cloud the HNCO antenna temperature is 3.1 K, an order of magnitude greater than in the other clouds. On the other hand the $C^{18}O$ spectra do not show a similar increase. The $1_{01} \rightarrow 0_{00}$ HNCO transition at 22.0 GHz was detected at Haystack and supports the view that HNCO is overabundant in the Sgr A cloud as opposed to other molecular sources.

2. We have continued our studies of hyperfine intensity anomalies in the NH_3 spectra from some molecular clouds. In collaboration with Prof. G. Winnewisser, University of Köln, we have found 13 sources which are known to exhibit anomalous hyperfine intensities. It is believed the unusual intensities arise from selective trapping of the infrared radiation from the J,K = 2,1→1,1 within the various hyperfine levels making up the transition. The observations can be used to constrain the overall gas density within rather narrow limits, typical values being $10^6 cm^{-3}$. An unusual outcome of these studies is that all sources which exhibit hyperfine intensity anomalies in their NH_3 spectra also have H_2O masers. The significance of this is not fully understood.

3. Our studies of the continuum emission from the galactic center region have continued. We have detected a number of sources associated with the NH_3 peaks in the Sgr A molecular cloud. Most of the sources are thermal and may be regions of recent, or current, star formation. One source is

nonthermal, crescent shaped, and appears to exhibit polarization with the electric-vector oriented normal to the crescent. This is suggestive of the magnetic field being oriented along the crescent, perhaps serving to confine the crescent.

4. A long-term study of the radio properties of star-burst galaxies has been initiated. These galaxies have a bright nucleus, infrared color excess, and optical emission lines whose full width is less than 300 km/sec. Since these properties correspond to the properties of young, hot stars in extragalactic HII regions, these galaxies have been called "star-burst" galaxies. We have obtained HI spectra at Arecibo from 46 galaxies of this type and CO J = 1→0 spectra from 7 (perhaps 10) of these galaxies. The CO and HI spectra are very similar. Observations of the J = 2→1 CO transition are planned to improve the spatial resolution. We also plan observations of H_2O at a wavelength of 1.35 cm.

13.1 Galactic and Extragalactic Radio Astronomy

National Science Foundation (Grant AST82-14296)
Bernard F. Burke

Overview

This is a set of broadly-based radio astronomy studies of extragalactic radio sources, being carried out, aimed at understanding the distribution of matter in galaxies and clusters of galaxies, the interactions of the ICM, IGM, and ISM with the relativistic plasma ejected by active galaxies, and to explore the extension of VLBI observations to shorter and longer wavelengths. A major emphasis will be a new set of observations aimed at improving our quantitative understanding of dark matter in the universe.

The largest amount of the research will be carried out at national or quasi-national, research centers. The VLA, the Green Bank NRAO facilities, the VLB network, and the Haystack radio observatory will be principal foci. At the same time, we will be carrying out modest in-house hardware development to allow the pursuit of VLB explorations that otherwise would not be possible. This means that our students can still have an interaction with real hardware, an experience that is not commonly available.

The individual components of the program include the study of (1) interacting galaxies, (2) gravitational lensing, (3) time variations of lensed objects, (4) gravitational distortion, (5) quasar-galaxy pairs, 6) structural studies of radio sources, (7) radio source surveys, (8) 7-mm VLBI, (9) long-wavelength VLBI, and (10) continuation of molecular maser VLBI studies. Radio observations alone are frequently insufficient to address astrophysical problems in depth, and we are planning associated optical observations in many of the above areas: in some cases, through collaborating work with optical observers, but principally through utilization of the McGraw-Hill

Observatory, which we share with Michigan and Dartmouth and which will have a 95-inch telescope in operation in 1985.

For many years it has been common knowledge that the luminous matter in the universe, which is the easiest state of matter to detect, is only a fraction of the total mass that makes up large-scale structures such as galaxies, clusters of galaxies, and the universe as a whole. Any single datum might be discussed, but there is a persistent gap between the dynamical mass and luminous mass determined in practically every case. Historically, the mean density of our own galaxy inferred from dynamical studies has been greater than the density measured by a careful census of starts, dust, and gas, an inequality that has recently been revived by the studies of Bahcall, Ostriker, and their collaborators. One popular explanation at present is the massive galactic halo postulate, which simultaneously provides the missing matter and helps to stabilize the thin population I disk. The outstanding spectrographic work of Rubin and Ford demonstrated clearly that spiral galaxies have remarkably flat rotation curves that are most easily interpreted as evidence for massive halos of dark matter (although alternative models have been proposed, the reality remains that a substantial quantity of dark matter, not distributed like the stars, must exist in spiral galaxies).

Evidence for large quantities of matter in clusters of galaxies has long been recognized by application of the virial theorem to observed motions of galxies in clusters. Although some reservations are in order for some of the most spectacular examples, for example, Pegasus II, with $\sigma_{Nu} \sim 2000$ cm/sec is quite probably more than one cluster, with substantially smaller velocity dispersion within each cluster. There has been speculation that the mass fraction of dark material inferred from the mass-to-light ratio is proportional to the size of the system: the mass -to-light ratio is apparently 5 to 10 in the case of galaxies, some integral multiple of 10 for binary galaxies, and several hundred for most clusters of galaxies. So far, the best-understood system is probably the twin quasar 0957 + 561, discovered by Walsh, Carswell, and Weymann. Through the optical work of Young *et al.*, the VLA observations of Greenfield *et al.*, and the VLBI work of Porcas *et al.*, and Gorenstein *et al.*, it is clear that the lensing material associated with the observed foreground cluster must be composed mostly of dark matter distributed rather differently from the visible matter.

The evidence for dark matter is so strong that it must be accepted. The distribution and nature of the dark matter, however, is still far from clear, and study of this interesting and widespread phenomenon is obviously indicated. A number of promising new methods can be employed, and we are exploring three approaches: the study of the gravitational lensing phenomenon, the measurement of the dynamics of interacting pairs of galaxies, and the study of quasar-galaxy pairs.

The aim is to improve, in a comprehensive way, our knowledge of the distribution of matter in galaxies and clusters of galaxies.

13.2 Jovian Decametric Radiation

National Aeronautics and Space Administration (Grants S-10781-C and NAGW-373)
David H. Staelin, Philip W. Rosenkranz, Peter M. Garnavich

The Planetary Radio Astronomy (PRA) experiment on the Voyager 1 and 2 spacecraft observed Jovian decametric radio emission in 198 channels distributed over the band from 1.2 kHz to 40.5 MHz. "Arcs" in the frequency-time domain have been associated with radio emission near the local electron-cyclotron frequency with a hollow conical emission pattern. Theory suggests that such conical emission might be produced by magnetospheric currents generated by the satellite Io as it traverses the magnetospheric fields. These currents, on the order of 10^6 amps, are believed to propagate in an Alfvén wave that is reflected repeatedly between the northern and southern Jovian ionospheres. These currents traveling along the magnetospheric field lines should be spaced in Jovian longitude by an amount that depends upon the Jovian magnetic field strength and the plasma density in the magnetosphere, which is dominated by the plasma located in the "plasma torus" produced near the orbit of Io by volcanic activity. It would be natural to associate the spacing of the Jovian arcs with the spacing between the separate reflections of the Io-generated currents.

Examination of ~ 200 arcs and ~ 200 gaps between arcs observed by Voyager 1 and 2 did not reveal the expected correlation between arc gaps and longitude; in general the arc spacings were often half of the values expected and were only weakly dependent on longitude. This model assumed a constant cone angle. If, however, there is a simple relation between arc vertex frequency and longitude, the arc cone angle can be deduced; the half-cone angles deduced in this fashion varied between ~ 40° and 90°. Thus, if the Alfvén-wave model is correct, the cone angle must vary considerably from one current stream to the next, and may even have multiple values within a single current stream. This could also explain the close spacings observed for S-burst arcs, which may arise from similar currents.

Analysis of Jovian decametric data has been based primarily on 48-sec averages of 6-sec spectra which have been displayed with limited dynamic range, thus obscuring much structure. Software to display this data with 6-sec resolution and with an easily adjusted dynamic range has been developed. New phenomena and better images of old phenomena will be sought during 1984.

References

1. P.M. Garnavich, "Jovian Decametric Radiation: A Test of the Multiple-Reflection Alfvén Wave Model," S.M. Thesis, Department of Physics, M.I.T., June 1983.

13.3 Long-Baseline Astrometric Interferometer

National Science Foundation (Grant AST79-19553)
M.I.T. Sloan Fund for Basic Research
Michael Shao, David H. Staelin, Mark Colavita, D. Cosmo Papa

During 1983 the Mark II optical astrometric interferometer was successfully used at Mount Wilson Observatory in California to track stellar fringes in two colors for the first time. This instrument has two 10-inch siderostat mirrors 3.4 meters apart in a north-south direction. Within the ~ 2-inch aperture the positions of red and blue fringes are independently estimated every ~ 2-10 ms, thus permitting the state of the atmosphere to be measured and compensated over time intervals sufficiently short that the atmosphere can be considered "frozen".

One typical experiment (August 31) tracked Alpha Lyra for 80 seconds with ~ 0.07 arc sec rms deviation from mean position (1-sec position measurements) in the red band, and with ~ 0.02 arc sec rms deviations when both the red and blue fringe positions were considered. The formal error for 80 such 1-sec measurements, if their errors are uncorrelated, is ~ 0.002 arc sec, much better than ever before achieved for so brief a measurement.

The primary purpose of the Mark II experiment is demonstration and evaluation of the two-color technique for obtaining relative astrometric positions accurate to ~ 10^{-3} arc sec rms for stellar separations $<\sim 1°$. Experiments to demonstrate wide angle ($\gtrsim 10°$) and absolute astrometry are also being planned for the Mark II instrument in collaboration with the Naval Research Laboratory. Future versions of the interferometer are expected to achieve 10^{-4} arc sec relative position accuracy over 1-2° stellar separation, which would be adequate to detect a Jupiter near a one-solar-mass star at a distance of several parsecs, with a signal-to-noise ratio of ~ 10.

13.4 Tiros-N Satellite Microwave Sounder

National Oceanic and Atmospheric Administration (Grant 04-8-M01-1)
Philip W. Rosenkranz, David H. Staelin, Krishna S. Nathan

The National Oceanic and Atmospheric Administration (NOAA) routinely reduces data from one or two operational polar orbiting weather satellites; these now carry infrared spectrometers and a four-channel passive microwave spectrometer (MSU) for the purpose of mapping the three-dimensional temperature field of the atmosphere at six- or twelve-hour intervals. The purpose of this research program is continued improvement in the utilization of the passive microwave data produced by these NOAA satellites.

A two-dimensional spatial filter, optimum in the minimum-square-error sense, was used to retrieve

atmospheric temperature profiles from operational MSU observations. The apparent reduction in retrieved error due to use of two-dimensional techniques (rather than one-dimensional) is greatest in the troposphere and tropopause, and in regions where the verification data sets are more reliable. A large part of the improvement is due to the reduction of the short spatial wavelength errors. The two-dimensional method also significantly surpassed the traditional one-dimensional retrieval method over a severe storm front that contained layers of air with substantially different lapse rates.

During this year a preliminary design was formulated for the operational sounding data retrieval system for the next generation operational low-earth orbit meteorological satellites. In particular, efficient methods were formulated for incorporating both nonlinear physical effects and *a priori* statistics in the retrieval of atmospheric temperature and water vapor profiles from microwave and infrared images obtained from a proposed 20-channel microwave spectrometer and a comparable infrared system.

References

1. K.S. Nathan, "Application of a Multi-Dimensional Filter to Temperature Profile Retrieval," S.M. Thesis, Department of Electrical Engineering and Computer Science, M.I.T., May 1983.

13.5 Improved Microwave Retrieval Techniques

National Aeronautics and Space Administration (Grant NAG5-10)
Philip W. Rosenkranz, David H. Staelin

This program is directed toward development of improved techniques for retrieval of atmospheric temperature, wind, and humidity fields from passive microwave measurements of the earth, as obtained from satellites. It was concluded in the spring of 1983.

The major effort was continuation of the study of the growth of initialization errors (due to remote sensing errors) in numerical weather prediction models. The initial experiments were extended to a more complete study of the consequences of using different sets of basis functions for describing the altitude distribution of errors. A transition was made from the numerical prediction model on the Cray computer at the National Center for Atmospheric Research to the similar but slightly smaller and more economic model at the University of Wisconsin. This work is continuing under NASA sponsorship, as described below.

13.6 High-Spatial-Resolution Passive Microwave Sounding Systems

National Aeronautics and Space Administration (Grant NAG5-10)
Philip W. Rosenkranz, David H. Staelin, Alain C. Briançon, John W. Barrett

The theoretical portion of this new research effort will explore methods for obtaining high-spatial-resolution passive microwave remote sensing atmospheric data and for obtaining the maximum benefit from such data in numerical weather prediction systems. In the initial months this effort has focused on 1) evaluating the potential of aperture synthesis systems for use in geosynchronous orbit for rapid sounding of atmospheric temperature and humidity profiles with ~ 20–40 km resolution, and 2) continued experiments on the impact of initialization errors on high-spatial-resolution numerical weather prediction models.

Theoretical analysis of aperture synthesis methods suggests that a two-receiver 118-GHz interferometer employing two 35-cm apertures at spacings of zero to three meters, and at all rotation angles, can yield ~ 30-km spatial resolution and ~ 0.3 K rms sensitivity over 640,000 km^2 in a few minutes' time. Thus this technique appears quite promising for use in geosynchronous meteorological satellites.

The experimental portion of this effort involves development of a 118-GHz spectrometer for imaging frontal systems from aircraft. A basic system concept has been formulated and procurement of critical components will begin shortly in order to be ready for initial flights in 1985.

13.7 Scanning Multi-Channel Microwave Radiometer (SMMR)

National Aeronautics and Space Administration (Contract NAS5-22929)
Philip W. Rosenkranz, David H. Staelin, Xi Ru Xu

On October 24, 1978, the Nimbus-7 satellite was launched into polar orbit carrying the Scanning Multi-Channel Microwave Radiometer (SMMR) and other instruments. SMMR separately measures vertically and horizontally polarized terrestrial thermal radiation at wavelengths of 0.81, 1.4, 1.7, 2.8, and 4.6 cm. The mechanically scanned antenna maps all 10 channels completely over a 780-km wide swath beneath the spacecraft with a ground resolution ranging from ~ 30 km to ~ 150 km, depending on wavelength. Two efforts were concluded during 1983, those concerned with estimating water vapor abundances over arctic sea ice and firn, and snow accumulation rates over Antarctica and Greenland.

13.8 Video-Bandwidth Compression Techniques

Defense Advanced Research Projects Agency (Contract MDA 903-82-K-0521)
David H. Staelin, Donald E. Troxel, Alan S. Willsky, Ali D.S. Ali, Jeffrey G. Bernstein, Biswa Ghosh, Brian L. Hinman, Katherine H. Lambert, Henrique S. Malvar, Joan M. Sulecki

The monochrome video recording and display system has become fully operational and has been used extensively to record images and to test coding techniques. The video format most frequently

used is 128 x 120 pels at 15 frames per second (fps), where the same frame-store memory contents are displayed with interlace at 60 fps in a 256 x 240-pel bilinearly interpolated format. Images of 256 x 240 pels at 7.5 fps, bilinearly interpolated to 512 x 480 pels, can also be studied at 4 bits per pel, as can 128 x 50 or 64 x 100-pel images at 30 fps and 8 bits per pel. Other combinations are also operational, as limited by the peak data transfer rate to and from the disk memory. Up to 90-sec continuous sequences can be studied.

The most successful video coding technique tested to date is a form of adaptive transform coding using selective replenishment and the short-space Fourier transform (SSFT). The SSFT was developed by Jeffrey Bernstein and Brian Hinman, and is similar to the mutli-dimensional short-time Fourier transform. The SSFT-coded images exhibit no "blocking effects" of the type produced when discrete cosine transforms are employed in a block format. Fully recognizable 128 x 120-pel head-and-shoulders images with considerable head motion have been coded at ~ 56 kbps rates, and much improvement appears to be possible. Experiments were also performed using adaptive two-band (high's and low's) coding techniques with selective replenishment. Morphological coding methods, wherein the image is decomposed into strokes resembling the brush strokes of an artist, are also being studied. These methods suffer from noise introduced by inconsistent resolution of ambiguities, but do suggest a soft upper bound to compression ratios for certain classes of image compression techniques.

13.9 Resolution-Preserving Interpolation of Video Frames

Center for Advanced Television Studies

David H. Staelin, John W. Barrett, Jeffrey G. Bernstein, Brian L. Hinman, Henrique S. Malvar, Philip W. Rosenkranz

As part of the Advanced Television Research Program the use of resolution-preserving interpolation techniques to reconstruct missing frames in a frame sequence is being studied. The facility being used is the same as described above. A second Nova-4 computer and 130-Mbyte disk have also been added to the system. The initial research effort has three aspects, the study of 1) optimum interpolation techniques for subsampled signals in the presence of sampling noise and observer characteristics, 2) motion estimation and motion-compensated interpolation of video sequences, and 3) applications of the short-space Fourier transform to video signal processing. Theoretical work has begun on all three problems, and initial techniques for motion-compensated interpolation have been successfully implemented. A moving head-and-shoulders sequence has been sampled at 7.5 fps, and the missing frames have been reconstructed with sufficient accuracy so as to be nearly indistinguishable from the original sequence. Comparison with reconstructions using only dissolving techniques (i.e., linear combinations of adjacent frames) show a marked superiority for resolution-preserving techniques. Reconstruction of eight intermediate frames between frame pairs yields a slow motion sequence where interpolation artifacts are most visible. In this test slow

motion sequence the only artifacts evident were a slight periodicity at 7.5 Hz in the image blur, and a small apparent discontinuity in velocity vector direction at one point in the sequence.

14. Electromagnetic Wave Theory and Remote Sensing

Academic and Research Staff

Prof. J.A. Kong, Dr. W.C. Chew, Dr. S.-L. Chuang, Dr. T.M. Habashy, Dr. L. Tsang, Dr. M.A. Zuniga, Q. Gu, H.-Z. Wang, X. Xu

Graduate Students

H. Chuang, Y. Jin, J.F. Kiang, J.K. Lee, F.C.-S. Lin, S.L. Lin, D.W. Park, S.Y. Poh, A. Sezginer, R.T.I. Shin, A. Tulintseff, E. Yang

14.1 Electromagnetic Waves

Joint Services Electronics Program (Contract DAAG29-83-K-0003)

Jin Au Kong, Abdurrahman Sezginer, Tarek M. Habashy, Soon Yun Poh

Electromagnetic waves are studied with applications to microstrip antennas,[1,2] geophysical subsurface probing,[3,4] scattering from helical structures[5,6] and Smith-Purcell radiation from metallic gratings.[7] Radiation and resonance characteristics of two coupled circular microstrip disk antennas are studied rigorously using numerical techniques, matched asymptotic analysis, and the newly developed Hankel transform analysis.[1,2] The electromagnetic fields due to dipole antennas in a two-layer dissipative medium is solved using the quasistatic approximation.[3] The solutions in integral forms are calculated with brute force numerical integration methods, the multi-image approach with the steepest descent method, the normal mode approach with the residue method, and a hybrid approach with combinations of the above methods. Electromagnetic wave scattering from helical structures has been studied using the physical optics and modal approaches. The fields scattered by a thin wire helix of finite extent is investigated using physical optics and the geometrical theory of diffraction.[5] The geometrical theory of diffraction result is obtained as a high frequency limit of the physical optics approximation by applying the saddle point technique to the integral representation of the physical optics field. The electromagnetic wave scattering by a tape helix of infinite extent is studied by using Floquet wave expansion for its guided modes and scattered fields.[6] The Smith-Purcell radiation problem is solved taking into account the penetrable properties of metallic gratings.[7] When an electron beam streams across the surface of a metallic grating, emission of electromagnetic radiation occurs. It is shown that maximum radiation occurs when the surface plasmon mode is excited.

14.2 Remote Sensing with Electromagnetic Waves

National Science Foundation (Grant ECS82-03390)
Jin Au Kong, Leung Tsang

Remote sensing with electromagnetic waves has been studied with the theoretical models of random media, discrete scatterers, and randoin distribution of discrete scatterers. These models are used to stimulate snow-ice fields, forest, vegetation, and atmosphere.[8-10] Scattering and emission of electromagnetic waves by such media bounded by rough interfaces are investigated.[11-17] Multiple scattering effects of electromagnetic waves by a half-space of densely distributed discrete scatterers are studied.[18-20] The quasi-crystalline approximation is applied to truncate the hierarchy of multiple scattering equation and the Percus-Yevick result is used to represent the pair distribution function. Also, active remote sensing with dipole antennas and line sources has been studied for both monochromatic and pulse excitations.[3,4]

14.3 Acoustic Wave Propagation Studies

Schlumberger-Doll Research Center
Jin Au Kong, Shun-Lien Chuang, Abdurrahman Sezginer, Sching L. Lin, Soon Yun Poh

The transient electric field due to a step excited line source, located on the axis of a dielectric cylinder buried in another dielectric medium is evaluated by the singularity expansion method, and by an approximate explicit inversion approach.[4] The explicit inversion approach is facilitated with a technique that preserves the principle of causality. The singularity expansion method and the explicit inversion technique complement each other as the former provides accurate results for the smoothly varying parts of the time-domain response and the latter accurately reproduces abrupt changes in the response. In addition, wave scattering from a half-space of densely distributed discrete scatterers,[19,20] radiation and resonance of two coupled circular microstrip disks,[1,2] geophysical subsurface probing by dipole antennas,[3] and scattering of waves from helical structures have been studied.[5,6]

14.4 Remote Sensing of Vegetation and Soil Moisture

National Aeronautics and Space Administration (Contract NAG5-141)
Jin Au Kong, Robert T. Shin, Sching L. Lin

In the remote sensing of vegetation and soil moisture, scattering effects due to volume inhomogeneities and rough surfaces play a dominant role in the determination of radar backscattering coefficients and radiometric brightness temperatures.[9,13] The scattering of electromagnetic waves by a randomly perturbed quasi-periodic surface is studied for active remote

sensing of plowed fields.[21] Thermal emission from plowed fields has been solved using a rigorous modal theory which has been developed with the extended boundary condition approach.[11,12] These models have been used to interpret the remote sensing data from plowed fields which show strong dependence to the change in look direction relative to the row direction.[14,17] The strong fluctuation theory is also applied to the study of electromagnetic wave scattering by a layer of random discrete scatterers. The strong fluctuation theory is particularly pertinent for vegetation canopy since the contrast of permittivity between vegetation, which is essentially water droplets, and air is very large.

14.5 Passive Microwave Snowpack Experiment

National Aeronautics and Space Administration (Contract NAS5-26861)
Robert T. Shin, Jin Au Kong

Microwave radiometers at the frequencies of 10.8, 18, and 37 GHz are used to conduct the snowpack experiment in North Danville, Vermont area during the winter of 1983–1984. The test sites are prepared before snowfall so that microwave emission can be continuously monitored throughout the winter as snow accumulates on these specially prepared sites. Aluminum covered ground, rough ground, and natural ground have been prepared. Due to the weather cycles in the area, there were prominent ice layers created in the snowpacks. These ice layers cause the interference effects which modify the emission characteristics of the snowpack. Analysis of preliminary results indicates that there are distinctive interference effects due to ice layers that appear in the incidence angle dependence of the brightness temperature of the snowpack.

14.6 Remote Sensing of Earth Terrain

National Aeronautics and Space Administration (Contract NAG5-270)
Jin Au Kong, Robert T. Shin, Yaqui Jin

Numerous theoretical models that are applicable to the active and passive remote sensing of plowed fields, atmospheric precipitation, vegetation, and snow fields have been developed. The development of our theoretical models has been strongly motivated by the need to interpret the data obtained from various types of earth terrain which show distinctive characteristics. The problem of microwave scattering from sinusoidal surfaces has been studied to explain the large differences in the radar backscattering cross sections and the radiometric brightness temperatures between the cases where the incident wave vector is parallel or perpendicular to the row direction.[11,12,21] The radiative transfer theory is used to interpret the active and passive data as a function of rain rate.[8,10] Both the random medium model and the discrete scatterer model are used to study the remote sensing of vegetation fields.[9,13] Due to the non-spherical geometry of the scatterers there is strong azimuthal dependence in the observed data. Thus, the anisotropic random medium model[16] and the

discrete scatterer model with nonspherical particles[15] have been developed. In order to relate the remote sensing data to the actual physical parameters, we have studied scattering of electromagnetic waves from randomly distributed dielectric scatterers.[18-20] Both the rigorous random discrete scatterer theory and the strong fluctuation theory are used to derive the backscattering cross section in terms of the actual physical parameters and the results agree well with the data obtained from the snow fields.[14,17]

14.7 Active and Passive Remote Sensing of Ice

U.S. Navy - Office of Naval Research (Contract N00014-83-K-0258)
Jin Au Kong, Robert T. Shin, Jay Kyoon Lee

In the remote sensing of ice, one of the dominant effects in the determination of the radar backscattering cross sections and radiometric brightness temperatures is the anisotropy due to the structures on the brine inclusions in sea ice and air bubble shapes in lake ice. Due to the absence of a useful dyadic Green's function, there has been a fundamental difficulty in solving problems of radiation and scattering of electromagnetic waves in layered uniaxial media. Therefore, we have derived the dyadic Green's function for a two-layer anisotropic medium.[16] The anisotropic medium is assumed to be tilted uniaxial. The backscattering cross sections and the bistatic scattering coefficients for a two-layer anisotropic random medium have also been derived. The Born approximation is used along with the dyadic Green's function for the two-layer anisotropic medium to calculate the scattered fields.

References

1. T.M. Habashy, S.M. Ali, and J.A. Kong, "Impedance Parameters and Radiation Pattern of Two Coupled Circular Microstrip Disk Antennas," J. Appl. Phys. 54, 2, 493-506 (1983).
2. T.M. Habashy and J.A. Kong, "Asymptotic Evaluation of Resonance Frequencies for Two Coupled Circular Microstrip Disk Resonators," IEEE MTT-S International Microwave Symposium, Boston, Massachusetts, May 31-June 3, 1983.
3. T.M. Habashy, J.A. Kong, and L. Tsang, "Quasistatic Electromagnetic Fields Due to Dipole Antennas in Bounded Conducting Media," to be published.
4. A. Sezginer and J.A. Kong, "Transient Response of Line Source Excitation in Cylindrical Geometry," to be published.
5. A. Sezginer and J.A. Kong, "Physical Optics Approach for Scattering by Thin Helical Wires," Radio Sci. 18, 639-649 (1983).
6. A. Sezginer, S.L. Chuang, and J.A. Kong, "Modal Approach to Scattering of Electromagnetic Waves by a Conducting Tape Helix," IEEE Trans. Antennas Propag., to be published.
7. S.L. Chuang and J.A. Kong, "Smith-Purcell Radiation from a Charge Moving Above a Penetrable Grating," IEEE MTT-S International Microwave Symposium, Boston, Massachuetts, May 31-June 3, 1983.
8. Y.Q. Jin and J.A. Kong, "Passive and Active Remote Sensing of Atmospheric Precipitation," Appl. Opt. 22, 2535-2545 (1983).
9. J.A. Kong, S.L. Lin, S.L. Chuang, and R.T. Shin, "Remote Sensing of Soil Moisture and Vegetation," URSI Symposium, Boulder, Colorado, January 5-7, 1983.

10. Y.Q. Jin and J.A. Kong, "Mie Scattering of Electromagnetic Waves by Precipitation," Optical Society of America Topical Meeting on Optical Techniques for Remote Probing of the Atmosphere, Lake Tahoe, Nevada, January 10–12, 1983.
11. S.L. Chuang and J.A. Kong, "Wave Scattering and Guidance by Dielectric Waveguides with Periodic Surface," J. Opt. Soc. Am. 73, 669–679 (1983).
12. J.A. Kong, S.L. Lin, and S.L. Chuang, "Microwave Thermal Emission of Periodic Surface," IEEE Trans. Geosci. Remote Sensing, accepted for publication.
13. R.T. Shin and J.A. Kong, "Thermal Microwave Emission from a Scattering Medium with Rough Surfaces," URSI Symposium, Boulder, Colorado, January 5–7, 1983.
14. Y.Q. Jin and J.A. Kong, "Strong Fluctuation Theory for Electromagnetic Wave Scattering by a Layer of Random Discrete Scatterers." J. Appl. Phys., accepted for publication.
15. L. Tsang, J.A. Kong, and R.T. Shin, "Radiative Transfer Theory for Active Remote Sensing of a Layer of Nonspherical Particles," Radio Sci., accepted for publication.
16. J.K. Lee and J.A. Kong, "Dyadic Green's Functions for Layered Anisotropic Medium," Electromagnetics, accepted for publication.
17. Y.Q. Jin and J.A. Kong, "Wave Scattering by a Bounded Layer of Random Discrete Scatterers," URSI Symposium, Boulder, Colorado, January 11–14, 1984.
18. L. Tsang and J.A. Kong, "Scattering of Electromagnetic Waves from a Half-Space of Densely Distributed Dielectric Scatterers," Radio Sci. 18, 1260–1272 (1983).
19. L. Tsang and J.A. Kong, "Scattering of Electromagnetic Waves from a Half-Space of Densely Distributed Dielectric Scatterers," IEEE/APS Symposium and URSI Meeting, Houston, Texas, May 23–26, 1983.
20. L. Tsang and J.A. Kong, "Theory of Microwave Remote Sensing of Dense Medium," URSI Symposium, San Francisco, California, 1983.
21. R.T. Shin and J.A. Kong, "Scattering of Electromagnetic Waves From a Randomly Perturbed Quasi-Periodic Surface," to be published.

15. Electronic Properties of Amorphous Silicon Dioxide

Academic and Research Staff

Prof. M.A. Kastner, S. Oda

Graduate Students

J.H. Stathis

Joint Services Electronics Program (Contract DAAG29-83-K-0003)

Marc A. Kastner

Since last January a number of significant changes and advancements have taken place in our investigation of defects in amorphous SiO_2 (a-SiO_2). These advancements have been facilitated by a move to a larger lab and the acquisition of several new pieces of equipment.

Although the initial plan was to probe the intrinsic defects using photoluminescence, this has been superceded, for the time being, as a result of a remarkable discovery. We have found that the charge state of some of or all of the intrinsic defects in a-SiO_2 is changed, in a metastable way, by exposure to sub-bandgap ultraviolet light. This change is manifested in several ways: (a) a mid-gap absorption band (4.8 eV); (b) a large enhancement of the intensity of the 1.9 eV photoluminescence band; and (c) the appearance of an electron-spin-resonance (ESR) signal. The discovery of photoinduced ESR in a-SiO_2 is perhaps the most significant development. ESR provides a local probe of the structure of the defects which is complementary to the optical probes (absorption, luminescence). Experiments now in progress will enable us to correlate the photoinduced ESR and photoinduced optical effects, giving us specific information about the structure and properties of the defects instrinsic to SiO_2. Although similar studies have been performed in the past to correlate ESR and optical measurements, with some success, these studies have relied on ionizing radiation (gamma or x-ray) to generate significant numbers of paramagnetic centers from the normally diagmagnetic ground state of the intrinsic defects. Photoinduced ESR has the advantage of providing another parameter, namely the photon energy. This gives us a spectroscopic tool which we are using to measure the energy needed to change the charge state of the defect.

By changing the photon energy we have been able to resolve the ESR into several components. We have found that at the highest photon energy currently available to us, 7.9 eV, the ESR spectrum is very similar, although not identical, to that observed after gamma irradiation, and that 10^{16}-10^{17} paramagnetic centers per cubic centimeter can be photogenerated, the same number as produced by gamma rays. When lower photon energies are used part of the spectrum is absent, and the relative intensities of other components are changed. Paramagnetic centers can be generated by photon

energies at least as low as 5 eV, corresponding to roughly half the band-gap. The centers responsible for the 1.9 eV luminescence are also created by these lower photon energies, but the centers giving the mid-gap absorption are not.

Our investigation of the photo-generation of the 4.8 eV absorption and the 1.9 eV luminescence centers has been accepted for publication. We demonstrated that these two optical transitions arise at different types of defects, belying previous speculations that a single defect was responsible. We also found that the photoresponse of a-SiO_2 depends markedly on the amount of OH present in the material. SiO_2 which is specially prepared in a way which prevents the incorporation of OH is much more sensitive to ultraviolet light than material containing ~1200 ppm OH impurity.

During this past year we also initiated experiments to study electrical transport in SiO_2. These experiments use the phenomenon of internal photoemission to inject electrons or holes into the conduction or valence band of thin SiO_2 samples, where their subsequent transport and interaction with traps can be studied using the time-of-flight technique.

16. Photon Correlation Spectroscopy and Applications

Academic and Research Staff

Prof. S.-H. Chen

Graduate Students

M. Kotlarchyk, Y.S. Chao, S. Cooper, C.L. Lin, C. Mizumoto, E. Sheu

16.1 Research Program

National Science Foundation (Grant PCM81-11534)
Sow-Hsin Chen

A high-resolution spectroscopic technique based on scattered light intensity fluctuation measurement has been in use for some time. Our method is a variation of the digital time-domain pulse correlation technique using a 256-channel clipped correlator developed in the laboratory. The correlator-multichannel memory system is controlled by a PDP 11/MINC computer system which is capable of high-speed data acquisition and analysis necessary for the study of time-varying phenomena.

We have developed theoretical methods to analyze quasi-elastic light-scattering spectra from cells undergoing Brownian motions or self-propelled motions in liquid media. The methods have been successfully tested with a model bacterium Escherichia coli, and applicability of the model calculation to cells of dimensions of the order of a micron has been ascertained. The combined theoretical and experimental progress now enables us to perform the following three categories of experiments:

1. Motility characteristics of bacteria in response to external stimuli such as light and chemical
2. Study of traveling-band formation of bacteria as a result of chemotaxis
3. Study of instability and spatial pattern formation in a chemotactic band of Escherichia coli
4. Study of competition between aerotaxis and magnetotaxis in bacteria aquaspirillum magnetotacticum
5. Study of Brown Dynamics in strongly interacting colloids

Recently another powerful technique has been brought into our study of macromolecular solutions. Small angle neutron scattering has been shown to be an exceptionally versatile tool for studies of structure and interactions of strongly interacting colloids. The following experimental program is

being pursued at small angle scattering centers at Oak Ridge and Brookhaven National Laboratories.

1. Investigation of Intra- and Inter-Micellar Structure

2. Structure of Three-component Microemulsion Near the Critical Point

3. Structure and Interaction of Globular Proteins in Solutions

Publications

Chen, S.-H. and F.R. Hallett, "Determination of Molide Behavior of Prokaryotic and Eukaryotic Cells by Quasi-elastic Light Scattering," Quarterly Rev. Biophys. 15, 1 (1982).

Tanner, R.E., B. Herpigny, S.-H. Chen, and C. Rha, "Conformational Change of Protein/SDS Complexes in Solution — A Study by Dynamic Light Scattering," J. Chem. Phys. 76, 3866 (1982).

Bendedouch, D., S.-H. Chen, W.C. Kochler, and J.S. Lin, "A Method for Determination of Intra- and Inter-Particle Structure Factors of Macroions in Solution from Small Angle Neutron Scattering," J. Chem. Phys. 76, 5022 (1982).

Kotlarchyk, M., S.-H. Chen, and J S. Huang, "Temperature Dependence of Size and Polydispersity in a Three Component Microemulsion by Small Angle Neutron Scattering," J. Chem. Phys. 86, 3273 (1982).

Bendedouch, D., S.-H. Chen, and W.C. Koehler, "Structure of Ionic Micelles From Small Angle Neutron Scattering," J. Chem. Phys. 87, 153 (1983).

Bendedouch, D., S.-H. Chen, and W.C. Koehler, "Determination of Interparticle Structure Factors in Ionic Micellar Solutions by Small Angle Neutron Scattering," J. Chem. Phys. 87, 2621 (1983).

Bendedouch, D. and S.-H. Chen, "Study of Intermicellar Interaction and Structure by Small Angle Neutron Scattering," J. Chem. Phys. 87, 1653 (1983).

Bendedouch, D. and S.-H. Chen, "Structure and Interparticle Interactions of Bovine Serum Albumin in Solution Studied by Small Angle Neutron Scattering," J. Phys. Chem. 87, 1473 (1983).

Kotlarchyk, M., S.-H. Chen, and J.S. Huang, "Critical Behavior of a Microemulsion Studied by Small-Angle Neutron Scattering," Phys. Rev. A 28, 508 (1983).

Chen, S.-H., C.C. Lai, J. Rouch, and P. Tartaglia, "Critical Phenomena in a Binary Mixture of n-hexane and nitrobenzene: Analysis of viscosity and Light Scattering Data," Phys. Rev. A 27, 1086 (1983).

Chen, S.-H. and D. Bendedouch, "Structure and Interactions of Proteins in Solutions Studied by Small Angle Neutron Scattering," in H.S. Hirs and S.N. Tinashelf (Eds.), Methods in Enzymology, (Academic Press), accepted for publication.

AD-A148 109 RLE (RESEARCH LABORATORY OF ELECTRONICS) PROGRESS REPORT NUMBER 126(U) MASSACHUSETTS INST OF TECH CAMBRIDGE RESEARCH LAB OF ELECTRONICS J ALLEN ET AL. 2/3

UNCLASSIFIED JAN 84 DAAG29-83-K-0003 F/G 9/3 NL

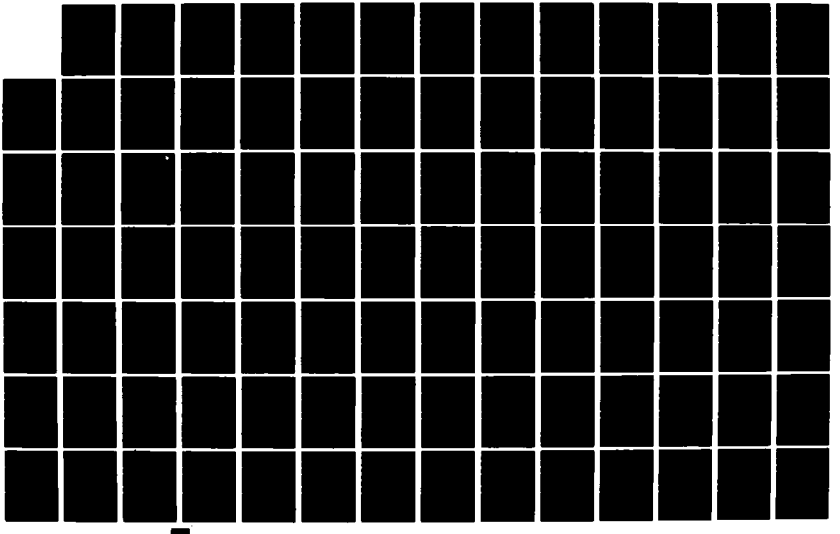

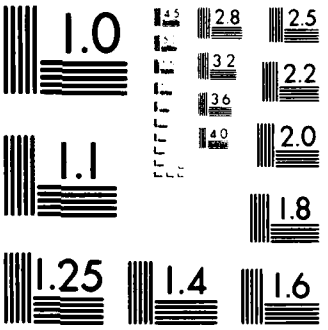

17. Submicron Structures Technology and Research

Academic and Research Staff

Prof. H.I. Smith, Dr. A.M. Hawryluk, Dr. C.M. Horwitz, Dr. J. Melngailis, Dr. C.V. Thompson, D.P. Chen, T. Yonehara

Graduate Students

E.H. Anderson, H.A. Atwater, S.Y. Chou, S.S. Dana, M. Islam, C.J. Keavney, R.F. Kwasnick, H. Lezec, J.C. Licini, I. Plotnik, M. Schattenburg, J.A. Stein, D. Summa, A.C. Warren, C.C. Wong

17.1 Submicron Structures Laboratory

The objective of the Submicron Structures Laboratory at M.I.T. is to develop techniques for fabricating surface structures having linewidths in the nanometer to micrometer range, and to use these structures in a variety of research projects. This laboratory contributes to an expansion of microsystems research at M.I.T. Fabrication techniques include various forms of lithography (optical, electron beam, x-ray, ion beam), etching (aqueous, reactive plasma, sputtering), growth (oxidation, plating, epitaxy), and deposition (evaporation, chemical vapor deposition, sputtering). The research projects of the laboratory, which are described briefly below, fall into four major categories: submicron structures fabrication techniques (no. 2); submicrometer electronics (nos. 3 to 5); crystalline films on amorphous substrates (nos. 6 to 8); periodic structures and applications (nos. 9 to 12).

17.2 Microfabrication at Linewidths of 0.1 μm and Below

Joint Services Electronics Program (Contract DAAG29-83-K-0003)
U.S. Navy - Office of Naval Research (Contract N00014-79-C-0908)
National Science Foundation (Contract ECS82-05701)
Erik H. Anderson, Andrew M. Hawryluk[3], Irving Plotnik, Henry I. Smith, Henri Lezec, John Melngailis

A variety of techniques for fabricating structures with linewidths of 0.1 μm and below are under development. These include: holographic lithography, spatial frequency doubling, x-ray lithography, and reactive-ion etching. Two new holographic techniques have been developed, which provide greatly improved control of resist profile over areas ~5.0 cm in diameter. In one technique, thick resist, of the order 0.5 μm, is used and a grating is produced in the top surface only. This is

[3]Lawrence Livermore Laboratory

shadowed obliquely with chromium and then reactive-ion etched in oxygen. The result is a periodic structure with vertical side-walls and well-controlled line-space ratio. In a second technique, an undercut profile is achieved in the resist by positioning the standing wave maximum at the resist-substrate interface. This is achieved by tilting the substrate normal out of the plane of the holographic interferometer. In spatial-frequency doubling (in collaboration with D. Ehrlich, M.I.T. Lincoln Laboratory), an ArF laser is used in conjunction with a 0.2 μm-period parent mask. In one experiment, a multilayer dielectric mirror was deposited on the mask to suppress the zero-order beam. Gratings of 0.1 μm-period (50 nm linewidth) were exposed in PMMA. These optical techniques are seldom used to expose patterns directly on experimental substrates. Instead, x-ray lithography masks are fabricated. In most cases, a Carbon K x-ray source (λ = 4.5 nm) is used in conjunction with PMMA resist to replicate the mask pattern. Details on the mask <100 Å are reproduced. Reactive-ion etching of structures with linewidths ~0.1 μm and below is investigated to improve control of cross-sectional profiles. This research employs transmission electron microscopy.

17.3 Electronic Conduction in Ultra-Narrow Silicon Inversion Layers

Joint Services Electronics Program (Contract DAAG29-83-K-0003)

Robert F. Kwasnick, Jerome C. Licini, Marc A. Kastner, John Melngailis, Patrick A. Lee

In order to study conduction phenomena in a quasi-one-dimensional electron gas, field-effect transistors have been fabricated with a ~70 nm wide and 7 μm long gate. The conductance of such metal-oxide-silicon transistors exhibits non-monotonic variation with electron density at temperatures below 15 K. The variations are largest at low electron concentrations, where the current is thermally activated, and they are the result of variations of the activation energy E_o. We find the striking result that the current is exponentially dependent on the voltage V_D along the inversion layer when E_o is much larger than its typical value. In fact, above 2 K both the temperature and V_D dependences of the current can be described by an activated form with activation energy $E_o - feV_D$ where f~0.3-0.5. This dependence on V_D is too strong to be explained by either electron heating or variable-range hopping. Instead, it indicates that the current is limited by spatial barriers which contain tunneling channels at discrete energies, as in the model of Azbel. Recently, structures with improved gate uniformity have been fabricated by evaporating Al in controlled O_2 atmosphere.

17.4 Corrugated Gate MOS Structures

Joint Services Electronics Program (Contract DAAG29-83-K-0003)

Alan C. Warren, Dimitri A. Antoniadis, John Melngailis, Henry I. Smith

The principal aim of this work is to demonstrate and understand the effects of a periodic potential variation on the conduction electrons in Si inversion layers. Toward this goal, MOS transistors are fabricated with a 0.2 μm-period chromium grating over the gate oxide. This serves as a first gate. A second gate (continuous Al sheet) is located above this, separated by 0.2 μm SiO_2. This dual-gate structure allows one to adjust the periodic potential in the Si inversion layer between source and drain. Test devices have been fabricated, and demonstrated a successful fusion of standard MOS processing and submicron structures fabrication. The immediate goal is to test devices at very low temperatures (~1-3°K) and to demonstrate the quantum effects due to a quasi-one-dimensional density of states (conduction parallel to the grating) and due to superlattice dispersion (conduction perpendicular to the gratings).

17.5 Submicron FET's in Si

Joint Services Electronics Program (Contract DAAG29-83-K-0003)
Stephen Y. Chou, Dimitri A. Antoniadis, John Melngailis, Henry I. Smith

The techniques of carbon-K x-ray lithography and reactive ion etching are being combined with standard MOS processing to fabricate Si FET devices having gate lengths ranging from 0.05 μm to 2 μm. The DC characteristics of these devices will be compared with predictions based on device-scaling models.

17.6 Graphoepitaxy of Si, Ge, and Model Materials

National Science Foundation (Contract ECS82-05701)
U.S. Navy - Office of Naval Research (Contract N0001-79-C-0908)
Carl V. Thompson, Takao Yonehara, Chee C. Wong, Henry I. Smith, Erik H. Anderson

Graphoepitaxy, in which an overlayer of film is crystallographically oriented by an artificial surface pattern, was demonstrated some years ago. However, to achieve single-crystal films on a variety of substrates for electronic and optical devices, the mechanisms of nucleation, growth, coalescence and reorientation need to be understood so that orientation spread and defects can be eliminated. We conduct basic studies of graphoepitaxy mechanisms in Si, Ge, and model materials (i.e., materials that exhibit large interfacial anisotropies and easy reorientation). This research is aimed at developing means of producing crystalline films of semiconductors and optically-active materials on insulating substrates. Two low-temperature approaches are pursued: SiI_4-chemical vapor deposition (CVD), and solid-state secondary grain growth. In the experiments on solid-state grain growth, ultra thin (less than 1000 Å) films are used. In this way, grain growth is driven by surface-energy anisotropy resulting in large grains of a specific crystallographic texture. The phenomena of surface-energy-driven secondary grain growth and solid-state agglomeration have

been observed in both Si and Ge films and appear promising for low-temperature graphoepitaxy.

17.7 Zone-Melting Recrystallization of Si for Solar Cells

U.S. Department of Energy (Contract DE-AC02-82-ER-13019)
Harry A. Atwater, Henry I. Smith, Carl V. Thompson

Zone-melting recrystallization (ZMR) of Si on SiO_2 has produced high-quality crystalline films with (100) texture, suitable for MOSFET devices. We are investigating the feasibility of using ZMR to produce low-cost solar cells. A transparent substrate, such as a low-cost glass coated with SiO_2, would serve as the window for the solar cell module. Because the substrate is insulating, back-surface-contact cells will be required. A "vertical-constriction" technique was developed which produces (100) texture in Si films 60 μm-thick. By patterning a Si film with an array of crystallization barriers prior to ZMR, a narrow distribution of in-plane orientations was achieved, a technique we call orientation filtering. Cells were fabricated by non-optimized processes in 10 μm-thick Si films. An efficiency of 7% was achieved in this initial attempt.

17.8 Zone-Melting Recrystallization of III-V Materials

U.S. Navy - Office of Naval Research (Contract N00014-79-C-0908)
Christopher J. Keavney, Harry A. Atwater, Chee C. Wong, Henry I. Smith, Carl V. Thompson

The success of Si zone-melting recrystallization (ZMR) in producing device-quality films has prompted us to investigate if similar results can be achieved with the III-V materials. These materials present special problems of adhesion, stoichiometry control, and differential vapor pressure at the melting point. Initial efforts have used InSb, which was deposited by flash evaporation. The natural oxide of InSb was found to be the best encapsulation layer. Large-grained films with <111> texture were achieved. Grains contain subboundaries where excess Sb collected and formed a eutectic phase. Techniques of planar constriction and subboundary entrainment were demonstrated.

17.9 Submicrometer-Period Gold Transmission Gratings and Zone Plates for X-Ray Spectroscopy and Microscopy

Joint Services Electronics Program (Contract DAAG29-83-K-0003)
Lawrence Livermore Laboratory (Contract 2069209)
Andrew M. Hawryluk[4], *Mark Schattenburg*[5], *Henry I. Smith, Natale M. Ceglio*[4]

[4]Lawrence Livermore Laboratory

[5]M.I.T. Center for Space Research

Gold transmission gratings with periods of 0.2 and 0.3 μm, and thicknesses ranging from 0.5 to 1 μm are fabricated using a combination of holographic lithography, x-ray lithography, and electroplating. These gratings are either supported on polyimide membranes or are made self-supporting by the addition of crossing struts. They are used for spectroscopy of the x-ray emission from plasmas produced by high-power lasers. Fresnel-zone-plate patterns are created on x-ray masks by electron-beam lithography in collaboration with IBM T.J. Watson Research Laboratory, Lincoln Laboratory and Cornell University. These are then used to x-ray expose patterns in thick resist. After electroplating, the finished structures are used in soft x-ray imaging experiments.

17.10 High-Dispersion, High-Efficiency Transmission Gratings for Astrophysical X-Ray Spectroscopy

National Aeronautics and Space Administration (Contract NGL-22-009-638)

Mark L. Schattenburg[5], Claude R. Canizares[5], Andrew M. Hawryluk[4], Henry I. Smith

Gold gratings with spatial periods of 0.1 – 10 μm make excellent dispersers for high resolution x-ray spectroscopy of astrophysical sources in the 100 eV to 10 KeV band. These gratings are planned for use in the Advanced X-ray Astrophysics Facility (AXAF) which will be launched in the early 1990's. In the region above 3 KeV, the requirements of high dispersion and high efficiency dictate the use of the finest period gratings with aspect ratios approaching 10:1. To achieve this we first expose a grating pattern in 1.5 μm thick PMMA over a gold plating base using Carbon-K x-ray lithography. To date, we have worked with gratings having periods of 0.3 or 0.2 μm (linewidth 0.15 – 0.1 μm). Gold is then electropolated into the spaces of the PMMA to a thickness of 1 μm.

17.11 Switchable Zero-Order Diffraction Gratings as Light Valves

U.S. Navy - Office of Naval Research (Contract N00014-84-K-0073)

Josephine A. Stein, Deborah A. Summa, John Melngailis, Jan A. Rajchman, Henry M. Paynter

Simple inexpensive light valves, which can be fabricated in a line-addressable matrix configuration, may make possible flat back-lighted displays or optical signal processing elements for converting electronic information into spatial light modulation. Our aim is to build and demonstrate a single such switchable light valve. This light valve would operate by displacing two facing phase gratings in a transparent medium with respect to each other. In one position the zero order of diffraction would be cancelled, in another it would not. The displacements needed are on the order of 1 μm. Techniques for fabricating the gratings have been developed and used, and the optical principles have been verified. Several schemes for producing the micromotion have been tried and a chevron configuration has evolved as the most promising. The micro-motion will be produced using the very

strong piezoelectricity of the transparent plastic poly-vinylidine fluoride (PVF_2). The geometry that is now being built involves motion producing elements in an open chevron configuration which, in effect, produces an amplification of the motion generated by the piezo-electric effect. Photolithography masks for fabricating this structure have been designed.

17.12 Studies of Surface Acoustic Wave Propagation in Gratings

National Science Foundation (Grants ECS80-17705 and ENG79-09980)
Dong-Pei Chen, Mohammed Islam, Hermann A. Haus, John Melngailis

The attenuation of Rayleigh waves due to scattering into the bulk by a periodic grating has been experimentally measured and theoretically calculated. Results have been obtained for both normal incidence and oblique incidence gratings on Y-cut Z-propagating lithium niobate. The radiation causes considerable loss in up-chirp reflective array compressors which are widely used in radar and in signal processing. Since the loss can now be predicted, the design of these devices becomes more quantitative.

The reflection of surface acoustic waves from normal incidence metal overlay gratings has been calculated using the coupling of modes formalism. The reflection is due to field shorting and to mass loading. Under special circumstances these two effects can be made to cancel. This result may be of importance in the design of surface acoustic wave transducers where reflection is an unwanted effect. Experiments are in progress to test the theory.

17.13 Collaborative Projects

The unique equipment and expertise of the Submicron Structures Laboratory has served as a resource for numerous researchers from other laboratories. Some examples are:

a) Very directional reactive-ion etching was used in the construction of a multilayer device called the joint-gate CMOS transistor. Collaboration with A.L. Robinson.

b) Submicron-period gratings, both topographic and metal overlay, have been fabricated on silicon optical detector structures by G. Ghavamishahidi. The gratings serve to reduce the lifetime of the optically generated carriers thus making the detector faster.

c) Surface-acoustic-wave transducers have been fabricated on InP by E. Wintner for the purpose of detecting waves generated by pulsed laser light which is incident on the surface.

Publications

Maby, E.W., H.A. Atwater, A.L. Keigler, and N.M. Johnson, "Electron-Beam-Induced Current Measurements in Silicon-on-Insulator Films Prepared by Zone-Melting Recrystallization," Appl. Phys. Lett. 43, 482 (1983).

Horwitz, C.M., "Rf Sputtering-Voltage Division Between Two Electrodes," J. Vac. Sci. Tech. A 1, 60 (1983).

Horwitz, C.M., "New Dryetch for Al and Al-Cu-Si Alloy: Reactively Masked Sputter Etching with SiF_4," Appl. Phys. Lett. 42, 898 (1983).

Smith, H.I., C.V. Thompson, M.W. Geis, R.A. Lemons, and M.A. Bosch, "The Mechanism of Orientation in Si Graphoepitaxy by Laser or Strip-Heater Recrystallization," J. Electrochem. Soc. 130, 2050 (1983).

Smith, H.I., M.W. Geis, C.V. Thompson, and H.A. Atwater, "Silicon-on-Insulator by Graphoepitaxy and Zone-Melting Recrystallization of Patterned Films," J. Cryst. Growth 63, 527 (1983).

Hawryluk, A.M., H.I. Smith, and D.J. Ehrlich, "Deep UV Spatial-Frequency Doubling by Combining Multilayer Mirrors with Diffraction Gratings," J. Vac. Sci. Technol. B 1, 1200 (1983).

Lezec, H.J., E.H. Anderson, and H.I. Smith, "An Improved Technique for Resist-Profile Control in Holographic Lithography," J. Vac. Sci. Technol. B 1, 1204 (1983).

Ceglio, N.M., A.M. Hawryluk, and M.L. Schattenburg, "X-Ray Phase Lens Design and Fabrication," J. Vac. Sci. Technol. B 1 1285 (1983).

Horwitz, C.M., "Hollow Cathode Reactive Sputter Etching — A New High-Rate Process," Appl. Phys. Lett. 43, 977, (1983).

Anderson, E.H., C.M. Horwitz, and H.I. Smith, "Holographic Lithography with Thick Photoresist," Appl. Phys. Lett. 49, 874 (1983).

Kwasnick, R.F., M.A. Kastner, J. Melngailis, and P.A. Lee, "Non-Monotonic Variations of the Conductance with Electron Density in ~70nm Wide Inversion Layers," Phys. Rev. Lett. 52, 224 (1984).

Atwater, H.A., C.V. Thompson, H.I. Smith, and M.W. Geis, "Orientation Filtering by Growth-Velocity Competition in Zone-Melting Recrystallization of Silicon on SiO_2," Appl. Phys. Lett. 43, 1126 (1983).

Atwater, H.A., H.I. Smith, C.V. Thompson, and M.W. Geis, "Zone Melting Recrystallization of Thick Silicon on Insulator Films," Mater. Lett., to be published.

Thompson, C.V. and H.I. Smith, "Silicon-on-Insulator by Surface-Energy-Driven Secondary Recrystallization with Patterning," Appl. Phys. Lett., March 15, 1984, to be published.

Geis, M.W., H.I. Smith, B.Y. Tsaur, J.C.C. Fan, D.J. Silversmith, R.W. Mountain, and R.L. Chapman, "Zone-Melting Recrystallization of Semiconductor Films," in J. Narayan, W.L. Brown, and R.A. Lemons (Eds.), Laser-Solid Interactions and Transient Thermal Processing of Materials, Materials Research Society Symposium Proceedings, Vol. 13 (North-Holland Publishing Co., 1983), p. 477.

Johnson, N.M., M.D. Moyer, L.E. Fennell, E.W. Maby, and H.A. Atwater, "Detection of Electronic Defects in Strip-Heater Crystallized Silicon Thin Films," in J. Narayan, W.L. Brown, and R.A. Lemons (Eds.), Laser-Solid Interactions and Transient Thermal Processing of Materials, Materials Research Society Symposium Proceedings, Vol. 13 (North-Holland Publishing Co., 1983), p. 491.

Atwood, D.T., N.M. Ceglio, H.M. Medecki, H.I. Smith, A.M. Hawryluk, T.W. Barbee, Jr., W.K. Warburton, J.H. Underwood, B.L. Henke, T.H.P. Chang, M. Hatzakis, D.P. Kern, P.J. Coane, W.W. Molzlen, A.J. Speth, G.L. Stradling, and D.W. Sweeney, "Current Developments in High Resolution X-Ray Measurements," in T.J. McIlrath and R.R. Freeman (Eds.), American Institute of Physics Conference Proceedings, Laser Techniques for Extreme Ultraviolet Spectroscopy, Boulder, Colorado, 1982.

Keavney, C.J., H.A. Atwater, H.I. Smith, and M.W. Geis, "Zone Melting Recrystallization of InSb on

Oxidized Silicon Wafers," Electrochemical Society Symposium on III-V Opto-Electronics Epitaxy and Device-Related Processes, San Francisco, California, May 1983.

Smith, H.I., E.H. Anderson, and M.L. Schattenburg, "Planar Techniques for Fabricating X-Ray Diffraction Gratings and Zone Plates," in D. Rudolph and G. Schmahl (Eds.), Symposium on X-Ray Microscopy, Gottingen, Federal Republic of Germany, Sept. 14-16, 1983 (Springer-Verlag, 1983).

Wong, C.C., C.J. Keavney, H.A. Atwater, C.V. Thompson, and H.I. Smith, "Zone Melting Recrystallization of InSb Films on Oxidized Si Wafers," presented at the Materials Research Society Symposium, Boston, Massachusetts, November 1983, to be published in Materials Research Society Symposia Proceedings, "Energy Beam-Solid Interactions and Transient Thermal Processing," (Elsevier Science Publishing Co.).

Yonehara, T., C.V. Thompson, and H.I. Smith, "Abnormal Grain Growth in Ultra-Thin Films of Germanium on Insulator," presented at the Materials Research Society Symposium, Boston, Massachusetts, November 1983.

Smith, H.I., C.V. Thompson, M.W. Geis, H.A. Atwater, T. Yonehara, and C.C. Wong, "Graphoepitaxy and Zone Melting Recrystallization of Patterned Films," to be published in N.M. Johnson and J.C.C. Fan (Eds.), Materials Research Society Symposia Proceedings, "Energy Beam-Solid Interactions and Transient Thermal Processing," (Elsevier Science Publishing Co., 1984).

Kwasnick, R.F., M.A. Kastner, and J. Melngailis, "Electronic Conduction in Ultra-Narrow Si Inversion Layers," presented at March 1983 Meeting of the American Physical Society, Bull. Am. Phys. Soc. 28, 322 (193).

Warren, A.C., D.A. Antoniadis, J. Melngailis, and H.I. Smith, "Submicrometer-Period Channel Modulation of a MOSFET," presented at the 1983 International Symposium on Electron, Ion, and Photon beams, Los Angeles, California, May 31-June 3, 1983.

Schattenberg, M.L., C.R. Canizares, H.I. Smith, and A.M. Hawryluk, "Submicrometer-Period Transmission Diffraction Gratings for X-Ray Astronomy," presented at the 1983 Symposium on Electron, Ion and Photon Beams, Los Angeles, California, May 31-June 3, 1983.

Anderson, E.H. and H.I. Smith, "TEM Analysis of Vertical-Slab Cross Section of Submicrometer Structures," presented at the 1983 International Symposium on Electron, Ion, and Photon Beams, Los Angeles, California, May 31-June 3, 1983.

Thompson, C.V., and H.I. Smith, "Silicon-on-Insulator by Solid State Surface-Energy-Drive Secondary Recrystallization," 1983 Electronic Materials Conference, Burlington, Vermont, June 1983.

Smith, H.I., "Graphoepitaxy to Circumvent Lattice Matching Constraints," presented at the Fourth International Conference on Integrated Optics and Optical Fiber Communication (Post-Conference Meeting), Tokyo, Japan, July 2, 1983.

Smith, H.I., "Graphoepitaxy and Zone-Melting Recrystallization of Patterned Films," presented at the VII International Conference on Crystal Growth, Stuttgart, Federal Republic of Germany, September 12-16, 1983.

Thompson, C.V. and H.I. Smith, "Silicon-on-Insulator by Surface-Energy-Driven Secondary Recrystallization with Patterning," presented at the VII International Conference on Crystal Growth, Stuttgart, Federal Republic of Germany, September 12-16, 1983.

Atwater, H.A., "Control of silicon Film Recrystallization Using Lithography with Application to Photovoltaics," S.M. Thesis, Department of Electrical Engineering and Computer Science, Massachusetts Institute of Technology, June 1983. Also VLSI Memo 83-149, July 1983.

Keavney, C.J., "Zone-Melting Recrystallization of InSb on Oxidized Silicon Wafers," S.M. Thesis, Department of Materials Science and Engineering, Massachusetts Institute of Technology, June 1983.

Ahlers, E.D., "Method of Photolithographic Projection System Characterization," B.S./M.S. Thesis, Department of Electrical Engineering and Computer Science, Massachusetts Institute of

Technology, June 1983.

Dana, S.S. "Nucleation on Surface Relief Structures by Chemical Vapor Deposition," Ph.D. Thesis, Department of Physics, Massachusetts Institute of Technology, September 1983.

Domestic Patents Filed

"Orientation Filtering," H.I. Smith, C.V. Thompson, H.A. Atwater, and M.W. Geis, filed April 1, 1983.

"Thick Crystalline Films on Foreign Substrates," H.I. Smith, H.A. Atwater, and M.W. Geis, filed May 9, 1983.

Plasma Dynamics

18. Plasma Dynamics

Academic and Research Staff

Prof. G. Bekefi, Prof. A. Bers, Prof. B. Coppi, Prof. T.H. Dupree, Prof. L.M. Lidsky, Prof. J.E. McCune, Prof. M. Porkolab, Prof. L.D. Smullin, Dr. R.H. Berman, Dr. G. Bertin, Dr. P.T. Bonoli, Dr. T. Boutros-Ghali, Dr. K-I. Chen, Dr. R.C. Englade, Dr. V. Fuchs[6], Dr. D. Hewett[7], Dr. K. Hizanides, Dr. J.H. Irby, Dr. V.B. Krapchev, Dr. J.S. Levine, Dr. S.C. Luckhardt, Dr. P.A. Politzer, Dr. A.K. Ram, Dr. J. Ramos, Dr. M.E. Read, Dr. N.N. Sharky, Dr. R.E. Shefer, Dr. L.E. Sugiyama, Dr. D.J. Tetreault, E.W. Fitzgerald, R. Li, I. Mastovsky, Y.Z. Yin, M.-L. Xue.

Graduate Students

J.G. Aspinall, P.E. Cavoulacos, K.D. Cogswell, G.B. Crew, J. Fajans, A.S. Fisher, M.E. Foord, G. Francis, R.C. Garner, T.R. Gentile, P.J. Gierszewski, K.E. Hackett, A.M. Hamza, L.P. Harten, D. Hinshelwood, D.A. Humphreys, K.D. Jacob, M. Kanapathipillai, D.A. Kirkpatrick, S.F. Knowlton, B.L. LaBombard, W.P. Marable, J.J. Martinell, M.E. Mauel, M.J. Mayberry, F.S. McDermott, A. Pachtman, Y. Pu, C.M. Rappaport, R.R. Rohatgi, S.E. Rowley, D.R. Thayer, S.H. Voldman

18.1 Relativistic Electron Beams and Generation of Coherent Electromagnetic Radiation

National Science Foundation (Grants ECS82-00646 and ECS82-13485)
U.S. Air Force - Office of Scientific Research (Contracts F33615-81-K-1426, F49620-83-C-0008, and AFOSR-84-0026)
U.S. Navy - Office of Naval Research (Contract N00014-83-K-2024)
Sandia National Laboratory (Contracts 31-5606 and 48-5725)
George Bekefi, Ruth E. Shefer

Relativistic electron beam research at M.I.T. focuses on the generation of intense coherent electromagnetic radiation in the centimeter, millimeter and submillimeter wavelength ranges. The primary radiation mechanism which is being studied at the present time is the free electron laser instability which is excited when an electron beam passes through a spatially periodic, transverse magnetic field (wiggler field). This instability is characterized by axial electron bunching and has emission wavelengths associated with the Doppler upshifted wiggler periodicity.

---

[6] IREQ-Hydro Quebec, Montreal, Canada

[7] Plasma Fusion Center, M.I.T.

Intense coherent sources of centimeter and millimeter wavelength radiation find applications in many diverse fields of research and technology including heating and diagnostics of thermonuclear fusion plasmas, photochemistry, solid state physics, and biophysics. One advantage of free electron systems such as the free electron laser are the very high predicted efficiencies which may be attained. Another important advantage is frequency tunability which results from the fact that the radiation frequency is not locked to an atomic or molecular transition or to an electromagnetic mode of a resonant structure but is instead determined by the velocity of the beam electrons.

The experimental facilities available to this group include three pulsed high voltage accelerators capable of delivering up to 100 kA of current at 0.5 to 1.5 MV. Their characteristics are summarized below:

Pulserad 110 A

Voltage	1.5 MV
Current	20 kA
Pulse Length	30 ns

Pulserad 615 MR

Voltage	0.5 MV
Current	4 kA
Pulse Length	1μs

Nereus

Voltage	0.6 MV
Current	100 kA
Pulse Length	30 ns

In the following sections, various radiation generation experiments presently being carried using the above electron beam generators are discussed.

a. The Rippled Field Magnetron (Cross-Field Free Electron Laser)

To achieve efficient conversion of energy from a stream of free electrons to electromagnetic radiation, near synchronism must be attained between the velocity of the electrons and the phase velocity of the wave. In cross-field devices, of which the magnetron is a typical example, this synchronism occurs between electrons undergoing a $v = E_0^{\prime} \times B_0^{\prime}$ drift in orthogonal electric and magnetic fields, and an electromagnetic wave whose velocity is reduced by a slow-wave structure comprised of a periodic assembly of resonant cavities. The complex system of closely spaced resonators embedded in the anode block limits the conventional magnetron to wavelengths in the centimeter range. Moreover, at high voltages typical of relativistic magnetrons, RF or dc breakdown in the electron beam interaction space, and at the sharp resonator edges poses serious problems.

The rippled-field magnetron is a novel source of coherent radiation devoid of physical slow-wave structures and capable of radiating at much higher frequencies than a conventional magnetron. The

configuration of the anode and cathode is similar to the so-called "smooth-bore" magnetron, but it differs from the latter in that the electrons are subjected to an additional field, an azimuthally periodic (wiggler) magnetic field B_ω oriented transversely to the flow velocity v. The resulting $-e\vec{v} \times \vec{B}_\omega$ force gives the electrons an undulatory motion which effectively increases their velocity, and allows them to become synchronous with one of the fast TE or TM electromagnetic modes (phase velocity > c) characteristic of the smooth-bore magnetron.

The magnetron configuration is cylindrical rather than linear as in conventional FEL's, and the system is therefore very compact. The cylindrical geometry also allows for a continuous circulation of the growing electromagnetic wave, and because of this internal feedback, the rippled-field magnetron is basically an oscillator rather than an amplifier as is the case of the FEL.

We have obtained measurements of millimeter-wave emission from the rippled field magnetron.[1] In these experiments the magnetic wiggler field is produced by a periodic assembly of samarium-cobalt bar magnets positioned behind the smooth, stainless steel electrodes. Maximum radiated power in the 26.5-60 GHz frequency band is obtained with a wiggler periodicity of 2.53 cm and a wiggler field amplitude of 1.96 kG. Under these conditions a narrow band spectral line is observed with a line width at the half power points of less than 2.2 GHz. The center frequency of this line can be varied from 32 GHz to 46 GHz by varying B_z between 5.8 kG and 9 kG. No deterioration in line profile is observed over this range. The total radiated power above 26.5 GHz measured with this wiggler is 300 kW; which is more than a factor of thirty above the broadband noise observed with no wiggler.

We note that this device differs from the conventional FEL in that the electron source (the cathode) and the acceleration region (the anode-cathode gap) are integral parts of the RF interaction space. This makes for high space-charge densities which result in large growth rates of the instability; but it has the disadvantages that the current density and position of the interacting electrons in the gap are difficult to control. In the section below we describe an experiment in which a thin, hollow rotating electron beam is injected into the cylindrical wiggler structure. This configuration eliminates the need for the accelerating anode-cathode electric field E_o and allows us to easily control both the current density and the beam dynamics in the interaction gap.

b. A Rotating Beam Free Electron Laser

In this section we describe a variation on the rippled field magnetron in which a rotating electron beam interacts with a rippled magnetic field.[2] This work is being carried out at the University of Maryland in collaboration with Prof. W.W. Destler.

In the experiments, a 12 cm diameter, hollow, rotating electron beam (2 MeV, 1-2 kA, 5 ns) is generated by passing a hollow non-rotating beam through a narrow magnetic cusp. The rotating beam performs helical orbits ($\beta_\theta \simeq .95$, $\beta_z \simeq .2$) downstream of the cusp in an axial guide field of about 1450 Gauss. Radiation is produced by the interaction of the beam with an azimuthally periodic wiggler magnetic field produced by samarium cobalt magnets located interior and exterior to the

beam. In the present work, the wiggler field has an amplitude of about 1300 Gauss, six spatial periods around the azimuth, and a periodicity of 6.28 cm.

We have observed at least 200 kW of radiation above 91 GHz in initial experiments, a result consistent with the frequency expected for a linear free electron laser operating with comparable parameters. Radiation at these frequencies is not observed in the absence of the wiggler field. Numerical calculations of the electron orbits in the combined axial and wiggler fields indicate that the orbits are relatively unperturbed in the r–θ plane and that the perturbation of the orbits due to the wiggler is primarily axial, as desired. Measurements of the actual circulating current exciting the wiggler region with and without the wiggler magnets in place confirm that the wiggler field does not have a seriously adverse effect on the electron orbits.

Measurements of the radiation spectrum using a grating spectrometer and studies of the effects of wiggler amplitude and periodicity are currently underway.

c. A Low Voltage Free Electron Laser

Many theoretical studies have been devoted to free electron lasers comprised of an electron stream traversing a periodic, circularly polarized magnetic (wiggler) field, as can be generated with bifilar, helical, current-carrying wires. The electron dynamics in these systems exhibit simple properties that have considerable theoretical appeal. However, from the experimental point of view large amplitude, circularly polarized wiggler fields are difficult to attain because of the large currents that are required in their windings; and for long pulse or steady-state operation, bifilar conductors may be entirely out of the question. In view of the above, studies of free electron lasers have begun in which the electron beam is subjected to a periodic, linearly polarized transverse magnetic field such as can be produced, for example, by an assembly of permanent magnets.

An experiment is underway to investigate the microwave and electron beam characteristics of a Free Electron Laser amplifier using a linear wiggler field. In this experiment, a 35 keV, 1A electron beam is produced by a thermionic cathode. The beam pulse width is 1–5 μsec, with a 0.001 duty cycle. A guiding axial magnetic field, generated by a series of D.C. powered, water cooled solenoid coils, is variable up to a maximum of B_o = 3 kG. This field both prevents radial expansion of the beam and allows investigation of the FEL gain near the cyclotron resonance condition, $k_o V_z - \Omega_o/\gamma = 0$. ($K_o = 2\pi/\ell$, ℓ = wiggler period, $\Omega_o = (eB_o/m_o)$, $\gamma = (1 - \beta^2)^{-1/2}$). When this resonance condition is satisfied, the cyclotron wavelength of an electron in the uniform guiding magnetic field equals the wiggler periodicity. Enhanced growth of the radiation field is predicted as this condition is approached.

A set of 480 samarium cobalt permanent magnets produces a linearly polarized wiggler magnetic field. The wiggler is 60 periods long, with periodicity ℓ = 2.0 cm. The wiggler amplitude is variable from 0.1 to 1.0 kG.

The beam drift tube is a length of WR-137 band rectangular waveguide. The 6 GHz FEL output frequency lies in the lowest (TE_{10}) mode of the waveguide. A calibrated crystal detector and a conventional spectrum analyzer are used to make microwave power and frequency measurements. Determination of the electron beam axial velocity distribution is made using a gridded Faraday cup. At these low beam voltages, it is possible to use a repelling grid in the cup. Measurement of the beam properties and the microwaves can be made simultaneously.

d. An Intermediate Energy, Long Pulse Free Electron Laser

An intermediate energy free electron laser experiment designed to investigate cyclotron resonance effects is being carried out on the Pulserad 615 MR electron beam facility. The experimental parameters are given in the table below:

Beam Energy (keV)	150–200
Beam Current Density (A–cm^{-2})	70
Pulse Length (μs)	2
Axial Magnetic Field (kG)	0.7–7.0
Wiggler Field Amplitude (kG)	0–1.5
Wiggler Period (cm)	3.3
Number of Periods	50

The Pulserad 615 MR power source is a Marx generator which produces a repeatable, flat accelerating voltage pulse. It has the capability of operating with a thermionic (hot cathode) electron gun. In this experiment the thermionic cathode is immersed in a shaped focusing magnetic field. The perpendicular energy of the emitted electrons is estimated to be less than one percent of their total energy. This characteristic of the electron beam is important in free electron devices from the standpoint of producing coherent radiation with high efficiency.

The beam propagates in a two meter long drift tube, guided by a uniform axial magnetic field that can be varied between 0.7 and 7.0 kG. The wiggler fields are generated by a bifilar helical winding. An adjustable, adiabatic entrance profile is produced by staggering the wiggler termination windings.[3] This termination scheme allows us to increase the wiggler field amplitude to its full value slowly and with any amplitude profile desired at the upstream end of the wiggler. Computer simulations have shown that the entrance profile is very important in preserving low beam energy spread in both the transverse and axial directions as the beam enters the wiggler field. The system has been designed so that under normal operating conditions, the emitted radiation propagates in the lowest mode of the cylindrical drift tube.

We have observed microwave power levels of over 10 kW at approximately 10 GHz. Spectra observed with an X-band waveguide dispersive line show that most of the power is concentrated in a narrow peak ($\Delta f/f < .01$). Preliminary results indicate that the output frequency increases with beam energy with the functional form predicted by theory.

Measurements of the beam current have been made in the vicinity of the resonance $k_w v_o = \Omega_o$ that occurs when the cyclotron frequency of the guide magnetic field equals the frequency $k_w v_o$ associated with the wiggler (k_w = wiggler wave number). As the axial magnetic field is increased and passes through the resonance, the beam current transmitted through the wiggler drops sharply. Beyond this point, the current increases slowly to its original value. Measurements of microwave power levels and spectra near resonance are underway.

e. A Submillimeter Free Electron Laser using a High Quality Electron Beam

In this experiment, a high current density, high energy electron beam is used to produce submillimeter wavelength radiation. The measured parameters of the electron beam are:

Beam Voltage	1.6 MV
Beam Current Density	200 A–cm^{-2}
Axial Momentum Spread	$\leq$ 1%

Other experimental parameters are as follows:

Wiggler Period	2.0 cm
Number of Periods	50
Wiggler Field Amplitude	1200 Gauss
Output Frequency	456 GHz
Theoretical Single Pass Gain	23 dB
Saturated Efficiency	0.75%

The M.I.T. Pulserad 110A accelerator facility is used in conjunction with a five stage electrostatically focused field emission electron gun to produce a high quality intense relativistic electron beam. The beam is then guided into a bifilar helical wiggler field by means of a short solenoidal coil which acts as a focusing lens. The coil is positioned upstream of the wiggler and obviates the necessity of having a guiding magnetic field in the wiggler region. The lack of a guide field in the wiggler region eliminates the possibility of exciting the cyclotron maser instability.

The beam quality has been determined by measurements of beam emittance and beam momentum spread.[4] Emittance measurements were carried out by allowing the beam to impinge on an array of pinholes in a brass disk, and then observing the transmitted beamlets on a fluorescent screen at a known distance downstream. We find that the normalized emittance is $\leq$ 50 mr–cm. Beam momentum spread measurements were carried out using a magnetic spectrometer. The spectrometer is of the Browne-Buechner type and is capable of a resolution in $\gamma v_{\parallel}$ of less than 0.1%. Both time integrated and time resolved measurements carried out on this electron beam show an axial momentum spread of less than one percent.

References

1. G. Bekefi, R.E. Shefer, and B.D. Nevins, Proc. Int. Conf. on Lasers '82, in R.C. Powell (Ed.) (STS Press, McLean, Virginia 1982), p. 136.

2. G. Bekefi, R.E. Shefer, and W.W. Destler, Appl. Phys. Lett. 44, 280 (1984).
3. J. Fajans, J. Appl. Phys. 55, Jan. 1, 1984.
4. R.E. Shefer, D.A. Kirkpatrick, and G. Bekefi, Bull. Am. Phys. Soc. 28, 1063 (1983).

18.2 Tokamak Research: RF Heating and Current Drive

U.S. Department of Energy (Contract DE-AC02-78ET-51013)

George Bekefi, Miklos Porkolab, Kuo-in Chen, Stanley C. Luckhardt

The main theme of the Versator II program is to understand interactions between externally excited lower-hybrid waves and tokamak plasmas. For typical tokamak plasmas, the lower-hybrid wave has a frequency in the range of a few hundred MHz to a few GHz. In current experiments, the lower-hybrid wave is generated by a RF system which consists of a 150 kW, 800 MHz klystron, and a waveguide power splitter with four output channels. The phase of each output can be continuously adjusted (0° ~ 360°) with mechanical phase shifters. Such phase control allows traveling wave spectra to be launched either parallel or antiparallel to the direction of the electron ohmic drift, $\Delta\Phi = \pm 90°$, or a standing wave spectrum can be excited with $\Delta\Phi = 180°$.

Versator II is a medium-size tokamak with the following important physical and plasma parameters: major radius R = 40.5 cm, limiter radius a = 13 cm, toroidal field B_T ~ (8–15) kG, plasma current I_p ~ (30–60) kA, discharge length τ_{pulse} ~ (30–40) ms, central electron temperature T_{eo} ~ (250–450) eV, central ion temperature T_{io} ~ (120–180) eV, line average density $\bar{n}_e$ ~ (0.1–3) x $10^{13} cm^{-3}$ and Z_{eff} ~ 2.

The phase velocity of the lower-hybrid wave can be controlled by adjusting phases between launching waveguides. With proper phase velocity and plasma parameters (e.g., density, toroidal magnetic field, etc.), the lower-hybrid wave will interact with either plasma electrons or ions. Consequently, the physics problems of heating (electron or ion) and current generation by lower-hybrid waves can be studied.

The emphases of these experiments in 1983 are on the toroidal effects of wave penetration; by making a comparison of launching waves through a top port and a side port at the same toroidal position. Important experimental results and detailed diagnostic measurements are summarized below.

Present Status

18.3 I. Lower-Hybrid Current Drive (LHCD) Experiment

18.3.1 Top Launching vs. Side Launching

Ray tracing theory[1] has shown that traveling waves launched from the top of the torus in the direction $\hat{S} = \vec{B}_T \cdot \vec{I}_p \hat{\Phi}/|B_T||I_p|$ (where $\hat{\Phi}$ is the toroidal unit vector) experience an upshift in their $n_{\parallel}(= ck_{\parallel}/\omega)$ due to toroidal effects. Generally, for top launching in the $+\hat{S}$ direction, the wave slows down along field lines and is often absorbed in the first poloidal transit through the center of the plasma. However, when waves are launched from the midplane on the outside, $n_{\parallel}$ downshifted initially, making first pass absorption less likely due to the difficulty in satisfying the Landau resonance condition. In general, top launching is expected to give improved power absorption efficiency and an interaction with lower energy electron when compared with side launching. Measurement of comparative current drive efficiency with couplers mounted on the top and side of the torus therefore appears to be a test of the ray tracing prediction of toroidal shifts in $n_{\parallel}$. Nevertheless, it should be noted that according to a very simple picture of Fisch current drive theory,[2] the merit factor of current drive $I_{RF}/P_{RF} \propto 1/n_{\parallel}^2$, so the $n_{\parallel}$ upshift is expected to result in reduced current drive efficiency.

Table 1

	4-Guide Top	4-Guide Side	6-Guide Side
$\Delta\Phi$	+90°	+90°	+90°
$N_{\parallel o}^{PEAK}$	8	8	8
$\bar{n}_e$	$4\times10^{12}cm^{-3}$	$4\times10^{12}cm^{-3}$	$4\times10^{12}cm^{-3}$
I_p	36 kA	36 kA	32 kA
P_{NET}	13 kW	11 kW	8 kW
ΔI	3.0 kA	5.3 kA	3.5 kA
Δt	5 msec	5 msec	5 msec
$\tau_{L/R} \simeq$	15 msec	15 msec	15 msec
$I_{RF} \simeq \frac{\Delta I}{\Delta t}\tau_{L/R}$	9.0 kA	16 kA	13 kA
$S = \bar{n}_{15}\frac{R_o I_{RF}}{P_{NET}}$	0.11	0.23	0.26

A comparison of current drive efficiencies between side and top launching experiments

The basic experiment results are shown in Table 1 where comparison is made in terms of the scaling parameter S defined as $S = (I_{RF}/P_{NET})\,\bar{n}_{15}R_0$. It appears from these initial experiments that the side couplers have a factor of 2–3 higher current drive efficiency than the top couplers. This reduction in S may be caused by the toroidal effects on $n_{\perp}$ predicted by ray tracing theory.

18.3.2 Particle Confinement

Observed density increases during LHCD experiments have been investigated in detail in 1983. These density increases can possibly be caused either by extra influxes of neutral hydrogen and impurities or improved confinement produced by the RF. Spectroscopically, we have measured emissions of neutral hydrogen and impurities. Specifically, H_α emission is found to decrease; thus, the increased density is not the result of increased ionization of hydrogen and impurities.

The global particle balance equation $(dN_e/dt) = S - (N_e/\tau_p)$ (where N_e is the total number of electrons in the plasma, S is the source term, τ_p is the global particle confinement time) is used to deduce τ_p (see Fig. 18–1).

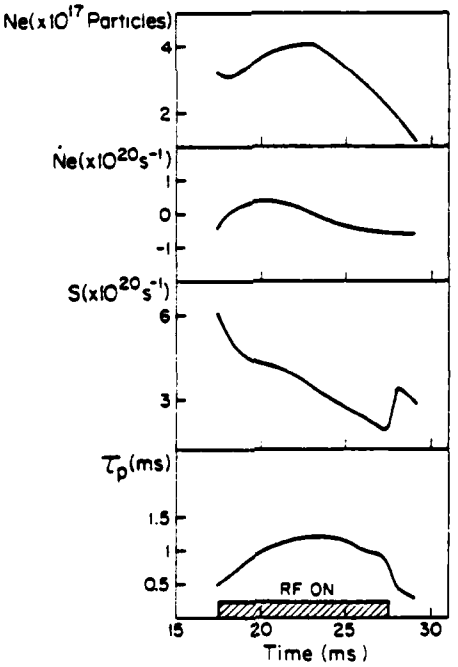

Figure 18-1: Analysis of global particle confinement

It appears the τ_p increases by approximately a factor of two during LHCD. This increase is

correlated with stabilization of the Parail–Pogutse runaway tail mode. This mode is normally present during low density ohmic discharges, and can be stabilized during RF current drive. When the instability does occur during the RF phase, the density suddenly decreases.

18.3.3 Current Profiles

Current profile changes can induce toroidal loop voltages inside the plasma, produce additional current, and complicate the interpretation of the current drive data. Therefore, a detailed study of current profile behavior during LHCD was carried out. One way to obtain information about the current profile is to do the analysis of the plasma equilibrium data. This analysis gives the time dependence of the quantity $\ell_i/2 + \beta_0$ (where ℓ_i is the internal inductance and β_0 the poloidal β value) through the Shafranov equilibrium condition. In the current drive density regime, β_0 is usually taken as small compared to $\ell_i/2$ so the data analysis gives essentially the time dependence of $\ell_i/2$. Increases in ℓ_i indicate the current profile is becoming more peaked and decreases indicate the current profile is flattening.

In the low density ohmic discharges we find that the value of ℓ_i is typically 2–3, and increases slowly as plasma current decays near the end of the discharge. During LHCD, the measurement shows that the current profile is essentially the same as that of the ohmic plasma and that internally induced voltages do not constitute significantly to the current in the Versator current drive experiment. Calculations of ℓ_i from model current profiles indicate that the current is peaked on axis with a radius of ~ 4 cm, r/a ~ 0.3.

Another way to obtain information on current profiles is to measure spatial profile of hard x-ray emissions from the plasma. Hard x-ray measurements have shown a very peaked spatial profile (FWHM ~ 6 cm or possibly smaller) before and during LHCD. This profile measurement seems to be consistent with previous $\ell_i/2 + \beta_0$ measurements.

18.3.4 Density Fluctuations and Wave Propagation

The microwave scattering experiment on Versator II uses scattering of a 140 GHz beam to measure density fluctuations. This experiment has been active, looking at both low-frequency fluctuations (20–500 kHz) thought to be associated with transport, and, more recently, the externally-driven 800 MHz lower-hybrid wave. The low-frequency fluctuations have been studied during LHCD; exponential frequency spectra have been measured. During current-drive the spectra are found to steepen as the density fluctuations (at fixed wavevector 7 cm^{-1}) decrease. The scattering experiment is now being used to detect the 800 MHz lower-hybrid wave, which is externally launched by a phased waveguide grill. To date a clean signal has been obtained and the wave has been observed. These experiments will continue in an attempt to study the propagation of the lower-hybrid wave in Versator plasmas.

18.3.5 Bulk and Tail Electrons

Soft and hard x-ray pulse height analysis (PHA) diagnostics are routinely used on Versator II to study the behavior of the superthermal electron tail during lower-hybrid current drive and heating experiments. A Si(Li) detector soft x-ray (1-30 keV) diagnostic is capable of radially scanning the entire plasma cross section from the side while a 3" x 3" NaI(Tℓ) hard x-ray (20 keV–1 MeV) detector can scan the entire plasma cross section from below. Measurements in the low density LHCD regime ($\bar{n}_e \lesssim 6 \times 10^{12}$ cm^{-3}) show the presence of a high energy electron tail with maximum detected energies exceeding 300 keV located in the central 5 cm of the 26 cm diameter plasma.

Time resolved measurements of soft and hard x-rays have shown a strong bursting behavior which correlates with the Parail-Pogutse runaway tail mode instability routinely observed in the low density current drive regime (see Fig. 18–2). The x-ray bursts originate from the central region of the plasma, but are much stronger in the top half of the plasma suggesting the possibility of ripple trapping of some electrons when they are pitch angle scattered from the parallel to the perpendicular direction by the instability. Future experiments will take place after the Versator upgrade is complete, and this will allow the OH electric field to be eliminated during current drive. Then, an attempt will be made to measure the anisotropy of the high energy RF sustained electron tail by scanning a NaI(Tℓ) detector in angle with respect to the magnetic field.

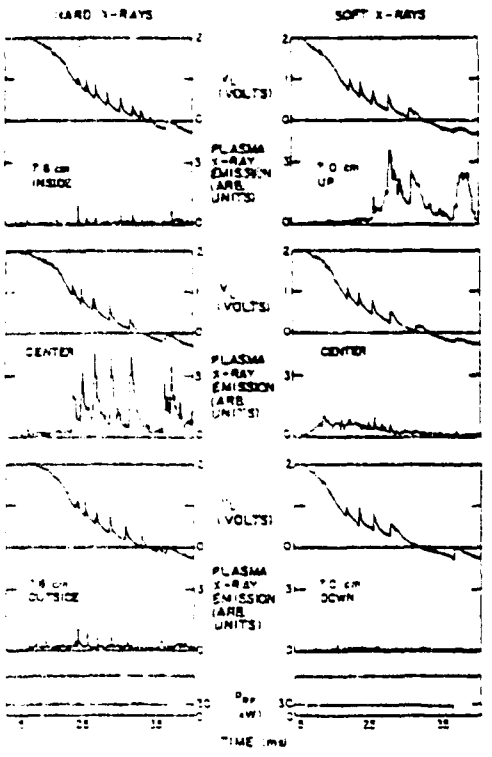

Figure 18-2: Parail-Pogutse instability observed by hard and soft x-ray diagnostics during LHCD

At higher densities, in the theoretical electron heating regime ($8 \times 10^{12} \lesssim \bar{n}_e \lesssim 1.5 \times 10^{13}$), a clear enhancement (up to x10) of the soft x-ray superthermal tail (4–25 keV) is observed. Under these conditions, the Parail-Pogutse instabilitiy is not usually present, either with or without RF. However, the electron temperature, obtained by fitting the slope of the continuum soft x-ray spectrum, does not change during RF injection. This result is confirmed by Thomson scattering measurements. Future experiments are needed to explain why the RF generated electron tail is not sufficient to thermalize with bulk electrons to produce bulk heating in this density regime.

18.3.6 $\omega < \omega_{pe}$ Emission Measurements

Emissions in frequency range from 1 GHz to 12.4 GHz have been measured during LHCD by a high frequency probe located behind the limiter radius. The signal is composed of a slowly varying "background" signal plus periodic bursting signals which are due to the waves driven unstable by the presence of an anisotropic tail of runaway electrons. The constant background signal ($f < 4$ GHz) during discharges with LHRF goes up by 10 dB compared to ohmic discharges (see Fig. 18–3). The frequency spectrum of bursting signals is broadened (significant signal extended out to 12 GHz) during LHCD compared to ohmic discharges (< 6 GHz) (see Fig. 18–4). The burst period is also changed from (0.25 ms–1 ms) for the ohmic case to (1 ms–3 ms) for the RF case. The frequency spectra of these bursting signals seems to be consistent with a theoretical model[3] in which waves are driven unstable at the anomalous Doppler resonance which only weakly damped at the Cerenkov resonance.

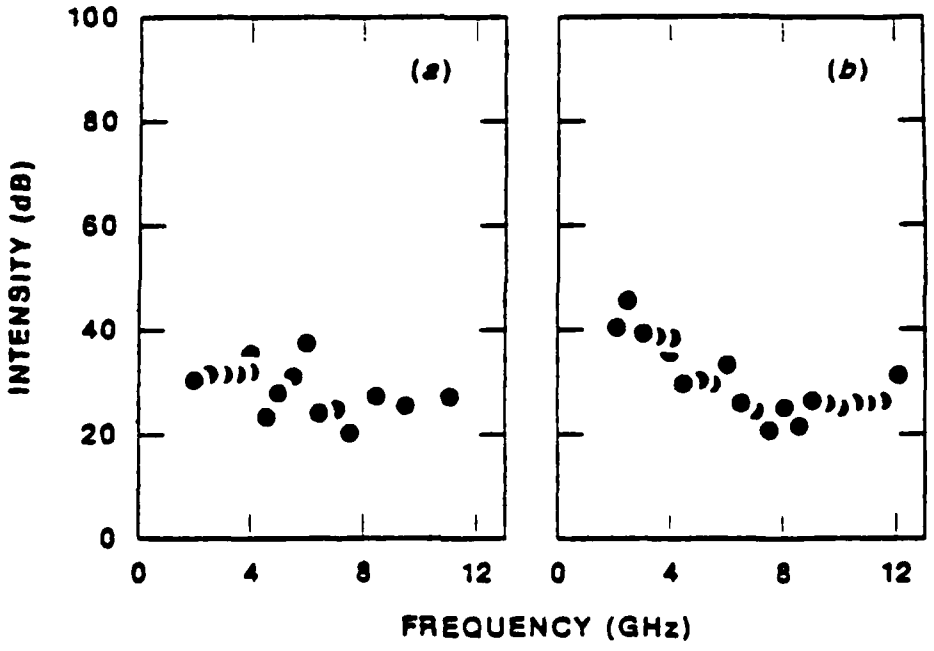

Figure 18-3: Spectra of the steady background emission at $\bar{n}_e = 4.5 \times 10^{12} cm^{-3}$ for (a) Ohmic (b) LHCD discharges

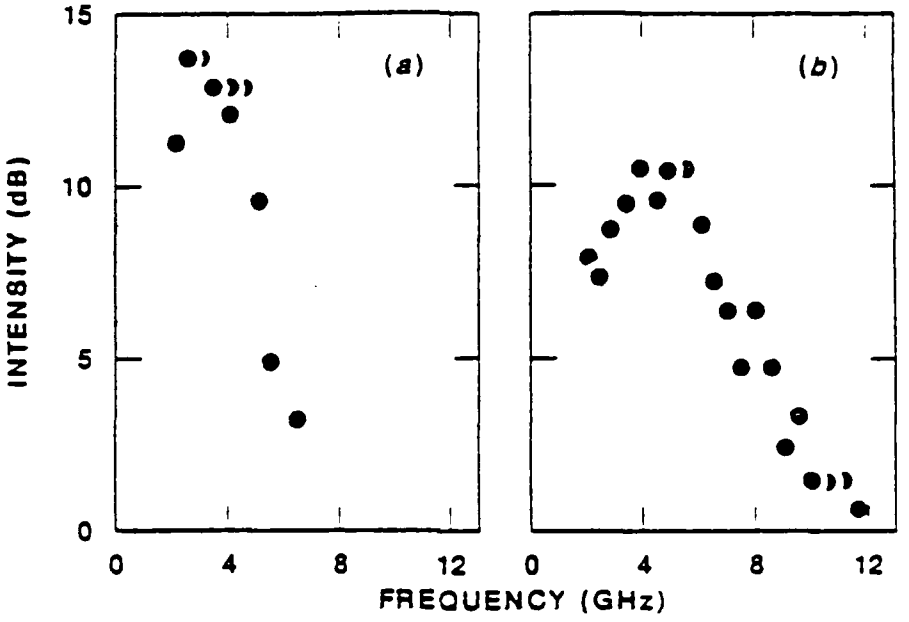

Figure 18-4: Spectra of the intense bursts of emission plotted in dB above the background emission level of $\bar{n}_e = 4.5 \times 10^{12} cm^{-3}$ for (a) Ohmic (b) LHCD discharges

II. Lower-Hybrid Ion Heating (LHH) Experiments

In ion heating studies encompassing the density range $1.3 \times 10^{13} cm^{-3} \leq n_e \leq 3.2 \times 10^{13} cm^{-3}$, no bulk heating of ion population was observed by UV Doppler broadening measurements during RF injection with the top-launching antenna for any value of the phase angle between waveguides ($45° \leq |\Delta\Phi| \leq 180°$). On the other hand, the perpendicular neutral charge-exchange flux showed a strong increase with RF injection. As in the case of side-launch injection, the decay of the neutral flux enhancement was no more than 150 μs following the shutoff of the RF power. The apparent temperature increase is dependent on the relative phase between waveguides, with the larger increases occurring at lower phase angles. The time-evolutions of the ion temperature inferred from perpendicular charge-exchange and UV measurements are shown in Fig. 18-5 for $\Delta\Phi = \pm 90°$ and 180° at $P_{RF} = 100$ kW and $\bar{n}_e = 2.6 \times 10^{13} cm^{-3}$

The apparent ion temperature increase indicated by the charge-exchange measurements is not believed to represent an actual increase in the bulk temperature, but most likely results from the presence of an ion tail near the edge of the plasma. The enhancement of the 0.5–1.0 keV neutral flux during RF injection with the top-launcher is consistent with the damping of higher $n_\parallel$ waves in the experiment (but it is in contrast with earlier side launcher studies). The larger $n_\parallel$ values at the damping locations may result from the higher average $n_\parallel$ spectrum launched by the narrow-waveguide top-launcher, and not necessarily from an upshift in $n_\parallel$ due to toroidal effects. The symmetry of the charge-exchange spectrum with $\Delta\Phi$ along with the lack of bulk ion heating

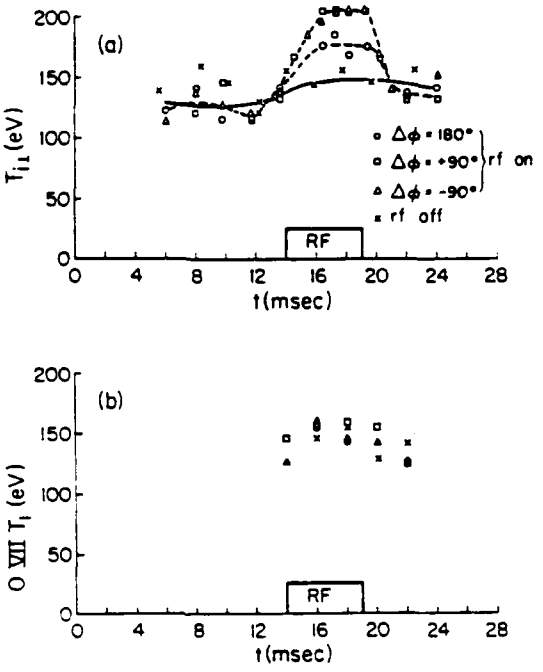

Figure 18-5: Temporal evolution of the central ion temperature during rf injection with the top–launcher

indicated by UV spectroscopic measurements is not consistent with the linear damping mechanism assumed in the ray-tracing calculations. Damping of parametric decay waves near the plasma edge may again be responsible for the observed effects on the ion energy spectrum. Consequently, the results of top–launching experiments can neither support nor refute the predictions of toroidal ray–tracing theory as it applies to lower–hybrid ion heating.

18.4 $2\omega_{ce}$ Emission and Absorption Experiments in ISX–B Tokamak

These experiments are under a joint project between the Versator II group and the ISX–B group at the Oak Ridge National Laboratory. The first goal of these measurements is to demonstrate that $2\omega_{ce}$ emissions can be used as a reliable diagnostic to measure electron temperature temporally and spatially. Secondly, to measure the absorption coefficient of $2\omega_{ce}$ extraordinary mode in a thermalized plasma accurately, so the measurement can be compared with analytic theoretical calculations and numerical model simulation results. This comparison is relevant in terms of planning future electron cyclotron heating experiments.

For studies of extraordinary mode emission at $\omega = 2\omega_{ce}$, the plasma is optically thick and $\omega = 2\omega_{ce}$ emission is approximately at the blackbody level. Electron temperatures at three spatial locations deduced from local $2\omega_{ce}$ emissions are shown in Fig. 18–6 for a typical neutral beam heated ISX–B discharge.

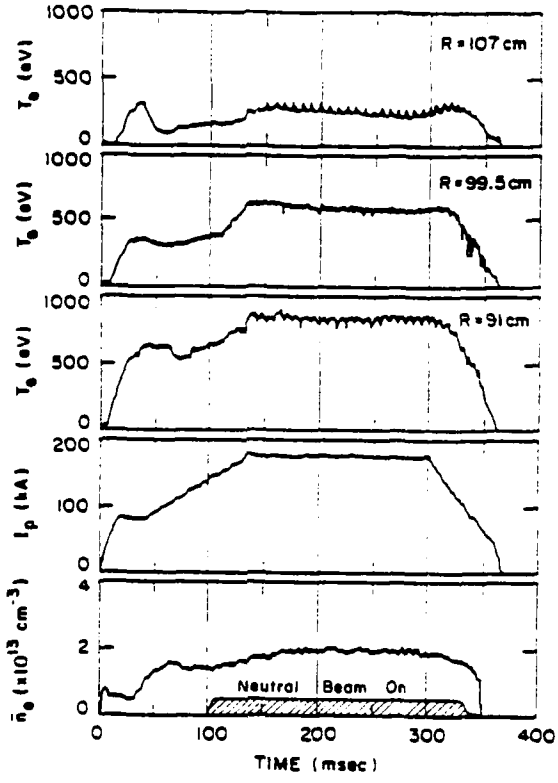

Figure 18-6: The electron temperature, Te, derived from $2\omega_{ce}$ emission for a typical neutral beam heated ISX-B discharge at B_o = 13.1 kG.

For the absorption measurement a transmitting antenna located on the high field side of the ISX-B vacuum vessel launches a wave along the equatorial plane of the torus and polarized in the extraordinary mode. The wave can be partially absorbed at the $\omega = 2\omega_{ce}$ layer. After passing through the plasma, the transmitted intensity is monitored by a receiving antenna located opposite on the low field side of the torus. By taking the diffraction of the input beam into account the absorption coefficient can be calculated from the input power and measured transmitted power. These absorption measurements are in good agreement with the analytic calculation of Ref. 4 and with the predictions of a fully relativistic numerical simulation developed by an Oak Ridge theory group.

References

1. P.T. Bonoli, E. Ott, Phys. Fluids 25, 359 (1982).
2. N.J. Fisch, Phys. Rev. Lett. 41, 873 (1978).
3. V.V. Parail, O.P. Pogutse, Nucl. Fusion 18, 303 (1978).
4. T.M. Antonsen, W. Manheimer, Phys. Fluids 21, 2295 (1978).

18.5 Nonlinear Wave Interactions—RF Heating and Current Generation in Plasmas

National Science Foundation (Grants ECS82-00646 and ECS82-13430)
U.S. Department of Energy (Contract DE-AC02-78-ET-51013)
U.S. Air Force - Office of Scientific Research (Contract F33615-81K-1426)
Abraham Bers, Vladimir Fuchs[8], Dennis Hewett[9], Kyriakos Hizanidis, Vladimir Krapchev, Abhay Ram, Gregory Francis, Leo Harten

The work and objectives of this theoretical and computational group were described in the RLE Progress Report No. 124, January 1982, pp. 112-113.

In the following seven subsections we report on our accomplishments of the past year on the following problems:

A. Theoretical modeling and analyses of current generation by lower-hybrid waves (subsections a and b). As described in our progress report of last year, this work is directly related to ongoing experimental efforts to produce a steady-state current for plasma confinement in toroidal geometry with the use of externally applied microwave power. More generally, this work seeks to understand the steady-states of high-temperature plasmas that are driven by RF waves.

B. Induced stochasticity in the dynamics of plasma particles by RF fields (subsections c and d). This work is part of our continuing studies of the nonlinear wave-particle interactions in a plasma. The important, new result reported in (d) is that an appropriately frequency modulated wave can induce stochastic motion in particles whose velocity is very different from the phase velocities of the wave fields, and at field amplitudes that are very much lower than those required for a single frequency wave.

C. Space-time evolution of relativistic instabilities (subsections e and f). Here we report on success in generalizing the absolute vs. convective instability analysis to include relativistic-electromagnetic interactions in plasmas. The applications of this work are to understanding instabilities in intensely heated plasmas by electron cyclotron RF power, and to explore the possibility of gyrotron-like devices at harmonics of the electron cyclotron frequency.

a. Theory of Lower-Hybrid Current Generation

The linearized, steady state, two-dimensional Fokker-Planck equation for electrons in the presence of strong RF diffusion has been solved analytically and the results have been compared with a

[8]Visiting Scientist from IREQ - Hydroquebec, Montreal, Canada

[9]Plasma Fusion Center, M.I.T., now at LLNL, Livermore, California

numerical integration of the equations. In this case the diffusion coefficient $D \equiv D_{QL}/\nu\, v_t^2 \gg 1$, where D is constant for $v_1 \leq v_{||} \leq v_2$ and zero otherwise. Here D_{QL} is the quasilinear diffusion coefficient, ν is the bulk collision frequency, $v_t = (T_B/m_e)^{1/2}$, T_B is the bulk temperature and $v_1(v_2)$ is the low (high) velocity boundary of the resonant domain.

We find a strong enhancement in the perpendicular temperature in the resonant plateau, $T_\perp \gg T_B$.[1] An analytical formula shows that $T_\perp = T_\perp (v_1, v_2)$ in reasonable agreement with the numerical results over a wide range of parameters. As a result of this there are many more current carriers in the tail and the two-dimensional current density is much larger than the one indicated from a one-dimensional theory.[2] This contradicts previous findings,[3] but agrees qualitatively with our numerical integration.[4] The two-dimensional figure of merit $(J/P_d)_2$ is 3 times larger than the prediction of the one-dimensional theory. This is in excellent agreement both with Ref. 3 and our numerical work.[4]

b. Relativistic Theory of Lower-Hybrid (LH) Current Generation

An analytical treatment based on the method of moments is developed. The relativistic Fokker-Planck equation for energetic electrons colliding with a thermal background of electrons and ions is derived as the Landau limit of the relativistic Balescu-Lenard collision operator.[5,6] Subsequently the energy, velocity and momentum moments of the relativistic Fokker-Planck equation are taken in the presence of RF diffusion. Since one is mainly interested in the average parallel and perpendicular momentum of the current carrying electrons the simplest possible distribution, which conveys this information, is employed — namely, one that consists of a product of displaced delta functions. This procedure provides us with the evolution equations of the average energy, momentum and current of the energetic electrons with LH diffusion. These equations when solved for the steady state provide us with the relations among the power dissipated, average energy and current carried by the energetic electron. The figure of merit as well as the average perpendicular energy are also calculated.

A numerical code of the 2D Fokker-Planck equation with relativistic effects taken into account has also been developed.[4,7,8] The numerical results indicate a significant enhancement of the perpendicular temperature as well as of the radial one. The current generated, power dissipated and perpendicular temperature are more or less insensitive to changes of the diffusion coefficient in the regime of strong RF-diffusion. Current and power dissipated change significantly with the location of the RF spectrum in parallel phase velocity. Relativity also affects significantly the current generated and the power dissipated but the figure of merit is only slightly affected. A very good agreement between the numerical results[9] for the perpendicular temperature and the simple analytic relativistic theory has been found.

The relativistic Fokker-Planck equation combined with RF diffusion has also been solved for arbitrary values of RF diffusion coefficient under conditions of detailed balance of the stationary joint

distribution involved.[10] The solution is in a closed form and therefore easily amenable to various analyses (small or large diffusion coefficients, etc.) in calculating current generated and power dissipated. The detailed balance condition also provides useful information about the functional form of the diffusion coefficients which are associated with the existence of a stationary steady state. The latter is also associated with a saturated spectrum of fluctuations in a plasma driven by a LH spectrum.

c. Stochastic Heating and Current Generation by Localized RF Fields

We consider the momentum transfer and diffusion of electrons interacting with a coherent one-dimensional wavepacket. Such a problem arises, for example, in lower-hybrid current drive, where electrons moving on a magnetic field surface around the torus interact periodically with a wave during the crossings of the resonance cone. With an effective length of the torus ℓ and a width of the resonance cone d we have typically $\ell \gg d$. This implies a large number of Fourier modes.

We consider an imposed field of such an amplitude that no particles from the bulk of the distribution are trapped. In that case the wave, maintained by the bulk particles, remains unchanged and we study the nonlinear dynamics of the high energy tail particles. The problem is treated both analytically and numerically. Earlier work on a similar problem is due to Stix[11] and Matsuda.[12]

For fields such that the autocorrelation time τ_{AC} is smaller than the trapping time τ_{TR} we find that the process is diffusive when the islands of neighboring Fourier modes overlap. The diffusion coefficient (D) is given essentially by the quasilinear formula, but with the important difference that only the overlapping modes should be included in calculating the r.m.s. field (E_{rms}) and τ_{AC}. With this modification we find an excellent agreement between theory and numerical experiments.[13,14] At larger amplitudes we find that D does not scales like E^2_{rms}. It does not follow the scaling of the resonance broadening theory, $\sim E^{3/2}_{rms}$, either. Depending on the width of the spectrum, the scaling is between $E^{1/2}_{rms}$ and E_{rms}. This numerical result should be explained by a theory for strong fields. In that case, we believe, the mechanism which leads to a diffusive motion is the crossing of the separatrices.

d. Induced Stochasticity by a Frequency-Modulated Wave

We have been studying the one-dimensional motion of an electron in a static confining potential and being perturbed by an electrostatic frequency modulated (fm) wave.[15] This problem models the motion of an electron along a d.c. magnetic field when it is confined by the field and an electrostatic potential. Such a situation would exist in the end-plugs of tandem mirror plasmas. The perturbing wave models an externally launched rf wave. The objective of this problem is to investigate the possibility of enhancing the electrostatic potential in the end-plugs by modifying the electron distribution function there so that the potential depends more favorably on the density than is given by the Boltzmann relation.

Our preliminary results[15] indicate that for very small amplitudes the fm-wave perturbs the electron

motion dramatically in regions of phase-space where the wave itself is not located. This happens for particular choices of the modulational index of the fm-wave and for frequencies which are close to the bounce frequency of the electron near the bottom of the confining potential. A large region of phase space can be driven stochastic by the fm-wave and the distribution function flattened in that region on a time-scale that is small compared to the electron-electron collisional time. The fm-wave can have its phase velocity far away in phase space so that it will not affect the passing electrons from the central cell. As an example, for TARA end-plug parameters, an fm-wave with an amplitude of 0.2 V/cm can flatten the electron distribution function for velocities, v, such that $0 \leq v \leq 2v_{te}$ (where v_{te} is the electron thermal velocity). This stochastic region of phase-space is nearly independent of the phase velocity, v_{ph}, of the wave as long as $v_{ph} \geq 2v_{te}$. This requires a frequency modulation of only 10% about the central carrier frequency — a spread that is easy to obtain experimentally.

e. Three-Dimensional Pulse Shapes of Absolute and Convective Instabilities for Relativistic Observers

The space-time growth and propagation of instabilities in a plasma is of considerable, general interest and has been recently reviewed.[16] The technique for distinguishing between absolute and convective instabilities is based upon the pinch-point analysis of the Green's function,[17] and the time asymptotic pulse shape of such instabilities is determined from the pinch points as seen by moving observers.[18] The latter was only developed for nonrelativistic observers and hence is, strictly speaking, applicable only to nonrelativistic plasma dynamics and unstable modes that propagate with velocities that are much smaller than the velocity of light, c (e.g., unstable electrostatic modes). We have recently generalized the pinch point analysis so that asymptotic pulse shapes can be obtained for relativistic-electromagnetic instabilities in three dimensions.[19,20] The following is a summary of our major results.

Let the dispersion relation, in the laboratory frame of reference, be $D(\vec{k},\omega) = 0$. For an observer moving with velocity $\vec{V}$ relative to the lab frame the Fourier-Laplace transform of the Green's function is then given by $D_V^{-1}(\vec{k}',\omega',\vec{V}) \equiv D^{-1}[\vec{k}(\vec{k}',\omega',\vec{V});\ \omega(\vec{k}',\omega',\vec{V})]$ where the unprimed and primed quantities are related by well-known relativistic transformation equations.[21] The pinch-points $(\vec{k}'_0,\omega'_0)$ are the proper solutions of $D_V = 0$ and $(\partial D_V/\partial \vec{k}') = 0$. Their dependence upon $\vec{V}$ is given by the following differential equations:

$$\frac{\partial \omega'_0}{\partial \vec{V}} = -\gamma^2 \vec{k}'_{0\parallel} - \gamma \vec{k}'_{0\perp} \tag{18.1}$$

$$\delta\vec{k}'_0 \cdot \overleftrightarrow{G}' = \delta\vec{V} \cdot \overleftrightarrow{F} \tag{18.2}$$

where

$$\overleftrightarrow{G}' = \left(\frac{\partial}{\partial \vec{k}'_\perp} + \frac{\partial}{\partial \vec{k}'_\parallel}\right)\left(\frac{\partial}{\partial \vec{k}'_\perp} + \frac{1}{\gamma}\frac{\partial}{\partial \vec{k}'_\parallel}\right) D_v \tag{18.3}$$

$$\overleftrightarrow{F} = -\gamma \frac{\partial D_v}{\partial \omega'} \overleftrightarrow{\delta} - \left[\frac{\gamma \omega_o'}{c^2} \left(\frac{\partial}{\partial \vec{k}_\perp'} + \gamma \frac{\partial}{\partial k_\parallel'} \right) \right. \tag{18.4}$$

$$\left. + \frac{(\gamma - 1)}{V} \left(k_\parallel' \frac{\partial}{\partial \vec{k}_\perp'} - \vec{k}_\perp' \frac{\partial}{\partial k_\parallel'} \right) \right] \left(\frac{\partial}{\partial \vec{k}_\perp'} + \frac{1}{\gamma} \frac{\partial}{\partial k_\parallel'} \right) D_v$$

$\gamma = [1 - (V^2/c^2)]^{-1/2}$, and all derivative operators are to be evaluated at the pinch-point $(\vec{k}_0', \omega_0')$. The time-asymptotic pulse shape is then obtained from the plot of $[(\max \omega_{oi}')/\gamma]$ vs. $\vec{V}$, where $(\max \omega_{oi}')$ is the maximum imaginary part pinch-point frequency.

Alternatively, in the laboratory frame of reference the pinch points $(\vec{k}_0', \omega_0')$ have corresponding values $(\vec{k}_0, \omega_0)$. As a function of $\vec{V}$, $(\vec{k}_0, \omega_0)$ are determined by the pinch-point solutions of $D = 0$ and $(\partial D/\partial \vec{k}_\perp) + \gamma(\partial D/\partial \vec{k}_\parallel) + \gamma \vec{V}(\partial D/\partial \omega) = 0$. They obey the following, simpler differential equations:

$$\frac{\partial \omega_o}{\partial \vec{V}} = -\frac{\partial D}{\partial \omega} \left[\overleftrightarrow{T} \right]^{-1} \cdot \vec{V} \tag{18.5}$$

$$\delta \vec{k}_o \cdot \overleftrightarrow{T} = -\frac{\partial D}{\partial \omega} \delta \vec{V} \tag{18.6}$$

where

$$\overleftrightarrow{T} = \left(\frac{\partial}{\partial \vec{k}} + \vec{V} \frac{\partial}{\partial \omega} \right)^2 D \tag{18.7}$$

and the derivative operators are evaluated at $(\vec{k}_o, \omega_o)$. For any fixed $(\vec{r}/t) = \vec{V}$ the time-asymptotic Green's function is proportional to $t^{-3/2} \exp[i(\vec{k}_o \cdot \vec{V} - \omega_o)t]$, and, its logarithmic magnitude is thus given by $(-\vec{k}_{oi} \cdot \vec{V} + \omega_{oi})t = \omega_{oi}' t' = (\omega_{oi}'/\gamma)t$. The time-asymptotic pulse shape is hence again determined from $[(\max \omega_{oi}')/\gamma]$ as a function of $\vec{V}$.

f. Relativistic-Electromagnetic Instabilities at Electron Cyclotron Harmonics

The analysis of absolute and convective instabilities[16-18] has been generalized for application to relativistic and fully electromagnetic instabilities in plasmas.[19,20] In particular, we have applied our analysis to electromagnetic instabilities propagating along a constant magnetic field,[19,22] $(\vec{B}_0)$, in which the plasma is immersed, as well as to those propagating perpendicular to $\vec{B}_0$.[20] These instabilities are driven by a highly anisotropic distribution function of relativistic electrons. Such a situation is found to be relevant in explaining the observed nonthermal radiation in the ECRH plasmas on TMX-Upgrade.[23] Our model analysis for waves along $\vec{B}_0$[19,22] shows that two distinct instabilities exist — the whistler instability and the relativistic instability. The former may be stabilized by introducing a thermal spread in the distribution function while the latter can only be stabilized by

increasing the density. For waves propagating perpendicular to $\vec{B}_0$,[20] electromagnetic instabilities occur at harmonics of the electron cyclotron frequency (ω_{ce}). The nature and the strength of the instabilities is highly sensitive to the plasma density. For low densities the dominant instability is at ω_{ce}. It is an absolute instability and its phase-velocity is greater than the speed of light (c). The instabilities at harmonics of ω_{ce} are convective in nature. As the density is increased the phase velocity of the instability at ω_{ce} becomes less than c while it still remains absolute. However, the instability at $2\omega_{ce}$ has the highest growth rate. It becomes an absolute instability with its phase velocity less than c.

References

1. V. Krapchev, D. Hewett, and A. Bers, "Steady State Solution of a 2D Fokker-Planck Equation with Strong RF Diffusion," M.I.T. Plasma Fusion Center Report PFC/JA-83-32; V. Krapchev, D. Hewett, and A. Bers, "Steady State Solution of a Two-Dimensional Fokker-Planck Equation with Strong RF Diffusion," Bull. Amer. Phys. Soc. 28, 1090 (1983); V. Krapchev, D. Hewett, and A. Bers, "Analytic Solution of the 2D Fokker-Planck Equation for LH Current Drive," US-Japan Workshop on RF Heating and Current Generation, GA Technologies, Inc., San Diego, California, 1983.
2. N.J. Fisch, Phys. Rev. Lett. 41, 873 (1978).
3. C.F.F. Karney and N.J. Fisch, Phys. Fluids 22, 1817 (1979).
4. D. Hewett, K. Hizanidis, V. Krapchev, and A. Bers, "Two-Dimensional and Relativistic Effects in Lower-Hybrid Current Drive," Proceedings of the IAEA Technical Committee on the Non-Inductive Current Drive in Tokamaks, Culham, England, April 1983, Culham Report CLM-CD, 1983; D. Hewett, V. Krapchev, J. Freidberg, and A. Bers, "Fokker-Planck Investigations of RF Current Drive," Sherwood Theory Meeting, Arlington, Virginia, 1983; M. Shoucri, V. Krapchev, and A. Bers, "A SADI Numerical Scheme for the Solution of the 2-D Fokker-Planck Equation," IEEE International Conference on Plasma Science, San Diego, California, 1983.
5. K. Hizanidis, K. Molvig, and K. Swartz, J. Plasma Physics 32, 223 (1983).
6. V.P. Silin, Sov. Phys. JETP 13, 1244 (1961).
7. K. Hizanidis, V. Krapchev, and A. Bers, "Relativistic Two-Dimensional Theory of RF Current Drive," Proceedings of the Fifth Topical Conference on Radio Frequency Plasma Heating, Madison, Wisconsin, February 1983.
8. K. Hizanidis, D.W. Hewett, K. Rugg, and A. Bers, "Steady State RF-Current Drive Theory Based Upon the Relativistic Fokker-Planck Equation," Bull. Amer. Phys. Soc. 28, 8, 1090 (1983).
9. K. Hizanidis, D.W. Hewett, and A. Bers, "Solution of the Relativistic 2-D Fokker-Planck Equation for LHCD," US-Japan Workshop on RF Heating and Current Generation, GA Technologies, Inc., San Diego, California, 1983; K. Hizanidis, V. Krapchev, and A. Bers, "Relativistic 2-Dimensional Theory of Lower-Hybrid Current Drive," Sherwood Theory Meeting, Arlington, Virginia, 1983.
10. H. Risken, Z. Physik 251, 231 (1972), and references therein.
11. T.H. Stix, Proceedings of the Joint Varenna-Grenoble International Symposium on Heating in Toroidal Plasmas 2, 363 (1978).
12. K. Matsuda, Reports GA-A16303 (1980), GA-15816 (1981).
13. V. Fuchs, V. Krapchev, A. Ram, and A. Bers, "Diffusion of Electrons by Coherent Wavepackets," M.I.T. Plasma Fusion Center Report PFC/JA-83-26, Physica D Nonlinear Phenomena, accepted for publication.
14. V. Fuchs, V. Krapchev, A. Ram, and A. Bers, "Stochasticity Induced by Coherent Wavepackets," Proceedings of the Fifth Topical Conference on Radio Frequency Plasma Heating, Madison,

Wisconsin, February 1983; V. Fuchs, V. Krapchev, A. Ram, and A. Bers, "Scattering and Stochasticity of Electrons Interacting with Coherent Wavepackets," Sherwood Theory Meeting, Arlington, Virginia, 1983.

15. A. Ram, M. Mauel, V. Krapchev, and A. Bers, Bull. Amer. Phys. Soc. 28, 1183 (1983).
16. A. Bers, "Space-Time Evolution of Plasma Instabilities — Absolute and Convective," in M.N. Rosenbluth and R.Z. Sagdeev (Gen. Eds.), Handbook of Plasma Physics; A.A. Galeev and R.N. Sudan (Vol. Eds.), Vol. 1, Basic Plasma Physics, Chapter 3.2, (North Holland Publishing Co. 1983).
17. R.J. Briggs, Electron Stream Interaction with Plasmas, (M.I.T. Press 1964).
18. L.S. Hall and W. Heckrotte, Phys. Rev. 166, 120 (1968).
19. A. Bers and A. K. Ram, "Relativistic Pulse Shapes of Absolute and Convective Instabilities," Bull. Am. Phys. Soc. 27, 919 (1982).
20. A. Bers, A. Ram, and G. Francis, "Relativistic Stability Analysis of Electromagnetic Waves Propagating Across a Magnetic Field," Bull. Amer. Phys. Soc. 28, 1158 (1983).
21. A. Bers, "Linear Waves and Instabilities," in C. DeWitt and J. Peyraud (Eds.), Plasma Physics — Les Houches 1972, (Gordon and Breach Science Publishers 1975), p.134.
22. A. Ram and A. Bers, Annual Sherwood Controlled Fusion Conference, Arlington, Virginia, 1983.
23. Y.J. Chen, W.M. Nevins, and G.R. Smith, LLNL, private communication.

Other Publications

Bers, A. and K.S. Theilhaber, "Three-Dimensional Theory of Waveguide-Plasma Coupling," Nucl. Fusion 23, January 1983.

Fuchs, V., M.M. Shoucri, G. Thibaudeau, L. Harten, and A. Bers, "High-Q Thermally Stable Operation of a Tokamak Reactor," IEEE Trans. on Plasma Science PS-11, 4 (1983).

Ram, A., and A. Bers, "Antenna-Plasma Coupling Theory for ICRF Heating," Proceedings of the Fifth Topical Conference on Radio Frequency Plasma Heating, Madison, Wisconsin, February 1983 and M.I.T. Plasma Fusion Center Report PFC/CP-83-1 (1983).

Ram, A., and A. Bers, "Coupling Theory for ICRF Heating of Large Tokamaks," Nucl. Fusion, accepted for publication in 1984; M.I.T. Plasma Fusion Center Report PFC/JA-83-40 (1983)

18.6 Physics of Thermonuclear Plasmas

U.S. Department of Energy (Contract DE-AC02-78ET-51013)

Bruno Coppi

The general objective of this program is the theoretical study of plasmas in thermonuclear regimes and it extends from the design of "burning core" experiments for both D-T and advanced fuel reactors to the basic study of plasma transport and stability questions. Continuous collaboration and theoretical guidance are provided for the Alcator and Versator experimental programs that involve high density regimes, with record values of the confinement parameter, as well as low and intermediate density regimes where current drive and r.f. heating can be produced. Much of the support involves the development, modification, and use of realistic simulation codes that are among the most advanced in the research community, particularly in the transport and r.f. areas.

Other areas of interest in which considerable progress has been made in 1983 are: the theoretical

explanation and description of enhanced electron and ion thermal conductivity observed in present day experiments and its relevance to future ones in which heating due to the fusion reaction products will prevail; the particle transport processes that occur in high density plasmas with either neutral gas (so-called "puffing") or pellet injection; the identification and analysis of heating sequences from low to high-β regimes (β being the ratio of particle pressure to magnetic pressure) that remain macroscopically stable; and the implications of these sequences for future reactor concepts and new types of experiments, such as PBX, that have been proposed since we have pointed out the theoretical possibility to reach relatively high values of β by exploiting the favorable factors that lead to the "second stability region"; the excitation of internal macroscopic modes by the fusion reaction products and their influence on the time needed to reach ignition; the relevant stability analysis of collisionless modes that involve magnetic reconnection; the investigation of new physical processes to make the experimental study of advanced fuel (such as D-D and D-He^3) burning feasible within the limits of present day technology; the burning conditions of plasmas with spin polarized nuclei, the collective modes that can be excited in them and the relevance that some of these modes have to ion cyclotron heating, to anomalous slowing down of the charged fusion reaction products and to the rate of spin depolarization.

As is traditional with our mode of operation, during 1983 we have maintained an effective system of close collaborations with national and overseas institutions for both our theoretical and experimental program. Our contributions have been presented at major national and international meetings.

Communication Sciences and Engineering

19. Optical Propagation and Communication

Academic and Research Staff

Prof. J.H. Shapiro, Dr. R.H. Rediker, Dr. P. Kumar

Graduate Students

P.L. Bogler, R.S. Bondurant, F. Hakimi, M.W. Maeda, M.B. Mark, P.L. Mesite, T.T. Nguyen, J. Ocenasek, R.P. Schloss, P.D. Shapiro, E.A. Swanson, A.H. Tewfik, H.V. Tran, S.S. Wagner, A.K. Wong

The central theme of our programs has been to advance the understanding of optical and quasi-optical communication, radar, and sensing systems. Broadly speaking, this has entailed: developing system-analytic models for important optical propagation, detection, and communication scenarios; using these models to derive the fundamental limits on system performance; and identifying, and establishing through experimentation the feasibility of, techniques and devices which can be used to approach these performance limits.

19.1 Atmospheric Optical Communication Systems for Network Environments

National Science Foundation (Grant ECS81-20637)

Jeffrey H. Shapiro, Trung T. Nguyen, Hai V. Tran, Albert K. Wong

A local computer network is prototypically a high-bandwidth (1–10 Mbps) geographically compact (0.1–10 km diameter) packet-switched network that employs coaxial cable or fiber optics as its transmission medium. These networks interconnect host computers within a single company, often within a single building. They are distinguished from long-haul packet networks in that the high-bandwidth, short delay, low-cost transmission media employed in local networks permit simplified protocols and control strategies.

Atmospheric optical communication links are a natural choice for certain high-bandwidth short-haul terrestrial transmission applications in which cable rights-of-way are unobtainable, or frequent link and network reconfiguration is necessary. Such systems will experience occasional outages due to local adverse weather conditions, but, via the results of our prior work,[1,2] low-visibility atmospheric optical communication links can now be analyzed with some confidence. It turns out that exploitation of scattered light can permit useful link operation beyond the limit set by extinction of the direct beam. However, although technology development can help extend scattered-light operating range, true all-weather capability at high data rates over kilometer or longer path lengths cannot be guaranteed.

The natural advantages of atmospheric optical links make them attractive candidates for such local network applications as bridges between buildings containing cable networks, and temporary quick-connects for new outlying hosts for which cable runs are unavailable. Whether these advantages will lead to widespread usage of atmospheric optical communication in local computer networks is uncertain at this time. There is a substantial gap that exists between link-understanding and network-understanding of atmospheric optical communications. In particular, high-level network protocols are designed to provide 100% reliability message transmission end-to-end through the network. Thus, in designing and implementing atmospheric optical links for such networks appropriate compromises must be established between the physical link design and low-level protocol design to best provide fairly reliable packet transmission for the high-level protocols to act upon. We have undertaken a combined analytical and experimental effort to attack these network problems. A brief summary of the status of these efforts follows.

Theory

The analysis of computer networks is generally carried out within a layered architecture model. Our purpose for analysis is to study how a local area network, employing one or more atmospheric optical links, is affected by the weather-dependent performance of these optical links.[3] Thus far, we have examined the trade-off between the delay created by an optical link making an unannounced transmission rate reduction to maintain reliable data communication in deteriorating visibility conditions versus the increased fraction of weather conditions in which operation is made possible by this rate reduction. We have also proposed and analyzed several state control procedures under which an optical link's transmission rate can be adjusted and communicated to the remainder of the network without creating a state-oscillation problem. Such a problem occurs when the optical nodes oscillate between states, sending their constantly changing status to the rest of the network at a rate much faster than the rate at which the network can make use of this information.

The preceding work addresses issues arising at the lowest layers of the hierarchy, namely, the physical layer (delay due to unannounced rate reduction), and the data link layer (state control procedure). We have begun blocking out the key issues to be studied at the higher layers.

Experiment

A major component of our research program is to experimentally probe the utility of atmospheric optical communication links in local area networks. Toward that end, we have constructed[3,4] a pair of optical transceivers capable of digital transmission at a rate up to 10 Mbps over line-of-sight paths as long as 1 km in weather conditions down to optical thickness 3. Initial laboratory tests of the equipment were performed using video terminals and a pair of specially constructed transmission rate converters. Building-to-building communication tests are now underway using the recently acquired LSI 11/23 computer to generate long sequences of packets for transmission to a remote video terminal via the link and one of our transmission rate converters.

In addition to the preceding communication link tests, we have been in contact with members of the

M.I.T. Laboratory for Computer Science regarding the future use of the optical links in network experiments.

References

1. W.S. Ross, W.P. Jaeger, J. Nakai, T.T. Nguyen, and J.H. Shapiro, "Atmospheric Optical Propagation: An Integrated Approach," Opt. Engr. 21, 775–785 (1982).
2. J.H. Shapiro and C. Warde, "Optical Communication through Low-Visibility Weather," Opt. Engr. 20, 76–83 (1981).
3. T.T. Nguyen, J.H. Shapiro, A.K. Wong, and D.J. Epstein, "Atmospheric Optical Communication for Local Area Networks," Globecom '83 (IEEE, New York, 1983) pp. 416–420.
4. A.K. Wong, "A Variable-Rate Atmospheric Optical Link for Computer Network Communication," S.M. Thesis Proposal, Department of Electrical Engineering and Computer Science, M.I.T., November 1983.

19.2 Two-Photon Coherent State Light

U.S. Navy - Office of Naval Research (Contract N00014-81-K-0662)

Jeffrey H. Shapiro, Prem Kumar, Roy S. Bondurant, Mari W. Maeda, Josef Ocenasek, Stuart S. Wagner

Recent work has highlighted the applications of two-photon coherent states (TCS), also known as squeezed states, in optical communications and precision measurements. These states have non-classical noise statistics, and their predicted generation schemes include degenerate parametric amplification (DPA), degenerate four-wave mixing (DFWM), the free-electron laser, and multi-photon optical bistability. The preceding generation schemes have been analyzed to varying degrees of approximation, but no experimental observation of TCS has been reported as of yet. We are engaged in a program to: generate and verify the quantum noise behavior of TCS light; and analyze the physics and applications of such light. Our recent progress is summarized below.

TCS Generation and Detection

Two-photon coherent states are in essence minimum uncertainty states for the quadrature components of the electromagnetic field possessing an asymmetric noise division between the quadratures. To detect them, one seeks to demonstrate their non-classical behavior. To generate them, one seeks interactions which mix annihilation operators and creation operators.

Our approach is to generate TCS light via pulsed DFWM,[1] and to exhibit its anti-bunching behavior via photon counting.[2] An initial experiment of this type with sodium vapor as the DFWM medium was performed,[3-5] with negative results. Basically, a combination of experimental difficulties prevented DFWM/photon counting operation in the regime wherein non-classical behavior should prevail. Additional analysis[3,5,6] has clarified pump and loss issues in DFWM TCS generation. Work is now proceeding toward a continuous-wave homodyne detection experiment.

TCS Applications

The main thrust of our TCS applications research has been in the area of phase sensing. We showed in[7] how multi-mode TCS permit arbitrarily high accuracy to be achieved in simultaneous amplitude and phase measurements made via optical heterodyne detection. In[8] we demonstrate how the preceding heterodyne apparatus could be used to greatly exceed the standard quantum limit on phase sensing gravity-wave interferometers.

References

1. H.P. Yuen and J.H. Shapiro, "Generation and Detection of Two-Photon Coherent States in Degenerate Four-Wave Mixing," Opt. Lett. 4, 334-336 (1979).
2. R.S. Bondurant, P. Kumar, J.H. Shapiro, and M.M. Salour, "Photon-Counting Statistics of Pulsed Light Sources," Opt. Lett. 7, 529-531 (1982).
3. R.S. Bondurant, "Theoretical and Experimental Aspects of Quantum Noise Reduction and Precision Measurement," Ph.D. Thesis, Department of Electrical Engineering and Computer Science, M.I.T., July 1983.
4. P. Kumar, R.S. Bondurant, J.H. Shapiro, and M.M. Salour, "Quantum Noise Measurements on Degenerate Four-Wave Mixing," in L. Mandel and E. Wolf (Eds.), Coherence and Quantum Optics V (Plenum Press, New York, 1983).
5. R.S. Bondurant, P. Kumar, J.H. Shapiro, and M. Maeda, "Degenerate Four-Wave Mixing as a Possible Source of Squeezed-State Light," Phys. Rev. A., submitted for publication.
6. R.S. Bondurant, M. Maeda, P. Kumar, and J.H. Shapiro, "Pump and Loss Effects on Degenerate Four-Wave Mixing Quantum Statistics," in L. Mandel and E. Wolf (Eds.), Coherence and Quantum Optics V (Plenum Press, New York, 1983).
7. J.H. Shapiro and S.S. Wagner, "Phase and Amplitude Uncertainties in Heterodyne Detection," IEEE J. Quantum Electron., submitted for publication.
8. R.S. Bondurant and J.H. Shapiro, "Squeezed States in Phase-Sensing Interferometers," Phys. Rev. D., submitted for publication.

19.3 Atmospheric Propagation Effects on Infrared Radars

U.S. Army Research Office - Durham (Contract DAAG29-80-K-0022)

Jeffrey H. Shapiro, Martin B. Mark, Paula L. Mesite, Ahmed H. Tewfik

Compact coherent laser radars have the potential for greatly improved angle, range, and velocity resolution relative to their microwave radar counterparts. This program is aimed at obtaining a quantitative understanding of target reflection and atmospheric propagation effects on the performance of compact coherent laser radars through a combination of theory and experiments. Under a collaboration arrangement with the Opto-Radar Systems Group at the M.I.T. Lincoln Laboratory, the experimental portions of the research are being carried out on the compact CO_2-laser radars under development there. During the past year our work has focused on experiments using the 2-D Doppler imager radar, and analyses of 3-D imaging systems, as described below.

Doppler-Radar Measurements

Two important features of Doppler radar operation are hard-target speckle and clutter. We have found[1,2] that target-returns from a moving flame-sprayed aluminum calibration plate do show the expected speckle behavior in the Doppler radar's far field, but evidence an as yet unaccounted for reduction of the speckle fluctuations in the radar's near field. Work is continuing on the latter case. In tree-clutter measurements[1,2] we have shown that observed spectra obey a micro-motion/macro-motion decomposition that we had previously proposed. Amplitude statistics for clutter returns are being investigated.

High Time-Bandwidth Radars

We have been studying,[2,3] analytically, the use of high time-bandwidth (TW) waveforms for 3-D imaging. In particular, we have been concerned with the effects of range-spread speckle targets on the range accuracy of such systems.

References

1. P.L. Mesite, "Laser Speckle and Clutter Effects on Moving Targets Observed with an Optical Radar," S.M. Thesis, Department of Electrical Engineering and Computer Science, M.I.T., September 1983.
2. J.H. Shapiro and P.L. Mesite, "Performance Analyses for Doppler and Chirped Laser Radars," IRIS Active Systems Specialty Group, 1983.
3. A.H. Tewfik, "Range-Spread Speckle Target Effects on CW Coherent Laser Radar Range Measurements," S.M. Thesis Proposal, Department of Electrical Engineering and Computer Science, M.I.T., September 1983.

19.4 Fiber-Coupled External-Cavity Semiconductor High Power Laser

U.S. Navy - Office of Naval Research (Contract N00014-80-C-0941)
Robert H. Rediker, Robert P. Schloss, Farhad Hakimi

The external-cavity laser has been operated with all five semiconductor gain elements lasing simultaneously and being controlled by the external cavity. The wavelength of lasing of each gain element has been controlled by controlling the temperature of its heat sink to 0.5×10^{-3}°C. Lasing has been obtained with various spatial filters in the focal plane between the two lenses which focus the collimated beam from the laser and recollimate the beam so it is incident on the end mirror of the cavity. These spatial filters include a 200 μm pinhole, a 100 μm pinhole and a 170 μm slit.

The insertion of the spatial filters perturb the lasing wavelengths of the various gain elements differently, requiring re-adjustment of parameters to put the lasing wavelengths again in coincidence. The external-cavity has not lased when the spatial filter which contains thirteen 3 μm slits on 10.5 μm centers is used. This spatial filter is the diffraction pattern of the gain elements radiation if these

elements are emitting in coherence. It is believed this latter spatial filter has also perturbed the wavelength at which the various gain elements would lase and, of course, stable interference is not possible for different wavelength gain-elements. Without lasing of the individual elements there is no systematic way to re-establish coincident wavelengths. Frequency-selective etalons are now being incorporated into the cavity to eliminate the wavelength perturbation. It is believed that once the gain elements have locked together that the perturbation issue will no longer exist.

20. Communication Networks

Academic and Research Staff

Prof. R.S. Kennedy, S.S. Wagner

Graduate Students

E.B. Sia

M.I.T. Vinton Hayes Fund

The goal of this newly initiated research program is to determine and demonstrate the principles that should be followed in the design of local communication networks as typified by local area networks, private branch exchanges and internetted collections of such structures.

Two fundamental assumptions distinguish the research from much of the ongoing work in this area. One is that a single integrated system is to provide a set of highly diverse communication services such as interactive terminal service, database access, file transfers, graphics, voice and video. The other is that single mode optical fiber links with very wide bandwidths can be employed economically. These assumptions are not satisfied by the networks now being designed, but based upon the perceived trend toward such integrated diverse services and the declining cost of single mode fiber technology, it is probable that they will be at some time in the future.

The research will involve theoretical, experimental and design activities. The theoretical work will provide the basis for choosing between broad alternative design approaches and will be guided by the existing and projected capabilities of single mode fiber technology. As the basic structure of the network becomes more defined, the feasibility of various design approaches will be evaluated experimentally. A longer term goal will be to design and build a prototype network to verify, and provide an experimental basis for extending, the results of the research.

The broad characteristics of the traffic the network is expected to carry also will provide important guidelines for the work. Those characteristics cannot be anticipated with certainty, but they can be plausibly estimated by conducting experimental studies of the traffic on existing M.I.T. networks and on the network that is being installed to serve the M.I.T. Project Athena.

The assumptions that highly varied information services are to be provided and that very wideband optical fiber technology is to be employed raise two subjective issues that provide some important guidance for the research.

One issue is whether or not all network users are required to employ the same network interface. It

arises because the need for a broad diversity of information services very often will result from a heterogeneous population of users requiring quite different services rather than from a homogeneous population of users all requiring the same broad spectrum of services.

When the network serves a homogeneous population of users it is reasonable to require that all interfaces to it be essentially identical; as do almost all existing and proposed networks. However, as the user requirements become more varied and the link bandwidths become larger it becomes more important to keep the cost of a user's network connection, or interface, roughly less than their other costs. For example, many interfaces that would be economical for a full graphics work station with very high peak data rate requirements would be far too costly for a user whose only requirement is for interactive keyboard traffic. Note that as used here, the interface costs includes both hardware and software.

Of course, if the needs of the most capable user can be met with a network interface that is also economical for the least capable user, that interface should be employed by all. The possibility of developing such a universally capable and economical interface certainly will be explored in the course of this research. However, since such a fortuitous outcome is not to be expected, we will give equal attention to approaches that can accommodate a family of interfaces whose "costs" appear to be monotonically related to the levels of service they can provide.

The other issue relates to the network topology and the means of coupling to it. It arises because, in contrast to the receivers used in lower frequency networks, optical receivers require a significant amount of energy per information bit. This difference is due to the importance of quantum effects at optical frequencies and limits the number of users among whom the available information bearing power can be equally shared. To the degree that such a division of power is made there is a significant limit to the number of users that can be accommodated without repeaters. Stated alternatively, the network topology is severely constrained when many users are to be served without any repeaters.

The determination of network topology that can be used with a family of interfaces and that are well suited to implementation with optical technology will be an important part of the research but the more fundamental issue is whether or not the information bearing power need be shared among users.

Clearly, inactive users should not be coupled to the network in a way that removes power from it. Moreover, once an active user is aware that the information being transmitted is not intended for them there is no reason for them to extract power from the network until the transmission of that information has been completed. Conversely, if they are the intended receiver their coupling to the network can be increased during this same interval so as to extract all of the available power. Thus, in principle, and perhaps in practice, the network can appear to have only one receiver connected to it during the transmission of any given message.

The energy that is used for addressing and/or network control must be shared by all users to determine whether they should reduce or increase their coupling to the network for the next message transmission. But that energy can be increased to accommodate as many users as desired by increasing the time allocated to the transmissin of power carrying control and addressing information. Thus the number of users can be increased until the time available for message transmission, as opposed to network control, becomes acceptably small.

It is far too early to say whether or not network interfaces with such controllable coupling can be implemented practically or whether or not the benefits of using them outweigh the additional complexity they introduce. However, the alternatives are sufficiently limited to warrant an exploration of the possibilities. Thus the feasibility and potential merit of using controllable coupling in the network interfaces will be investigated.

In summary, the research will be shaped by the assumptions that a broad spectrum of highly diverse communication services are to be provided by the network and that it is to be implemented with optical fiber technology. These assumptions suggest that the scope of the research should not be limited to networks in which all interfaces are the same and the coupling to the network is fixed but should include networks that employ user interfaces with controllable coupling whose "costs" vary according to the services they must handle.

21. Digital Signal Processing

Academic and Research Staff

Prof. A.V. Oppenheim, Prof. A.B. Baggeroer, Prof. J.S. Lim, Prof. B.R. Musicus, Dr. D.R. Mook, Dr. G.L. Duckworth

Graduate Students

T.E. Bordley, P. Chan, S.R. Curtis, D.S. Deadrick, W.P. Dove, F.U. Dowla, D.W. Griffin, W.A. Harrison, D. Izraelevitz, D.M. Martinez, E.E. Milios, C. Myers, T.N. Pappas, M.D. Richard, H. Sekiguchi, R. Sundaram, P.L. Van Hove, M.S. Wengrovitz

21.1 Introduction

The Digital Signal Processing Group is carrying out research in the general area of digital signal processing. While a major part of our activities focus on the development of new algorithms, there is a strong conviction that theoretical developments must be closely tied to applications and to issues of implementation. The application areas which we deal with principally are speech, image and geophysical data processing. In addition to specific projects being carried out on campus, there is close interaction with Lincoln Laboratory and with the Woods Hole Oceanographic Institution.

In the area of speech processing, we have over the past several years worked on the development of systems for bandwidth compression of speech, parametric modeling of speech using pole-zero models, time-scale modification of speech and enhancement of degraded speech. Recently we have obtained some important new results on time-scale modification of speech, growing out of a more general set of issues involving the estimation of a signal after its short-time Fourier transform has been modified. We are also exploring new techniques for speech enhancement using adaptive noise cancelling when multiple microphones are available.

There are also a number of projects related to image processing that we are currently pursuing. One project is restoration of images degraded by additive noise, multiplicative noise, and convolutional noise. Out of this project, we have developed a new image restoration system which is applicable to restoring images degraded by various different types of degradation. Our current work in this project involves development of new image restoration systems by exploiting additional available information such as the range map in infrared radar images. Another project is development of new image coding techniques by reducing quantization noise in PCM image coding or by reducing blocking effect in cosine transform image coding. Our approach to first decorrelate the quantization noise, and then reduce the quantization noise by a noise reduction system, led to a noticeable improvement in the performance of a simple PCM image coding system. We are currently working on the extension of these results to a more complex PCM image coding system. To reduce the blocking

effect in cosine transform image coding, we have studied two approaches. In one approach, the coder is modified to account for the blocking effect and in the second approach, the coded image with blocking effect is processed to reduce the blocking effect. In both approaches, we have developed specific algorithms that significantly reduce the blocking effect in cosine transform coding. Another project that we are currently exploring is the development of a very low bit rate (below 50 kbits/sec) video-conferencing system. The specific approach we are currently studying is to model a human face, which is a regular feature in typical video-conferencing applications, with a set of parameters and then synthesize the image at the receiver from the coded parameters. This approach is analogous to modeling human speech for speech coding, which led to significant bit rate reduction without seriously degrading the speech intelligibility.

In the area of geophysical data processing, there are a variety of on-going and new projects. During March-May 1980, we led a large acoustics and geophysics experiment, FRAM II, in the eastern Arctic. This was followed by an even more extensive program in March-May 1982, FRAM IV. Both of these experiments implemented an array of hydrophones and geophones with multichannel digital data recording. Work has been carried out on applying adaptive array processing to the measurement of the reverberation associated with the resulting acoustic signals, as well as the phase and group velocities of the seismic paths within the seabed and water column for refraction and bottom interaction studies. Work is also currently under way to examine the properties of several velocity function inversion techniques for multi-channel seismic ocean-bottom interaction data. The array data at FRAM II and FRAM IV are also being used to measure the scattering function of the channel at low frequencies and the directional spectra of the ambient noise in the Arctic. Associated with the acoustics experiment is a project aimed at extending the parabolic wave equation approximation for modeling underwater acoustics.

The summer of 1983 saw the successful beginning of a series of geophysical and acoustic experiments in the marginal ice zone of the Arctic. In this first MIZEX experiment, a large multichannel telemetered array was used to receive acoustic signals propagated across ocean and crustal paths marking the transition between the open waters of the Atlantic, and the ice covered regions of the Arctic Ocean. The goal of this experiment, and a more extensive one to be carried out in the same region in 1984, is to study the acoustic transmission properties of the laterally inhomogeneous and time varying water column, and to characterize the crustal velocity-depth function in this region. To carry out this work, much emphasis has been placed on the use of digital signal processing algorithms to decompose the multichannel data into domains that are easily related to the model parameters of interest. This is the beginning of the chain of analysis that leads to inversion of the observations for the model parameters.

Two additional projects related to geophysical signal processing in the context of ocean acoustics are the development of an algorithm for data processing to measure the acoustic reflection coefficient from the ocean bottom both for the deep water and shallow water cases. Out of this work

has come a Hankel transform algorithm as well as a new method for generating synthetic data.

In both the context of image processing and geophysical data processing we have obtained some significant results in the multi-dimensional high resolution spectral estimation problem. Specifically, we have developed new algorithms for maximum entropy power spectrum estimation which are computationally simple relative to previous approaches and applicable to both equally spaced and non-equally spaced data for both one-dimensional and two-dimensional signals. This algorithm has been applied to investigate the characteristics of multi-dimensional maximum entropy spectral estimates. In addition, we are investigating several approaches to improve the performance of the maximum likelihood method for spectral estimation.

Recently, we have proposed a new approach to the problem of estimating multiple signal and/or parameter unknowns using incomplete and noisy data. Our Minimum Cross-Entropy Method applies an information theoretic criterion to optimally estimate a separable probability density for the signal model. Not only does this new approach include all the various Maximum Likelihood and Maximum A Posteriori methods as degenerate cases, but it also directly leads to a simple iterative method of solution in which we alternate between estimating the various unknowns, one at a time. We are now exploring applications to statistical problems, iterative signal reconstruction, short-time analysis/synthesis, and noisy pole/zero estimation.

Another interesting area of research is the connection between signal processing algorithms and computer architectures. The "speed" of an algorithm depends not only on how many operations it requires, but also on how suitable it is for the computer architecture it runs on. With the advent of VLSI technology, it is now possible to build customized computer systems of astonishing complexity for very low cost. Exploiting this capability, however, requires designing algorithms which not only use few operations, but also have a high degree of regularity and parallelism, or can be easily pipelined. Directions we are exploring include systematic methods for designing multi-processor arrays for signal processing, isolating signal processing primitives for hardware implementation, and searching for algorithms for multi-dimensional processing which exhibit a high degree of parallelism.

There also are a number of projects directed at the development of new algorithms with broad potential applications. For some time we have had considerable interest in the broad question of signal reconstruction from partial information such as Fourier transform phase or magnitude. We have shown theoretically how under very mild conditions signals can be reconstructed from Fourier transform phase information alone. We have also developed a variety of theories and algorithms relating to signal reconstruction from Fourier transform magnitude and from partial short-time Fourier transform information. We are also exploring the application of some of these theoretical results to problems such as speech and image coding.

A recent and growing emphasis in our group is the combination of signal processing and artificial intelligence techniques. There are a variety of problems in signal analysis that can be approached

either from the analytical viewpoint characteristic of signal processing or the symbolic viewpoint characteristic of knowledge-based systems and artificial intelligence. We believe there is considerable potential for combining these two viewpoints into what we refer to as knowledge-based signal processing. There are currently two projects under way directed at developing this approach in the context of specific signal processing problems. One attempts to exploit artificial intelligence concepts to develop a knowledge-based pitch detector and the second, to explore knowledge-based signal processing in the context of signal enhancement. We have also coupled our work on knowledge-based signal processing into a project at Lincoln Laboratory on distributed sensor nets.

21.2 Improved Paraxial Methods for Modeling Underwater Acoustic Propagation

U.S. Navy – Office of Naval Research (Contracts N00014-81-K-0742 and N00014-77-C-0266)
Arthur B. Baggeroer, Thomas E. Bordley

In modeling long-range sound propagation through the world's oceans, the severe computational and informational demands of the processing render straightforward solution of the hyperbolic wave equation governing the fields prohibitively expensive. For this reason, much effort has been expended to develop approximate solutions which effectively exploit the near stationarity of the channel with range. In mode methods, for example, the inhomogeneities in range are totally or partially ignored. The more general of these techniques, invoking the quasi-adiabatic approximation, assume that the primary effect of slow change in the channel is slow change in the shape of the modes, so that coupling between the modes is negligible. Other approaches such as ray methods simplify the problem by considering only the high frequency asymptotes of the field. In addition, a more general solution, the method of Gaussian beams, has been developed which treats the diffusive effects ignored by conventional ray tracing.

Of particular importance when the full field must be modeled and the inhomogeneities cannot be neglected are paraxial methods. These techniques solve a simplified form of the wave equation, obtained by splitting the field into transmitted and reflected components, and then neglecting the reflected field. The justification for this approach is that for a stationary media, no energy is reflected back to the source, so for a media which varies slowly with range, the reflected field should be small. In practice, current techniques perform well except when bottom interaction is important — for example, in areas such as the Arctic Ocean where no SOFAR channel exists. Even when these methods fail, however, their underlying assumption remains true: the energy transmitted forward greatly dominates the energy reflected back. Therefore, effective modeling within the framework of this approximation should be possible.

The concern of this research is to develop paraxial methods less restricted in angle, yet retaining the numerical stability and efficiency which have made this class of solutions so valuable. Two

methods are considered. The first, a multiple beam approach, finds a series of local solutions for the field, accurate in the neighborhood of the ray paths, and patches these solutions together to generate the total field. In the second, a dynamic splitting algorithm, the notion of a split is generalized to allow variation in range and depth, and the solution is determined iteratively with the current estimate of the field used to generate a better split for the next step. The effectiveness of these techniques is examined in the context of modeling sound propagation in the Arctic Marginal Ice Zone.

21.3 Adaptive Image Restoration

U.S. Navy - Office of Naval Research (Contract N00014-81-K-0742)
National Science Foundation (Grant ECS80-07102)
Jae S. Lim, Philip Chan

There have been many mathematically optimal linear noise smoothing techniques developed for noisy images with the assumption of stationarity over the entire image. The use of space invariant filters results in blurring of edges in the processed images. Space-variant filters offer an attractive alternative to space-invariant filter. This class of filters does not assume global stationarity nor require detailed *a priori* knowledge of the image and noise processes. These methods are adaptive to varying details over the image. In addition, these algorithms are simple to implement.

One effective adaptive noise smoothing algorithm estimates the *a priori* mean and variance of each pixel from its local mean and variance in a window. Then, the minimum mean-square error estimator in its simplest form is applied. Essentially, the algorithm multiplies the difference between the pixel value and the pixel mean by a gain factor and adds it to the local mean to obtain the output pixel. The gain factor k is a function of the local image and noise variances. For images with low SNR, this algorithm does not result in sufficient noise removal, especially near the high-contrast regions.

To achieve better control on the trade-off between the degree of noise smoothing and the degree of edge preserving, we introduce a contrast expansion factor β and modify the gain factor to k^{β}. For $\beta = 0$, the image remains unprocessed and for $\beta = \infty$, the filter reduces to simple local averaging. In addition, we have made a modification in the algorithm implementation, which leads to significant improvement both in performance and computations. Specifically, we use up to four one-dimensional filters oriented at 0, 45, 90, and 135 degrees respectively. Because each filter is adaptive in the same manner as the basic algorithm, a sharp edge inclined at a large angle to the filter direction remains intact, while the noise in the edge area is removed by one of the filters that lies closest to the direction of the edge. The same factor β is used to control the degree of smoothing as before. The result is the simultaneous reduction of noise and preservation of edges.

The algorithm is being developed and tested on images corrupted by additive Gaussian noise at a SNR as low as 3 dB. Preliminary results show remarkable improvement over other methods in its

ability to preserve edges and remove noise in all regions including the edge areas.

21.4 Signal Reconstruction from Partial Fourier Domain Information

U.S. Navy - Office of Naval Research (Contract N00014-81-K-0742)
National Science Foundation (Grant ECS80-07102)
Bell Laboratories Fellowship
Alan V. Oppenheim, Susan R. Curtis

In a variety of practical problems, only the magnitude or the phase of the Fourier transform of a signal is available, and it is desired either to reconstruct the signal exactly or to synthesize a signal which retains many of the important characteristics of the original signal. We are working on several distinct problems in this area. One set of problems is to identify those portions of the FT which contain most of the "intelligibility" information, and to develop conditions under which a signal can be exactly reconstructed from only this partial information. Another set of problems involves finding practical algorithms for doing the reconstruction and finding applications where such a reconstruction is desirable.

On the intelligibility problem, past work has shown that a signal synthesized with the correct phase or signed-magnitude maintains many of the important characteristics of the original signal, whereas a signal synthesized from the correct magnitude and zero or random phase does not. We have also found that a signal synthesized from one bit of phase alone is intelligible. Since this one bit of phase is contained in both the signed-magnitude and the phase but not in the magnitude alone, this result helps to explain the earlier results.

Past work on exact reconstruction involved the development of conditions under which signal reconstruction is possible from only the magnitude, phase, or signed-magnitude of the FT. We have developed a number of new extensions and generalizations of these results. Recently, we have also developed some surprising new results on signal reconstruction from one bit of phase alone, without any magnitude information.

We have also applied algorithms often used for reconstruction from magnitude or phase towards the problem of reconstruction from one bit of phase. An iterative reconstruction procedure, which involves imposing constraints in both time and frequency domains, only yields good results if the FT is significantly oversampled. Another procedure, involving the solution of linear equations, yields excellent results for small signals, but is impractical for large signals. We hope to develop an algorithm which works well for larger signals.

Despite the potential applicability of results on reconstruction from partial information to a wide

range of problems, so far the results have been mostly of theoretical value. Thus, we are also interested in finding applications of these results. One application we have been exploring is the design of FIR filters to match a given magnitude and phase specification. Our approach is to first find an FIR filter to match the phase specification using phase-only reconstruction techniques, and then use the Parks-McClellan algorithm to compensate for the resulting magnitude. We are also interested in exploring applications of our results on reconstruction from one bit of phase.

21.5 Helium Speech Enhancement from the Short-Time Fourier Transform Magnitude

U.S. Navy – Office of Naval Research (Contract N00014-81-K-0742)
National Science Foundation (Grant ECS80-07102)
Jae S. Lim, Douglas S. Deadrick

Since sound travels faster in a hyperbaric helium-oxygen atmosphere than in air at normal pressure, speech uttered in this type of environment suffers from certain severe degradations. This effect handicaps communication systems for deep-sea divers and others who must work in such an atmosphere.

The effects of the helium can be easily identified using short-time Fourier analysis. Specifically, the frequencies of the speech formants are increased non-linearly and the formant bandwidths are increased. These phenomena take place while the pitch information is left relatively undisturbed. Models exist for translating the formants of helium speech back to their normal frequencies, and these models are suitable for use with the short-time Fourier transform (STFT).

Previous attempts to enhance such speech using the STFT have introduced noise into the pitch magnitude and phase information. This work will apply pitch detection algorithms to the enhancement scheme in order to reduce the amount of noise. Moreover, since the required modifications to the STFT are valid only for its magnitude, recent techniques for estimating a signal from its STFT magnitude will be used to construct the enhanced speech.

21.6 Knowledge-Based Pitch Detection

Amoco Foundation Fellowship
U.S. Navy - Office of Naval Research (Contract N00014-81-K-0742)
National Science Foundation (Grant ECS80-07102)
Alan V. Oppenheim, Randall Davis, Webster P. Dove

Knowledge-based signal processing is an effort to design signal processing programs that go beyond purely numerical processing of the data and try to symbolically reason about the problem in

order to better solve it. Problems appropriate for this area are those whose model is either too complex to be solved directly with a numerical algorithm, and those for which the model is not well understood.

Pitch detection falls into this category both because the speech signal model is not well specified, and because the model for the generation of pitch is not fully understood.

This project is developing a program called the Pitch Detector's Assistant (PDA) which will both serve to reduce the effort involved in generating hand edited pitch and provide a laboratory for studying and programming the knowledge that makes humans better pitch trackers than existing automatic algorithms.

Existing methods of semi-automatic pitch detection[1] require the user to make a voicing decision and select a pitch individually for every frame. The PDA program is intended to analyze as much of the utterance as it is sure of and then help the user with the remaining difficult portions. Thus we expect a dramatic reduction in the time from the current 30 minutes per second of speech analyzed.

Although there have been projects which combine signal processing and AI technology for particular problems such as speech understanding[2,3] and underwater acoustic signal recognition,[4] the actual signal processing present in these systems has only been used as a means for generating symbolic objects. These objects are then manipulated by the AI portions of the program until an interpretation of the data is complete. The symbols do not provide information to assist subsequent numerical processing, and thus the information flows one way from numeric to symbolic form. The pitch detection problem choice is motivated by the observation that these other problems are ones of recognition (i.e. signals in, symbols out) and naturally lead to solutions which process numerically first and symbolically later.

By choosing a problem which involves signal output we assure the use of numerical processing in later portions of the program. The creation and study of programs which emphasize the interaction between symbolic and numerical processing, is the primary purpose of the knowledge-based signal processing effort at MIT.

References

1. C.A. McGonegal, L.R. Rabiner, and A.E. Rosenberg, "A Semiautomatic Pitch Detector (SAPD)," IEEE Trans. ASSP 23, 570-574 (December 1975).
2. L. Erman, R. Hayes-Roth, V.R. Lesser, and D.R. Reddy, "The Hearsay-II Speech Understanding System: Integrating Knowledge to Resolve Uncertainty," Computing Surveys 12, 213-254 (June 1980).
3. B. Lowerre and R. Reddy, "The HARPY Speech Understanding System," in W. Lea (Ed.), Trends in Speech Recognition (Prentice-Hall, 1980) pp. 340-360.
4. H.P. Nii, E.A. Feigenbaum, J.J. Anton, and A.J Rockmore, "Signal-to-Symbol Transformation: HASP/SIAP Case Study," AI Magazine 3, 23-35 (Spring 1982).

21.7 Multi-Dimensional High-Resolution Spectral Analysis and Improved Maximum Likelihood Method

U.S. Navy - Office of Naval Research (Contract N00014-81-K-0742)
National Science Foundation (Grant ECS80-07102)
Jae S. Lim, Farid U. Dowla

Although MEM, MLM, and AR-modeling spectral estimation are high resolution spectral estimation algorithms, in multidimensional situations there are problems with each of these methods. The MEM algorithms are iterative and their applications to real world problems is prohibitive from numerical viewpoints. MLM does not quite achieve the resolution which one would like it to have. The AR-modeling has problems as the shape of the spectrum is distorted when the filter mask does not conform to certain symmetry.

We are developing a closed-form high resolution spectral estimation algorithm based on the concepts of MLM, MEM, and AR spectral estimation. We have found a useful relationship between the MLM and AR signal modeling in multidimensions. By exploiting this relationship and by studying the problem of array design in multidimensions for these algorithms, we propose to present an algorithm with computational properties like the MLM but whose resolution property is better than the MLM.

The performance of the algorithm is being evaluated on synthetic data and on real data in a multichannel radar tracking problem.

21.8 Speech Synthesis from Short-Time Fourier Transform Magnitude Derived from Speech Model Parameters

U.S. Navy - Office of Naval Research (Contract N00014-81-K-0742)
National Science Foundation (Grant ECS80-07102)
Jae S. Lim, Daniel W. Griffin

Previous approaches to the problem of synthesis from estimated speech model parameters have primarily employed time-domain techniques. Most of these methods generate an excitation signal from the estimated pitch track. Then, this excitation signal is filtered with a time-varying filter obtained from estimates of the vocal tract response. This approach tends to produce poor quality "synthetic" sounding speech.

In this research, a new approach to speech synthesis from the same estimated speech model parameters is investigated. In this approach, a desired modified short-time Fourier transform magnitude (MSTFTM) is derived from the estimated speech model parameters. The speech model

parameters used in this approach are the pitch estimate, voiced/unvoiced decision, and the spectral envelope estimate. The desired MSTFTM is the product of a MSTFTM derived from the estimated excitation parameters and a MSTFTM derived from spectral envelope estimates. (The word "modified" is included in MSTFTM in these cases to emphasize that no signal exists, in general, with this MSTFTM). Then, a signal with short-time Fourier transform magnitude (STFTM) close to this MSTFTM is estimated using the recently developed LSEE-MSTFTM algorithm.[1,2] Preliminary results indicate that this method is capable of synthesizing very high quality speech, very close to the original speech.

This method has applications in a number of areas including speech coding and speech enhancement. In speech coding applications, the excitation parameters and spectral envelope can be coded separately to reduce transmission bandwidth. Then, these coded parameters are transmitted and then decoded and recombined at the receiver. In speech enhancement applications, the excitation parameters and the spectral envelope can be separated, processed separately, and then recombined.

References

1. D. W. Griffin and J. S. Lim, "Signal Estimation from Modified Short-Time Fourier Transform," Proceedings of the 1983 Int. Conf. on Acoustics, Speech and Signal Processing, Boston, Massachusetts, April 14–16, 1983, pp. 804–807.
2. D. W. Griffin and J. S. Lim, "Signal Estimation from Modified Short-Time Fourier Transform," IEEE Trans. ASSP 32, 2, 236–243 (1984).

21.9 Speech Enhancement Using Adaptive Noise Cancelling Algorithms

U.S. Navy – Office of Naval Research (Contract N00014-81-K-0742)
National Science Foundation (Grant ECS80-07102)
Jae S. Lim, William A. Harrison

This research is directed towards evaluating the performance of some general adaptive noise cancelling algorithms in a distributed noise environment. General adaptive noise cancelling algorithms utilize one or more reference microphones that record a correlated version of noise that is additively corrupting a desired signal in the primary microphone. In practice, the desired signal is often recorded by the reference microphones. Under these conditions, the algorithm will attempt to cancel part or all of the desired signal. Under certain conditions, modifications in an adaptive noise cancelling algorithm such as the Widrow-Hoff least mean square algorithm, allows one to still reduce the background noise without severely distorting the desired signal. One application of this work is in reducing the background noise in a jet fighter pilot's speech. Test cases conducted with simulated data have shown some promise that the ANC algorithm can be used to improve the SNR of the pilot's speech.

21.10 Overspecified Normal Equations for Autoregressive Spectral Estimation

U.S. Navy – Office of Naval Research (Contract N00014-81-K-0742)
National Science Foundation (Grant ECS80-07102)
Jae S. Lim, David Izraelevitz

There is a one-to-one relationship between a set of P normalized positive definite correlation estimates and the P predictor coefficients derived using autoregressive modeling. Several researchers have proposed the use of M > P correlation estimates to provide a better Pth order model. Specifically, the normal equations are augmented to provide M linear equations between the correlation estimates and the predictor coefficients. Since the system of equations is now overspecified, a least squares solution is required.

In this research a study is presented of some of the properties of the method of overspecified normal equations as applied to the problem of spectral estimation. The main contribution of this research is the derivation of the relationships between the number of correlations used, the model order and the signal-to-noise ratio of the signal, to the characteristics of the resulting spectral estimate. The characteristics studied are the spectral height, bandwidth and area. The method is shown to be a spectral density estimator like the ME method, where spectral areas rather than spectral values should be interpreted as estimates of power.

The relationships derived point to the number of correlations used over the minimum, i.e., model order, as a signal-to-noise enhancer. The resulting spectrum is equivalent to the ME spectrum under higher signal-to-noise conditions. Another result is the requirement of a proportionality constant dependent on the number of correlations and the model order which is necessary for unbiased signal-to-noise measurements. This constant is not required however, for measurements of relative power within the same spectral estimate, as in the power ratio of two sinusoids in noise.

The second part of the research presents some empirical studies using computer simulations which verify the theoretical predictions and provide the region of validity of the analysis. Further experiments study the interfering effect of several closely spaced sinusoids. The method of overspecified normal equations is shown to be much more sensitive to this interference than the ME method. Finally, some further empirical studies are made of the resolution capabilities of the method. Using the data derived, an empirical model is derived which seems to agree to some extent with the data.

This work was completed in June 1983.

21.11 Restoration of Image Sequences with Motion

U.S. Navy - Office of Naval Research (Contract N00014-81-K-0742)
National Science Foundation (Grant ECS80-07102)
Jae S. Lim, Dennis M. Martinez

The problem of image restoration for static, single frame images has received much attention in signal processing research. Most of the effort has been devoted to the problem of restoring single image frames which have been degraded in some way (additive noise, quantization noise, etc.). However, in many situations one is dealing with sequences of image frames, which when viewed in temporal succession constitute a scene with motion. Either in communicating or processing of such signals, various degradations can also occur.

In developing algorithms for restoring sequences of image frames, there are a number of issues which are not present in the single frame case. For example, there is the possibility of utilizing inter-frame as well as intra-frame information in performing restoration. Inter-frame methods take advantage of the fact aht most motion video frames have a high degree of temporal correlation. However, because the scenes are changing with time, there is the added problem of motion compensation to be contended with.

This research is concerned with developing methods for using motion information in performing restoration of scenes with motion. There are two important questions presently under consideration. Even before attempting to use motion information in restoration algorithms, a fundamental question concerns how accurate motion estimates have to be in order to be useful in performing restoration. One goal of the presen work is to determine how the performance of several different restoration algorithms vary as the accuracy of a motion estimate deteriorates. Once this has been determined, attention will be focused on developing restoration algorithms which can combine motion estimation with restoration.

21.12 Knowledge-Based Array Processing

U.S. Navy - Office of Naval Research (Contract N00014-81-K-0742)
National Science Foundation (Grant ECS80-07102)
Alan V. Oppenheim, Evangelos E. Milios

The objective of this research is to explore the integration of signal processing knowledge with symbolic knowledge about the physical objects that generated the signal in the context of acoustic sensor array processing. A taxonomy of array processing techniques is being formed on the basis of their assumptions and performance in the real world of acoustic sensor array processing. This knowledge will be matched with information about the motion of the sources of sound and the system

will possibly be coupled with another system that performs low-level interpretation of signal processing results. For now, the interpretation system will be simulated by a human interpreter.

In order to explore the issues involved in planning, diagnosis, monitoring, design and prediction within the array processing context, a simpler problem is being considered, that of performing spectral analysis of a single acoustic waveform with the purpose of classifying the source that generated it. The signal processing issues in one-dimensional spectral analysis are much better understood than in the multidimensional case to which the array processing problem can be reduced. For this reason, it is felt that the one-dimensional problem is an appropriate first step toward exploring the signal-symbol integration. It is believed that research in the one-dimensional case will generate the necessary ideas to enable the design of the more general knowledge-based array processing system.

21.13 The Use of Speech Knowledge in Speech Analysis

Schlumberger-Doll Research Center Fellowship
U.S. Navy - Office of Naval Research (Contract N00014-81-K-0742)
National Science Foundation (Grant ECS80-07102)
Sanders Associates, Inc.
Alan V. Oppenheim, Cory Myers

The problem of speech modeling is one which has been of great interest in the signal processing community. As part of our efforts to explore methods by which signal processing and symbolic processing techniques can be made to interact we are building a system for symbolic reasoning about speech analysis. The system produces a time-varying parametric model of the speech signal where, not only do the parameters change over time, but the models used may also change over time. For example, the system may perform all-pole modeling of the signal but may change the number of poles which are to be used in different portions of the signal. The system attempts to develop a parametric model of a speech signal given both the speech signal (or a noisy version of it) and a symbolic description of how the signal was produced. The symbolic description of the signal includes information about the speaker, such as gender and age, and information about the recording environment, such as noise characterization, sampling rate and speech bandwidth. The system is also given a symbolic description of the content of the signal in the form of a time-aligned phonetic transcription. The output from the system is a time-varying parametric representation of the speech signal (excluding excitation information).

The system generates its parametric representation in three stages. First a symbolic reasoning system takes the description of the signal, breaks the signal into sections, and recommends a signal analysis method for each section of the signal. These recommendations include choice of model and choice of analysis parameters, e.g. model order, window size, analysis rate, etc. The second stage of

the system runs the signal analysis methods recommended by the first stage. Estimates of modeling accuracy are also generated during the signal analysis. The third stage of the system examines the results from the signal analysis and the accuracy measures. It uses these and the original symbolic information to determine new models to try or modifications to make to the values from the models. Modifications are suggested according to both modeling error criteria and model smoothness criteria. The choice of appropriate modification criteria varies with the symbolic information available. The third stage continues to make modifications until a satisfactory set of models has been found.

21.14 Estimation of the Degree of Coronary Stenosis Using Digital Image Processing Techniques

U.S. Navy - Office of Naval Research (Contract N00014-81-K-0742)
National Science Foundation (Grant ECS80-07102)
Jae S. Lim, Thrasyvoulos N. Pappas

The aim of this research is the development of an algorithm for evaluating the degree of coronary artery stenosis from coronary cine-angiograms. A cine-angiogram is a sequence of x-ray pictures of the coronary arteries in which a contrast agent has been injected via a catheter. The precise measurement of the stenosis of the coronary arteries is important in the treatment of patients with ischemic heart disease.

The first step will be the determination of the percentage diameter reduction from a single frame of the cine-angiogram. This will require the detection of the boundaries of the coronary arteries and the analysis of the variation of their diameter. Preprocessing of the image for noise reduction will hopefully lead to improved boundary detection.

Subsequent steps will involve the analysis of multiple frames of the cine-films, and the investigation of densitometric procedures, which use the brightness information within the artery to obtain estimates of the cross-sectional percentage area reduction.

21.15 Automatic Target Detection in Aerial Reconnaissance Photographs

U.S. Navy - Office of Naval Research (Contract N00014-81-K-0742)
National Science Foundation (Grant ECS80-07102)
Jae S. Lim, Michael D. Richard

The detecting of small anomalous regions in images has aroused much interest in such areas as optical aerial reconnaissance, radar analysis, terrain classification, and medical diagnosis through imagery. A recently developed algorithm[1] has proven highly successful in detecting small objects or

targets in natural terrain such as trees, grass, and fields of aerial photographs. The algorithm uses a significance test to distinguish each image pixel as either background or non-background (i.e., target). Specifically, the background is assumed to be characterized by a nonstationary Gaussian probability distribution. The algorithm further represents the background by a two dimensional (2-D) autoregressive model. The resulting significance test is expressed as the error residuals of 2-D linear prediction.

This research will explore several new areas to either develop a superior detection algorithm or to significantly improve the existing one. First, the issue of target modelling will be explored. The current algorithm models only the background and treats targets simply as anomalies in the background. The question arises as to how a suitable model for targets can be incorporated in a detection algorithm. Second, methods to detect and to fully determine the boundaries of larger objects will be considered. The present algorithm can detect only small point objects representing statistical irregularities in the background random process. The issue of detecting larger targets poses significant questions regarding object detection, image segmentation, and boundary extraction. Additional research in these two areas should improve the somewhat favorable results obtained by using linear predictive techniques to detect anomalous regions in images.

References

1. T.F. Quatieri, "Object Detection by Two-Dimensional Linear Prediction," M.I.T. Lincoln Laboratory Technical Report 632, 28 January 1983.

21.16 Separation of Desired Speech from Interference Speech Reverberating in a Room

Toshiba Company Fellowship
U.S. Navy - Office of Naval Research (Contract N00014-81-K-0742)
National Science Foundation (Grant ECS80-07102)
Bruce R. Musicus, Hiroshi Sekiguchi

An important problem in the area of speech processing is speech enhancement. The objective of speech enhancement is ultimately to improve the intelligibility of the desired speech or to separate the desired speech from interfering signals, such as noise, other speech, or echoes.

A specific problem in speech enhancement, which this research will deal with, is the separation of an acoustically added speech signal simultaneously uttered in a confined room from the desired signal. This type of problem is often observed in the real world. One example is a broadcast news room environment. When a news anchor person is on the air in a broadcast studio, studio engineers running the broadcast often transmit to the news anchor person specific cues or messages to inform him/her of what is to be done next. If these messages are sent out over an audio monitor placed near the news anchor person, the microphone into which the newscaster speaks would also pick up the

messages played out by the audio monitor. It would be then necessary to subtract out the monitor signal together with any acoustic reflections from the microphone signal. This research will seek a practical and effective algorithm for canceling interfering speech in a real news room environment.

One class of enhancement methods attempts to subtract the interfering speech signal by exploiting the harmonic nature of speech. This class is called the one-data channel method, since only one microphone is used. One of these methods utilizes the difference in the fundamental frequencies, or pitch periods, between the interfering speech signal and the desired speech signal to selectively eliminate the interfering speech from the microphone signal using a comb filter. The two-data channel method primarily employs adaptive noise canceling schemes. Related work has been done by Mark Paulik, in which he utilized the noise cancellation scheme of Benard Widrow because both the microphone signal and the monitor signal are available to the algorithm. Although his work was restricted to exploring the theoretical feasibility of the adaptive noise cancellation approach, based on modeling the reverberant impulse response with a 21 tap filter with known coefficients, his results suggest that the approach may be quite practical.

The aim of this research is to investigate various types of modeling and estimation techniques for a reverberant environment. These include the periodogram technique, the pole-zero modeling technique, and the FIR technique. Facts which complicate the problem include: 1) The room reverberant impulse response may last more than 200 msec. This would produce more than 2000 parameters which would need to be estimated in the FIR technique at a 10 KHz sampling rate. It also indicates that at least 5 Hz frequency resolution may be required in the periodogram technique. 2) The news anchor person may move around in the studio with the microphone. Therefore, the estimation algorithm must adjust itself to the change of the system function adaptively. This requires a real-time algorithm fast enough to keep track of the change. The results of this algorithm will be combined with the noise cancellation scheme previously proposed by Mark Paulik, and the applicability of this new approach to a real studio environment will be studied. Hopefully, it will present an algorithm effective enough to display good performance in canceling the interfering signal in an actual studio.

21.17 Low Bit Rate Video Conferencing

M.I.T. Vinton Hayes Fellowship
U.S. Navy - Office of Naval Research (Contract N00014-81-K-0742)
National Science Foundation (Grant ECS80-07102)
Jae S. Lim, Ramakrishnan Sundaram

The attempt of this research is to achieve a drastic reduction in the channel capacity requirements for video transmissions. Currently, such transmissions require bandwidth of the order of 100 Mbps. An algorithm based on local averaging and adaptive thresholding has been developed which reduces

an 8-bit picture to a 1-bit binary picture without significant loss in quality. The resulting image is then smoothed by adaptive median filtering to remove random bit transitions. This is then suitable for run length coding. Compression factors of up to 60 are expected to result. Other forms of data encryption are also being examined. Currently the emphasis is only on intraframe redundancy reduction. The work is expected to lead on to interframe analysis.

21.18 Improved Techniques for Migrating Acoustic Fields

Hertz Foundation Fellowship
U.S. Navy - Office of Naval Research (Contract N00014-81-K-0742)
National Science Foundation (Grant ECS80-07102)
Alan V. Oppenheim, George V. Frisk[10] Michael S. Wengrovitz

The problem of inverting an acoustic field from a continuous-wave point source in the ocean to determine information about the bottom is being studied. Although there has been recent progress in this area, a successful inversion using real experimental data has not yet been performed. One apparent source of degradation in the inversion is the variation of sensor height off the ocean floor as a function of range. Numerical experiments with synthetic data have shown the importance of compensating for this variation.

Several algorithms which migrate the field to a fixed height off the bottom have improved the inversion results. These algorithms are based on the principle of a single dominant ray arriving at each range point. This concept suggests that improved migration schemes might account for multiple ray arrivals.

This research will explore new migration algorithms which exploit simple, robust ray approximations to acoustic data. These techniques may also be applicable to direct profile inversion using offset/ray-parameter data, mode determination in an acoustic waveguide, and reflected/direct field separation in acoustic experiments.

---

[10] Woods Hole Oceanographic Institution

22. Speech Communication

Academic and Research Staff

Prof. K.N. Stevens, Prof. J. Allen, Prof. M. Halle, Prof. S.J. Keyser, Prof. V.W. Zue, A. Andrade[11], Dr. D. Bradley[11], Dr. Martha Danly[12], Dr. F. Grosjean[13], Dr. S. Hawkins[14], Dr. R.E. Hillman[15], E.B. Holmberg[16], Dr. A.W.F. Huggins[17], C. Hume, Dr. H. Kawasaki, Dr. D.H. Klatt, Dr. L.S. Larkey, Dr. John Locke[18], Dr. B. Lyberg[11], Dr. J.I. Makhoul[17], Dr. E. Maxwell, Dr. L. Menn[19], Dr. P. Menyuk[20], Dr. J.L. Miller[13], Dr. J.M. Pardo Munoz[11], Dr. J.S. Perkell, Dr. P.J. Price, Dr. S. Shattuck-Hufnagel, S.-Q. Wang[11], T. Watanabe[11]

Graduate Students

A.M. Aull, C. Aoki, C. Bickley, F. Chen, K. Church, S. Cyphers, C. Espy, J. Glass, R. Goldhor, D. Huttenlocher, L. Lamel, H. Leung, M. Randolph, S. Seneff, C. Shadle

C.J. LeBel Fellowship
Systems Development Foundation
National Institutes of Health (Grants 5 T32 NS07040 and 5 R01 NS04332)
National Science Foundation (Grant 1ST 80-17599)
U.S. Navy - Office of Naval Research (Contract N00014-82-K-0727)
Kenneth N. Stevens, Dennis H. Klatt, Joseph S. Perkell, Stefanie Shattuck-Hufnagel, Victor W. Zue

---

[11] Visiting Scientist

[12] Staff Member, Wang Laboratories, Inc.

[13] Associate Professor, Department of Psychology, Northeastern University

[14] Postdoctoral Fellow, Haskins Laboratories

[15] Assistant Professor, Department of Speech Disorders, Boston University

[16] Research Scientist, Department of Speech Disorders, Boston University

[17] Staff Member, Bolt, Beranek and Newman, Inc.

[18] Director, Graduate Program in Speech-Language Pathology, MGH Institute of Health Professions, Massachusetts General Hospital

[19] Assistant Professor, Department of Neurology, Boston University School of Medicine

[20] Professor of Special Education, Boston University

22.1 Studies of Acoustics and Perception of Speech Sounds

We have continued our investigations of the acoustic and perceptual correlates of the features that distinguish between utterances in different languages. The aim of these studies is to establish the inventory of acoustic properties that are used to make these distinctions, and to attempt to uncover the principles governing the selection of this inventory of properties that appear to be used across all languages. The techniques we are using in this research include acoustic analysis of utterances representative of the distinctions, and human perception of synthetic utterances in which the relevant properties are systematically manipulated. The phonetic features that we have been studying over the past year include: the nonnasal-nasal distinction for vowels in certain languages of India (as well as the influence of nasal consonants on vowels in English); the use of duration of a preceding vowel or nasal consonant to signal voicing for an obstruent consonant in Portuguese; the distinction between tense and lax vowels in English, including differences in duration, formant trajectories, and relative prominence of spectral peaks; the acoustic properties that distinguish between the liquids and glides /l, r, w, y/ in English; the relative roles of formant transitions and bursts in stop-consonant perception; the distinction between velars and uvulars in Arabic; and the distinctions between dental, alveolar, and palatal consonants in certain Australian languages.

In addition to our studies of the segmental aspects of speech production and perception, we are continuing our investigation of the influence of fundamental frequency on the comprehension of sentences. We have found apparent differences between speakers in the contribution of the F0 contour in a reaction-time task involving sentence comprehension, and we are investigating the source of these individual differences.

A program of research aimed at an acoustic analysis of Japanese syllables and sentences had been initiated. The purpose is to see if it might be feasible to synthesize Japanese sentences by rule within the general framework specified in Klattalk, and further, to determine the minimal data set that would permit such an effort to succeed. We have recorded syllables and sentences from three speakers, and have made measurements of formant motions in the CV syllables and durations in sentences. Phonological recoding phenomena in sentences are being studied and tentative rules have been formulated. We are in the process of analyzing these data.

A digitized data base consisting of 129 CVC English words spoken by 12 men, 12 women, and 12 children has been acquired from a cooperating group. The words include many different CV and VC syllables. This data base will be analyzed in the coming year to determine the extent to which the synthesis-by-rule framework described elsewhere in this report can be used to characterize the data, produce meaningful averages, and perhaps suggest better ways to approach the problem of phonetic recognition by machine.

As we proceed with these phonetic studies, we are continuing to revise and to elaborate on our theoretical views concerning invariant acoustic correlates of phonetic features and the role of

redundant features in enhancing phonetic distinctions.

22.2 Speech Production Planning

Spontaneous speech error patterns suggest at least two conclusions about normal speech planning:

(1) it involves the formulation of representations in terms of sublexical elements like phonemic segments (C.V), syllable onsets (CC), and syllable rhymes (VC); and

(2) it includes processing mechanisms that manipulate these units, e.g., a serial ordering process. We are examining the nature of the sublexical planning processes by analyzing constraints on and patterns in the manipulation of these units, in speech errors (both spontaneous and experimentally elicited) and pig-latin-like play languages. Recent findings provide information about the following questions:

What are the planning units? Although spontaneous speech errors often involve syllabic units like single C's and V's, consonant clusters, and -VC's, they seldom move or change whole syllables (unless the syllable also corresponds to a morpheme). This suggests that at some point in production planning, syllable-like frames provide the organizing schema for syllabic processing units. Using tongue twisters like "play cat plot coy," we are pursuing the question of how and when onset clusters like /pl/ come apart in errors, and when they function as whole units. In a second line of investigation we are examining the spontaneous and elicited output of speakers who use play languages that manipulate sublexical fragments in various ways, in order to gain insight into the nature of the representation of syllabic and subsyllabic units.

What are the representational dimensions? On the assumption that shared representational dimensions make two elements more likely to interact in an error, we have examined spontaneous errors to see which dimensions are shared by pairs of target and intrusion elements. One obvious finding is position similarity: Two target segments can interact when they appear in similar positions (like initial /t/ and /d/ in "top dog"). Elicitation experiments have shown that shared position in the word is more conducive to errors than is shared position in the stressed syllable (e.g., /j/ and /d/ are more likely to interact in "july dog" than in "legit dog"). This indicates that word-sized units play a role in the representation of an utterance at the point where sublexical ordering errors occur.

A second finding is phonemic context similarity: Interacting consonant segments are often followed by identical vowels, as in /f/ and /p/ in the error "pat fack" for "fat pack." Experimental elicitation errors show this same contextual similarity constraint.

We are now using an elicitation technique to ask whether context similarity affects some error types more than others. Such a finding would support a model in which different sublexical error types (exchanges, substitutions, shifts, etc.) are associated with different aspects of phonemic processing

(see next section).

What are the sublexical processing stages or mechanisms? Is there a single sublexical planning mechanism or are there several? If there are several, then it is a reasonable assumption that each is susceptible to its own particular type and pattern of errors. Against the simplest assumption of one mechanism are several findings in the elicited error data: (1) Words behave differently from nonwords. (2) Content words and function words participate differently in sublexical errors in spontaneous speech: many more sublexical errors occur in content words than in function words, even though function words are more frequent. (3) Stressed-syllable-position similarity does not interact with word-position similarity in facilitating sublexical interaction errors.

Taken together, these results suggest the existence of at least two planning mechanisms in normal speech processing that make reference to sublexical units: one that involves the organization of real words and morphemes of English into grammatically well-formed utterances, and another that controls the organization of strings of phonemic elements (whatever their grammatical status) into utterable sequences. Experiments now in progress test this hypothesis in the following ways: by comparing sublexical errors in content words vs. function words, in the recitation of prespecified lists and phrases vs. the generation of fresh new utterances, and between segments in similar phonemic contexts vs. dissimilar ones.

22.3 Auditory Models and Speech Processing

In an attempt to gain insight into the mechanisms used by human listeners in the processing of speech, we are developing models of the peripheral auditory system and we are examining the response of these models to selected classes of speech sounds. These models contain sets of bandpass filters with critical bandwidths, and process the outputs in different ways. One of the models incorporates a special procedure for detecting synchrony in the waveform at the filter outputs, and provides a representation of vowellike sounds with enhanced spectral prominences. This model is being tested with a variety of nonnasal and nasal vowels produced by speakers with a range of fundamental frequencies, and its behavior is being compared with the results of more conventional types of spectral analysis. Another model is oriented toward simulating the auditory response to speech events characterized by rapid frequency and amplitude changes, and incorporates adaptation properties similar to those observed in the peripheral auditory system. The behavior of this model is being tested with speech and speechlike sounds that simulate stop gaps of various durations and degrees of abruptness, and sounds in which various rates of spectrum change occur near an onset.

This work on implementation of auditory models has been paralleled by the continuing development of theoretical ideas concerning the potential utility of these models, and the directions for future research on auditory modeling. Ideas that have been produced in published papers include: (1) the necessity for reexamining and possibly broadening the bandwidths that are appropriate for speech analysis at low frequencies; and (2) the types of "central filtering" that are appropriate, beyond the

stage of peripheral processing.

22.4 Physiology and Acoustics of Speech Production

A pilot study of jaw movements produced during selected speech and nonspeech tasks performed at different rates has been completed. Several hypotheses have been developed as a result of this study, and these have been concerned with the relation between articulatory effort and the articulatory targets selected by a subject when producing alternating jaw movements at different rates. In preparation for a more detailed study of these questions, algorithms have been developed to automatically extract movement distance, time, peak velocity and peak acceleration from displacement, velocity and acceleration signal stream data. These algorithms will be used to increase the efficiency of data processing, thereby allowing us to explore constraints on jaw movements with larger numbers of subjects and more varied experimental conditions. Experiments will be designed to test the hypotheses that were addressed in or have grown out of the pilot study.

Progress has been made in evaluating a full prototype of an alternating magnetic field transducer system for simultaneous tracking of several midsagittal-plane points inside and outside the vocal tract. The prototype electronics were completed and are being tested in conjunction with a new, small transducer. For this testing, several precision mechanical components have been designed and built. These components include a plastic jig to hold the transmitter coils and eventually mount them on a subject's head, a plastic testing device which enables us to move a transducer in circles of different radii and through straight lines with different degrees of transducer tilt, and an apparatus that enables us to precisely translate and tilt a transducer with respect to the transmitters for calibrating the field. A procedure has been devised to record data directly into the computer. Data processing algorithms have been developed to convert the raw data into Cartesian coordinates in the midsagittal plane, and an algorithm has been developed to plot midsagittal-plane trajectories of transducer displacement. The data processing and plotting algorithms have been used to evaluate the performance of the system in tests which include the input of circles and straight lines using the testing device. Several problems with the electronics and calibration techniques have been encountered and overcome, and testing is near completion. Work on the finished laboratory apparatus has begun.

In collaboration with Dr. Robert Hillman and Ms. Eva Holmberg at Boston University, we have continued work on a project on the use of non-invasive aerodynamic and acoustic measures during vowel production to study hyperfunctional and other voice disorders. Recording and data processing techniques have been further refined, and data collection and processing is proceeding on a number of normal and pathological subjects. This work is exploring the utility of measures of glottal resistance to airflow, vocal efficiency and various measures derived from glottal airflow waveforms as predictors of voice dysfunction. Preliminary work on devising test procedures has pointed out the importance of carefully controlling speaking mode and rate for obtaining oral measurements which can be used for the reliable estimation of glottal function.

Studies of the characteristics of turbulence noise sources in speech production have been continued with further measurements of the amplitude and spectrum of sound that is generated when air is passed through constrictions in mechanical models and impinges on obstacles (simulating the teeth or lips). Evidence has been gathered to show that the source of sound produced in this way has the characteristics of a dipole source, and can be modeled in one dimension by a series source of sound pressure. Further experiments and theoretical analysis is proceeding with various configurations of the constrictions and obstacles in mechanical systems that simulate human production of fricative sounds.

22.5 Speech Recognition

The overall objectives of our research in machine recognition of speech are:

— To develop techniques for incorporating acoustic-phonetic and phonological knowledge into speech recognition systems;

— To carry out research aimed at collecting, quantifying, and organizing such knowledge; and

— To develop prototype systems based on these principles.

During the past year progress has been made on several projects related to these broad objectives.

22.5.1 An Isolated-Word Recognition Model Based on Broad Phonetic Information

In 1982, we conducted a study on the structural constraints imposed by a language on the allowable sound patterns. Words were indexed into a lexicon based on broad phonetic representations, and it was found that the number of words sharing a common representation in this form is very small. As a result, we proposed an approach to isolated word recognition for large vocabularies. In this proposal, the speech signal is first classified into a string of broadly-defined phonetic elements. The broad phonetic representation is then used for lexical access, resulting in a small set of word candidates. Finally, fine phonetic distinctions determine which of these word candidates were actually spoken.

We have extended this model in several directions. First, the potential role of word-level prosodic information in aiding lexical access was examined. Again using the Merriam Websters Pocket dictionary as our database, we found that knowledge of the three-level (i.e., stressed, unstressed, and reduced) stress pattern of a given word, or simply the position of the most stressed syllable, significantly reduces the number of word candidates in lexical access. A project is underway to determine the stress patterns of isolated words from the acoustic signal while utilizing the constraints on allowable stress patterns.

Second, refinements were made to our original model in order to minimize the effect of acoustic

variability and front-end errors. Specifically, lexical access is based on prosodic information, and segmental information derived from stressed syllables, where the acoustic information is known to be robust. We are developing a preliminary implementation of a word hypothesizer based on partial phonetic information.

22.5.2 Speaker-Independent Continuous Digit Recognition

We also explored for continuous speech the use of constraints like those described in the previous section. Specifically, we focused on the task of continuous digit recognition as a feasibility demonstration. In our proposed model, the first step is the broad classification of the segmentable portions of the acoustic signal. Next, the segment lattice is scanned for all possible digit candidates spanning the utterance. Finally, the best digit string is selected as the answer based on further detailed acoustic comparison of the digit candidates. We have completed a preliminary implementation of the system up to the point of lexical access. Formal evaluation indicated that the "fatal" error rate is about 1%. In other words, 1% of the time the correct digit cannot be recovered. The number of digit candidates has correspondingly been reduced by about 60%.

22.5.3 Properties of Consonant Sequences within Words and Across Word Boundaries

It is well known that, for a given language, there are powerful constraints limiting the permissible sound sequences within words. Sound sequences across word boundaries, on the other hand, are only limited by the allowable combination of words. In some cases, knowledge of the phoneme sequence in continuous speech uniquely specifies the location of the word boundary, while in other cases, phonotactic knowledge is not sufficient. For example, the word boundary can be uniquely placed in the sequence /... m g l ... /, as in the word pair "same glass", whereas the word boundary location is ambiguous in the phoneme sequence /... s t r ... / without further acoustic information. The /... s t r ... / may have a word boundary in one of three places as in "last rain", "mouse trap", and "may stretch."

As a step towards a better understanding of the acoustic phonetic properties of consonant sequences within and across word boundaries, we have studied the distributional properties of these sequences. We focused our inquiry on whether there exist structural constraints limiting the potential consonant sequences across word boundaries in English. The database consists of several text files from different discourses, ranging in size from 200 to 38,000 words. In each case we tabulated the number of distinct word-initial, word-medial, word-final, and word-boundary consonant sequences and their frequency of occurrence. It was found that, on the average, only 20% of the observed word-boundary sequences also occur in a word-medial position. Of those word-boundary sequences that can only occur across word-boundaries, approximately 80% have a unique boundary location.

The results of this study suggest that, given a detailed phonetic transcription, it may be possible to propose word boundary locations even if words are not delineated by pauses. When the consonant

sequence cannot uniquely specify the location of a word boundary, different placement of word boundaries often results in allophones with substantially different acoustic characteristics, as described in the our last report.

22.5.4 Automatic Phonetic Alignment of Phonetic Transcription with Continuous Speech

The alignment of a speech signal with its corresponding phonetic transcription is an essential process in speech research, since the time-aligned transcription can provide pointers to specific phonetic events in the waveform. Traditionally, the alignment is done manually by a trained acoustic phonetician, who listens to the speech signal and visually examines various displays of the signal. This is a very time-consuming task requiring the expertise of acoustic phoneticians, of whom there are very few. Furthermore, there is the problem of the lack of consistency and reproducibility of the results, as well as human errors associated with tedious tasks.

During the past year, we have developed a system to automatically align a phonetic transcription with the speech signal. The speech signal is first segmented into broad classes using a non-parametric pattern classifier. A knowledge-based dynamic programming algorithm then aligns the broad classes with the phonetic transcriptions. These broad classes provide "islands of reliability" for more detailed segmentation and refinement of boundaries. Acoustic phonetic knowledge is utilized extensively in the feature extraction for pattern classification, the specification of constraints for time-aligned paths, and the subsequent segmentation/labeling and refinement of boundaries. Doing alignment at the phonetic level permits the system to tolerate some degree of inter and intra-speaker variability.

The system was recently evaluated on sixty sentences spoken by three speakers — two male and one female. Ninety-three percent of the segments are mapped into only one phoneme, and 70% of the time the offset between the boundary found by the automatic alignment system and a hand transcriber is less than 10 ms.

We expect that such a system will enable us to collect and label a large speech database, which will directly contribute to our enhanced knowledge in acoustic phonetics. Furthermore, the automatic time alignment system can also serve as a testbed for specific recognition algorithms in that the success of the time alignment procedure depends critically on our ability to describe and identify phonetic events in the speech signal.

22.6 Speech Synthesis

A review of speech synthesis technology has been updated. The review includes a discussion of various methods for synthesizing speech from small building blocks and a description of the techniques used to convert text to speech.

Rules for synthesis of consonant-vowel syllables using a formant synthesizer have been updated

and described in a publication. It is argued that consonant-vowel coarticulation has systematic acoustic influences that are described fairly elegantly by hypothesizing up to three distinct allophones for each consonant — one before front vowels, one before back unrounded vowels, and one before back rounded vowels. Within each category, consonant spectra are remarkably invariant for one speaker, and consonant-vowel formant transitions obey a modified locus theory. It remains to be seen whether these results (quite satisfactory for synthesis purposes, as shown by CV intelligibility testing) apply to all English talkers (see analysis research described elsewhere in this report).

A text editor system for the blind has been assembled using a Rainbow personal computer and a Dectalk synthesizer to speak information that a sighted user obtains from a terminal screen during creation and editing of a text file. The software is currently undergoing evaluation and use by two blind professionals. Additional efforts are underway to get Dectalk used in other applications involving the handicapped.

In a theoretical paper, relations between synthesis by rule and linguistic theory have been discussed. Some of the solutions chosen in the search for a suitable abstract linguistic description of sentences in Dectalk, as well as some of the detailed rules for allophone selection and synthesis, may have implications for phonological theory. Synthesis activities not only provide a unique opportunity to test specific postulated rules, but may also guide thinking on the nature of universal phonological frameworks and descriptions. Examples of current descriptive controversies include a determination of the number of lexical stress levels in English. Experience with Klattalk seems to indicate that secondary lexical stress, if it is to be distinguished from unstressed/unreduced, has very restricted uses, no matter what acoustic cues are postulated to distinguish it. An example of Klattalk rules having implications for universal phonetic frameworks is the system of duration rules. Even if the detailed durational system of a language is considered a part of the language-specific feature implementation rules, ways must still be developed to represent the input to these rules adequately.

22.7 Issues of Variability and Invariance in Speech

National Institutes of Health (Grant 1 R13 NS 20005)
National Science Foundation (Grant BNS 83-11063)
Research Laboratory of Electronics

A symposium on "Invariance and Variability of Speech Processes" was held on October 8–10, 1983. The symposium was organized by members of the Speech Communication Group in collaboration with Prof. Gunnar Fant of the Royal Institute of Technology, Stockholm and Prof. Bjorn Lindblom of Stockholm University. About seventy researchers from the fields of speech production, perception, acoustics, pathology, psychology, linguistics, language acquisition, synthesis and recognition were invited. Twenty-four participants submitted drafts of papers which were distributed in advance of the meeting to serve as foci of discussion for all participants. Final manuscripts of focus and comment

papers are being prepared for inclusion in a proceedings book which is scheduled for publication late in 1984.

Among the contributions to the symposium were two papers from the Speech Communication Group. One of these papers reviews currently popular speech recognition techniques in light of the variability normally seen in speech. The paper presents arguments to show why techniques such as dynamic programming, automatic clustering, vector quantization, and LPC distance metrics are limited in their success. In each case, more knowledge of the processes actually contributing to irrelevant variability, as well as knowledge of that portion of the signal contributing useful context-dependent information, would help improve recognition systems. The same paper includes a description of the IBM speech recognition system in terms that permit comparisons between it and other approaches. The "learning" technique employed by IBM is very powerful, but other design choices in the IBM system were not so fortunate. Suggestions for combining the best ideas from LAFS (Lexical Access From Spectra) and IBM are included in the discussion. The positive features of LAFS as a way to incorporate knowledge of acoustic-phonetic details into a recognition system are discussed.

Another contribution to the symposium gives a review of the concepts of distinctive and redundant features, and presents a number of examples of the enhancing properties of redundant features and their role in phonology.

22.8 Computer-Based Speech Research Facilities

A new VAX-750 computer system to replace the old PDP-9 system has been installed. Software from the PDP-9 has been rewritten or modified in order to be useful on the VAX.

KLSYN Synthesizer. A formant synthesizer has been rewritten in floating point and augmented with a new more natural voicing source. Parameter specification from terminal commands has been implemented, and a VT-125 display package has been written to permit visualization of parameter tracks. Interactive graphics will be written when a VS-100 display and graphic input device arrive.

MAKETAPES Stimulus Generation. A program has been written to generate perceptual tests and to produce both answer sheets and response sheets automatically. Test types initially available include (1) identification tests, (2) 4IAX tests, and (3) fixed standard paired comparison tests.

KLSYN Spectral Analysis. A program to replace FBMAIN has been written. It can compare spectra for several waveforms at one time, and has four different spectral representations to choose from: (1) dft, (2) spectrogram-like, (3) critical-band, and (4) linear prediction. Hard copies of spectra and waveforms can be plotted.

SPECTO Crude Spectrogram. A program has been written to produce a crude spectrogram-like printout on the line printer, and a listing of f0 and formant estimates every 10 msec. The program is

useful when trying to synthesize from a natural model, and when using KLSPEC with a long utterance so as to "find your way".

KLATTALK. The Klattalk text-to-speech software has been made accessible to users. Stimuli can be prepared, or listings of parameter values can be obtained as a starting point for hand synthesis using KLSYN.

The development of an interactive speech research facility on our Lisp machines has also continued over the past year. In addition to refinements and additions to the capability of the SPIRE and SPIREX systems described in our last report, we have also developed a facility that enables researchers to study the distributional constraints imposed by a language. Researchers can ask questions such as: "How many three-syllable words in the database have primary stress on the first syllable?", or "How often is the homorganic rule violated in the database?", and obtain statistically meaningful results. The software package, including SPIRE, SPIREX, and ALEXIS, are available to interested parties through the MIT patent office.

23. Linguistics

Academic and Research Staff

Prof. A.N. Chomsky, Prof. J.A. Fodor, Prof. M.F. Garrett, Prof. K.L. Hale (on leave Fall 1983), Prof. M. Halle, Prof. J.W. Harris, Prof. S.J. Keyser, Prof. R.P.V. Kiparsky (on leave Fall 1983), Prof. J.R. Ross

Graduate Students

D. Archangeli, M. Baker, A. Barss, M. Browning, N. Fabb, E. Falk, N. Fukui, I. Haik, K. Johnson, M.-Y. Kang, J. Kisala, J. Levin, L. Levin, M. Magnus, R. Manzini, D. Massam, M. Montalbetti, W. Poser, P. Pranka, D. Pulleyblank, T. Rapoport, M. Rappaport, A. Rochette, S. Rothstein, M. Saito, J. Simpson, M. Speas, R. Sproat, L. Travis, E. Walli, J. Wager

Morris Halle

The ultimate objective of our research is to gain a better understanding of man's mental capacities by studying the ways in which these capacities manifest themselves in language. Language is a particularly promising avenue because, on the one hand, it is an intellectual achievement that is accessible to all normal humans and, on the other hand, we have more detailed knowledge about language than about any other human activity involving man's mental capacities.

Scientific descriptions of language have for a very long time followed a standard format. A number of topics are almost invariably discussed; for example, pronunciation, the inflection of words, word formation, the expression of syntactic relations, work order, and so forth. Moreover, the manner in which these have been treated has also been quite standard. While traditional grammars have many shortcomings, their great practical utility is beyond question; generations of students have acquired adequate command of innumerable languages with the help of grammars of the standard type. A plausible inference that might be drawn from this fact is that languages are somehow not very different from one another and that the traditional standard format has succeeded in capturing essential aspects of what all languages share in common. Accordingly, much of the research of the group has been devoted to studying the common framework that underlies different languages, the general principles that are exemplified in the grammar of different languages. Results strongly indicate that this assumption is indeed correct as far as the linguistic evidence is concerned.

The preceding discussion leads quite naturally to the question, "What evidence from outside of linguistics might one adduce in favor of the hypothesis that all languages are constructed in accordance with a single plan, a single framework?" It seems to us that the most striking evidence in favor of the hypothesis is, on the one hand, the rapidity with which children master their mother

tongue, and, on the other hand, the fact that even a young child's command of his mother tongue encompasses not only phrases and utterances he has heard but also an unlimited number of phrases and utterances he has not previously encountered. To account for these two sets of facts, we must assume that in learning a language a child makes correct inferences about the structural principles that govern his language on the basis of very limited exposure to the actual sentences and utterances. In other words, we must assume that with regard to matters of language a child is uniquely capable of jumping to the correct conclusions in the overwhelming majority of instances, and it is the task of the student of language to explain how this might be possible.

A possible explanation might run as follows. Assume that the human organism is constructed so that man is capable of discovering only selected facts about language and, moreover, that he is constrained to represent his discoveries in a very specific fashion from which certain fairly far-reaching inferences about the organization of other parts of the language would follow automatically. If this assumption is accepted, the next task is to advance specific proposals concerning the devices that might be actually at play. The obvious candidate is the theoretical framework of linguistics for, while it is logically conceivable that the structure of language might be quite distinct from that of the organism that is known to possess the ability to speak, it is much more plausible that this is not the case, that the structures that appear to underlie all languages reflect quite directly features of the human mind. To the extent that this hypothesis is correct — and there is considerable empirical evidence in its favor — the study of language is rightly regarded as an effort at mapping the mysteries of the human mind.

The research conducted by the linguistics group has almost from its inception been an integral part of the M.I.T. Ph.D. program in linguistics, which at present is housed in the Department of Linguistics and Philosophy. Many of the results obtained by the group were first presented by faculty or graduate students as part of a regularly scheduled class or are to be found in papers or dissertations written by students in partial fulfillment of different requirements for their Ph.D. degrees. Since dissertations in linguistics often remain unpublished or are published only after considerable delays it has been decided to publish abstracts of the dissertations accepted during the year 1983 in the present RLE Progress Report. It is our plan to publish dissertation abstracts in each subsequent Progress Report.

During 1983 seven dissertations in linguistics were accepted by the Department of Linguistics and Philosophy. Of these, one is in phonology, two deal with the interaction between syntax and word formation, whereas the remaining four concern various problems in syntactic theory viewed from the vantage points of the theory of government and binding (see N. Chomsky Lectures on Government and Binding (Foris 1981)) and lexical functional grammar (see J. Bresnan, The Mental Representation of Grammatical Relations (M.I.T. Press 1982)).

Aspects of Warlpiri Morphology and Syntax

Jane Helen Simpson

Submitted to the Department of Linguistics and Philosophy in
April 1983, in partial fulfillment of the requirements for the degree
of Doctor of Philosophy

Abstract

I present a fragment of Warlpiri grammar, within the framework of Lexical-Functional Grammar (LFG), focusing on the morphological and syntactic representation of the relations between arguments and argument-taking predicates. In Chapter 2, I discuss the assignment of grammatical functions to arguments within finite clauses headed by verbs or nominals. I argue for a rule which assigns grammatical functions freely to the daughters of S. This rule is the source of free work-order in Warlpiri. I also argue for a rule allowing an argument-taking predicate to introduce a null pronominal for any grammatical function which is linked to an argument of that predicate. This rule is the source of zero anaphora in Warlpiri.

Chapter 3 shows that case-suffixes have two main uses: to indicate that a nominal bears a particular grammatical function, such as SUBJECT, or that it is an attribute of another argument, and to act as an argument-taking predicate analogous to an English preposition. To preserve the *Lexical Integrity Hypothesis*, this last use requires the assignment of grammatical functions within the morphology, as part of the word-building process. I show that this assignment allows an account of the unusual phenomenon of double case-marking.

Chapters 4 and 5 treat the use of nominals as secondary predicates. The existence of discontinuous nominal expressions marked with the same case-suffix is shown to follow from independently needed rules. I claim that nominal secondary predicates are normally independent adjuncts, rather than subcategorizing arguments, as in English. A striking illustration of this is provided by the great freedom resultative attributes in Warlpiri have, compared with their English counterparts.

In Chapter 6, I examine the use of nominalized verbs, action nominals, and complementizer suffixes as secondary predicates. Such clauses have null pronominal SUBJECTs which bear case, suggesting that they must be *anaphorically* controlled. I show that the properties of complementizer suffixes can be represented in the same way as the properties of case-suffixes, with the exception that complementizer suffixes specify the grammatical function of their controllers. I present a classification of Warlpiri complementizer suffixes, in terms of their controllers and their tense properties, including a discussion of clauses with controlled OBJECTs.

Thesis Supervisor: Kenneth Locke Hale

Title: Ward Professor of Modern Languages and Linguistics

Syntax and Word Formation

Paula Marie Pranka

Submitted to the Department of Linguistics and Philosophy on
May 23, 1983 in partial fulfillment of the requirements for the Degree
of Doctor of Philosophy in Linguistics

Abstract

This dissertation concerns the morphophonological alternation of lexical items, determined by syntactic position. It considers three types of inflection, positional allomorphy and certain examples of phenomena collectively called "contraction", and argues that the notion of lexical insertion into d-structure, underlying many current syntactic theories, has difficulty in accounting for these cases. The difficulty is that the variation of forms for particular syntactic contexts is often a reflection of certain post-d-structure syntactic operations, such as move-X. Lexical insertion into d-structure occurs too early to be able to consistently insert the proper alternate for a given construction.

I argue that the lexical insertion concept conflates two independent processes: the projection from the lexicon of the categorial information composing the phrase structure of the sentence, and the phonological realization of the lexical items constituting the sentence. I propose a model of grammar incorporating the Government-Binding syntactic framework combined with the Lexical Phonology model of the lexicon. This model replaces the traditional notion of lexical insertion with the processes of *Categorial Construction and Phonological Insertion.* Phonological Insertion occurs after s-structure, i.e., after the syntax has completed its rearrangement of the base structure. In this way, the appropriate members of phonologically alternating items can be identified for a given syntactic context.

I also introduce two types of "incorporation" processes within the grammar. Merger occurs at s-structure, combining the grammatical features of two independent lexical items into a single composite set of features. Merger underlies the inflection phenomena studied here. Fusion takes place at PF and has access to both the grammatical and the phonological features of the words it affects. Fusion is responsible for the contraction data examined. Both processes explain the alternation of strings of items in one context with single items in another context by deriving the "incorporated" form from the base-generated string.

The model of grammar combining merger and fusion, along with Categorial Construction and Phonological Insertion, accommodates the alternation data in a natural way.

Thesis Supervisor: Kenneth Locke Hale

Title: Ward Professor of Modern Languages and Linguistics

Tone in Lexical Phonology

Douglas Pulleyblank

Submitted to the Department of Linguistics and Philosophy on
May 27, 1983 in partial fulfillment of the requirements of the Degree
of Doctor of Philosophy

Abstract

This thesis examines certain issues of tonal phonology within the theory of lexical phonology. Tonal phenomena require the enrichment of the lexical framework to include a post-lexical phonetic component. This component is shown to play a crucial role in accounting for the array of phenomena known as downdrift/downstep.

By separating phonological processes from phonetic processes, and by distinguishing between two classes of phonological processes — namely, those that apply lexically and those that apply post-lexically — we move towards an understanding of why particular tonal rules exhibit the properties that they do. For example, phonological constraints on autosegmental linkings may hold of rules applying lexically, but not of rules applying post-lexically — or such constraints may hold of rules applying lexically and post-lexically, but not phonetically.

The role of underspecification in tonal phonology is investigated. It is proposed that when rules of linking, spreading, etc. have not supplied any given tone-bearing unit with a tone, then a tonal autosegment is assigned by universal default rules. It is proposed that such universal default rules cannot be extrinsically ordered with respect to language-specific phonological rules. Once their allocation to the lexical, syntactic or phonetic component has been determined, the ordering of default rules is predicted by general principles.

Central to the approach taken in this thesis is a revised set of tonal association conventions, where spreading of tones onto free tone-bearing units is not automatic. Spreading takes place by language-specific rule only. A number of the consequences of this revision are investigated. In particular, it is shown that accentual diacritics can be eliminated as a device for determining the location of tonal melodies.

As a final theoretical point, it is shown that the notion of "extrametricality" is required for tone, as well as for stress. Moreover, it is shown that "extrametrical" tonal constituents obey the same "Peripherality Condition" that has been proposed as a constraint on extrametricality in stress systems.

The evidence presented in this dissertation is drawn from a number of languages, including the following: Dschang-Bamileke, Margi, Tiv, Tonga and Yoruba.

Thesis Supervisor: Paul Kiparsky Title: Professor of Linguistics

The Syntactic Forms of Predication

Susan Deborah Rothstein

Submitted to the Department of Linguistics and Philosophy on
July 20, 1983 in partial fulfillment of the requirements for the
Degree of Doctor of Philosophy in Linguistics

Abstract

In this dissertation I propose a rule of predicate-linking, which accounts for the distribution of non-argument maximal projections. These XPs are considered predicates, and are treated as one-place syntactic functions, requiring completion, or saturation. This saturation is achieved by linking each predicative XP to an argument XP, its syntactic subject. "Subject" is always defined relative to a particular XP, and not as "subject of an S". The predicate-linking rule, which is a condition on well-formedness at S-structure, defines the syntactic conditions under which such linking takes place. There are two major advantages of representing S-structure in terms of syntactically defined subjects and predicates. In the first place, it allows us to account for constraints on phrase-structure not subsumed under X-bar theory. In particular, the phrase-structure rule S → NP INFL VP becomes redundant, and the occurrence of both small clause and main clause predicates is accounted for by the same principle. The predicate-linking rule should be seen as complementary to the theta-criterion; the latter is a constraint on the distribution of argument XPs, whilst the former is a constraint on the distribution of non-argument, or predicative XPs. In the second place, this representation makes available a simple algorithm which maps from S-structure, via LF, to the semantic component, using syntactic information to build a semantic representation in which semantic subject-predicate relations are encoded. Chapters III and IV of this dissertation discuss how it is ensured that a semantically appropriate argument is the subject of a particular XP. We see that there are general lexical principles which dictate that certain thematic arguments will always be interpreted as the subject of the maximal projections of the lexical heads which select them. We also see how the interaction between the lexicon and the syntactic and semantic components accounts for the assymetries between subjects and objects. Chapter IV argues that the movement of arguments (i.e. cases where the trace left by Move- is A-bound) and the insertion of pleonastics are syntactic mechanisms which have the effect of providing subjects for predicates which are not assigned one by lexical principles. Chapter V distinguishes between two forms of syntactic predicates: primary, or clausal predicates, and secondary predicates, or small clauses. Chapter VI analyzes the structural properties of NPs and S's, and suggests why, unlike the other maximal projections, these XPs which may be predicative, may also be, and in most cases are, theta-marked arguments.

Thesis Supervisor: James Higginbotham

Title: Associate Professor of Linguistics and Philosophy

Complementation in Moroccan Arabic

Janet Stephanie Wager

Submitted to the Department of Linguistics and Philosophy on August 5, 1983 in partial fulfillment of the requirements for the degree of Doctor of Philosophy in Linguistics

Abstract

This dissertation presents an investigation of the phenomenon of complementation in the syntax of Moroccan Arabic, a language which has not been the subject of extensive research in theoretical syntax.

In particular, the present study examines a construction which I have termed "Matrix-Object Dislocation." This construction is similar to Left-Dislocation, in that the interpretive operation in both constructions is the same, namely anaphoric binding. Matrix-Object Dislocation differs from Left-Dislocation, however, in that, with the former, an element dislocated from a closed complement appears in the position of object of the matrix verb, while with Left-Dislocation the dislocated element does not occur in the domain of any verb.

Chapter I constitutes an introduction to the syntax of simple sentences in Moroccan, presented within the theoretical framework of Lexical-Functional Grammar (LFG) of Bresnan (1982a,b,c) and Kaplan and Bresnan (1982). Chapter II is a discussion of Moroccan complex sentences, and together Chapters I and II provide the theoretical assumptions and details of Moroccan grammar upon which the work in the final two chapters is based.

Chapter III presents an extensive study of the Matrix-Object Dislocation construction, in which the dislocated element is shown to be in matrix object position, but at the same time does not function as a normal object with respect to certain syntactic operations. This apparently anomalous behavior has its roots in the fact that, though the dislocated element is a constituent-structure object of the matrix verb, it is not, in most cases, a thematic argument of that verb. The dislocated element, bearing the function OBJ to the matrix verb, serves to give prominence to an argument in the complement clause, and therefore also bears the TOPIC function with respect to that clause. Verbs in Moroccan subcategorize for this TOPIC function, as not all verbs that take closed complements allow Matrix-Object Dislocation.

Chapter IV constitutes an investigation of complements to verbs other than the Matrix-Object Dislocation verbs. These complements superficially appear to be open complements, but closer examination reveals that, for the most part, they are functionally closed complements. Only a small class of verbs are found to take open adjectival complements.

Thesis Supervisor: Kenneth Locke Hale

Title: Ward Professor of Modern Languages and Linguistics

Structural Invariance and Symmetry in Syntax

Dominique Sportiche

Submitted on October 5, 1983 to the Department of Linguistics
and Philosophy in partial fulfillment of the requirements for the
Degree of Doctor of Philosophy

Abstract

This essay investigates the incidence of the Isomorphy Principle, a principle of thematic invariance across levels of syntactic representations, on the nature of the relations between these levels, within the model of Universal Grammar proposed by the Transformational Generative Theory (the Government and Binding framework). This leads us to undertake a reanalysis of various syntactic dependencies -move Np, move-wh...- and to develop a theory of Φ-categories and correlatively a theory of Binding relations.

Move NP is exclusively studied from the point of view of syntactic chains, from which its properties will be shown to be entirely derivative: this result entails primarily that D-structure is not an independent level of representation.

Move-wh and more generally the theory of the set of A'/A relations is investigated. We show that this set is symmetric with respect to the value of any binary classificatory features used. In particular, we conclude that invariance across levels is one such feature so that A'/A relation types partition equally depending on whether they remain invariant across levels or not: we also deduce that clitic constructions do not involve an A'/A relation.

The set of Φ-categories is also shown to be closed under symmetry. From this, we conclude that there is no type distinction between expletive PRO and NP-trace, and between pronouns, resumptive pronouns, wh-traces and pro. This last result is the conceptual cornerstone of our treatment of Weak Crossover, Strong Crossover and Parasitic Gap structures. We conclude as well that PRO is a "pure" anaphor and that the theory of its referential properties -Control Theory- partly reduces to Binding Theory, partly to the theory of the range of non-overt operators.

Thesis Supervisor: Noam Chomsky

Title: Institute Professor

Restructuring and Reanalysis

Maria Rita Manzini

Submitted to the Department of Linguistics and Philosophy on
October 20, 1983 in partial fulfillment of the requirements for the
Degree of Doctor of Philosophy in Linguistics

Abstract

This thesis, assuming the existence of restructuring and reanalysis processes in grammar, seeks to provide a precise and minimally simple definition of such processes (Chapter 2), which successfully applies to restructuring and reanalysis phenomena both held to be such independently of this thesis (causative constructions, Chapter 4), and introduced as such in this thesis (middle constructions, Chapter 3).

Chapter 2 comprises the theoretical core of the thesis. Section 2.1 seeks to formalize the intuitive idea that restructuring is defined by the presence of more than one structure for one and the same sentence in one and the same level of grammar. Section 2.2 seeks to formalize the intuitive idea that reanalysis is defined by the merger of the subcategorization properties of an element with the subcategorization properties of another element.

Chapters 3 and 4, on the other hand, comprise the core of the thesis' empirical discussion. Chapter 3, in particular, uses middle constructions, concretely Italian si constructions, to illustrate the theory of restructuring arrived at in section 2.1; while Chapter 4 uses causative constructions, concretely in French, to illustrate the theory of reanalysis arrived at in section 2.2.

Various theoretical and empirical issues essentially independent of restructuring and reanalysis are taken up in the course of the thesis as the opportunity presents itself. Perhaps the most sizable example of this is to be found in Chapter 3; where, in taking into consideration Italian si for the purposes of restructuring, we independently present what to our knowledge is the first unified theory of its impersonal and reflexive constructions, as well as of its middle ones.

Thesis Supervisor: Noam Chomsky

Title: Institute Professor

24. Cognitive Information Processing

Academic and Research Staff

Prof. W.F. Schreiber, Prof. D.E. Troxel, Dr. C.W. Lynn, Dr. L. Picard, Dr. K.P. Wacks, Dr. Yao-Ming Chao, Dr. Malik Khan, Qiding Du, S. Corteselli, J. Ward

Graduate Students

J. Allen, P. Cantarutti, D. Chan, D. Clemens, R. Fortino, A.Garcia, G. Hamilton, S. Hsu, M. Isnardi, E. Krause, C. Lee, H. MacDonald, D. Pan, D. Pian, J. Sara, G. Saussy, R. Ulichney, G. Vachon, J. Wang, K. Yun

24.1 Picture Coding

a. Sampling and Reconstruction

Most present-day picture coding is digital; virtually all input and output images are analog. Thus the conversion from one form to the other is everpresent and important to the quality and efficiency of the overall process. To elucidate the phenomena involved, a systematic study was carried out on a wide variety of pre-sampling and interpolation filters. It was found that, as suspected, the "ideal" low-pass filter was far from best, subjectively, since the least rms error criterion is not valid for human observers. Aliasing resulting from "violation" of the sampling theorem is visually traded off against sharpness and visibility of the sampling structure which occurs with other filters. Several filters studied performed substantially better than the ILPF. The best combination of performance and computational simplicity was found in the "sharpened Gaussian" filter, which has an impulse response not unlike that of human vision.[1]

b. Differential Pulse Code Modulation

This most common of image data compression systems has been widely studied. Its performance depends in marked degree on the characteristics of the signal source, since the presence of very sharp transitions requires an unfavorable trade-off between slope overload and the granular noise which occurs in blank areas. Nevertheless, when this factor is carefully taken into account, we have gotten good results with a form of DPCM in which the companding characteristic is adaptively adjusted to local image properties. In speech coding effective adaptation is possible based only on the coded signal. Because of the isotropic character of vision and images, this is not possible — extra data must be transmitted. Even including this extra data, we have obtained nearly "original" quality at 2.2 bits/pel, non-statistical, and 1.5 bits/pel statistical.[2]

c. Two-channel Coding System

For a number of years we have studied a picture transmission system in which the signal is divided into two channels, a two- dimensional low-pass signal ("lows") which is coarsely sampled and finely quantized, plus the remainder ("highs") which is finely sampled and coarsely quantized with the aid of a tapered randomized quantizer.[3] While this can be thought of as a crude form of transform coding, the two- or three-channel approach permits tailoring the separate channel coding parameters to well-known human visual properties. While the performance of the non-adaptive version of this system is not as good as the adaptive DPCM system mentioned above, it does feature rather simple implementation and excellent (PCM-like) performance in the presence of channel errors. Under a grant from the Sony Corporation, a real-time hardware system was implemented.[4]

d. Adaptive Two-channel Color Coding System

The abovementioned system can be substantially improved by adapting the highs quantization to the local signal properties. Blank-area signal-to-noise ratio of 50 db at about 3 bits/pel is possible in most cases. The system is extended to color coding by transmitting a three-color lows signal plus an adaptively-companded achromatic highs signal. The color lows signal is further compressed by mapping to a perceptually uniform color space, akin to the Munsell system of subjective color notation. Excellent quality full color images are possible at four bits/pel, compared with 24 for the uncoded signal. Further compression is possible by statistical (entropy) coding of the two-channel coder output.[5]

24.2 Graphic Arts Applications

The vast majority of pictures produced every day are made on printing presses. The printing industry is one of the largest in the country — five times as large as radio and TV broadcasting, and three times as large as the semiconductor industry. This industry is undergoing a true revolution in technology based on electronics and computers. For this and other reasons, our activities in recent years have been focused on understanding and improving the complicated chain of processes used to translate images of natural scenes, or man-made graphics, into printed pages. This orientation affects our activities in a number of ways:

1. Our sponsors generally plan to use the products of our research and development in daily production. Thus, the systems must be practical, reliable, and cost-effective.

2. Graphic arts images are of very high quality compared to those usually used by computer image processors. This requires careful attention to certain factors, such as tone reproduction, not always considered of great importance. High quality also implies very large amounts of data to be processed.

3. The images we deal with are intended for human viewing, and the systems we design are always operated by people. Human perceptual and operational capabilities are central to our work. The

principal operations which must be performed are the scanning and editing of individual page components, the selection and arrangement of elements on the page (composition, often erroneously called pagination), the arrangement of pages on the sheet (imposition), and the control of machines which make printing plates for letterpress, offset, and gravure printing.

24.3 Automated Engraving of Gravure Printing

Providence Gravure, Inc. (Grant)
William F. Schreiber, Donald E. Troxel

Gravure printing is characterized by high platemaking costs but inexpensive and very stable operation of the printing press. Thus it is suited primarily to long runs, particularly of color work, of both high and low quality. Substantial economic benefit would accrue from reducing the cost and time required to prepare printing cylinders, perhaps even making it practical to extend gravure printing to certain very significant applications such as daily newspapers.

In the system under development, all photographic steps between the original copy and the cylinder are eliminated by scanning into a computer system. Pictures are interactively edited, and then all components for each page are assembled into a single disk file. Cylinders are engraved directly from computer storage. (In other forms of printing, four color separation films would be made for each page instead). Imposition and correction for ink and paper are performed in "real" time simultaneously with engraving.[6]

The differences between this system and other existing pre-press systems include substantially reduced storage requirements due to data compression, high cost-effectiveness, the elimination of the need for the operators to have long experience in color printing, a high-speed page composition system, and the ability to perform multiple tasks at the same time.

24.4 Computer Graphics Architectures

International Business Machines Corporation (Grant)
William F. Schreiber, Donald E. Troxel

We are investigating architectures suitable for high resolution, high speed interactive graphics displays. We consider cost-performance trade-offs both for today's costs and those projected for the future. Both memory and processing costs are expected to decrease dramatically. However, reduced cost of special purpose computation suitable for high speed graphics displays by means of custom VLSI circuits may well be achievable only with volume production. The primary focus of our research has been to investigate appropriate trade-offs for a hierarchically-structured graphics memory architecture consisting of a combination of disk, bulk random-access memory, and high

speed image refresh memory. The overall aim is to provide a cost-effective architecture which will still permit rapid access to very large images. We are aiming to provide windowing, zooming, and roaming capabilities for images of arbitrary size, where these images are generated from a combination of data structures appropriate to scanned-in continuous tone images (contones), scanned-in line art, and algorithmically generated images, e.g., from a vector display list and/or a text file.

There has been considerable literature and increasing use of anti-aliasing in order to generate more pleasing displays for a given spatial sampling grid. This, of course, impacts architectural considerations as the size of the required image refresh memory can be reduced, thus altering the trade-offs. An interesting question concerns the trade-off between the spatial and gray scale resolution, i.e., how available memory should be allocated to optimize quality. Another area of research concerns the computation required to produce an anti-aliased display as pertaining to the benefits to be derived from anti-aliasing. When roaming or zooming quickly through an image, it is more important to give fast response than to optimize quality. When motion ceases, then the highest quality is desired.

A thesis project completed this year involved the simulation of three different hierarchical memory structures.[7]

References

1. J.N. Ratzel, "The Discrete Representation of Spatially Continuous Images," Ph.D. Thesis, Department of Electrical Engineering and Computer Science, M.I.T., August 1980.
2. A. Zarembowitch, "Forward Estimation Adaptive DPCM for Image Data Compression," S.M. Thesis, Department of Electrical Engineering and Computer Science, M.I.T., May 1981.
3. D.E. Troxel, et al., "Bandwidth Compression of High Quality Images," International Conference on Communication, June 1980, pp. 31.9.1-31.9.5.
4. D.E. Troxel, et al., "A Two-Channel Picture Coding System: I - Real Time Implementation," IEEE Trans. Commun. COM-29, 12, 1841-1848 (1981).
5. W.F. Schreiber and R.R. Buckley, "A Two-Channel Picture Coding System: II - Adaptive Companding and Color Coding," IEEE Trans. Commun. COM-29, 12, 1849-1858 (1981).
6. D.E. Troxel, et al., "Automated Engraving of Gravure Cylinders," IEEE Trans. Syst. Man Cybern. SMC-11, 9, 585-596 (1981).
7. P. Cantarutti, "Display Architectures for Interactive Graphics," S.M. Thesis, Department of Electrical Engineering and Computer Science, M.I.T., December 1983.

25. Custom Integrated Circuits

Academic and Research Staff

Prof. J. Allen, Prof. L.A. Glasser, Prof. P. Penfield, Jr., Prof. R.L. Rivest, Prof. G.J. Sussman, Prof. J.L. Wyatt, Jr., Dr. H. Shrobe, Jr.

Graduate Students

R. Armstrong, C. Bamji, C. Hauck, S. McCormick, L. Seiler

25.1 Conversion of Algorithms to Custom Integrated Circuits

U.S. Air Force - Office of Scientific Research (Contracts F49620-81-C-0054 and F49620-84-C-0004)
Jonathan Allen, Paul Penfield, Jr., Ronald Rivest, Gerald Sussman, Howard Shrobe

We have viewed the design of custom integrated circuits as an overall process of transformations starting at a high-level functional description and ending at a detailed masked specification for a particular process technology. At the highest level, a functional specification for the circuit must be generated, which should be specified in a form that permits the depiction of all of the possible parallelism present in the task. A great many high-level hardware design languages have been specified, but so far none have been utilized for integrated circuit design that provide an appropriate semantic foundation while permitting compilation to a fully parallel graph. In recent years, however, a great deal of research has taken place in the data flow computation area leading to the specification of languages that permit such a compilation to a graphical structure where all of the latent parallelism is revealed. It is important to realize that these results can be exploited for many purposes without the need to make any commitment to utilization of data flow architectures at the implementation level. We are currently building on this experience in order to derive a well founded formalism for functional specifications that is amenable to such optimal compilation techniques. Such a compilation will not only reveal the parallelism between diverse unrelated tasks, but can also unwind iterative loops in a way that reveals parallelism if in fact there is no sequential dependency between these iterations. Once the fully parallel graph structure is revealed, our techniques then focus on a phase of architectural exploration in order to allow the designer to select and utilize the degree of parallelism appropriate to the performance levels required in the application environment. At this stage, a large number of different techniques can be utilized. Techniques for transforming signal flow graphs into a variety of highly parallel architectures (including systolic forms) have been derived, as well as new techniques for retiming that provide the appropriate foundation for the establishment of a timing discipline in the overall system. It is clear that there is a substantial collection of these architectural exploration techniques that have been devised by a variety of researchers interested in various aspects of architectural exploration. In this study, our purpose is to unify these treatments into an overall theory of the interrelatedness of architectural forms and transformations between these

representations. We are also complementing this formalism with new results on area time trade-offs that go beyond results that have been achieved using asymptotic complexity theory. Instead, numerical estimates for constants in these asymptotic bounds are being derived, so that reliable engineering estimates of these performance variables can be made at the level of architectural exploration. We see this work as fundamental, and as comprising the core of an interactive program that permits the designer to systematically explore design alternatives. It is interesting that previously, different architectures for a particular task were often seen as unrelated. These new results, however, indicate that all of these architectural forms are systematically related through transformations, the form of which is just now being derived. For this reason, there is a new opportunity for the derivation of a basic theory of computer architecture having a formal and systematic basis, rather than the current heuristic basis for much of computer architecture.

Once a particular architecture is established, it remains to generate the detailed layout for the constituent cells. During the previous year, we had considerable success in devising a new PLA generator based on the specification of a minimal exemplar of a PLA circuit style, combined with a detailed logical specification for that PLA. We are now going on to generalize this approach by designing a new system that can generate a wide variety of regular structures. In each case, the user need only specify the individual constituent cells and their local connectivity, together with a high-level "concept file" that characterizes the nature of the overall module to be produced. It is interesting to note that if the only constraints provided by the designer at this point are those due to local connectivity, then a substantial (certainly not unique) variety of modules can result. It is the role of the concept file to remove this ambiguity and to place a form on the overall structure that suits the intended task while maintaining the local connectivity constraints. This approach is exceedingly general, but can be used for a wide variety of structures including register arrays, arithmetic logic units, program logic arrays, multiplexors, memory, and even specialized units such as array multipliers. Another facet of this work is the utilization of topological abstractions for the constituent cells, so that a wide variety of design rules, and hence processes, can be utilized. Once the overall module is created by use of the local connectivity constraints and the concept file, then a compaction phase is entered which introduces the technology constraints associated with a particular set of design rules. The result is a single mechanism that provides for a wide class of optimal circuit generators. Associated with each of these generators is a class of performance estimators that characterize the area consumed by the module, the time delay associated with it, and it's power dissipation. In addition to these specialized generators, a general purpose processor architecture will also be provided, since we believe that most realistic systems cannot be realized in their entirety by utilization of these specialized function generators. It is, of course, the task of the architectural exploration phase to specify the overall design in terms of the specialized generators as well as the general purpose architecture in a form that satisfies the performance constraints dictated by the user. Two additional activities associated with the function generator phase are also worthy of note. We are designing a new CMOS multiplier, where the target speed for a 16x16 multiply is 50 nanoseconds. This is a regular design being carried out in conjunction with Professor Hoelflinger of Purdue

University. We are also completing the design of a special purpose function generator for a floating point unit, since many of our applications are in the area of digital signal processing which increasingly demands floating point capability on chip.

During this year, we finished work on a high accuracy circuit extraction program. Together with a comprehensive circuit simulator, this tool can be used to carefully evaluate the designs created by the function generators, and hence to derive procedures for the calculation of area, time, and power estimates previously mentioned. For digital signal processing applications, where not only high parallelism but aggressive circuit performance is required, this ability to accurately characterize automatically generated designs is essential. If, as a result of the performance estimates applied to the individual modules of the overall system, the user decides that the overall design will be acceptable, then we may go ahead to a placement and routing phase which uses the PI program which has been under development for several years within our project. This program creates a layout from the constituent modules, where each module is assumed to be rectangular in shape and orthogonally related to the other modules, with interconnect on all four sides. Routing strategies are already highly developed, and several placement packing strategies are under investigation.

From the above discussion, it is clear that the elements of an overall design system are being assembled in a fundamental way. We believe that the utilization of functional languages that characterize the deep semantics of the task and which are suitable for compilation to fully parallel representations provides a fundamental and new initial phase to integrated circuit design systems. We also recognize that a great many efforts involving architectural transformations have taken place within limited spheres of concern, but that these may now be unified into a more general framework, and this is the direction of much of our research. The use of local constraints and the "concept file" idea has permitted us to generate a wide variety of specialized modules that are highly efficient, and hence supplies us with one framework that is easily specialized to the many requisite modules of an overall design. Finally, the placement and routing strategies used employ well-tuned heuristics that can lead to a densely packed chip with little open area.

Lastly, we comment that construction of a hardware design rule checker has been completed, and that we have been able to demonstrate an improvement of two orders of magnitude in speed over conventional software design rule checkers by utilization of a single circuit board of specialized hardware, which is easily added to a standard general purpose computer. In this way, a significant amount of the computational burden in IC design is reduced to a level that is compatible with highly efficient interactive design.

25.2 A Circuit Theory for Digital VLSI Systems

National Science Foundation (Grant ECS81-18160)

Lance A. Glasser, Paul Penfield, Jr., John L. Wyatt, Jr., Isaac Bain, Charles Zukowski

VLSI circuit theory is an extension of classical non-linear circuit theory to networks that are so large as to make complete analysis infeasible. The goal is to allow precise partial circuit analysis, while exploiting many of the typical properties of VLSI circuits to achieve speed. These properties include the use of regular structures, simple design methodologies, and restoring digital signals.

The first area of VLSI circuit theory being pursued is design methodology verification. To deal with complexity, large circuits are often constructed with simple rules that ensure proper operation in some respect. For example, the proper connection of ratioed logic will always eventually produce valid logic signals at the outputs given valid and stable inputs. Therefore, verification that the rules of construction are not violated constitutes a useful partial analysis of a circuit.

Previous work in the area of methodology verification has involved producing programs that check for a particular set of rules. We are currently testing a language that can express very general methodologies. This is being used as an input to a syntax checking program. Circuits are specified for the syntax checker using an experimental circuit design language for expressing a designer's intent.

The second area of VLSI circuit theory being pursued is waveform bounding. Instead of finding the exact response of a network as in classical circuit analysis, the goal of waveform bounding is to merely narrow down the set of possible solutions to the extent necessary. The analysis is still precise, but the amount of information obtained about a circuit is sacrificed for greater speed. Bounding is feasible for digital circuits because signal uncertainty is restored.

For many purposes in the design and analysis of VLSI circuits, exact circuit simulation is impractical. Solving for the exact response of an accurate circuit model is very time consuming for large circuits and an exact solution is not always essential, e.g., for a first pass design. To combat this problem, new simulators have been developed that calculate the response of much simpler circuit models. Such an approach decreases computation at the expense of accuracy.

In the waveform bounding approach, instead of approximating a more complex model by a simpler one, a simpler model is derived that "bounds" the behavior of the more complex one. Given upper and lower bounds on the response of the complex model, one can produce an approximate response by averaging the bounds, as well as a maximum error. In addition to measuring the errors made in simplifications, bounds can naturally incorporate uncertainties in a simulation, such as device parameter variations and imperfectly characterized input waveforms.

VLSI circuits are often designed to meet various external constraints such as a maximum delay. In this case approximating simulators are never reassuring design verifiers while bounding simulators are adequate in many cases. Given a delay specification, a bounding simulator can produce one of three conclusions: the circuit definitely meets the specification, it definitely does not meet the specification, or further calculation is needed to determine if the specification is met. Assuming that a

bounding simulator can be adjusted to trade speed for accuracy, the fact that maximum errors are calculated allows the computation speed to be reduced only when more accuracy becomes necessary.

A large amount of work has been done on the generation of rigorous bounds on common VLSI subcircuits: RC interconnect models, restoring logic gates, and pass transistor circuits. Circuit theorems have been proved about monotonic relationships between the basic circuit elements and the responses of these sub-circuits. The error produced by various bounds based on these theorems is currently being investigated. The theory of combining bounds on subcircuits into bounds on entire networks is also being pursued. Ultimately, this work could contribute to a new generation of VLSI circuit simulation programs.

Publications

Wyatt, J.L., Jr., C. Zukowski, L.A. Glasser, P. Bassett, and P. Penfield, Jr., "The Waveform Bounding Approach to Timing Analysis of Digital MOS IC's." Proc. IEEE International Conf. on Computer Design/VLSI in Computers, 1983, pp. 392–395.

Zukowski, C., "Circuit Simulation with Iterating Bounds," VLSI Memo, pp. 84–159.

25.3 Very Large Scale Integrated Circuit Research

U.S. Air Force - Office of Scientific Research (Contracts F49620-81-C-0054 and F49620-84-C-0004)

Lance A. Glasser, Mark Matson

Our work in this area focuses on two issues: modelling and optimization algorithms. We are developing precise models to describe the behavior of MOS logic gates. These models deal not with voltages and currents, but rather with delays and loading conditions. For example, our models predict a gate's output waveform shape as a function of input waveform shape and output capacitance. Details such as the logic gate's voltages and currents are implicitly accounted for by the model. By working at this higher level of abstraction, we have considerably improved computational speed while maintaining accuracy.

We have carefully analyzed the characteristics of our design problem, and found it well suited to a divide and conquer strategy where we break the problem into several subproblems which are then solved almost independently. We are applying optimization algorithms, in conjunction with sophisticated data structures, which use this strategy, resulting in improved computational efficiency.

At present we have implemented the modelling and optimization software, and have tested them on simple circuits. The tests were successful; our program demonstrated that it could compute transistor sizes that met a speed specification while minimizing power. Just as importantly, computer execution speed was fast (about 2 cpu seconds per design parameter).

We are now refining these implementations for more accuracy and higher computational speed, and

plan to test them on more complex circuits, such as microprocessors' arithmetic-logic units.

Publications

Glasser, L.A. and J. Hoyte, "Delay & Power Optimization in VLSI Circuits," to be presented at the 21st Design Automation Conference, June 25–27, 1984.

25.4 Waveform Bounding for Fast Timing Analysis of MOS VLSI Circuits

National Science Foundation (Grant ECS83-10941)

John L. Wyatt, Jr., Paul Penfield, Jr., Lance A. Glasser, Charles Zukowski, Han-Ngee Tan, Pearl Yew, Peter O'Brien

This project continues, enlarges, and applies one of the research avenues first uncovered in the work described in Section 25.2 of this report. That section outlined the basic rationale for waveform bounding: here we discuss some of the methodologies in more detail.

To obtain rigorous upper and lower bounds on the voltage response at all the nodes of a dynamic circuit, one has to study the differential equations describing it. Digital MOS circuits are highly nonlinear, but they have special features that make them analytically somewhat tractable. These include monotonicity of key element constitutive relations, the absence of inductors in most circuit models, a limited number of d.c. paths to supply voltage and ground, the restoring character of logic circuits, and the presence of a capacitance from every node to ground in most circuit models.

This research began with Rubenstein, Penfield and Horowitz' derivation of closed-form response bounds for linear network models of MOS interconnect.[1] Subsequent work by Wyatt extended the method to unbranched line models incorporating realistic monotone nonlinearities.[2] Qingjian Yu and Omar Wing of Columbia University then discovered a way to include branched nonlinear lines.[3] Dr. Yu will be in residence with our group during the summer of 1984 in a temporary postdoctoral position.

A current research goal is to tighten the bounds on delay through linear interconnect models given in Ref. 1. One approach is based on a spatial monotonicity property of the time derivative of voltage first noted in Ref. 4 and proved in Ref. 5. Another is based on second-order bounds, i.e., bounds that can be computed in a length of time which grows quadratically with the number of elements in the circuit model. To exploit these second order bounds we have recast the problem in the form of a linear minimum- and maximum-time optimal control problem with linear state constraints. Han Tan hopes to completely solve the optimal control problem this summer (1984) with some assistance from Professor Violet Haas, a visiting professor from Purdue University who specializes in optimal control.

Interconnect is at worst only mildly nonlinear: logic gates are highly nonlinear and require a

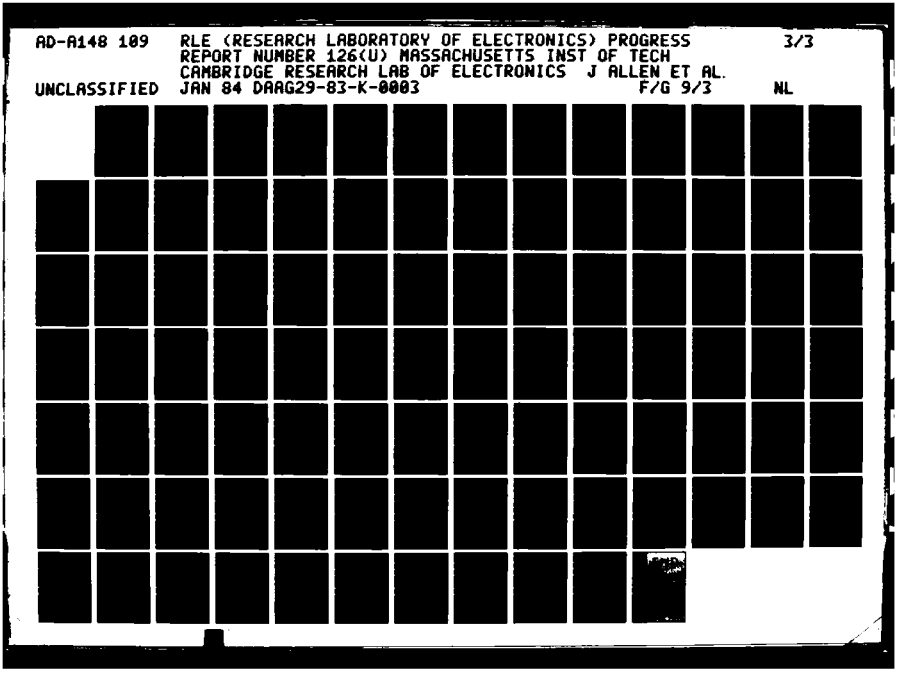
AD-A148 109
RLE (RESEARCH LABORATORY OF ELECTRONICS) PROGRESS
REPORT NUMBER 126(U) MASSACHUSETTS INST OF TECH
CAMBRIDGE RESEARCH LAB OF ELECTRONICS J ALLEN ET AL.
3/3
UNCLASSIFIED
JAN 84 DAAG29-83-K-0003
F/G 9/3
NL

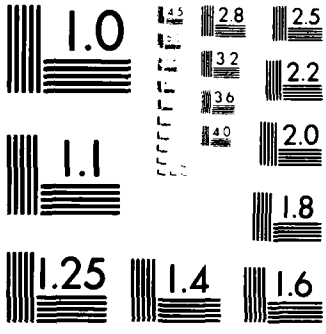

different approach. We have found a way to use the first variational equation to study the sensitivity of delay through MOS logic circuits to the shape of the input waveform.[6,7] The main result is that for inverters the time of maximum sensitivity is the moment when the pulldown makes the transition between the ohmic and saturation regions.

The most fruitful approach to date for bounding the response of MOS logic circuits is to exploit the monotone character of the MOSFET v–i curves. In this way one can model a complex multiple-input gate by a much simpler network and be confident of the sign of the error produced by the model simplification.[8]

Perhaps the most exciting development in this project is an effort to marry waveform bounding techniques to methods of circuit simulation based on waveform relaxation.[9] At its simplest, the idea is to use waveform bounding to provide a good global initial guess for an exact simulator like RELAX. A more advanced version of the idea is to perform iterations on the bounds themselves.[10] In the interest of speed the iterations need not be carried to convergence: computation can be terminated when the bounds are tight enough. Charles Zukowski is writing his doctoral thesis on this approach to simulation, and John Wyatt will spend August of 1984 at IBM Yorktown Heights collaborating with the developors of RELAX on its implementation.

References

1. J. Rubenstein, P. Penfield, Jr., and M.A. Horowitz, "Signal Delay in RC Tree Networks," IEEE Trans. Comput. Aided Design, CAD-2, 3, 202–211 (1983).
2. J.L. Wyatt, Jr., "Monotone Sensitivity of Nonlinear, Nonuniform RC Transmission Lines, with Application to Timing Analysis of Digital MOS Integrated Circuits," IEEE Trans. Circuits, Syst., accepted for publication.
3. Q. Yu and O. Wing, "Waveform Bounds of Nonlinear RC Trees," Proceedings of the IEEE International Symposium on Circuits and Systems, Montreal, Canada, May 1984, pp. 356–359.
4. M.A. Horowitz, "Timing Models for MOS Circuits," Ph.D. Thesis, Department of Electrical Engineering, Stanford University, December 1983.
5. P. O'Brien, "Analytical Results for Waveform Bounding," S.B. Thesis, Department of Electrical Engineering and Computer Science, M.I.T., May 1984.
6. J.L. Wyatt, Jr., "The Sensitivity of Inverter Delay to Details of the Input Waveform: A Variational Approach," VLSI Memo 82–126, November 1982.
7. P. Yew and J.L. Wyatt, Jr., "A Variational Approach to Delay in MOS Logic Circuits," Proceedings of the IEEE International Symposium on Circuits and Systems, Montreal, Canada, May 1984, pp. 852–855.
8. J.L. Wyatt, Jr., C. Zukowski, L.A. Glasser, P. Bassett, and P. Penfield, Jr., "The Waveform Bounding Approach to Timing Analysis of Digital MOS IC's," Proceedings of the IEEE International Conference on Computer Design: VLSI in Computers, Port Chester, New York, November 1983, pp. 392–395.
9. E. Lelarasmee, A.E. Ruehli, and A.L. Sangiovanni-Vincentelli, "The Waveform Relaxation Method for Time-Domain Analysis of Large Scale Integrated Circuits," IEEE Trans. Comput. Aided Design, CAD-1, 3, 131–145 (1982).
10. C.A. Zukowski, "Circuit Simulation with Iterating Bounds," VLSI Memo 84–159, January 1984.

26. Communications Biophysics

A. Signal Transmission in The Auditory System

Academic and Research Staff

Prof. N.Y.S. Kiang, Prof. W.T. Peake, Prof. W.M. Siebert, Prof. T.F. Weiss, Dr. M.C. Brown, Dr. R.A. Eatock, Dr. D.K. Eddington, Dr. J.J. Guinan, Jr., Dr. E.M. Keithley, Dr. J.B. Kobler, Dr. W.M. Rabinowitz, Dr. J.J. Rosowski, J.W. Larrabee, F.J. Stefanov-Wagner, D.A. Steffens

Graduate Students

D.M. Freeman, M.L. Gifford, A.D. Krystal, M.P. McCue, X-D Pang, C. Rose

26.1 Basic and Clinical Studies of the Auditory System

National Institutes of Health (Grants 5 PO1 NS 13126, 1 RO1 NS 18682, and Training Grant 5 T32 NS 07047)

Nelson Y.S. Kiang, William T. Peake, William M. Siebert, Thomas F. Weiss

Studies of signal transmission in the auditory system continue in cooperation with the Eaton-Peabody Laboratory for Auditory Physiology at the Massachusetts Eye and Ear Infirmary. The goals of these studies are to determine the anatomical structures and physiological mechanisms that underlie vertebrate hearing and to apply that knowledge where possible to clinical problems. We report projects that were completed during 1983.

Mechanisms of mechanoelectric transduction in hair cells have been investigated in the alligator lizard.[1,4,5] Comparison of responses of hair cells and cochlear neurons to acoustic clicks and tone bursts have indicated that: adaptation of the response is a property of synaptic transmission at the receptor-neuron junction; frequency selectivity of the steady-state response to tones is a property of the mechanical input of the hair cell and/or a property intrinsic to each hair cell; important nonlinear phenomena accompany mechanoelectric transduction; the production of the receptor potential involves a low-pass filtering stage that follows mechanoelectric transduction.

Electric responses to sounds which are recorded outside the cochlea are widely used in auditory experiments to monitor the state of the cochlea as well as to assess its mechanical input. These responses are mixtures of potentials generated by different sources in the cochlea. To investigate their composition, electric responses to clicks and tones were recorded at the round windows of anesthetized alligator lizards before and after the neurotoxin "tetrodotoxin" (TTX) was added to scala tympani.[5] By combining click responses obtained in the presence and absence of TTX and at high

and low click repetition rates, click responses were trisected into three components: (1) a rate-insensitive, TTX-insensitive component (that was identified as the cochlear microphonic potential or CM and assumed to be generated by hair cells); (2) a rate-sensitive, TTX-sensitive component (that was identified as the neural component); (3) a rate-sensitive, TTX-resistant component (which has not been identified previously and which was called component X). Component X is generated in the inner ear and has a latency between that of the CM and neural component. Several origins for component X are possible of which the most likely is that component X represents the compound post-synaptic potential of the nerve terminals. Measurements of responses to tones in the presence and absence of TTX demonstrate that the contribution of the neural component to the round-window response is appreciable below 1.5 kHz and negligible above this frequency.

The olivocochlear bundle (OCB) is a major efferent pathway from the central auditory system to the periphery. Both the anatomy[3] and physiology[2] of this pathway have been investigated in cats. The main anatomical finding is that the projections from both the medial superior olivary complex (MSOC) and from the lateral superior olivary complex (LSOC) to the cochlea are topographic but that while the LSOC mapping appears to connect locations with the same best frequencies, the MSOC mapping does not appear to do so. Electrical stimulation of the OCB at the midline of the brainstem is known to suppress sound-evoked responses of cochlear nerve fibers. A study was completed[2] in which the synchronized responses of fibers to tones were examined. The results are consisent with a model in which two processes that excite cochlear nerve fibers summate, and only one is affected by the electrical stimulation of the OCB.

The afferent neurons innervating hair cells in cats are of two types. Type I neurons innervate inner hair cells and Type II neurons innervate outer hair cells. A great deal is known about the physiological activity of the former and virtually nothing about the activity of the latter. An attempt was made to record from the central axons of Type II neurons with metal electrodes[7] (which have a low electrical noise level) and to look for long-latency events in response to electric shocks delivered to the cochlea. The rationale is based on the relatively small diameters of the axons of these neurons and their consequent small conduction velocities. It was possible to obtain long-latency spikes, but the amplitudes were barely above the noise levels of the electrodes. When sound was introduced, the electrode recorded gross responses of the cochlea that obscured these spikes. Thus it was concluded that other approaches to recording the activity of Type II neurons would need to be developed.

References

1. K. Baden-Kristenson and T.F. Weiss. "Receptor Potentials of Lizard Hair Cells with Free-Standing Stereocilia: Responses to Acoustic Clicks," J. Physiol. 335, 699-721 (1983).
2. M.L. Gifford and J.J. Guinan, Jr., "Effects of Crossed-Olivocochlear-Bundle Stimulation on Cat Auditory Nerve Fiber Responses to Tones." J. Acoust. Soc. Am. 74, 115-123 (1983).
3. J.J. Guinan, Jr., W.B. Warr, and B.E. Norris, "Differential Olivocochlear Projections from Lateral Versus Medial Zones of the Superior Olivary Complex," J. Comp. Neurol. 221, 358-370 (1983).

4. T. Holton and T.F. Weiss, "Receptor Potentials of Lizard Cochlear Hair Cells with Free-Standing Stereocilia in Response to Tones," J. Physiol. 345, 205–240 (1983).
5. T. Holton and T.F. Weiss, "Frequency Selectivity of Hair Cells and Nerve Fibers in the Alligator Lizard Cochlea," J. Physiol. 345, 241–260 (1983).
6. M.S. Kaplan, B.G. Szaro, and T.F. Weiss, "Components of Cochlear Electric Responses in the Alligator Lizard," Hearing Res. 12, 323–351 (1983).
7. N.Y.S. Kiang, E.M. Keithley, and M.C. Liberman, "The Impact of Auditory-Nerve Experiments on Cochlear Implant Design," Ann. N.Y. Acad. Sci. 405, 114–121 (1983).
8. E.A. Richter, B.E. Norris, B.C. Fullerton, R.A. Levine, and N.Y.S. Kiang, "Is There a Medial Nucleus of the Trapezoid Body in Humans?" Am. J. Anat. 168, 157–166 (1983).

B. Auditory Psychophysics and Aids for the Deaf

Academic and Research Staff

L.D. Braida, R. Boduch, H.S. Colburn, J. Coker, L.A. Delhorne, L.C. Dowdy, N.I. Durlach, C.L. Farrar, L.J. Ferrier, M.S. Florentine, D.M. Freeman, M. Furst, K.J. Gabriel, W. Jesteadt, J. Koehnke, N. Macmillan, K. Morey, W.M. Rabinowitz, C.M. Reed, J. Reid, R.P. Russell, M.C. Schultz, P.M. Zurek

Graduate Students

T.T. Allard, C.A. Bickley, D.K. Bustamante, M.M. Downs, K.K. Foss, E. Gilbert, D.M. Horowitz, Y. Ito, M. Jain, S.J. Leivy, D.F. Leotta, D. Opalsky, R.C. Pearsall II, J.C. Pemberton, P.M. Peterson, R.D. Reohr, R.J. Rohlicek, G.M. Skarda, M.J. Tsuk, R.M. Uchanski, R.G. Waissman

26.2 Intensity Perception and Loudness

National Science Foundation (Grant BNS77-16861)
National Institutes of Health (Grant 1 F 33 NS07202-01)
Louis D. Braida, Nathaniel I. Durlach, Neil Macmillan, William M. Rabinowitz, Michael J. Tsuk, Roberto G. Waissman

This research involves theoretical and experimental studies directed at a unified quantitative theory of intensity perception and loudness. It involves the development and integration of models of sensory processes, short-term memory, perceptual-context effects, and decision making, as well as psychophysical experimentation. During this period our work has consisted of i) development of a new model for context coding, ii) development of maximum-likelihood techniques for estimating sensitivity parameters, and iii) model-based analysis of categorical perception experiments.

i) The new model for context coding accounts for the increase in sensitivity, observed near the extremes of the range when unidimensional stimuli are identified, by assuming that sensations are estimated relative to noisy perceptual anchors with a stochastic ruler. In this model, the mean and variance of the anchor locations, and the mean number of ruler steps used to cover the sensation range, are the only free parameters. Further, these parameters are assumed to be independent of the stimulus parameters for the experiment. By fitting data (Braida and Durlach, 1972) from sets of intensity identification experiments in which the stimulus range was varied systematically, we have estimated that the mean anchor locations are roughly 2.0 jnd's outside the sensation range, the anchor variance is roughly 3.0 times the sensation variance, and roughly 35 steps are used to measure the sensation range. Independent estimates of the anchor position to sensation variance ratio have been derived based on the relation between sensitivity in fixed-level two-interval

discrimination experiments and small-range one-interval identification experiments (1.2–4.0), and from data on the dependence of fixed-level discrimination on interstimulus interval (0.5–3.0). We plan to develop a model for the formation and maintenance of anchors in order to determine whether these parameters can be determined from more fundamental considerations, such as the composition of the stimulus set. A manuscript (Braida et al., 1984) describing this model has been accepted for publication.

ii) Estimates of sensitivity in identification experiments are often derived crudely merely by fitting straight lines to ROC curves by eye. Lippmann (1974) developed a procedure for computing maximum likelihood estimates under the assumption that the underlying densities were Gaussian and of equal variance. We are attempting to improve the computational efficiency of this procedure (which must solve sets of simultaneous nonlinear equations) and to relax the equal-variance assumption Some preliminary work is reported on by Waissman (1983).

ii) We have begun to apply the Preliminary Theory of Intensity Resolution (Durlach and Braida 1969) to data obtained in categorical perception experiments. According to the theory, two memory modes are used in processing perceptual continua. In the trace mode, observers compare stimuli with the memory traces of other stimuli, and performance is limited by the inter-stimulus interval. In the context mode, observers compare stimuli to perceptual anchors, and performance is limited by the stimulus range. The theory predicts that sensitivity in discrimination experiments should be proportional to that in identification. For many continua used in categorical perception research, this prediction is upheld; for some (the fricative-affricate "continuum") it is not, suggesting that stimuli actually differ multidimensionally. Different stimulus domains were found to differ in (a) the amount of trace variance, (b) the amount of context-coding variance, and (c) the existence and location of anchors; but no single parameter captured the categorical/continuous distinction. Memory variances and anchor locations can be estimated from experiments in which fixed-level discrimination, as well as identification and roving-level discrimination, is measured. Among the few experiments with categorically-perceived continua that have used the critical fixed-level condition are some in which discrimination peaks arise from anchors, and others in which they reflect regions of high basic sensitivity. A manuscript reporting on this work has been prepared for publication (Macmillan, 1984).

References

1. L.D. Braida and N.I. Durlach, "Intensity Perception II: Resolution in One-Interval Paradigms," J. Acoust. Soc. Am. 51, 483–502 (1972).
2. L.D. Braida, N.I. Durlach, J.S. Lim, J.E. Berliner, W.M. Rabinowitz, and S.R. Purks, "Intensity Perception XIII: Perceptual Anchor Model of Context Coding," J. Acoust. Soc. Am., accepted for publication (1984).
3. N.I. Durlach and L.D. Braida, "Intensity Perception I: Preliminary Theory of Intensity Resolution," J. Acoust. Soc. Am. 46, 372–383 (1969).
4. R.P. Lippmann, "Effect of Payoff Matrix on Absolute Identification," S.M. Thesis, Department of Electrical Engineering and Computer Science, Massachusetts Institute of Technology, 1974.
5. N.A. Macmillan, "Beyond the Categorical/Continuous Distinction: A Psychophysical Approach to

Processing Modes," in S. Harnad (Ed.) Categorical Perception, submitted for publication.
6. R.S. Waissman, "Maximum Likelihood Estimation of Decision Model Parameters," S.M. Thesis, Department of Aeronautics and Astronautics, Massachusetts Institute of Technology, 1984.

26.3 Binaural Hearing

National Institutes of Health (Grant 5 RO1 NS10916)

H. Steven Colburn, Nathaniel I. Durlach, Kaigham Gabriel, Manoj Jain, Janet Koehnke, Sander J. Leivy, David Opalsky, Patrick M. Zurek

Research on binaural hearing has consisted of i) experimental work, ii) theoretical work, and iii) development of facilities.

i) We have measured the effect of masker bandwidth and frequency on binaural detection for masker bandwidths from 6.4 Hz to 10 kHz and center frequencies of 250 and 4000 Hz. Specifically, a complete set of N0S0 and N0SPi thresholds were measured for two subjects using an adjustment procedure and for a third subject using a forced-choice, adaptive procedure. There were no significant differences between results from the two procedures. Both the N0S0 and the N0SPi data are being used in connection with modeling studies.

Also, we have continued with measurements of sensitivity to interaural correlation of narrowband noises in the presence of a spectral fringe of interaurally correlated noise. Preliminary results indicate that the presence of a spectral fringe interferes with detection of a narrowband stimulus more than one would expect from the critical bandwidth notion as it is applied in detection.

We are continuing to study the relation of detection to correlation. The outcomes of in-depth measurements from a small number of normal hearing subjects are testing our ability to predict detection from correlation and visa versa. Specifically, we are measuring psychometric functions for both tests. Early results, when plotted on common axes according to the calculated equivalent correlation coefficient or signal to noise ratio, indicate that the functions appear to be steeper for the detection experiment than for the correlation experiment. Further data are needed. These results will also be compared to those obtained from hearing-impaired subjects (Gabriel, 1983).

ii) In our theoretical work we continue to pursue both physiologically based models (e.g., Colburn, 1983) as well as stimulus-response models (e.g., Siegel and Colburn, 1983; Zurek, 1984). Although our analysis of physiological models is proceeding, most of our work this year has been focused on models that are easily described and analyzed without the complexity of the description of the peripheral transduction from pressure to neural firing patterns. We use available physiology as a guide, but believe that there are many models that can be made compatible with the physiology and that progress at this time is most likely to come from the black-box approach.

Predictions were made from the energy-detection model of Green and Swets for the N0S0 thresholds measured in the MLD-Bandwidth study. The fits are good with some choice of critical bandwidth (similar to values in the literature) and integration time (also similar to previous estimates). These quantities are of interest because the critical bandwidth estimate is used in predicting the N0SPi thresholds. Further, if it is assumed that one and the same integrator is effective in both homophasic and antiphasic detection tasks, then fitting the N0S0 data can provide an estimate of what we have been calling 'binaural sluggishness'. Indeed, an interesting prediction of this 'single-integrator' model is that as T (integration time) varies (from subject to subject), larger T's produce lower N0S0 thresholds and higher N0SPi thresholds. (The MLD thus varies inversely with T.) This co-variation is seen, roughly, in the data of our three subjects.

A simple model of binaural interaction incorporating a temporal averager for interaural differences has been developed and tested on results from both normal and hearing impaired subjects. This model has been successful at predicting NOSPi detection results and correlation discrimination results from observed interaural time and interaural intensity jnds.

Also, we have calculated the cross-correlation between the envelopes of band-pass noises that are identical except that they have an either an antiphasic tone or uncorrelated noise added. These quantities are needed to analyze detection and correlation discrimination at high frequencies where the envelope is assumed to be the effective binaural stimulus.

iii) Considerable efforts were applied to the development of two related but distinct experimental facilities, a VAX-based facility in the main laboratory and a stand-alone, 11/23-based, easily transportable facility that is designed for use in our anechoic chamber (Leivy, 1983; Opalsky, 1983). For the VAX-11/750 system, we have been developing a sophisticated stereo interface with microsecond interaural delay capabilities: the hardware is complete, but work still remains on the software development. For the 11/23-based system, a stand-alone experimental station designed for binaural experiments has been developed and is currently being used to perform a variety of different psychophysical experiments. A complete hardware/software package has been implemented which allows the manipulation and presentation of digitally stored or computed stimulus waveforms as well as the recording, storage and retrieval of subject responses. The experimental data recording routines have been developed around a data-base management system which enables the storage and retrieval of experimental results along with experimental and stimulus parameters. All of the software has been written the language FORTH. Because of the interpretive nature of this language, the user-system interaction is relatively simple compared with other experimental systems, and hence, novice users are more easily able to develop experimental programs.

References

1. H.S. Colburn, "Recent Developments in Binaural Modeling," in R. Klinke (Ed.), Hearing-Physiological Bases and Psychophysics 1983.
2. K.J. Gabriel, "Binaural Interaction in Hearing-Impaired Listeners," Ph.D. Thesis, Department of Electrical Engineering and Computer Science, M.I.T., August 1983.

3. Sander J. Leivy, "A FORTH Program for Psychophysical Experiments," B.S. Thesis, Department of Biomedical Engineering, Boston University, 1983.
4. David Opalsky, "Binaural Psychophysical Experimental Facility," B.S. Thesis, Department of Biomedical Engineering, Boston University, 1983.
5. R.A. Siegel and H.S. Colburn, "Internal and External Noise in Binaural Detection," Hearing Res. 11, 117–123 (1983).
6. P.M. Zurek, "A Predictive Model for Binaural Advantages and Directional Effects in Speech Intelligibility," J. Acoust. Soc. Am., accepted for publication.

26.4 Hearing Aid Research

National Institutes of Health (Grant 5 RO1 NS12846)

Louis D. Braida, Diane K. Bustamante, Lorraine A. Delhorne, Nathaniel I. Durlach, Kristin K. Foss, Dennis M. Freeman, Eric Gilbert, Patrick M. Peterson, Miles P. Posen, Charlotte M. Reed, Roy P. Russell, Karen Silletto, Rosalie M. Uchanski, Victor W. Zue, Patrick M. Zurek.

This research is directed toward improving hearing aids for persons with sensorineural hearing impairments. We intend to develop improved aids and to obtain fundamental understanding of the limitations on such aids. The work includes studies of i) effects of noise on intelligibility, ii) amplitude compression, iii) frequency lowering, and iv) clear speech.

i) Although many persons with impaired hearing experience difficulty understanding speech in noise backgrounds which are not particularly deleterious for persons with normal hearing, the extent to which this reflects aspects of the impairments beyond loss of sensitivity is unknown. To obtain insight into this problem we have measured monaural speech intelligibility for CV syllables presented in a background of Gaussian noise with the spectral shape of babble. Speech and noise are added prior to spectral shaping with either a flat or a rising frequency-gain characteristic. Data has been obtained from five hearing-impaired subjects with roughly 40–60 dB losses and wide variety of audiometric configurations.

The results have been analyzed in terms of a model which assumes that the hearing loss is caused by an equivalent additive noise, (e.g., Dugal et al., 1980), and Articulation Theory is used to predict intelligibility. Plots of consonant identification scores versus Articulation Index for the conditions tested, including a few conditions with normal listeners, show a very strong degree of overlap. That is, these results indicate that, once the materials are 'calibrated' with normal listeners, consonant reception is highly predictable (within limits of test variability and between-subject variability in normal listeners) from knowledge of the speech and noise spectra and the listener's absolute thresholds.

ii) Many sensorineural hearing impairments are characterized by reduced dynamic range and abnormally rapid growth of loudness. Multiband amplitude compression has been suggested to improve speech reception for listeners with such impairments, but the intelligibility advantages associated with multiband compression are limited by distortion of speech cues associated with the

short term spectrum (e.g., Braida et al., 1983, De Gennaro et al., 1984). To overcome this problem we are studying 'Principal Component Compression,' a means of inter-band control of compressor action that seems capable of achieving significant reductions in level variation with minimal distortion of the short term spectrum.

The basic structure of the principal component compression system is as follows. First, the speech signal is analyzed into bandpass components using a 16-channel critical-band filter bank. The bandpass signals are modulated to yield baseband signals. Estimates of the short-term RMS band level functions (envelopes) or band energies are derived by smoothing the squared baseband signals. The logarithms of the band energy signals provide estimates of the log-coded short-term speech amplitude spectrum. The principal component representation of the amplitude spectrum is obtained via the principal component transform; that is, the vector of band energies is multiplied by a matrix of the principal component basis vectors to yield a vector of principal component coefficients. The principal component coefficients are processed, which generally entails compression of one or more low-order coefficients. The inverse principal component transformation is applied to the compressed coefficients, another vector-matrix multiplication, yielding a set of modified band energies. The difference between the processed and unprocessed log band energies yields the band gain functions in dB. The original filter bank output signals are processed accordingly and summed to yield the processed speech signal.

Promising compression algorithms have been evaluated on the basis of three criteria; 1) effectiveness in reducing short-term speech level variations, 2) preservation of the shape of the short-term spectrum of various speech sounds and 3) intelligibility for normal hearing listeners in quiet and in noise. Results of these evaluations indicate that system configurations which substantially compress (e.g., by a factor of 50) only the first principal component or the first two principal components are most successful in reducing level variation across frequency while preserving important spectral cues. Compression of the first PC significantly compresses overall level and also provides some compression of spectral tilt. Compression of the second PC compresses spectral tilt, which effectively can provide high frequency emphasis for falling spectra and low frequency emphasis for rising spectra. However, the compression systems have been selected to avoid compressing the spectral tilt of rising spectra, which generally correspond to fricatives (i.e., /s/ and /sh/), as this would diminish high frequency energy in these spectra, the major cue for these sounds. Perceptual evaluations of two PC compression systems, one which compresses PC 1 and one which compresses both PC 1 and PC 2 will be performed on the basis of speech intelligibility experiments with severely impaired sensorineural hearing loss listeners.

iii) Frequency-lowering is a form of signal-processing intended to make high-frequency speech cues available to those who cannot hear high-frequency sounds. We have evaluated a frequency-lowering technique studied by Lippmann (1980). In this system speech levels in high-frequency bands modulate 1/3 octave bands of noise at low frequencies, which are then added

to unprocessed speech. We found, in agreement with Lippmann, that processing improved the recognition of stop and fricative consonants when the listening bandwidth is restricted to 800 Hz. However, we also found that processing degrades the perception of nasals and (particularly) semivowels, consonants not included in Lippmann's study. We modified Lippmann's signal processing by reducing the level of the modulated noise when low-frequency components dominate the speech signal. Preliminary results indicate that the modified system does not degrade nasals and semivowels, but maintains the processing advantage for stops and fricatives. Further details of this work are available in Posen (1984).

A preliminary study of artificially coded consonants and vowels has been completed (Foss, 1983). In this study low-frequency (under 500 Hz) sounds have been synthesized to represent CV syllables. After training, identification scores were 90% correct, roughly 20 percentage points higher than those obtained on single tokens of low-pass filtered natural speech. These results suggest that, at present, the limitations to an effective frequency-lowering system depend upon signal processing constraints rather than auditory factors. Furthermore, the cues used in identifying the coded sounds appear to be relatively robust: the error rates and confusions observed for the full-size set were generally consistent with those obvserved on smaller training sets. For the filtered natural speech, performance was found to depend on the number of tokens used to represent each stimulus type: scores decreased from 70% to 35% when the type/token ratio increased from 1 to 3. This indicates that the cues used to identify small sets of filtered natural speech may prove unreliable when the set size is increased substantially. Comparison of these results with those of Miller and Nicely (1953), suggests that increases in the type-token ratio beyond 3 should have minimal effects on performance.

iv) Research on clear speech is directed toward understanding the improvements in intelligibility that can be achieved through techniques which focus on the speech source rather than signal processing. Previous research (e.g., Picheny, 1981; Chen, 1980) has established substantial intelligibility gains for "clear" speech relative to "conversational" speech. During the past year, work has focused on using principal components (PC) analysis to characterize the short term acoustic spectral differences between these two types of materials. PC basis vectors have been computed from the smoothed band energies of sixteen frequency bands with bandwidths that approximate critical bands.

To a first approximation, each of the first few PC basis vectors has a shape roughly independent of speaker and mode. This is consistent with the absence of long-term spectral differences (over speakers or modes) for these materials. In addition, the cumulative percent of the total variance in the first four basis vectors is constant, 91-93%, for all speakers and both speaking modes. However, we have also found that the sum of the variances of the smoothed energy bands increases from conversational to clear speech, i.e. there is a greater total variability in band levels for clear speech. In addition, PC1 (roughly corresponding to overall level) accounts for less of this variability in clear

than in conversational speech for each speaker. By contrast, PC2 (roughly corresponding to spectral tilt) accounts for a larger portion of this variability in the clear speech of the talkers who achieved the greatest increase in intelligibility when speaking clearly. In an absolute sense, variation in spectral tilt increases from conversational to clear for each speaker studied, and is correlated with intelligibility, both within and across speaking modes. Equivalently, the proportion of total variability accounted for by PC1 is negatively correlated with intelligibility.

References

1. L.D. Braida, "Speech Processing for the Hearing Impaired," Proc. 2nd Int. Conf. on Rehab. Engr., Ottawa, Canada, 1984.
2. F.R. Chen, "Acoustic Characteristics and Intelligibility of Clear and Conversational Speech at the Conversational Level," S.M. Thesis, Department of Electrical Engineering and Computer Science, M.I.T., 1980.
3. S.V. De Gennaro, L.D. Braida, and N.I. Durlach, "Multichannel Syllabic Compression for Severely Impaired Listeners," Proc. 2nd Int. Conf. on Rehab. Engr., Ottawa, Canada, 1984.
4. R.L. Dugal, L.D. Braida, and N.I. Durlach, "Implications of Previous Research for the Selection of Frequency-Gain Characteristics," in G.A. Studebaker and I. Hochberg (Eds.), Acoustical Factors Affecting Hearing Aid Performance and Measurement (University Park Press 1980).
5. K.K. Foss, "Identification Experimentation on Low-Frequency Artificial Codes as Representation of Speech," S.B. Thesis, Department of Electrical Engineering and Computer Science, M.I.T., 1983.
6. R.P. Lippmann, "Perception of Frequency Lowered Consonants," J. Acoust. Soc. Am. 67, S78 (1980).
7. G.A. Miller and P.E. Nicely, "An Analysis of Perceptual Confusions among Some English Consonants," J. Acoust. Soc. Am. 27, 338-352 (1953).
8. M.A. Picheny, "Speaking Clearly for the Hard of Hearing," Ph.D. Thesis, Dept. of Electrical Engineering and Computer Science, M.I.T., 1981.
9. M.P. Posen, "Intelligibility of Frequency Lowered Speech Produced by a Channel Vocoder," S.M. Thesis, Department of Electrical Engineering and Computer Science, M.I.T., 1981.

26.5 Discrimination of Spectral Shape

National Institutes of Health (Grant 1 RO1 NS16917)

Louis D. Braida, Lorraine A. Delhorne, Nathaniel I. Durlach, Catherine L. Farrar, Mary S. Florentine, Yoshiko Ito, Charlotte M. Reed, Patrick M. Zurek

This research is concerned with determining the ability of listeners with normal and impaired hearing to discriminate stimuli with broadband, continuous, speechlike spectra, and to relate these measurements to underlying auditory abilities. The stimuli were generated by filtering Gaussian noise through a parallel synthesizer whose resonance parameters were adjusted to correspond to the spectra of steady-state unvoiced fricatives /f,s,sh/ and the burst portion of the unvoiced plosives /p,t,k/). In some tests, a masker having the spectral characteristics of cafeteria-noise babble was introduced. To prevent listeners from basing judgments on loudness cues, overall levels were roved. Discrimination data have been obtained for three experimental conditions (/p-t/ with 30-msec

duration, /p-t/ with 300-msec duration, and /f-sh/ with 300-msec duration), each with a different group of five normal-hearing listeners. Roughly speaking, the shape of the psychometric function, d' vs. S/B (averaged over level pairs), is the same for all stimulus configurations and all subjects tested; this function is very shallow and has a slope of approximately 0.13 (change in d' per dB change in signal to babble ratio). Preliminary data have been obtained from two listeners with sensorineural loss indicate that they require a 20-30 dB increase in S/B to achieve discrimination performance comparable to that of listeners with normal hearing. The extent to which this shift in S/B should be assigned to effects of the impairment rather than to other differences between the subjects has not yet been determined.

A second set of experiments measured pure-tone thresholds in the background of a masker composed of a synthetic speech stimuli (30 msec /p/ and /t/ bursts) in quiet (where the /p-t/ discrimination was easy) or at S/B = − 4 dB (where the discrimination was difficult). For all four masker complexes, the fixed-level masked thresholds generally follow the spectral shape of the masker at the three levels tested (45, 75, and 95 dB SPL). The most notable deviation from linearity of masking is observed at 125 Hz for the lower levels, where the threshold increase is smaller than the increase in masking level. Masking difference patterns, obtained by subtracting thresholds in the /p/-shaped masker complex at a given S/B from those obtained in the /t/-shaped masker complex at the same S/B, show (as expected) much larger differences in quiet than in babble. In quiet, these differences, which are several dB larger for the 75- and 95-dB SPL maskers than for the 45-dB masker, were highest in the frequency region 500-2000 Hz (averaging roughly − 15 dB for the highest masker level) and smallest at 4000 Hz (3 dB). For S/B = − 4 dB, the masking differences fluctuate around zero except at 3500 Hz for the 45-dB level, where the /t/-shaped masker complex provides roughly 7 dB more masking than the /p/-shaped masker.

In order to interpret the relation between spectral shape discrimination and basic auditory abilities, we are developing black-box models of both peripheral processing, which derives an internal spectrum from the physical input, and central processing, which relates the hypothesized internal spectrum to psychophysical performance. Our general approach to this modelling task is to start with models that are as simple as possible, apply them to an increasingly wide range of data, and elaborate them as dictated by these applications. Initial work on the peripheral processor has used a conventional filter-bank model and has assumed ideal central processing. Each filter output level is assumed to be estimated by rectification, integration, and a logarithmic transformation. The processing is corrupted by adding Gaussian internal noise after the level estimate. This model has been applied to our own data on discrimination and detection and also to results on frequency discrimination of tone bursts in broadband noise. For a given choice of filters and integration times, the model has one free parameter, K, corresponding to the level of noise added after the logarithmic transformation. Results show that (1) except for our own data on the detection of 30-msec tones in /t/-shaped masking noise (with no babble), all empirical curves can be reasonably well fit by some choice of model parameters; and (2) in the exceptional case just mentioned, the best fitting

theoretical curve is too high at high frequencies and too low at low frequencies. The values of K required to fit the data vary by a unacceptable amount. However this variation can be substantially reduced if the effects of external noise fluctuations are taken into account. Our work on ideal central processing has assumed, for simplicity, that the internal spectrum (with the roving level included) can be characterized as an N-dimensional random vector whose components are Gaussian random variables. We have computed the optimal performance of such a receiver as a function of the variance of the roving overall level, and shown that this performance is equivalent to that for a receiver which processes only level-differences between adjacent bands optimally. In general, the roving of overall level is predicted to have only small effects on the discriminability of stimulus pairs equated in terms of overall energy or loudness.

26.6 Tactile Perception of Speech

National Institutes of Health (Grant 1 RO1 NS 14092-05)
National Science Foundation (Grant BNS 77 21751)
Louis D. Braida, Raymond Boduch, Jackie Coker, Lorraine A. Delhorne, Maralene M. Downs, Leonard C. Dowdy, Nathaniel I. Durlach, Daniel F. Leotta, Joseph C. Pemberton, William M. Rabinowitz, Charlotte M. Reed, Jean Reid, Richard D. Reohr, J. Robin Rohlicek, Roy P. Russell, Martin C. Schultz, Gregory M. Skarda

The ultimate goal of our research program is to develop tactile aids for the deaf and deaf-blind that will enable the tactile sense to serve as a substitute for hearing. Among the various components of our research in this area are (i) study of tactile communication methods employed by the deaf-blind, (ii) development of an augmented Tadoma system, (iii) development of a synthetic Tadoma system, and (iv) design and evaluation of a wearable, portable aid.

i) Experimental work is being conducted on two methods of communication (tactile fingerspelling and tactile signing) that are in common use among members of the deaf-blind population. One goal of our research is to examine the rates of communication attainable through these two methods and to compare these rates to those obtained through the Tadoma method. For tactile fingerspelling, five deaf-blind subjects have been tested on several sentence-repetition tasks and on tracking of continuous text. Sentences were presented by an experienced fingerspeller at rates varying from roughly 2 to 6 letters/sec. For "conversational" sentences, experienced deaf-blind receivers of fingerspelling achieved perfect scores for rates at and below 5 letters/sec (the equivalent of 1.5 syllables/sec, which is roughly three times slower than normal speaking rates). These subjects were able to track text at an average rate of roughly 30 words/min (a result similar to that obtained by experienced Tadoma users and roughly one-third of that obtained under normal auditory conditions). For tactile signing, the sentence materials used in the Tadoma and fingerspelling research have been translated into ASL and videotaped by a native signer who then serves as the "sender" in tests with experienced deaf-blind users of ASL. Results (currently available for three subjects) are being

analyzed by glossing the subjects' responses and determining their semantic and syntactic accuracy as a function of rate of presentation in signs/sec.

ii) Work is underway to evaluate an "augmented" Tadoma system in which the normal Tadoma signal (received by placing a hand on the talker's face and neck) is supplemented by information on tongue position (derived by sensing the contact pattern of the tongue with the upper palate and displayed to a finger of the opposite hand through a tactile transducer array). A programmable interface has been developed between a Palatograph and an Optacon transducer and software allows tabular specification of vibrator action on a 24x6 array corresponding to 63 palate contact points. The mapping currently in use preserves the general shape of the palate on the vibratory array. Current experiments are concerned with the ability of laboratory subjects using augmented Tadoma to discriminate pairs of stimuli that contrast different tongue positions and are difficult to discriminate using normal Tadoma. Experiments will then be extended to include other subjects (deaf-blind Tadoma users) and other types of tasks and test materials (e.g., identification of speech segments and reception of continuous speech).

iii) To better understand the success of the Tadoma method and to explore transformations of the method that cannot be achieved directly, we are developing a synthetic Tadoma system in which an artificial talking face is driven by signals recorded from the facial actions of a real talking face. During the past year work has continued on the processing (digitizing, editing, filtering, etc.) of the tape-recorded facial-action signals into computer files appropriate for driving the artificial face (Skarda, 1983). The library has been substantially increased to include additional speech materials from the original male talker and materials from a second male talker and two female talkers.

On the artificial face, a four-channel position-control system has been constructed to drive the DC servomotors which effect the lip and jaw movements. Each motor operates closed-loop with feedback of shaft velocity (tachometer) and position (optical encoder). The system response (of shaft position over input voltage) is set to approximate a third-order Butterworth lowpass characteristic with a 3-dB cutoff of 32 Hz, which allows for (smoothly) driving the articulators at normal and higher rates. An interface (of specialized hardware and software) for outputing the facial-action signal files from our laboratory computer system to the artificial-face electronics has also been completed. Artificial-face representations for the two remaining facial actions, laryngeal vibration and oral airflow, are currently being installed and experiments will soon begin with laboratory-trained normal subjects and deaf-blind Tadoma users to assess the adequacy of the system as a simulation of Tadoma.

iv) A further project in this area concerns the development of a multi-channel, wearable/portable, tactile aid. (This project is being conducted under the auspices of the Rehabilitation Engineering Center at Gallaudet College.) The aid incorporates a linear array of vibrators and displays short-term spectral information to the abdomen. Efforts during the past year have focused on laboratory-based experiments to guide various design choices (Rohlicek, 1983). These experiments have provided

rough estimates of absolute thresholds, intensity and frequency discrimination thresholds, modulation thresholds, and spatial and temporal masking thresholds. In addition, preliminary discrimination experiments were performed using a computer-controlled eight-channel tactile vocoder on speech segments to explore the effects of various signal processing schemes, e.g., amplitude compression (to combat small dynamic range), temporal truncation (to combat masking of consonants by vowels), and spectral peak picking (to combat spatial masking). None of the processing schemes tested improved the discrimination of speech segments significantly. Work has now begun on hardware development of the wearable aid.

References

1. J.R. Rohlicek, "Some Perceptual Constraints on the Tactile Coding of Speech," S.M. Thesis, Department of Electrical Engineering and Computer Science, M.I.T., 1983.
2. G.M. Skarda, "An Analysis of Facial Action Signals during Speech Production Appropriate for a Synthetic Tadoma System," S.M. Thesis, Department of Electrical Engineering and Computer Science, M.I.T., 1983.

C. Transduction Mechanisms in Hair Cell Organs

Academic and Research Staff

Prof. L.S. Frishkopf, Prof. T.F. Weiss, Dr. D.J. DeRosier[21], Dr. C.M. Oman

The overall objective of this project is to study the sequence of steps by which mechanical stimuli excite receptor organs in the phylogenetically related auditory, vestibular, and lateral-line organs. The receptor cells in these organs are ciliated hair cells. Specific goals include the characterization of the motion of the structures involved, particularly the hair cell stereocilia; study of the nature and origin of the electrical responses to mechanical stimuli in hair cells; and investigation of the role of these responses in synaptic and neural excitation.

26.7 Length-Dependent Mechanical Tuning of Free-Standing Stereociliary Bundles in the Alligator Lizard Cochlea is the Basis of Neural Tuning

National Institutes of Health (Grants 5 R01 NS 11080 and GM-21189)

Lawrence S. Frishkopf, David J. De Rosier

As reported earlier,[1] we have studied the motion in response to sound of free-standing stereociliary bundles of hair cells in the alligator lizard basilar papilla as a function of stimulus frequency, hair cell location, and bundle length. We have established that such motion provides a basis for frequency selectivity and tonotopic organization observed in nerve fibers to the organ. Our results indicate (1) that stereociliary bundles behave like damped mechanical resonators; (2) that resonant frequency varies inversely with bundle length raised to a power between 1.5 and 2; and (3) that bundle resonant frequency and neural CF are close in value in corresponding regions of the papilla and nerve. These findings are consistent with an explanation of frequency analysis in the papilla based on length-dependent mechanical tuning of stereociliary bundles.

We have reported these results fully in a recent paper;[2] other findings that corroborate this interpretation have been recently published as well.[3]

References

1. L.S. Frishkopf and D.J. DeRosier, "Evidence of Length-Dependent Mechanical Tuning of Hair Cell Stereociliary Bundles in the Alligator Lizard Cochlea: Relation to Frequency Analysis," M.I.T. Research Laboratory of Electronics Progress Report No. 125, pp. 190-192 (1983).
2. L.S. Frishkopf and D.J. DeRosier, "Mechanical Tuning of Free-Standing Stereociliary Bundles and Frequency Analysis in the Alligator Lizard Cochlea," Hearing Res. 12, 393-404 (1983).

[21] Professor, Department of Biology, Brandeis University

3. T. Holton and A.J. Hudspeth, "A Micromechanical Contribution to Cochlear Tuning and Tonotopic Organization," Science 222, 508–510 (1983).

27. Physiology

Academic and Research Staff

Prof. J.Y. Lettvin, Dr. J. Gardner, Dr. S. Jhaveri, Dr. L.A. Kamentsky, Dr. D. Perlman, Dr. G.M. Plotkin, Dr. S.A. Raymond, Dr. S. Wiesner, G. Geiger

Graduate Students

L.R. Carley, A. Grant, B. Howland, A. Medina-Puerta, G. Pratt

27.1 Nervous Signals in the Neuropil of Tectum

Bell Laboratories, Inc.
Ortho Instruments
Jerome Y. Lettvin, Edward R. Gruberg[22], Eric Prenowitz

In 1959[1] we reported not only on the retinal operations in frog's eye as recorded in optic nerve but also on what seemed the same signals recorded extracellularly in tectal neuropil. We assumed, and thereafter the subsequent literature from other laboratories took for granted, that this sort of tectal record represented the invasion of the terminal bush of an optic nerve fiber. The proliferation of branches in the bush, so we thought, might multiply the local signal current of the fiber by the number of branches and, so, bring the invading signal well above noise level. This hypothesis seemed to explain why we could not record from the fibers in passage but only where they terminated.

But in 1982 and early 1983, Drs. Edward Gruberg and Jerome Lettvin discovered some material that provided a very different account. The tectal neurons have two major known inputs, one from the eye, the other from nucleus isthmi, an ipsilateral slave nucleus to the tectum in that its sole input is from tectal cells, and its output, ipsilaterally, is back to the same cells. This arrangement, by the way, is ubiquitous in land vertebrates from frog through reptiles and birds to mammals, as has been shown by Dr. Harvey Karten.[2] From a variety of experiments by others as well as by us, the ipsilateral n. isthmi fibers are inhibitory to tectal cells. What we discovered was this: Direct stumulation of n. isthmi produced no obvious extracellular signals in the ipsilateral neuropil, while stimulation of optic nerve produced fine signals. The terminals of n. isthmi fibers alternate with optic nerve fibers as specific layers in the depth of the neuropil. It was, therefore, disconcerting to find no electrical sign of their activity in extracellular records.

From n. isthmi, a small fraction of the fibers go contralaterally to the opposite tectum, as was described in earlier papers by us. These fibers mediate the crossed information used in the frog's

[22] Temple University

binocular vision. Like the direct optic nerve fibers to the opposite tectum, they are also excitatory, and electrical stimulation of these crossed fibers produces excellent extracellular signals in the superficial neuropil of the opposite tectum.

It became obvious to us that the sharp, discrete nerve spikes we were recording in tectal neuropil may not be the electrical signals on afferent fibers in the neuropil, but be the subsynaptic responses to the excitatory afferents. This hypothesis is not easily checked except by happy accident. The extracellular electrical spikes in tectum, seen through low resistance metal microelectrodes (of our new design, ~20 kΩ at 1 KHz for a 5 μ tip diameter) are fairly often not simple signals but can comprise up to five distinct phases and, so, be well individuated from other signals. These complex transients are of constant amplitude and shape if the electrode tip is not displaced. We found two cases where the overlapping receptive fields of the direct optic fiber of one eye and the relayed fiber from the opposite n. isthmi, representing the same part of the visual field in the other eye, evoked exactly the same characteristic complex spike at the same point in the superficial neuropil. This convinced us that there was a common signal generator activated by both fibers, and could only be the common area on the dendrite on which both ended.

The importance of this finding is great. To explain the significance: It is possible, if our finding is proper, to work out electrophysiologically the topography of endings on dendrites of cells in the central nervous system. The self-same kinds of spikes, appearing in neuropil where the cell bodies are remote, are found everywhere in the brain and spinal cord. They have been dismissed as fibers of passage, etc. Intracellular records only give a distant and smeared integrated view of all the synaptic activity in all the dendrites of the impaled cell. This method locates precisely active excitatory endings of known provenance. By their nature, inhibitory endings, which evoke shunts to the V_{K^+} or V_{Cl^-} across cell membrane, cannot produce the same current-generating responses as excitatory endings. Thus we now have the tool for telling whether a particular input to a neuron is excitatory.

References

1. J.Y. Lettvin, H.R. Maturana, W.S. McCulloch, and W.H. Pitts, "What the Frog's Eye Tells the Frog's Brain," Proc. I.R.E., 47:1940–1951, 1959.
2. H.J. Karten and R.O. Kuljis, "The Frog and the Peptide Swamp," to be published.

27.2 Sensing of Texture by Retinal Ganglion Cells

Bell Laboratories, Inc.
Ortho Instruments
Jerome Y. Lettvin, Arthur Grant

In 1959[1] we reported a variety of ganglion cells from the frog retina that became known as the "bug" detector. This element is the most frequent sort to be found in the retina and constitutes well over 50% of the population. However, it has a small cell body, and its axon is approximately 0.2 μ in

diameter at most, so that it is difficult to detect by its electrical signal. Initially, we found this type in optic nerve, using electrodes that, for some reason, have never become very popular. (They are a modified form of the Dowben-Rose probe that uses platinum-black at the tip. The real component of the input resistance of such a tip in contact with physiological saline solution is ~20 KΩ at 1 KHz for ~4 μ diameter, so that the noise is extraordinarily low. But they require individual preparation — they cannot be batch-produced.) This retinal element, type II, however, is readily detected in tectal neuropil by the responses described in the previous section.

The literature since 1959 has more or less rejected our initial description, not because the experimental results could not be repeated, but because there was a simpler description to be had by the responses to less complex stimuli. That is to say, the details that we found so interesting were to be considered ancillary, epiphenomenal.

Our original description, while incomplete, had the misfortune of being improperly named as "net convexity" detector, and this name, rather than the substance of the account, became the object of attack and the grounds for denying the complexity of image processing that we found. It is worthwhile, therefore, to recall the original findings so as to set the basis for the new work to be reported here.

A type II ganglion cell in frog retina has an intrinsic receptive field of ~5° in visual angle. That is, on a screen, 15" away from the eye, the area to which it is directly sensitive is about 1" in diameter and is fairly sharply defined. The sensitivity is indicated by the production of pulse trains in the fiber. This area is directly surrounded by an annular region whose outer border is vague and variable; it is called the "surround". Visual events in the surround diminish the responses made to other events in the central receptive field. This surround annulus can be over 2" thick; the bad definition of the outer border simply reflects the lessening of the inhibitory influence of a stimulus by its distance from the border of the central receptive field, hereafter call simply "center RF", so that one can talk of center RF/surround RF relations.

The center RF is located by moving a small black spot ~15' of arc in diameter over a blank white screen. The position of its center (to be called "focus") is estimated, and the spot is moved radially toward it from about 2°-3° away. The border of the center RF is defined by the occurrence of a pulse train where the spot crosses the boundary between surround RF and center RF. The outline of center RF is somewhat circular or oval, but occasionally is cardioid. Movement of the black spot centrifugally from the focus of the center RF produces a smaller response (see below).

Once the eye of the frog is fixed against any rotation, the center RF of a type II neuron is well etermined on a fixed screen and can then be studied for the relation between visual events and the pulse trains given by the neuron.

Two important insensitivities are found immediately. First, no steady state of the region covered by

the center RF and surround RF excites any nervous response in the fiber. The background white screen can be supplanted by a large color photograph of a complex scene, and the neuron is indifferent. Second, no uniform change of illumination on the screen excites a response. The general lighting in the room can be switched on and off to the complete indifference of the neuron.

The only excitement of the fiber occurs when a phase boundary comes into being or is moved within the center RF. For simplicity, let us talk of two phases, black and white, where the black phase has ~0.12 the luminosity of the white. For a response to occur there are three conditions:

A. A single area within the center RF, up to and including the whole center in area must be sharply darkened, and the dark phases must have a sharp edge. The smallest area that produces a response in this way is about 2' of arc in diameter. The largest is slightly larger than the area of the center RF (which had been outlined by the radial moving spot method). The effect of blurring the edge of the dark spot compromises the response more than diminishing the contrast between the dark and light phases. The response is maximal at the time the black phase suddenly appears, then dies off in time. After about 20 sec, but often somewhat longer, the dark phase against the light background becomes a steady state system and is ineffective.

B. If a single black spot, fixed in area and shape and lying completely within the center RF, is moved in steps within the center RF, it excites the fiber with each step. The excitement is greatest when there is no centrifugal lightening by the movement. Thus a small black spot approaching the center of the center RF has a leading edge and a trailing edge. The response is large, except as the trailing edge moves predominantly away from the focus. Thus, for example, a black spot growing in size radially away from the focus gives a good response. So does a single black spot, part of whose border is co-extensive with the border of the center RF but which grows to occupy the whole of the center RF without trespassing onto the surround. All movements or growth of a black spot produce a good response so long as the spot is not in some sense "retreating", i.e., growing smaller or moving centripetally.

C. The moving dark phase or sharply appearing dark phase must be a single continuous spot, a single phase. This was the condition that excited enough disbelief that, apparently, it was never seriously checked or pursued. So, for example, three black spots, each capable of exciting a good response if alone, when rigidly spaced from each other and moving rotationally or translationally as a triad in the center RF, do not excite much of a response, if any. However, if the space between the dots is blackened so as to give a single black triangle, the response to its movement is again excellent. Furthermore, if yet a fourth spot is added and rigidly coupled, the neuron is insensitive to the tetrad. But if the fourth spot is decoupled from the other three and moved independently of them, it again excites the type II element.

A pair of rigidly coupled spots is not as exciting as a solid black bar of the same width and length as if the space between the pair had been filled. But the cell, nevertheless, does respond to a pair, if with

diminished vigor. Finally, a single black spot with a tortuous serrated edge, is almost as exciting as a black spot with a smooth edge.

It is evident from these three conditions that the type II element is sensitive in its center RF not only to phase boundary but to phase continuity. (This second aspect prophylactically rid us of Minsky and Papert's[2] later perceptron model).

Interaction of the center with the surround was also complex. For example, suppose against a blank white background a large black sheet of paper to be moved edge first into the surround RF and thence, jerkily, but with steady advance so as to intersect and finally pass through the center RF. There is absolutely no response. However, if the sheet is moved, corner first, into and through the receptive field in the same way, the response is strong. Several later researchers, notably Gaze and Jacobsen,[3] felt that the growth of darkening from the rim of the center RF inward was excitatory purely as darkening if nothing occurred at the same time in the surround RF. In the case of the black sheet, edge first, the surround was darkened at the same time as the center was darkened, and, so, edge need not be involved — the interaction was simply a case of inhibition from the surround and on the basis only of diminution of flux. They conveniently ignored the case of the black sheet moved corner first. For some reason, the notion of shape detection in the retina was felt to be suspect. It needed, so the received wisdom held, the amenities of mammalian cortex. Edges possibly might, by some peculiar circuitry, be sensed by single retinal cells as was later found also in pigeon or rabbit, but certainly nothing as complex as shape or texture could be detected. Gaze and Jacobsen's[3] experiment was thereafter cited as the example of how to reduce what seemed to be a complex system into an easily explained inhibitory interaction between center and surround on the basis of flux change alone.

With these comments as background, we can now describe our current work, emphasizing one specific aspect, that relating phase and texture. The primitive experimental setup is this: We locate a center RF of a type II neuron as described earlier. Then we cut a hole in the white screen slightly smaller than the center RF. The hole is backed with a wide, white cardboard flap that allows introduction of stimuli between it and the screen. Thus no stimuli ever appear in the surround. Five distinct stimuli are prepared. They are all circular paper discs, all of the same size, about half the diameter of the hole. Each is glued to a thin flat steel washer that can be moved over the face of the flap by a magnet behind the flap. The five stimuli are these:

1. A uniform black disc.

2. A white disc with several identical black spots on it. The area of the black spots is about the same as the area of the white ground of the disc.

3. Black disc with several white spots on it. Again, within the disc the areas of white and black are about equal.

4. A gray disc with half the luminance of a white disc.

5. A white disc with a black spot on it the size of those in stimulus 2.

While it is not technically correct to say it, stimuli 3 and 4 have the same first-order statistics and differ only in the second order.[4] They differ also in another way. In stimulus 2, the continuous phase is white, in stimulus 3 it is black.

There is a good response to stimuli 1 and 4, and a good response also, though not as vigorous, to stimulus 5 when they are introduced into the center RF from behind the screen. There is no response to stimulus 2 but a fairly good and distinct response to stimulus 3.

If the hole is itself masked by a white sheet of paper and the stimulus set in phase behind it so that it suddenly appears when the sheet is sharply withdrawn, the same order of stimulus effectiveness is seen, and almost no response to stimuli 2.

These initial simple experiments are not as easy as they sound. The frog must be robustly healthy, immobilized in body and eye, the pupil must be constricted, and the retinal circulation good. Dilated pupil, poor circulation, the presence of barbituates or other anesthetic and any more curare than is just necessary for immobilization, all militate against successful study.

These early results show several things. Simple average darkening of a portion of the center RF is not a stimulus. Otherwise the responses to 2, 3 and 4 would be the same. Amount of edge is not pertinent, otherwise 2 and 3 would be equally excitatory. In distinguishing between the stimuli 2 and 3, there is the choice between saying the stimuli differ in second-order statistics or in which phase is continuous. There is, obviously, a weak relation between the two statements, except that we cannot see how continuity of phase can be inferred from the second-order statistics, while the other way round is fairly transparent although not simple. Furthermore, the textures, which we call microtextures to distinguish them from those which Julesz analyzed, are abstracted by one ganglion cell alone, not from an ensemble of such cells.

There has been one interesting by-product of this work. For a long time we have felt that something was wrong, extremely wrong, in using video screens as tools in studying the retina. It is evident enough for the frog that the envelope of dots in stimulus 2 is a far cry from the continuous single phase boundary of stimuli 1 and 4. Oddly enough the same microtexture prevents the perception of form in human peripheral vision. Form is not given by an envelope of dots if they are clearly discrete as pixils, but only by what are actually (rather than virtually) phase boundaries.

References

1. J.Y. Lettvin, H.R. Maturana, W.S. McCulloch, and W.H. Pitts, "What the Frog's Eye Tells the Frog's Brain," Proc. I.R.E., 47:1940-1951, 1959.
2. M. Minsky and S. Papert, Perceptrons (M.I.T. Press 1969).
3. R.M. Keating and J.M. Gaze, "Observations on the "Surround" Properties of the Receptive Fields of Frog Retinal Ganglion Cells," Quart. J. Exp. Physiol., 55, 129–142 (1970).
4. B. Julesz, "Experiments in the Visual Perception of Texture," Sci. Am. 232, 34–43 (1975).

27.3 Analogue Model of a Photoreceptor

Bell Laboratories, Inc.
Ortho Instruments
Jerome Y. Lettvin

Conceive a photosensitive pigment in a receptor that is several wave-lengths of light in width — a few microns. The pigment has a uniform spectral absorption. When all the pigment is in native state, it captures 2% of the photons entering the receptor in a flash of light.

The pigment has four states. It is photosensitive only in the native state, A. When a molecule in state A captures a photon, it switches very rapidly to state B, the first intermediate product. A population of molecules in state B switches then to state C, the second intermediate, with a rate constant of β. In turn, a population in state C switches to the fully bleached state, D, with a rate constant of γ. And those in state D are returned to state A by an energetic process and with rate constant of δ. In respect to the rate constants, $\beta > \gamma > \delta$, as is required for stability of the state loop. The system is described by a simple ring, using state letters to signify the fractions of pigments in those states. φ is the flux entering the receptor, and Z is the capture fraction by the pigment when A = 1. Then

$$\frac{-dA}{dt} = A\varphi z - D\delta$$

$$\frac{-dB}{dt} = B\beta - A\varphi z$$

$$\frac{-dC}{dt} = C\gamma - B\beta$$

$$\frac{-dD}{dt} = D\delta - C\gamma$$

Under steady state of φ all these expressions equal 0.

We define two constants, $K_1 = \beta/\gamma$ and $K_2 = \beta/\delta$; and an attenuating constant

$$\frac{1}{K_3} < 1.$$

The state variables are then represented by conductances in the following circuit (Fig. 27-1), which is a primitive model of our present design:

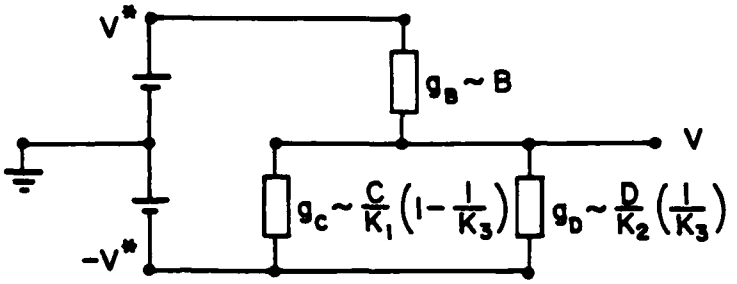

Figure 27-1

By Kirchoff's rule

$$\frac{V}{V^*} = \frac{g_B - (g_C + g_D)}{g_B + (g_C + g_D)} = S, \text{ the signal value } -1 \leq S \leq +1$$

and $S = 0$ at all steady states of φ.

Suppose the system has come to steady state and then a small step of $\Delta\varphi$ occurs.

At the time of the step

$$\Delta S = \frac{\Delta g_B}{2g_B} \quad \text{since } g_B = g_C + g_D \text{ just before the step.}$$

Thus $\Delta S_T \sim \frac{\Delta\varphi_T}{\varphi}$, which is the Weber-Fechner law (the subscript T signifies threshold).

If the step is maintained, S returns to ~0 with the approximate rate constant of β. When D is in steady state with C and B, for any step $\Delta\varphi$ away from the steady state φ_0, at the instant of the step

$$\Delta S \simeq \tanh \frac{1}{2} \ell n \left(\frac{\Delta\varphi + 1}{\varphi}\right)$$

the operating characteristic. It is approximately what Norman and Werblen measured in actual cones.

And if the step is maintained, S returns to 0.
Note that ΔS is independent of φ_0 and depends only on $\frac{\varphi}{\varphi_0}$.

Note also that the saturating function S is almost linear with $n\frac{\Delta\varphi}{\varphi_0}$ between $\frac{1}{3} \leq \frac{\Delta\varphi}{\varphi_0} \leq 3$

which is the decade needed for handling reflectances. Note also the effects when $D > K_2B$ and when $D < K_2B$ and compare them with experience. This is not the final version, which takes account of the ohmic interconnectedness of cones, but it conveys the major ideas.

We will not go into how such a model accounts for several previously unaccountable phenomena and laws (e.g., the Rushton–Dowling law that for threshold to a flash under complete darkness

$$\frac{\log(\text{density of photons in a threshold flash})}{K} \sim D$$

where K can lie between 2 and 20, depending on the species of animal and the species of photoreceptor. The law holds for $.01 < D < .99$ as Dowling showed.) Instead we want to discuss what is involved in the strategy.

Since our eyes move about constantly in microsaccades and saccades to maintain the image, C takes a short-term running history of the fluxes encountered, and D takes a long-term running history. In brief, D does in time the averaging over many phases in many places of the scene because our eyes move about, while C does the averaging of the phases in the immediate region of the image. C is used for the normalization, the short-term adaption, and does not represent an independent measure or constraint. D supplies what was needed in the dimensional analysis without recourse to feedback from later processing.

This is a novel and, so far as we know, an unprecendented use of pigment intermediate breakdown products to supply the method for both the immediate local processing and the additional representation of the surround so as to account for the degrees of freedom in color vision. But the same theory also explains the Norman and Werblen "operating characteristic" measured on cones — $a \tanh \frac{1}{2} \ell n \frac{\varphi}{\varphi_0}$ where φ_0 is the adapting light. The mechanism for such a process has not yet appeared or, to our knowledge, been suggested.

27.4 Enhancement of Form Perception Under Textural Masking

Bell Laboratories, Inc.
Ortho Instruments
Jerome Y. Lettvin, Gad Geiger

In eccentric vision, i.e. perception away from the fixation axis, there is a distinct interplay between form and texture. It occurs in foveal as in extrafoveal or peripheral vision and has been called lateral masking. Most easily demonstrated with letter and other shaped signs, it can be illustrated thus:

N X TENET

When the X is fixated with either or both eyes, the isolated N is quite visible; the N in TENET is not, although the two are equidistant from the X. This phenomenon was systematically investigated first by

Bouma.[1] Now there are over a score of relevant papers as given in the bibliography, which is far from exhaustive. To some extent the shape of a sign has much to do with its ability to mask or be masked, as does its boldness, contrast, distance from other signs and the sharing of direction between parts of neighboring signs. These relations have been examined extensively by Bouma and those who followed. But what remains as common in all cases is that the interaction between separate adjacent signs suppresses something related to their form so that the interior signs of a string are hard to identify. The most eccentric sign of an eccentric string is commonly the easiest to make out, and the least eccentric is the next easiest.

There has been a feeling, voiced again and again from Estes,[2] that such interaction, which makes eccentric vision less clear than would be expected from measurement of spatial resolving power, has its key in the nature of cortical receptive fields. In a sense this must be the case, the only reservation being whether those receptive fields have been well-enough described so as to accommodate the observations.

The reason for this doubt is that we have found an enhancing or unmasking interaction between the center of gaze and the eccentric field. Unmasking could not occur if the masking process was at so elementary a level that the information by which shaped signs are judged has already been lost. Interactions of this sort are transient as opposed to the masking which endures. They were sought and discovered in a simple way; the experiments to be described refined the observations so as to rule out various epiphenomenal causes.

Experiments

Two slide projectors were mounted behind and aimed at a translucent diffusing screen such as occurs in large film-readers. Inscribed on the screen was a fixation mark. Both projectors were equipped with current-driven shutters able to open or close in three milliseconds. The currents were governed by conventional gating operations whose timing could be set accurately. One projector displayed a test image on the screen for a period that could be adjusted up to 150 ms, but no more. Within this period the probability of one microsaccade is low — of two is negligible, and there is no time for a voluntary eye movement. From our point of view, the conditions for tachistoscopy are met, given the fixation of the eye up to and during the exposure.

The test image was followed by an "erasing" image, usually a square grid crossed by a grid of the diagonals. This erasing image always occurred with a delay after the test image was turned off. The delay from the onset of the test image never exceeded 250 ms. Erasure was important in establishing repeatability and reliability of the data. Otherwise there could be distinct variations that were related, we felt, to the use of after-images or to changes in adaptation.

The complex signs used in the test-image were bold, upper-case block letters of high contrast. They were about 35 minutes high in angular size from where the subject sat, and at most 30 minutes broad, and when presented in strings, were separated by 35 minutes between the centers so as to

provide clear spacing. These signs are called "complex". Another sort of sign, the "simple" one, consisted of bars with the same thickness of line as the letters but presented in different orientations.

Initially, while the subject gazed at the fixation point, a string of three signs was flashed eccentrically 2°40' away. The length of exposure and timing of erasure were adjusted until the subject reported correctly slightly less than 100% of the time, i.e., 80%–90%. This less-than-fully correct calling was quite stable and repeatable and often was retested at the end of a run. Thus, when the same strings were flashed at 8° eccentricity, which we used as a standard distance, the accuracy of report dropped to a fairly low level. This ensured that all tests were done below the threshold for recognition. Thus a base was provided against which enhancement of recognition could be tested for isolated signs or strings. Enhancement usually gave a 20%–50% improvement in the density of correct calls.

The subject used both eyes in the experiment, since we wanted to avoid comparing nasal and temporal fields in each eye.

Results

In the same image flash we began with two signs, one at the fixation point, one at 8° eccentricity. The signs were either identical or different. With disparate signs, identification of that at 8° was poor. But when the two signs were the same letter, identification was distinctly enhanced. This enhancement, however, applied only to complex signs. When simple signs were used, bars at the same orientation or at disparate orientations, no enhancement occurred.

With strings of three complex signs in a horizontal line, the center sign at 8°, there was distinct enhancement of any letter in the string when the identical letter was flashed simultaneously at the fixation point. When a letter not in the string was flashed at the fixation point, there was little or no enhancement, as if no fixation-point letter was flashed. And again, there was no enhancement with the same experiments done with simple signs instead of complex ones — the masking in the eccentric field stayed unchanged.

Similar experiments were done at greater eccentricities, and from them emerged two populations. The greater number of subjects showed neither resolution nor enhancement beyond 10°–12° eccentricity. A small group, to our surprise, showed enhancement at 15°–18° eccentricity. (The blind spot does not figure here, since the tests were done with binocular fixation.) This latter group were all characterized by significant reading difficulty. We mention this as an aside.

Finally, in admixtures of complex and simple signs in eccentric strings of three, enhancement always occurred when the identical complex signs lay at the fixation point and in the string, and never occurred when identical simple signs were in the same pair of positions.

Discussion

So far the work has addressed what may be called an interplay between texture and form. The interior sign in a string of eccentric complex signs has an odd quality when there is no enhancement. Something seems to be there — it has boundary in a way — but the spatial order is lacking by which that boundedness is given form. It is a textural part of the string, a vaguely prehended distribution, an innominate *chiaroscuro*, and the subjects do not guess wrong letters. They simply say they could see nothing clearly. When it stands out by enhancement in this transient display, it takes on an almost distinct form. We are driven to suppose, therefore, that there is a texture-breaking interaction between the fixation point and the eccentric string — an enhancing of unmasking influence.

If the masking was a primitive and information-destroying process, it would be hard to imagine how such enhancement was possible. The recognition is triggered only when the correct sign lies in the string. Otherwise there is no distinct percept at all. Therefore, the information that such and such a letter lies in the string must still be available in what appears, without enhancement, as formless — the masked center of the string.

We have as yet no way of accounting for this phenomenon, but its very existence calls into question those mechanisms that have been proposed to explain lateral masking.

While lateral masking is a robust and stable interaction, unmasking (enhancement) is transient and fragile. We needed tachistoscopy to show the interplay. The fragility of enhancement can be illustrated by the effects on it of microtexture. By microtexture we mean that the quality of the sign is not uniform; i.e., instead of being unrelievably white against black or black against white with sharp boundaries in either case, it is comprised of an assembly of dots or stripes, or what have you, for which we read the envelope as being the sign. With signs of this sort, such as are had from a dot matrix or TV screen, not only is masking most effective, but enhancement is singularly weak if present at all. This should occasion no surprise, because envelopes (textural boundaries) are not treated the same as phase boundaries in early visual processing. (We had shown this in the receptive fields of frog optic nerve fibers (Lettvin et al., 1959). The ease of using computer displays as stimuli has, to some extent, suppressed such observations in mammals.) However, enhancement is undisturbed by macro-texture or embedding texture, e.g., a cloud of noise texture (like that of a noisy TV screen but expanded to where the black spots are the size of letters). This cloud is inserted between the fixation point and the eccentric 8° letter and extends from the fixation point to the letter.

There are also indications that, taking the fixation point as the center of the system, masking in the tangential direction differs from masking in the radial direction, with consequent changes in the enhancement.

The enhancing interaction described here occurs up to a 10°-12° distance in the visual field for most of our subjects and over a markedly larger field for a distinct subclass of them. But it occurs only with

complex signs such as block letters. It does not occur with simple signs such as bars. That the interaction is expressed in the recognition of the eccentric signs raises the question of how local processing, whether in primary or secondary cortex, can be so connected over large distances to permit it to work in such a way, under tachistoscopic presentation, as to prevent or break lateral masking.

There are, of course, methods of building filters to reveal on the instant all examples of a particular sign in some integral transform (e.g., a hologram) of a two-dimensional cloud of different signs. If such sophisticated processing must be invoked, it invites a rethinking of the nature of receptive fields, particularly those found in the cortex.

References

1. H. Bouma, Nature 226, 177–178 (1970).
2. W.K. Estes, Percept. & Psychophys. 12, 278–286 (1982).

27.5 Physical Reasons Behind Caisson Disease

Bell Laboratories, Inc.
Ortho Instruments
National Institutes of Health (Grant 5 TO1 EY00090)
Jerome Y. Lettvin, Edward R. Gruberg[23], Robert M. Rose[24], George M. Plotkin

Most guesses about why diving animals do not get the bends have focused on possible mechanisms for preventing nitrogen from dissolving in tissue under high pressure. Examples are: the forcing of inspired air from alveoli into bronchi and trachea whence negligible gas exchange occurs; the shunting of circulation away from sensitive tissues; etc. On the whole, these measures, used to the extent needed to account for the absence of bends, are so incompatible with active life as not to be plausible under any number of compensatory hypotheses.

Recent work by Ridgway and Howard [1] lays to rest any need for such nonce engines. In their study of dolphins diving to about 100 meters over and over again, the dissolved N_2 in the muscle tissue rose to three times the partial pressure found in dolphins that remained at the surface. Despite rapid ascents that would certainly have given the bends to a human diver, the dolphins seemed to be quite comfortable.

It is not likely that dolphins simply do not complain about their blood boiling; their blood cannot froth, since no mammal, man included, could survive frequent gas emboli in heart or brain.

---

[23]Temple University

[24]Department of Mechanical Engineering

Therefore, the findings of Ridgway and Howard indicate that attention be directed not at the prevention of supersaturation but rather at the absence of the formation of bubbles under supersaturated conditions. The basic phenomena are evident to the thoughtful drinker of beer: Bubbles occur at specific nucleation sites such as scratches on the glass container, or solid particles adherent to the container or inadvertently introduced into the beer itself. The effervescence can be substantially reduced or eliminated by the careful use of appropriate containers, e.g., a smooth, clean, fire-polished beaker. Observations on a glass of beer near a radioactive source led directly to the invention of the bubble chamber as an experimental tool for high-energy physics. Bubble formation is nucleated by the particles as they decay along their paths and nowhere else. Another important example is the formation of CO bubbles in molten steel, which is necessary in steelmaking, and which is induced by mechanisms that nucleate the melt.

Ebullition of dissolved gases in liquids can be adequately described by the classical theory of Volmer,[2] Weber,[3] Becker and Doring, [4] as corrected by Lothe and Pound.[5] The original theory was directed at the homogeneous nucleation of liquid drops from vapors, and later developed[6] to deal with heterogeneous nucleation and expanded to deal with solids and liquids. The nucleation of bubbles by solid substrates in superheated liquids have been considered by Frenkel[7] and Fisher.[8] In general, the nucleation rate should be proportional to the expression

$$(\Delta G^*)^{1/2}(1-\cos\theta^1)\exp(-\Delta G^*/KT) \tag{27.1}$$

where the activation energy G^* is given by

$$\Delta G^* = 16\,\pi\sigma^3\varphi(\theta^1)/3(P^*-P)^2 \tag{27.2}$$

and

$$\varphi(\theta^1) = \frac{(2+\cos\theta^1)(1-\cos\theta^1)^2}{4} \tag{27.3}$$

where σ is the surface energy, θ^1 is the complementary angle to the contact angle of the liquid to the substrate (i.e., π minus the contact angle), P is the imposed hydrostatic pressure and P^* is the partial pressure of the nitrogen gas inside the critical nucleus.

We suggest here that the difference in susceptibility between humans and, say, dolphins can be accounted for by the presence of more nucleation sites in humans and less chemical suppression of heterogeneous nucleation. With very few exceptions, heterogeneous nucleation is the rule in nature. Mammals provide numerous substrates for nucleation of nitrogen bubbles. For land mammals there are cartilaginous and calcific granules generated by the attrition of weight-bearing joints. There is a low but definite rate of lamellar fracture in cancellous centra of the vertebrae and the subchondral regions of the long bones. In most of us there are atheromatous plaques unevenly distributed in the

circulatory system which eventually calcify in arteriosclerosis. These "boiling chips" appear incipiently even in infants. There are huge numbers of other potential nucleation sites, e.g., calculi in gall bladder and urinary bladder; growths and scars on the edges of cardiac valves; etc. In fact, Eqs. (27-1) — (27-3) apply to flat substrates, and any re-entrant cavity will be a much more potent nucleation catalyst than a flat surface of the same tissue or material,[8] so that any surface with fine folds or convolutions, e.g., villi, will be an excellent heterogeneous nucleant. In essence, every belch and crepitation vouches for our intolerance, not for the deep so much as for any rapid translation from it.

If, then, dolphins are to tolerate high supersaturations of dissolved nitrogen gas without fizzing, two approaches are possible. One is the elimination of potential nucleation sites by achieving an internal smoothness of high order; that is to say, that the circulatory systems of diving animals such as whales, dolphins and seals are "fire-polished" by evolution. On the other hand, heterogeneous nucleation can be suppressed by chemical inhibitors which reduce the catalytic potency of the substrates. This point of view is suggested by the fact that many fish survive extended supercooling until they are scratched or otherwise nucleated, and only then will suddenly freeze. They possess a potent "anti-freeze", a glycoprotein, which clearly is not in sufficient concentration to depress the freezing point significantly and, therefore, must be a suppressor of heterogeneous nucleation. The same point has been made abundantly clear in the formation of kidney stones and bladder stones, where supersaturations are attained in the normal human kidney[9] only because heterogeneous nucleation has been suppressed. For the case of bubble formation, Eqs. (27-1) — (27-3) make it clear how such an inhibitor would work. A wetting agent would be highly effective, since complete wetting (or a zero contact angle) would take $\varphi(\theta)$[1] to unity and ΔG^* would be at its maximum value, i.e., the value appropriate to homogeneous nucleation of bubbles, and much higher supersaturations, up to those necessary for homogeneous nucleation, could be sustained. Alternatively, the number of nucleation sites may be so vastly increased in land-dwelling mammals that small quantities of nucleation suppressant may not suffice. In either case, it is possible to conceive of a chemical control for the "bends", if not on a chronic level at least for acute emergencies.

References

1. S.H. Ridgway and R. Howard, Science 206, 1182-1183 (1979).
2. M. Volmer, in Kinetic der Phasenbildung, Steinkopff, Dresden & Leipzig, 1939.
3. M. Volmer and A. Weber, Phys. Chem., 119, 277-301 (1926).
4. R. Becker and W. Doring, Ann. Physik. (5) 24, 719-752 (1935).
5. J. Lothe and G.M. Pound, J. Chem. Phys. 36, 2080-2085 (1962).
6. J.P. Hirth, Ann. N.Y. Acad. Sci. 101 805-815 (1963), review.
7. J. Frenkel, Kinetic Theory of Liquids, Oxford U. Press, London (1946).
8. J.C. Fisher, Appl. Phys. 19, 1062-1067 (1948).
9. Urolithiases: Physical Aspects, Nat'l. Acad. Sci. (1972).

27.6 Quantum Cryptography[25]

Ortho Instruments
Stephen J. Wiesner

A class of codes is made possibly by restrictions on measurement related to the uncertainty principal. Two concrete examples and some general results are given.

The uncertainty principle imposes restrictions on the capacity of certain types of communication channels. We will show that in compensation for this "quantum noise", quantum mechanics allows us novel forms of coding without analogue in communication channels adequately described by classical physics.

We will first give two concrete examples of conjugate coding and then proceed to a more abstract treatment.

Example One: A means for transmitting two messages, either, but not both of which, may be received.

The communication channel is a light pipe or guide down which polarized light is sent. Since the information will be conveyed by variations in the polarization, it is essential that the light, and that all polarizations of light, travel with the same velocity and attenuation.

The two messages are rendered into the form of two binary sequences. The transmitter then sends bursts of light at times that we will label T_1, T_2, etc. The amplitude of the bursts is adjusted so that it is unlikely that more than one photon from each burst will be detected at the receiving end of the light pipe.

Before emitting the ith burst (i = 1,2 ...), the transmitter chooses one of the two messages in a random manner by flipping a coin or selecting a bit from a table of random numbers. If the first message is chosen, the ith burst is polarized either vertically or horizontally depending on whether the ith digit of the first binary sequence is a zero or a one. If the second message is chosen, the ith burst is polarized in either the right or left-hand circular sense depending on whether the ith digit of the second message is a zero or a one, Fig. 27-2. The receiver contains a quarter-wave plate and birefringent crystal, or some other analyzer, that separates orthogonally polarized components of the light wave into spatially separate beams. Following this is a pair of the best available photomultiplier tubes. If the first message is to be received, the analyzer is arranged so as to send vertically polarized photons to one phototube and horizontally polarized photons to the other. If the second message is to be received, the separation is made with respect to right and left-hand circular polarization.

---

[25] As published in Association for Computing Machinery Special Interest Group on Automata and Computability Theory 15, 1, Spring 1983.

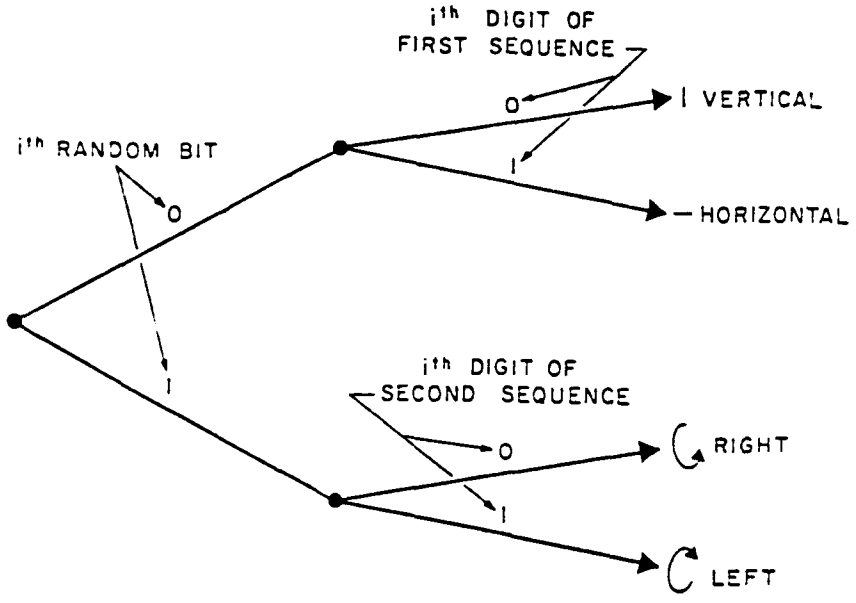

Figure 27-2: Polarization of the ith Burst

Now if the linear polarization of a photon is measured, all chance of measuring its circular polarization is lost. Thus, if the receiver is set to receive the first message, nothing at all is learned about the contents of the second message. Likewise, when the receiver is set to receive the second message, it destroys all information concerning the first message. If the receiver is set up to sort the photons with respect to some elliptical polarizations intermediate between linear and circular, less information about each message is recovered than when the receiver makes the best measurement for the reception of one message alone.

Of course, even when the receiver is set for the first message, a full knowledge of the first sequence is not recovered. In fact, half the digits of the first sequence never even influence the transmitted signal and at the corresponding times, when the second message is being transmitted, the receiver output has an equal probability of being a zero or a one. This noise introduced by the coding scheme, as well as the noise due to the channel, the photon shot noise, and the photomultiplier noise, may be overcome if an error-correcting code of the usual sort is used in forming the binary sequences from the original messages. Care must be taken, for too much redundancy would allow both messages to be recovered by the alternate reception of one sequence and then the other.

There is no way that the receiver can recover the complete contents of more than one of the conjugately coded messages so long as it is confined to making measurements on one burst of photons at a time. In principle, there exist very complicated measurements that allow recovery of all the transmitted information. To see this, consider the transmission of two messages of finite length. The transmitter will produce a signal consisting of a finite number of bursts of polarized light, and the entire signal may be described by a single vector ψ in a large Hilbert space spanned by all possible

finite transmissions. If one of the messages is changed, a state corresponding to a different vector ψ' is produced. The change from ψ to ψ' could be detected unambiguously by a receiver of the type previously described, if set to receive the message that was changed. For this to be possible, ψ must be orthogonal to ψ'. It follows that the set $\{\psi\}$ of the vectors corresponding to all possible pairs of finite messages is ortho-normal and, therefore, there exists an Hermetian operator or a set of commuting Hermetian operators corresponding to a measurement or measurements that can distinguish all the possible signals.

There is an easy extension to the case of three messages, no two of which may be recovered. One simply transmits a third binary sequence using light in the two polarization states at 45° to vertical and horizontal. Extension to more than three messages is not straightforward.

The above system for sending two mutually exlusive messages could be built at the present time. Though it is possible in principle to beat the system and recover both messages, to do so would require measurements that are completely beyond the reach of present-day technology. The system, therefore, works in practice but not in principle. The next example is in the opposite category; it is foolproof in principle, but it probably could not be built at the present time.

Example Two: Money that it is physically impossible to counterfeit.

A piece of quantum money will contain a number of isolated two-state physical systems such as, for example, isolated nuclei of spin 1/2. For each two-state system, let a and b represent a pair of ortho-normal base states and let $\alpha = 1/\sqrt{2}(a+b)$ and $\beta = 1/\sqrt{2}(a-b)$ represent another pair.

The two state systems must be well enough isolated from the rest of the universe so that if one of them is initially in the state a or α, there is little chance that a measurement made during the useful lifetime of the money will find it in the orthogonal states b or β, respectively. There is no device operating at present in which the "phase coherence" of a two-state system is preserved for longer than about a second; however, the continuing advance of cryogenic technique will surely change this.

Let us suppose, to be definite, that the money contains twenty isolated systems, S_i, $i = 1, 2, \ldots 20$. At the mint they create two random binary sequences of twenty digits each which we will call M_i and N_i, $i = 1,2, \ldots 20$, $M_i = 0$ or 1, $N_i = 0$ or 1. Then the two-state systems are placed in one of the four states a, b, α or β in accordance with the scheme shown in Fig. 27-3.

The money is also given a serial number which is printed on it in the usual way, and the two binary sequences describing its initial state are kept on record at the mint and perhaps at a number of branch banks.

When the money is returned to the mint, a check is made to see if each isolated system is still in its initial state, or whether it has switched to the orthogonal state.

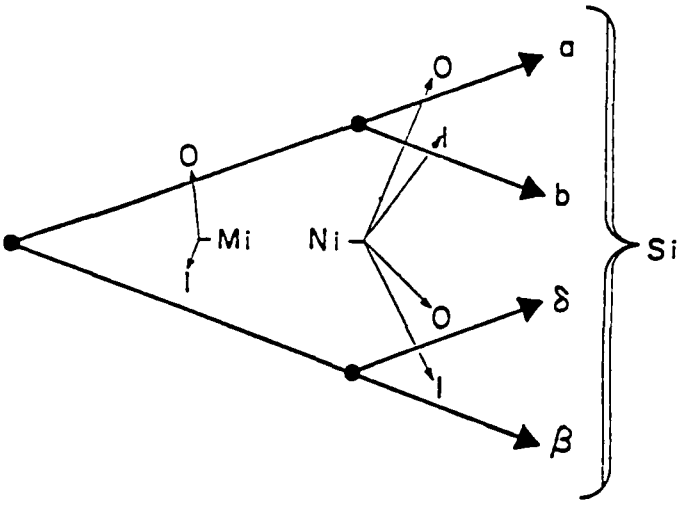

Figure 27-3

Now consider the problem of someone who would duplicate a piece of quantum money. He cannot recover N_i because, since he does not know M_i, he does not know what measurements to make on S_i. A measurement on a particular S_i that distinguishes a from b must necessarily destroy all chance of distinguishing α from β. Likewise, a measurement that distinguishes α from β destroys the chance of distinguishing a from b. Suppose a counterfeiter goes ahead anyway, makes some measurement on the S_i and produces money with the new S_i in the states found by his measurements. Then for each i, there is a 50% chance that he will make the wrong measurement, and in this event there is a 50% chance that a measurement at the mint will show S_i to be in the wrong state. Thus, there is a 1/4 chance of each digit being found wrong and the probability of the whole counterfeit coin passing inspection is only $(3/4)^{20} < 0.00317$.

Could there be some way of duplicating the money without learning the sequence N_i? No, because if one copy can be made (so that there are two pieces of the money), then many copies can be made by making copies of copies. Now given an unlimited supply of systems in the same state, that state can be determined. Thus, the sequence N_i could be recovered. But this is impossible.

Conjugate Bases

If the momentum of a particle is known, then nothing is known about its position; in other words, it is equally likely to be found in all regions possessing a fixed volume V. Likewise, if the position is known, then nothing is known about its momentum. The same relation holds between all pairs of conjugate variables, and this suggests an extension of the idea of conjugation from variables to basis sets.

Let $\{a_i\}$, $i = 1,2,\ldots N$ and $\{b_i\}$, $i = 1,\ldots N$

be two ortho-normal bases for an N dimensional Hilbert space. We call such a pair conjugate if and only if $|(a_i, b_j)|^2 = 1/N$ for all i and j[26]. Physically, if a system is in a state described by a_i, i = 1,... ,N, then it must have an equal probability of being found in any of the states b_i, i = 1,...,N and vice versa, if *it is in a state* b_i *it must have an equal probability to be found in any* a_j.

A collection of bases will be called conjugate if each pair of bases in the collection is conjugate. We can now present a definition.

A conjugate code is any communication scheme in which the physical systems used as signals are placed in states corresponding to elements of several conjugate basis of the Hilbert space describing the individual systems. Note that in the case where the sequence of signals has more than one element, the above definition does not require the vectors describing entire transmissions to be elements of conjugate base sets. This last condition was fulfilled in the second example but not in the first.

In addition to pairs of conjugate bases, there are triplets of conjugate bases. For example, in a two-dimensional system we have

$$\{a,\ b\} \qquad |a|^2=|b|^2=1 \quad (a,b)=0$$
$$\{1/\sqrt{2}(a+b),\ 1/\sqrt{2}(a-b)\}$$
$$\{1/\sqrt{2}(a+ib),\ 1/\sqrt{2}(a-ib)\}.$$

Three such bases were used in the scheme for sending three messages, no two of which can be received.

Are there sets bigger than triplets? The following theorem shows that there is no limit to the multiplicity of mutually conjugate basis sets.

Theorem: In an Hilbert space of dimension $2^{(N-1)!/2}$, there exists sets of N mutually conjugate basis sets. **Proof**: Suppose the theorem to be true for $N \leq M$. Let $\{A^\alpha\}$, $\alpha = 1...M$ be a set of mutually conjugate ortho-normal basis on an Hilbert space H of dem. $2^{(M-1)!/2} \equiv D$

$$A^\alpha\{a_i^\alpha\}\ i = 1 \ldots D$$

and

$$|(a_1^\alpha, a_j^\beta)|^2 = \frac{1}{D}$$

---

[26] (a_i, b_j) is the inner product $\langle a_i|b_j\rangle$ in the Dirac notation.

for all $\alpha \neq \beta$.

We can then construct M + 1 mutually conjugate bases on the space H ⊗ H ⊗ ... ⊗ H = H^M.[27] For the first M basis, we take a natural extension of the basis sets A^α. Call $A^{-\alpha}$ the basis set of H^M consisting of the vectors $a_1{}^\alpha \otimes a_j{}^\alpha \ldots \otimes a\ {}^\alpha$, i, j, ... D.

Note that is $\alpha \neq \beta$,

$$\left|(a_i{}^\alpha \otimes \ldots a\ {}^\alpha, a_m{}^\beta \otimes \ldots \otimes a_p{}^\beta)\right|^2 = \left|(a_i{}^\alpha, a_m{}^\beta)\right|^2 x \ldots x \left|(a\ {}^\alpha, a_p{}^\beta)\right|^2 = \left(\frac{1}{D}\right)^M$$

so these basis sets $\{A^{-\alpha}\}$ are mutually conjugate.

For the last basis, we take the vectors

$$V(q,\{P^\alpha\}) = \frac{1}{\sqrt{D}} \sum_{K=1}^{D} e^{2\pi i \frac{qK}{D}} x\, a_K{}^1 \otimes a^2_{p^2(K)} \ldots \otimes a^M_{p^M(K)}$$

here, q = 1 ... D and $\{P^\alpha\}$, α = 2, 3 ... M is a set of cyclic permutations on the integers 1 ... D, (i.e., $P^\alpha(n) = n + J_\alpha$ Mod(D) for some integer J_α.) Call this last basis V.

Since there are D cyclic permutations on D intergers, there are D^{M-1} sets $\{P^\alpha\}$ and $DxD^{M-1} = D^M$ vectors $V(q,\{P^\alpha\})$ in V; as there should be.

The proof that V is ortho–normal is obvious.

So, actually, is the proof that V is conjugate to the other basis sets, but I give it since it is the heart of the matter. Fix α and let $W \equiv a_i{}^\alpha \otimes \ldots \otimes a\ {}^\alpha$ be a typical vector of A_α. Then

$$\left|(W,V(q,\{P^\alpha\}))\right|^2 = \frac{1}{D}\left| \sum_{K=1}^{D} e^{2\pi i \frac{qK}{D}} \times \left(a_i{}^\alpha \otimes \ldots a\ {}^\alpha, a_K{}^1 \otimes \ldots a^M_{P^M(K)}\right)\right|^2$$

The inner product will be zero unless $a^\alpha_{P^\alpha(K)}$ equals the αth term of W. (Let P^1 be the identity.) This happens for just one value of K, call it k. Then $|(W,V(q,\{P^\alpha\}))|^2 = 1/D|(a_i{}^\alpha \otimes \ldots a\ {}^\alpha, a_k{}' \otimes \ldots a^M_{P^M(k)})|^2$
where the αth vector is the same on both sides of the inner product. As for the rest, $|(a_i{}^\alpha, a^\beta p^\beta{}_{(k)})|^2 = 1/D$

[27] ⊗ is the tensor product. H ⊗ H' is defined as the space of all linear functions from H into H'.

27.7 New Eye Testing Chart

Bell Laboratories, Inc.
Ortho Instruments
Bradford Howland, Antonio Medina-Puerta

Snellen optotypes have changed very little since this eye testing letter chart was introduced in 1862. Snellen letters achieved a wide and rapid success and they are now used all around the world in spite of being based in an arbitrary and inaccurate principle.

A novel eye testing chart has been developed consisting of letters (or figures) made of alternatively black and white stripes (or dots) on a gray background. Any cross section of any letter has a Fourier transform with a zero frequency component equal to the luminance of the gray background. When these letters are out of focus (or equivalently, low-pass filtered), the image of the letters on the retina rapidly fades into the gray background, rendering the letters invisible rather than simply blurred as in a standard chart.

We have optimized the operation of the chart as follows. When sharply imaged the letters are highly visible. Then, when the image is defocussed, the letters will disappear as completely as possible. Such operation would clearly permit the optometrist to separate the lines of large letters which are visible and the lines of smaller letters which cannot be seen.

Snellen's "optotypes", introduced in 1862, (Snellen, 1862) achieved a wide and rapid success. Most of the distance test charts today are modelled on Snellen's original chart. One of the disadvantages of eye testing charts using letters as test objects is the well known fact that different letters are not equally legible, (Sheard, 1921), (Le Grand and Guillemot, 1951), (Coates, 1935), (Lebensohn, 1965), (Popp, 1964). Furthermore, the relative legibilities of the various letters of the alphabet differ from one type style to another. Hence it is not surprising that the related questions of the style of type and the selection of letters to be employed have been the subject of much discussion. (See for example, Bennett, 1965).

The optotypes proposed in this paper are free from this limitation and they offer two additional properties. Firstly, the letters fade completely in the background when their retinal image is out of focus making them invisible rather than just blurred as in a standard chart. Secondly, the relation of the size of these new letters to the size of Snellen's letters for the same visual acuity is not a linear one. Instead we have found that a six-to-one size variation of the new letters is equivalent to a twenty-to-one size range of Snellen letters.

A. Description and Operation of the Chart

This chart uses letters of different size arranged in lines as in a standard chart. The letters are formed from a stripe of uniform width, having an odd number of black and white lines; the stripe is

symmetric. This is the type of letter used in our experiments, and we shall concentrate on this particular case although similar results should be achieved with a chart made with letters with a different number of elements or even with letters made of black dots on white. The condition required is that the Fourier transform of the light reflectance of a cross section of a stripe approaches zero as ω approaches zero. This way letters are mostly represented by high spatial frequencies. Since refractive errors produce an out-of-focus image on the retina, which is equivalent to a low-pass filtered image, the lack of low frequency components of our letters thus renders them invisible when out of focus.

Decomposing the cross section light reflectance function of a five-element stripe into three π functions plus a constant enables us to calculate the following Fourier transform:

$$F(\omega) = \frac{-\sin A\omega + \sin[(1-B)\omega] - G\sin\omega}{\omega/2} + G\,\delta(\omega) \qquad (27.4)$$

To make this function approach zero as ω tends to zero, we take the limit of $F(\omega) - G\,\delta(\omega)$ as ω tends to zero and set it equal to zero:

$$-A + (1-B) - G = 0$$
$$A + B = (1-G)$$

This equation determines the level of grey, given the width of the stripes.

The choices of A,B and hence G are determined by three additional considerations. First, we wish to minimize the values of $F(\omega)$ for small ω. Secondly, we wish to avoid very small values of A and B, since these would correspond to line widths too small to reproduce by the photographic process used to create the letters. Finally, we wish to find values of A and B closely approximated by simple fractions, so that the letter stripe can be easily specified.

Values of A, B and G meeting all these requirements were as follows: $A = 1/3$, $B = 2/9$ and $G = 5/9$. Thus, the letter stripe consists of black and white lines having relative widths of 1,2,3,2,1 units, and having a total width of 9 units.

An alternative to the above would be to directly synthesize a letter stroke which has zero response for a group of spatial frequencies. Thus, for example, we might choose a flat frequency spectrum for frequencies higher than a predetermined value and zero for the rest and transform back into the spatial structure of the cross section of the letter. This structure will not be a composition of π functions, and since it is difficult to create stripes with gradual shading, we have not presently used this approach.

The operation of our chart is quite different from that of the Snellen chart. Snellen letters or any black letters on a white background which are imaged out of focus became illegible because the blurred letter does not resemble the sharp letter any more. Our letters in no way become illegible, but

they become invisible, as defocus progresses, much earlier than illegibility is possible. Fig. 27–4 illustrates this.

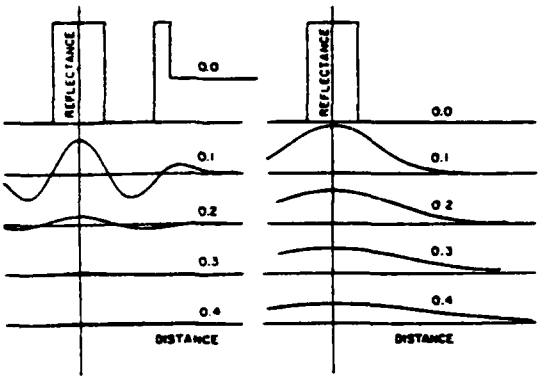

Figure 27-4: Result of Gaussian filter acting on single element and five–element letter stripes, with identical degrees of blur. The vertical line marks the center of the stripe

If we characterize the eye as a Gaussian low–pass filter, the curves on the right side of Fig. 27–4 represent the filtered image (in magnitude) on the retina of a single line for an increasingly narrow band of the filter. The curves on the left side show the image of a five–element stripe equivalently filtered. It is evident from the figure that the five–element stripe cross section becomes undetectable much faster than a single line.

B. Test of Operation with Subjects

Four subjects looked at the charts from a distance of 20 feet wearing different plus lenses on one eye (therefore converted to artificial myopes); the other eye was occluded. They were asked to read the lines in both charts. For each lens the line of smallest letters readable in both charts by the subject was recorded. This way lines of equal visibility were matched for every subject and later the values were averaged and plotted in Fig. 27–5. This figure shows the visual acuity necessary to read the letters of a determined height for the high frequency letters and for the Snellen letters. It is obvious from the plot that the new letters perform in a non–linear fashion, this means that there is no constant ratio between the size of the Snellen letters and the size of the high frequency letters for equal visibility. This result is a consequence of the peculiar spectra of the new letters and will be discussed further below.

This experiment, however, enables us tentatively to calibrate the new chart in the same way as the standard chart.

C. Discussions and Conclusions

To understand the results of comparative visibility tests of the Snellen and the new letters it is necessary to appreciate the differences in the operation of the letters. When the Snellen letters are rendered progressively more blurred, they gradually become unrecognizable as the blurred shapes of

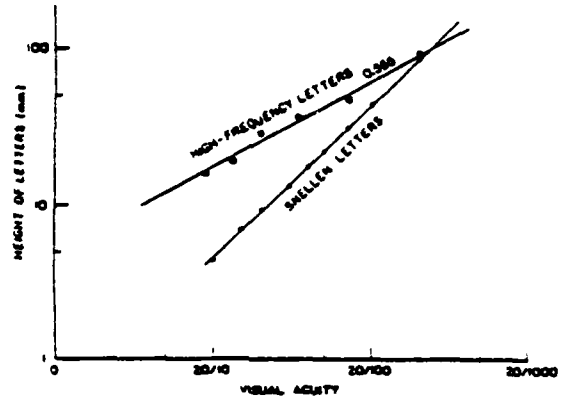

Figure 27-5: Plot of size of Snellen letters and the new letters as a function of visual acuity of subject

different letters become indistinguishable from one another. Even when the letter cannot be recognized, it is still present as a black blurred figure. With the new letters, the defocus acts to filter out the predominant frequency components of the stripe pattern, so as to render the image of the stripe indistinguishable from the surrounding grey area, i.e., the stripe is now invisible.

If one measures the predominant frequency component of the largest and the smallest of the new letters, corresponding to 20/200 and 20/10 vision, one finds spatial frequencies of 11 and 66 cycles/degree. It is known from the work of Fergus Campbell and associates (Campbell, 1968) that the eye's sensitivity to sine-wave gratings, i.e., its contrast sensitivity function varies markedly with spatial frequency, reaching a peak sensitivity at approximately 5 cycles/degree, and falling off rapidly for higher frequencies.

Thus, the smallest of our new letters, corresponding to 20/10 vision, and having 66 cycles/degree can withstand very little low-pass filtering before the predominate frequency component falls below the threshold of detectability of the retina. This, we believe, is the explanation as to why the sizes of the new letters are not proportional to the sizes of the Snellen letters of comparable visibility. Further work will be necessary to verify this hypothesis.

Although we have calibrated our new chart in the same way as the Snellen chart is calibrated, it should be noted that they do not measure exactly the same thing. The Snellen chart measures the highest frequency that the visual system is capable of detecting under the assumption that the transfer function of the subject's visual system is a "normal" transfer function, this is, the sensitivity to high frequencies progressively decreases. The Snellen chart cannot provide any additional information about the transfer function or contrast sensitivity function of the eye (Ginsburg, 1980). The new chart is made of letters of a narrow spatial frequency spectrum and, therefore, each line can be used to measure roughly the sensitivity of the human eye to that spatial frequency. Suppose, for example, that a subject could read lines 2 and 4, but not line 3 on the chart. It would suggest that his

contrast sensitivity function had a notch at that spatial frequency. Some pathological conditions of the eye have this peculiar characteristic (Walkstein et al., 1977, Regan et al., 1977), although Snellen acuity in these cases may be normal.

References

1. A.G. Bennett, British Journal of Physiological Optics 22, 238 (1965).
2. F.W. Campbell and J.G. Robson, "Applications of Fourier Analysis to the Visibility of Gratings," J. Physiol. 197, 551 (1968).
3. W.R. Coates, "Visual Acuity and Test Letters." Trans. Institute of Ophthalmic Opticians III, (1935).
4. A.P. Ginsburg, "Specifying Relevant Spatial Information for Image Evaluation of How We See Certain Objects," Proc. S.I.D 21, 3 (1980).
5. J.E. Lebensohn, "Visual Charts: Refraction," I.O.C. 5, 2 (1965).
6. Y. LeGrand and E. Guillemot, "Measurement of Visual Acuity with Blurred Tests," in Opt. Devel. 21, 2 (1951).
7. H.M. Popp, "Visual Discrimination of Alphabet Letters," Reading Teacher, January 1964.
8. C. Sheard, "Some Factors Affecting Visual Acuity," Am. J. Physiol. Opt. 2, (1968).
9. H. Snellen, "Letterproeven tot Bepaling der Gezigtsscherpte," P.W. van der Weijer, Utrecht, (1862).
10. D. Regan, R. Silver and T.J. Murray, "Visual Acuity and Contrast Sensitivity in Multiple Sclerosis: Hidden Visual Loss," Brain 100, 563 (1977).
11. M. Walkstein, A. Atkin and I. Bodis-Wollner, "Grating Acuity in Two Sites with Tapetoretinal Degeneration," Doc. Ophthal. 12, 45 (1977).

28. Publications and Reports

28.1 Meeting Papers Presented

10th Conference on Numerical Simulation in Plasma, San Diego, California
January 4–6, 1983

R.H. Berman, Symbolic Computation in Plasma Physics (invited paper)

R.H. Berman, D.J. Tetreault, and T.H. Dupree, Observation of Turbulent Self-binding Fluctuations in Simulation Plasma

National Radio Science Meeting, University of Colorado, Boulder, Colorado
January 5–7, 1983

Abstracts in Proceedings

J.A. Kong, S.L. Lin, S.L. Chuang, and R.T. Shin, Remote Sensing of Soil Moisture and Vegetation (p. 213)

R.T. Shin and J.A. Kong, Thermal Microwave Emission from a Scattering Medium with Rough Surfaces (p. 171)

161st Meeting, American Astronomical Society, Boston, Massachusetts,
January 9–12, 1983

Abstracts in Bull. Am. Astron. Soc. 14:4 (1982)

J.W. Dreher and C.R. Lawrence, Hot Spots in Extragalactic Radio Sources (p. 963)

D.H. Roberts, P.E. Greenfield, B.F. Burke, J.N. Hewitt, and A.K. Dupree, Recent VLA Observations of the Double Quasar 0957 + 561 (p. 974)

M. Shao, M. Colavita, P. Garnavich, D. Staelin, and S. Knowles, NRL–MIT Astrometric Interferometer (p. 884)

Winter '83 Meeting on "Optical Techniques for Remote Probing of the Atmosphere," Incline Village, Nevada
January 10–12, 1983

Papers in Technical Digest

Y.Q. Jin and J.A. Kong, Mie Scattering of Electromagnetic Waves by Precipitation (pp. MC2-1 – MC2-4)

Topical Meeting on Signal Recovery and Synthesis with Incomplete Information and Partial Constraints, Optical Society of America, Incline Village, Nevada
January 12–14, 1983

Papers in Digest of Technical Papers

A.V. Oppenheim and J.S. Lim, Signal Reconstruction from Partial Fourier Domain Information (pp. ThA12:1–ThA12:4)

T.F. Quatieri, S.H. Nawab, and J.S. Lim, Frequency Sampling of the Short-Time Fourier Transform Magnitude (pp. ThA9:1–ThA9:4)

P.L. Van Hove, J.S. Lim, and A.V. Oppenheim, Signal Reconstruction from Fourier Transform Amplitude (pp. ThA15:1–ThA15:4)

Sixth Midwinter Research Meeting of the Association for Research in Otolaryngology, St. Petersburgh, Florida
January 23–27, 1983

Abstracts in Proceedings

J.J. Rosowski and W.T. Peake, From the Ear Canal of the Alligator Lizard: Evidence for Multiple Inner-Ear Sources of Mechanical Non-Linearity (p. 101)

Fifth Topical Conference on RF Plasma Heating, University of Wisconsin, Madison, Wisconsin
February 21–13, 1983

Papers in Proceedings

P.T. Bonoli, R.C. Englade, and M. Porkolab, A Computational Model for Lower-Hybrid Current Drive (pp. 72–75)

V. Fuchs, V. Krapchev, and A. Bers, Stochasticity Induced by Coherent Wavepackets (pp. 156–159)

K. Hizanidis, V. Krapchev, A. Ram, and A. Bers, Relativistic Two-Dimensional Theory of RF Current Drive (pp. 160–163)

S.C. Luckhardt, S.F. Knowlton, K.I. Chen, M.J. Mayberry, S. McDermott, M. Porkolab, and R. Rohatgi, Lower-Hybrid Current Drive and Heating Experiments on the Versator II Tokamak (pp. 76–79)

M. Porkolab, J.J. Schuss, B. Lloyd, Y. Takase, S. Texter, R. Watterson, P. Bonoli, R. Englade, C. Fiore, R. Gandy, R. Granetz, M. Greenwald, D. Gwinn, B. Lipschultz, E. Marmar, S. McCool, D. Pappas, R. Parker, P. Pribyl, J. Rice, J. Terry, S. Wolfe, R. Slusher, and C.M. Surko, Lower Hybrid Current Drive and Heating Experiments up to the 1 MW Level in Alcator C (pp. 88–95)

A. Ram and A. Bers, Antenna–Plasma Coupling Theory for ICRF Heating (pp. 300–303)

R.L. Watterson, Y. Takase, M. Porkolab, J.J. Schuss, R.E. Slusher, and C.M. Surko, Study of Lower Hybrid Waves in Alcator C Using CO_2 Laser Scattering (pp. 80–83)

Workshop on "New Directions in Phase-Conjugate Nonlinear Optics," Los Alamos, New Mexico
February 22–24, 1983

J. Shapiro, Mysteries and Applications of Two-Photon Coherent States

1983 IEEE Workshop on Automatic Test Program Generation, San Francisco, California
March 15–16, 1983

G. Kramer, Test Generation Algorithms

1983 Sherwood Meeting, Arlington, Virginia
March 21–23, 1983

Abstracts in Proceedings

P.T. Bonoli, L. Sugiyama, and R.C. Englade, Lower Hybrid Heating in the Ignitor Device (p. 3P13)

B. Coppi, F. Pegoraro, and J.J. Ramos, Instability of Fusing Plasmas and Relevant Spin-Depolarization Process (p. 2C2)

G.B. Crew, B. Coppi, J. Martinelli, and J.J. Ramos, Collisionless Internal Kink Modes (p. 1P17)

R. Englade and P. Bonoli, Simulations of the Density, Phase and Toroidal Field Dependence of Lower Hybrid Current Drive (p. 1S1)

V. Fuchs, V. Krapchev, A. Ram, and A. Bers, Scattering and Stochasticity of Electron Interacting with Coherent Wavepackets

D.W. Hewett, V. Krapchev, J.P. Freidberg, and A. Bers, Fokker–Plank Investigations of rf Current Drive (p. 1P10)

K. Hizanidis, V. Krapchev, and A. Bers, Relativistic 2-Dimensional Theory of Lower-Hybrid Current Drive (p. 2Q3)

D. Humphreys and L. Sugiyama, Determination of a Value for the Anomalous Electron Thermal Conductivity (p. 1S26)

M. Mars, P.T. Bonoli, B. Coppi, and R.C. Englade, Degradation of Electron Energy Confinement Properties in the Presence of Auxiliary Heating (p. 1S11)

A. Ram and A. Bers, Relativistic Evolution of Electromagnetic Instabilities (p. 2Q24)

L. Sugiyama, Current and Particle Density Effects on Ignition in the Presence of Sawteeth (p. 2P16)

G. Vlad and B. Coppi, Finding of a "Bremsstrahlung Cortex" in Advanced Fuel Burning Plasmas (p. 1R9)

1983 March Meeting, American Physical Society, Los Angeles, California
March 21–25, 1983

Abstracts in Bull. Am. Phys. Soc. 28:3 (1983)

A. Erbil, R. Kortan, M.S. Dresselhaus, and R.J. Birgeneau, Two-Dimensional Phase-Transitions in Bromine Intercalated Graphite (p. 264)

J. Ihm, D.H. Lee, J.D. Joannopoulos, and A.N. Berker, Structure and Phase Transition of the Reconstructed Si(100) Surface (p. 416)

C. Jagannath and D.M. Larsen, Four-Wave Piezospectroscopy of the Ground-State of Donors in Silicon (p. 534)

R.F. Kwasnick, M.A. Kastner, and J. Melngailis, Electronic Conduction in Ultra-Narrow Silicon Inversion Layers (p. 322)

B.D. Larson, L.J. Yu, and J.D. Litster, Reorientational Behavior of Micelles in a Lyotropic *Liquid Crystal via Picosecond Absorption Spectroscopy of Probe* Dye Molecules (p. 332)

G. Timp, A.R. Kortan, L. Salamanca-Riba, R.J. Birgeneau, and M.S. Dresselhaus, High Resolution Diffraction Experiments on Graphite Potassium Amalgam (p. 347)

SPIE's Technical Symposium East '83, Arlington, Virginia
April 4–8, 1983

Papers in SPIE

D.M. Papurt, J.H. Shapiro, and S.T. Lau, Measured Turbulence and Speckle Effects in Laser Radar Target Returns (Vol. 415, pp. 166–178)

J.H. Shapiro, Random-Medium Propagation Theory Applied to Communication and Radar System Analyses (Vol. 410, pp. 98–102)

IEEE International Conference on Acoustics, Speech and Signal Processing, Boston, *Massachusetts*
April 14–16, 1983

Papers in ICASSP '83

M.A. Bush, G.E. Kopec, and V.W. Zue, Selecting Acoustic Features for Stop Consonant Identification (paper 16.8, pp. 742–745)

M.A. Clements, L.D. Braida, and N.I. Durlach, Speech Processing for Artificial Tactile Speech Displays (paper 28.13, pp. 1376–1379)

W. Dove, C. Myers, A. Oppenheim, R. Davis, and G. Kopec, Knowledge Based Pitch Detection (paper 28.6, pp.1348–1351)

C. Esmersoy and J.S. Lim, Subjective Evaluation of a PCM Speech Coding System with Quantization Noise Reduction (paper 24.6, pp. 1137–1140)

D.W. Griffin and J.S. Lim, Signal Estimation from Modified Short-Time Fourier Transform (paper 17.8, pp. 804–807)

J.S. Lim and F.U. Dowla, Improved Maximum Likelihood Method for a Two-Dimensional Spectral Estimation (paper 18B.3, pp. 851–854)

E.E. Milios and A.V. Oppenheim, The Phase-only Version of the LPC Residual in Speech Coding (paper 17.6, pp. 797–799)

B.R. Musicus, Iterative Algorithms for Optimal Signal Reconstruction and Parameter Identification Given Noisy and Incomplete Data (paper 6.1, pp. 235–238)

S.H. Nawab, T.F. Quatieri, and J.S. Lim, Algorithms for Signal Reconstruction from Short-Time Fourier Transform Magnitude (paper 17.7, pp. 800–803)

H.C. Reeve III and J.S. Lim, Reduction of Blocking Effect in Image Coding (paper 26A.1, pp. 1212–1215)

CANDE Workshop, Mescalera, New Mexico
April 17–22, 1983

L. Seiler and J. Allen, Special Hardware for Design Rule Checking

Department of Electrical Engineering Seminar, University of Maryland, College Park, Maryland
April 18, 1983

R.E. Shefer, Coherent Millimeter Wave Generation at M.I.T. (invited paper)

1983 Spring Meeting, American Physical Society, Baltimore, Maryland
April 18–21, 1983

Abstracts in Bull. Am. Phys. Soc. 28:4 (1983)

D. Kleppner, Spin Polarized Hydrogen for Polarized Source and Targets (p. 664)

Nineteenth Regional Meeting, Chicago Linguistic Society, Chicago, Illinois
April 21–22, 1983

in A. Chukerman, M. Marks, and J. F. Richardson (Eds.), CLS 19

K.L. Landhal and E.M. Maxwell, The /b/-/w/ Contrast and Considerations of Syllable Duration (pp. 234–243)

Electrochemical Society Symposium on III–V Opto-Electronics Epitaxy and Device-Related Processes, San Francisco, California
May 8–13, 1983

C.J. Keavney, H.A. Atwater, H.I. Smith, and M.W. Geis, Zone Melting Recrystallization of InSb on Oxidized Silicon Wafers

105th Meeting, Acoustical Society of America, Cincinnati, Ohio
May 9–13, 1983

Abstracts in J. Acoust. Soc. Am. Vol. 73, Suppl. No. 1, Spring 1983

H.S. Colburn, P.M. Zurek, and N.I. Durlach, Directional Hearing in Relation to Hearing Impairments and Aids (p. S17)

C.L. Farrar, C.M. Reed, N.I. Durlach, L.D. Braida, and P.M. Zurek, Spectral-Shape Discrimination of Synthetic Plosive Bursts (p. S93)

M. Furst, W.M. Rabinowitz, and P. Zurek, Combination-Tone Cancellation Phase: Comparison of Psychophysical and Ear-Canal Measurements (p. S78)

R. Goldhor, The Representation of Speech Signals in a Model of the Peripheral Auditory System (p. S4)

S. Hawkins and K.N. Stevens, A Cross-Language Study of the Perception of Nasal Vowels (p. S54)

H. Kawasaki, Fundamental Frequency Perturbation Caused by Voiced and Voiceless Stops in Japanese (p. S88)

D. Klatt, Timing Rules in Klattalk: Implications for Models of Speech Production (p. S66)

E.M. Maxwell and K.L. Landahl, The b/w Contrast and Considerations of Syllable Duration (p. S53)

P.J. Price and H.J. Simon, Age as a Factor in the Perception of Temporal Information in Speech (p. S103)

C.M. Reed, W.M. Rabinowitz, N.I. Durlach, and L.D. Braida, Research on the Tadoma Method of Speech Communication (p. S26)

P.M. Zurek, Conductive Hearing Loss and Interaural Discrimination Under Headphones (p. S77)

P.M. Zurek, N.I. Durlach, H.S. Colburn, and K.J. Gabriel, Masker Bandwidth and the MLD (p. S77)

49th Statistical Mechanics Meeting, Rutgers University, New Brunswick, New Jersey
May 12–13, 1983

R.E. Goldstein, Molecular Structure and Hydrogen Bonding at Lower Critical Solution Points

Conference on Lasers and Electro-Optics — CLEO '83, Baltimore, Maryland
May 17–20, 1983

R.S. Putnam, M.M. Salour, and T.C. Harman, Optically Pumped Mode-Locked LPE-Grown HgCdTe Lasers

IEEE 1983 Custom Integrated Circuits Conference, Rochester, New York
May 23–25, 1983

Papers in Proceedings

J. Allen, The Design of Custom Integrated Circuits for Signal Processing (pp. 364–368)

1983 IEEE International Conference on Plasma Science, San Diego, California
May 23–25, 1983

Abstracts in Conference Record

D.D. Hinshelwood, The Effect of Cathode Surface Impurities on Gap Closure (p. 125)

M.J. Mayberry, K-I. Chen, S.F. Knowlton, S.C. Luckhardt, F.S. McDermott, M. Porkolab, and R. Rohatgi, Soft and Hard X-ray Spectroscopy Radial Profile Measurements During Lower-Hybrid Current Drive and Heating Experiments on the Versator II Tokamak (p. 97)

J.J. Schuss, B. Lloyd, M. Porkolab, Y. Takase, S. Texter, R. Watterson, P. Bonoli, R. Englade, C. Fiore, R. Gandy, R. Granetz, M. Greenwald, D. Gwinn, B. Lipschultz, E. Marmar, S. McCool, D. Pappas, R. Parker, P. Pribyl, J. Rice, J. Terry, and S. Wolfe, Low Hybrid Current Drive and Heating Experiments at High Plasma Densities on Alcator C (p. 3)

R.E. Shefer, B.D. Nevins, and G. Bekefi, Experimental Results from a Rippled Field Magnetron (Cross-Field FEL) (p. 102)

R.E. Shefer, Y.Z. Yin, and G. Bekefi, Discrete Measurements of the Drift Velocity on Intense Relativistic Electron Beam (p. 102)

M. Shoucri, V. Krapchev, and A. Bers, A SADI Numerical Scheme for the Solution of the 2-D Fokker-Planck Equation (p. 67)

S. Texter, J. Rice, B. Lloyd, M. Porkolab, and J. Schuss, Measurement of X-ray Spectra During Lower Hybrid Current Drive Experiments on the Alcator C Tokamak (p. 97)

Y.Z. Yin and G. Bekefi, Dispersion Characteristics of an FEL with a Linearly Polarized Wiggler and Axial Guide Field (p. 28)

U.R.S.I. National Radio Science Meeting, University of Houston, Houston, Texas
May 23–26, 1983

Abstracts in Proceedings

L. Tsang and J.A. Kong, Scattering of Electromagnetic Waves from a Half-Space of Densely Distributed Dielectric Scatterers (p. 133)

IEEE Computer Society Trends and Applications Conference, Gaithersburg, Maryland
May 25–26, 1983

Papers in Proceedings

V.W. Zue and D.P. Huttenlocher, Computer Recognition of Isolated Words from Large Vocabularies (pp. 121–125)

IEEE Mini-Course "RF Heating and Current Drive in Magnetic Fusion Plasmas," San Diego, California
May 25–27, 1983

A. Bers, Interactions of Electromagnetic Waves with Magnetized Plasmas

1983 International Symposium on Electron, Ion, and Photon Beams, Los Angeles, California
May 31 – June 3, 1983

Papers in Proceedings

E.H. Anderson and H.I. Smith, TEM Analysis of Vertical-Slab Cross Section of Submicrometer Structures

A.M. Hawryluk, H.I. Smith, and D.J. Ehrlich, Deep UV Spatial-Period-Division by Combining Multilayer Mirrors with Diffraction Gratings

H.J. Lezec, E.H. Anderson, and H.I. Smith, An Improved Technique for Resist-Profile Control in Holographic Lithography

M.L. Schattenburg, C.L. Canizares, H.I. Smith, and A.M. Hawryluk, Submicrometer-Period Transmission Diffraction Gratings for X-Ray Astronomy

A.C. Warren, D.A. Antoniadis, J. Melngailis, and H.I. Smith, Submicrometer-Period Channel

Modulation of a MOSFET

Low-Hybrid Group Seminar, Princeton Plasma Physics Laboratory, Princeton, New Jersey

June 1, 1983

S.C. Luckhardt, Partial Confinement Measurements During Low-Hybrid Current Drive (invited paper)

Ninth Conference on Aerospace and Aeronautical Meteorology, Omaha, Nebraska
June 6-9, 1983

Papers in Preprint Volume of Extended Abstracts

D.H. Staelin, Atmospheric Temperature Sounding from Space (pp. 191-193)

Army Snow Meeting Workshop, Boulder, Colorado
June 7-8, 1983

J. Kong, Theoretical Models for Remote Sensing of Earth Terrain

Fifth Rochester Conference on Coherence and Quantum Optics, University of Rochester, Rochester, New York
June 13-15, 1983

Papers in Coherence and Quantum Optics V (Plenum Press)

R.S. Bondurant, M. Maeda, P. Kumar, and J.H. Shapiro, Pump and Loss Effects on Degenerate Four-Wave Mixing Quantum Statistics (pp. 767-774)

R.S. Bondurant and J.H. Shapiro, Squeezed States in Phase-Sensing Interferometers (pp. 629-636)

P. Kumar, R.S. Bondurant, J.H. Shapiro, and M.M. Salour, Quantum Noise Measurements in Degenerate Four-Wave Mixing (pp. 43-50)

***Seminar on Electrooptical Engineering*, National Chiao Tung University, Taiwan, Republic of China**
June 20, 1983

H.A. Haus, Optical Waveguide Structures for Picosecond Signal Processing (invited paper)

Gordon Conference on Plasma Physics, New London, New Hampshire
June 20-24, 1983

J.J. Ramos, Second Region of Stability of Kink and Ballooning Modes

Symposium for Senior Executives "Global Technological Change: A Strategic Assessment," Massachusetts Institute of Technology, Cambridge, Massachusetts
June 21–23, 1983

Papers in Proceedings

J. Allen, New Perspectives in Electronics Technology (pp. 61–85)

VLSI Workshop, Saratoga Spring, New York
June 23–25, 1983

J. Allen, Computer-Aided Design of Integrated Circuits for Digital Signal Processing

Electronic Materials Conference, Burlington, Vermont
June 23–25, 1983

H.A. Atwater, C.V. Thompson, H.I. Smith, and M.W. Geis, Orientation Filtering by Growth Velocity Competition in Zone-Melting Recrystallization of Si on SiO_2

IOOC '83 – Fourth International Conference on Integrated Optics and Optical Fiber Communication, Tokyo, Japan
June 27–30, 1983

Papers in Technical Digest

H.A. Haus and M. Kuznetsov, Radiation Loss of Coupled Waveguide Structures (pp. 360–361)

R.H. Rediker, T.A. Lind, and F.J. Leonberger, Integrated Optics Wavefront Measurement Sensor (pp. 248–249)

IUTAM–IUPAP Symposium on "Mechanical Behavior of Electromagnetic Solid Continua," Paris, France
July 4–7, 1983

Papers in G.A. Maugin (Ed.), The Mechanical Behavior of Electromagnetic Solid Continua (Elsevier Science Publishers, Amsterdam, The Netherlands, 1984)

F.R. Morgenthaler, On the Electrodynamics of a Deformable Ferromagnet Undergoing Magnetic Resonance (pp. 287–292)

Symposium: "Process for the Phonetic Coding and Decoding of Speech," Toulouse, France
July 15–16, 1983

Papers in Speech Communication — Special Issue, July 1983

K. Stevens, Invariant Acoustic Correlates of Distinctive Features: A Review of Some Evidence

V.W. Zue, The Use of Phonetic Rules in Automatic Speech Recognition (invited paper) (pp. 181–186)

11th International Congress of Acoustics, Paris, France
July 19–27, 1983

Papers in Proceedings

C. Shadle, Turbulence Noise in the Vocal Tract (pp. 171–174)

V.W. Zue, The Use of Phonetic Rules in Automatic Speech Recognition

Tenth International Congress or Phonetic Sciences, Utrecht, The Netherlands
August 1–6, 1983

Papers and Abstracts in Proceedings

J. Allen, Units for Speech Synthesis (pp. 107–111)

C.A. Bickley, Acoustic Evidence for Phonological Development of Vowels in Young Children (p. 624)

C.Y. Espy, Coarticulatory Effects Between /1/ and /r/ Allophones and Adjacent Vowels (p. 467)

S. Hawkins and K.N. Stevens, Perceptual Correlates of the Feature Nasal for Vowels (p. 510)

E. Holmberg, R. Hillman, and J. Perkell, Relationship Among Indirect Measurements of Glottal Resistance and Vocal Efficiency and Derived Glottal Waveform Characteristics for Normal Speakers (p. 445)

D.H. Klatt, The Problem of Variability in Speech Recognition and in Models of Speech Perception (pp. 287–298)

J. Perkell, Individual and Possible Language-Related Differences in Two Aspects of Coarticulation: Time Beginning of Anticipation and the Production of "Troughs" (p. 474)

P.J. Price, Voice Quality and the Glottal Waveform: Analysis and Synthesis (p. 413)

S. Shattuck-Hufnagel, Evidence for a Speech Production Planning Model from Spontaneous and Elicited Speech Errors (p. 792)

V.W. Zue, Proposal for an Isolated-Word Recognition System Based on Phonetic Knowledge and Structural Constraints (pp. 299–305)

Gordon Research Conference on Implantable Auditory Prostheses, Tilton, New Hampshire

August 21–26, 1983

W.M. Rabinowitz, Selection of Speech Intelligibility Test Materials and Artificial Speech Codes for Consideration with Cochlear Implants

American Association for Artificial Intelligence Annual Conference, Washington, D.C.
August 22–26, 1983

D.P. Huttenlocher, Phonotactic and Lexical Constraints in Speech Recognition

1983 IEEE Workshop on Digital Signal Processing, L'Aquila, Italy
September 6–8, 1983

J. Allen, The Impact of Parallelism on Hardware and Software

J. Allen, Software Engineering

A.V. Oppenheim, J.S. Lim, and S.R. Curtis, Signal Reconstruction from Partial Fourier Domain Information

Fifth International Topical Conference on High-Power Electron and Ion-Beam Research and Technology, San Francisco, California
September 12–14, 1983

D.A. Kirkpatrick, R.E. Shefer, Y.Z. Yin, and G. Bekefi, Energy and Velocity Diagnostics for Intense Relativistic Electron Beams

R.E. Shefer, G. Bekefi, R.D. Estes, C-L. Chang, E. Ott, T.M. Antonsen, and A.T. Drobot, Experimental and Theoreticl Results from a Rippled Field Magnetron (Cross-Field FEL)

VII International Conference on Crystal Growth, Stuttgart, Federal Republic of Germany
September 12–16, 1983

C.V. Thompson and H.I. Smith, Silicon-on-Insulator by Surface-Energy-Driven Secondary Recrystallization with Patterning

Symposium on X-Ray Microscopy, Gottingen, Federal Republic of Germany
September 14–16, 1983

Papers in G. Schnahl and D. Rudolph (Eds.), X-Ray Microscopy — Springer Series in Optical Sciences Vol. 43 (Springer-Verlag, Heidelberg, 1984)

H.I. Smith, E.H. Anderson, A.M. Hawryluk. and M.L. Schattenburg, Planar Techniques for Fabricating X-Ray Diffraction Gratings and Zone Plates (pp. 51–61)

IEEE International Symposium on Information Theory, St. Jovite, Quebec, Canada
September 26–30, 1983

Abstracts in Abstracts of Papers

J.H. Shapiro, Near-Optimum Receiver Realizations for Binary Two-Photon Coherent State Signals (p. 52)

1983 IEEE SOS/SOI Technology Workshop, Jackson Hole, Wyoming
October 4–6, 1983

C.V. Thompson and H.I. Smith, Silicon-on-Insulator by Surface-Energy-Driven Secondary Recrystallization in Ultra-Thin Films

Segundo Symposium de Ingenieria Biomedica, Madrid, Spain
October 5–7, 1983

Papers in Proceedings

B. Howland and A. Medina, A Novel Eye Testing Chart

Third Lerchendahl Conference on Systems Science, Technical University of Norway, Trondheim, Norway
October 10–12, 1983

M.A. Jenkins, The Role of Equations in Nial

3rd IEEE ASSP Workshop on Multi-Dimensional Digital Signal Processing, Lake Tahoe, California
October 19–21, 1983

F.U. Dowla and J.S. Lim, Relationship Between Autoregressive Signal Modeling and Maximum Likelihood Method for Spectral Estimation

1983 IEEE International Symposium on Ultrasonics, Atlanta, Georgia
October 31–November 2, 1983

D-P. Chen, A Variational Method for Estimation of the SAW Electromechanical Coupling Coefficient

E.M. Garber and H.A. Haus, Synthesis of High Performance Compact Saw Filters with Nonuniformly Spaced Fingers

N.A. Whitaker, Jr. and H.A. Haus, Backward Wave Effects in Acoustic Scattering Measurements

1983 IEEE International Conference on Computer Design/VLSI in Computers, Port Chester, New York
October 31–November 3, 1983

Papers in Proceedings

J.L. Wyatt, Jr., C. Zukowski, L.A. Glasser, P. Bassett, and P. Penfield, Jr., The Waveform Bounding Approach to Timing Analysis of Digital MOS IC's (pp. 392–395)

1983 Meeting, IRIS Specialty Group on Active Systems, Naval Postgraduate School, Monterey, California
November 1–3, 1983

J.H. Shapiro and P.L. Mesite, Performance Analyses for Doppler and Chirped Laser Radars

25th Annual Meeting of the Division of Plasma Physics, American Physical Society, Los Angeles, California
November 7–11, 1983

Abstracts in Bull. Am. Phys. Soc. 28:8 (1983)

B. Basu and B. Coppi, Gravity Driven Localized Modes in the Equatorial Ionosphere (p. 1130)

R.H. Berman, D.J. Tetreault, and T.H. Dupree, Simulation of Growing Phase Space Holes and the Development of Intermittent Plasma Turbulence (p. 1133)

A. Bers, A.K. Ram, and G.E. Francis, Relativistic Stability Analysis of Electromagnetic Waves Propagating Across a Magnetic Field (p. 1158)

G. Bertin and B. Coppi, Bending Waves and Current Disk Model of the Solar Wind (p. 1140)

P.T. Bonoli, R. Englade, and M. Porkolab, Simulation of Lower Hybrid Heating in Alcator C (p. 1163)

K.I. Chen, S.C. Luckhardt, S.F. Knowlton, M. Porkolab, A.S. Fisher, M.J. Mayberry, F.S. McDermott, and R. Rohatgi, A Study of Particle Confinement During Lower-Hybrid Current Drive Experiments on the Versator II Tokamak (p. 1031)

B. Coppi, Evidence of Gravity Driven Ballooning-type Modes in the Ionosphere (p. 1161)

B. Coppi, Transport in Plasma with Ohmic and Prevalent Injected Heating (p. 1211)

B. Coppi, Magnetic Reconnection and Velocity Space Instabilities (p. 1210)

B. Coppi, P. Detregiache, J.J. Ramos, and F. Pegoraro, Collective Mode Scattering of Fusion Reaction Products and Spin Depolarization (p. 1240)

B. Coppi and L. Sugiyama, Paths to the Second Stability Region (p. 1210)

P. Detregiache, B. Coppi, S.C. Cowley, R.M. Kulsrud, and E.J. Valeo, Velocity Space Instabilities for Two Component Plasmas (p. 1113)

R. Englade, P.T. Bonoli, and M. Porkolab, Lower Hybrid Current Drive Modeling (p. 1163)

A.C. England, O.C. Eldridge, J.S. Levine, M.E. Read, Y. Carmel, R. Seeley, T. Antonsen, Jr., K.R. Chu, B. Hui, F.S. McDermott, and G. Bekefi, Electron Cyclotron Heating Current Drive in ISX-B (p. 1255)

J. Fajans, Y.Z. Yin, G. Bekefi, and B. Lax, A Free Electron Laser in Combined Helical and Axial Magnetic Fields (p. 1063)

C.L. Fiore, M.J. Greenwald, S.V. Judd, Y. Takase, B. Lloyd, M. Porkolab, and J. Schuss, Results of Neutral Particle Measurements During Lower Hybrid Injection on Alcator C (p. 1163)

R.F. Gandy, D.H. Yates, B. Lloyd, M. Porkolab, and J. Schuss, Electron Plasma Frequency Emission During Current Drive on Alcator C (p. 1162)

A.M. Hamza, B. Coppi, and R. Petrasso, Analysis of Impurity Transport by Impurity Driven Modes (p. 1083)

D.D. Hinshelwood and R.J. Li, The Effects of Cathode Properties on Cathode Turn on in REB Diodes (p. 1146)

K. Hizanidis, D.W. Hewett, K. Rugg, and A. Bers, Steady State RF Current Drive Theory Based Upon the Relativistic Fokker-Planck Equation (p. 1090)

K.D. Jacobs and G. Bekefi, A Free Electron Laser (Ubitron) Experiment (p. 1142)

J. Kesner and B. Lane, Effect of Equilibrium Radial Electric Field on the Trapped Particle Instability in Tandem Mirrors (p. 1132)

S.F. Knowlton, S.C. Luckhardt, P.T. Bonoli, K.I. Chen, M.J. Mayberry, and M. Porkolab, Lower-Hybrid Heating Studies Using a Top-Launching Grill on the Versator II Tokamak (p. 1236)

V.B. Krapchev, D.W. Hewett, and A. Bers, Steady State Solution of a Two-Dimensional Fokker-Planck Equation with Strong RF Diffusion (p. 1090)

B. Lane, Collisional Effects on Trapped Particle Modes in Tandem Mirrors (p. 1183)

J.S. Levine, M.E. Read, Y. Carmel, R. Seeley, F.S. McDermott, G. Bekefi, A.C. England, and O.C. Eldridge, Electron Cyclotron Heating in the ISX-B Tokamak (p. 1255)

B. Lloyd, M. Porkolab, J.J. Schuss, Y. Takase, S.C. Texter, R. Watterson, P. Bonoli, R. Englade, and Alcator Group, Lower-Hybrid Current Drive and Heating Experiments in Alcator C (p. 1162)

S.C. Luckhardt, K.I. Chen, S.F. Knowlton, M.J. Mayberry, M. Porkolab, A.S. Fisher, and

R. Rohatgi, Lower-Hybrid Current Drive Experiments on the Versator II Tokamak (p. 1031)

E. Marmar, M. Foord, B. LaBombard, B. Lipschultz, J. Moreno, J. Rice, J. Terry, B. Lloyd, M. Porkolab, J. Schuss, Y. Takase, S. Texter, and the Alcator Group, Impurity Generation During Lower Hybrid RF Experiments on the Alcator C Tokamak (p. 1163)

M. Mars, B. Coppi, R. Englade, and P.T. Bonoli, Electron Thermal Energy Transport in Plasma with Auxiliary Heating (p. 1221)

M.J. Mayberry, S.C. Luckhardt, K.I. Chen, S.F. Knowlton, F.S. McDermott, M. Porkolab, and R. Rohatgi, X-Ray Measurements During Lower-Hybrid Current Drive Experiments on Versator II (p. 1031)

S. McDermott, G. Bekefi, K.I. Chen, A.S. Fisher, S.F. Knowlton, S.C. Luckhardt, M.J. Mayberry, M. Porkolab, and R. Rohatgi, Emission at $\omega \sim < \omega_{pe}$ During Low Power Lower-Hybrid RF Current Drive Experiments in the Versator II Tokamak (p. 1031)

D.S. Pappas, S.C. Texter, R. Gandy, B. Lloyd, and M. Porkolab, Limiter Hard X-Ray Emission Measurements During Lower Hybrid Injected Discharges (p. 1162)

A.K. Ram, M.E. Mauel, V. Krapchev, and A. Bers, Stochastic Motion of Mirror Confined Electrons by a Frequency Modulated Wave (p. 1183)

J.J. Ramos, B. Coppi, P. Detregiache, and F. Pegoraro, Deuteron Spin Depolarization by Resonant Interaction with Anisotropy Driven Plasma Instability (p. 1208)

R. Rohatgi, S.C. Luckhardt, G. Bekefi, K.I. Chen, A.S. Fisher, S.F. Knowlton, M.J. Mayberry, F.S. McDermott, and M. Porkolab, Scattering from Low-Frequency Fluctuations During Current Drive on Versator II (p. 1091)

R.E. Shefer, D.A. Kirkpatrick, and G. Bekefi, Emittance and Momentum Spread in a Multielectrode Electron Gun for FEL Applications (p. 1063)

L. Sugiyama and B. Coppi, Thermal Transport in High Temperature Ohmic Discharge (p. 1220)

Y. Takase, M. Porkolab, J.J. Schuss, R.L. Watterson, C.L. Fiore, R.E. Slusher, and C.M. Surko, Parametric Instability During Alcator C Lower Hybrid Experiments (p. 1163)

S. Texter, B. Lloyd, M. Porkolab, and J. Schuss, Plasma X-Ray Emission in the 20-500 keV Range During Lower Hybrid Current Drive on Alcator (p. 1162)

R.L. Watterson, Y. Takase, B. Lloyd, M. Porkolab, J.J. Schuss, R.E. Slusher, and C.M. Surko, Study of Lower Hybrid Waves in Alcator C Using CO_2 Laser Scattering (p. 1162)

106th Meeting, Acoustical Society of America, San Diego, California
November 7-11, 1983

Abstracts in J. Acoust. Soc. Am. Vol. 74, Suppl. No. 1, Fall 1983

C. Bickley, Development of Vowel Articulation in Children (p. S103)

D. Bustamante and L.D. Braida, Principal Component Amplitude Compression (p. S104)

F.R. Chen and V.W. Zue, Exploring Allophonic and Lexical Constraints in a Continuous Speech Recognition System (p. S15)

C.L. Farrar, Y. Ito, P.M. Zurek, N.I. Durlach, and C.M. Reed, Detection of Tones in Synthetic Plosive Bursts (p. S71)

K.J. Gabriel, Binaural Interaction in Hearing Impaired Listeners (p, S85)

K.J. Gabriel, H.S. Colburn, P.M. Zurek, and N.I. Durlach, A General Modification for Models of Binaural Interaction (p. S85)

D.P. Huttenlocher and V.W. Zue, Exploring Phonotactic Lexical Constraints in Word Recognition (p. S15)

H. Kawasaki, An Acoustic Study of Japanese Coronal Fricative Clusters Resulting from Word Devoicing (p. S90)

L.F. Lamel, The Use of Phonotactic Constraints to Determine Word Boundaries (p. S15)

L.S. Larkey and M. Danly, Fundamental Frequency and the Comprehension of Simple and Complex Sentences (p. S67)

E.M. Maxwell. Portuguese Nasalized Vowels and Nasal Consonants: Their Relation to Following Consonants (p. S90)

S. Seneff, Pitch and Spectral Estimation of Speech Based on Auditory Synchrony Model (p. S9)

S. Shattuck-Hufnagel, The Word-Position Similarity Constraint on Segmental Speech Errors: Further Experimental Results (p. S117)

SEMICRO Conference, Rio de Janeiro, Brasil
November 9, 1983

J. Allen, VLSI Education in United States

ASSP Spectrum EstimationWorkshop II, Tampa, Florida
November 10-11, 1983

Papers in Proceedings

D. Izraelevitz and J.S. Lim, Spectral Characteristics of the Overdetermined Normal Equation Method for Spectral Estimation (pp. 49-54)

Materials Research Society Symposium on "Energy Beam-Solid Interactions and Transient Thermal Processing," Boston, Massachusetts
November 14–17, 1983

Papers in Fan and Johnson (Eds.), Symposium Proceedings (Elsevier Science Publishing Company, New York)

C.C. Wong, C.J. Keavney, H.A. Atwater, C.V. Thompson, and H.I. Smith, Zone Melting Recrystallization of InSb Films on Oxidized Si Wafers

American Speech and Hearing Association Meeting, Cincinnati, Ohio
November 18–21, 1983

Abstracts in ASHA 25:10, October 1983

C.L. Farrar, C.M. Reed, N.I. Durlach, L.D. Braida, and P.M. Zurek, Spectral-Shape Discrimination of Synthetic Plosive Bursts (p. 67)

R.E. Hillman, E. Holmberg, M. Walsh, and J. Perkell, Source Characteristics of Esophageal Phonation (p. 72)

J.D. Koehnke and M.F. Cohen, The Effects of Masker Level on Binaural Masking Patterns (p. 156)

Conference on Fractals in the Physical Sciences, National Bureau of Standards, Gaithersburg, Maryland
November 21–23, 1983

M. Kardar and M. Kaufman, Competing Criticality of Short- and Infinite-Range Interactions on the Cayley Tree: Effective Dimensional Variation

GLOBECOM '83 Global Telecommunications Conference, San Diego, California
November 28 – December 1, 1983

Papers in Conference Record

T.T. Nguyen, J.H. Shapiro, A.K. Wong, and D.J. Epstein, Atmospheric Optical Communications for Local Area Networks (pp. 416–420)

8th International Conference on Infrared and Millimeter Waves, Miami, Florida
December 12–17, 1983

P.A. Wolff, Nonlinear Optical Studies of Picosecond Relaxation Times in Semiconductors

US-Japan Workshop on RF Heating and Current Generation, GA Technologies Inc., San Diego, California
December 19–21, 1983

K. Hizanidis, D.W. Hewett, and A. Bers, Solution of the Relativistic 2-D Fokker-Planck Equation for LH Current Drive

V.B. Krapchev, D.W. Hewett, and A. Bers, Analytic Solution of the 2-D Fokker-Planck Equation for LH Current Drive

1983 International Conference on Advanced Automation, Taiwan, Republic of China
December 19-21, 1983

V.W. Zue and D.P. Huttenlocher, Computer Recognition of Isolated Words from Large Vocabularies: Lexical Access Using Partial Phonetic Information

28.2 Journal Papers Published

D. Bendedouch, S-H. Chen, and W.C. Koehler, Determination of Interparticle Structure Factors in Ionic Micellar Solutions by Small Angle Neutron Scattering (J. Phys. Chem. 87:14, 2621-2628 (1983))

C.L. Bennett, C.R. Lawrence, and B.F. Burke, 5 GHz Source Variability and the Gain of the 300-Foot Telescope (Astrophys. J. Suppl. 54, 211-227 (1984))

P.J. Benson and P.C. Myers, Dense Cores in Dark Clouds. IV. HC_5N Observations (Astrophys. J. 270, 589-604 (1983))

R.H. Berman, D.J. Tetreault, and T.H. Dupree, Observation of Self-binding Turbulent Fluctuations in Simulation Plasma and Their Relevance to Plasma Kinetic Theories (Phys. Fluids 26:9, 2437-2459 (1983))

R.J. Birgeneau, C.W. Garland, G.B. Kasting, and B.M. Ocko, Critical Behavior Near the Nematic-Smectic-A Transition in Butyloxybenzylidene Octylaniline (Phys. Rev. A 24:5, 2624-2634 (1981))

D. Blankschtein, Y. Shapir, and A. Aharony, Potts Models in Random Fields (Phys. Rev. B 29:3, 1263-1267 (1984))

R.G. Caflisch and A.N. Berker, Oxygen Chemisorbed on Ni(100): A Renormalization-Group Study of the Global Phase Diagram (Phys. Rev. B 29:3, 1279-1286 (1984))

S.L. Chuang and J.A. Kong, Wave Scattering and Guidance by Dielectric Waveguides with Periodic Surfaces: Addendum (J.Opt. Soc. Am. 73:12, 1823-1824 (1983))

R.A. Close, A. Palevsky, and G. Bekefi, Radiation Measurements from an Inverted Relativistic Magnetron (J. Appl. Phys. 54:7, 4147-4151 (1983))

G.B. Crew and J.J. Ramos, Asymptotic Theory of the Internal Kink Mode in Current Carrying Toroidal Plasmas (Phys. Fluids 26:9, 2621-2634 (1983))

S.L. Dexheimer, T.A. Brunner, and D.E. Pritchard, Angular Momentum Limitation in Vibrationally Inelastic Collisions of $I_2(B^3\Pi)$ with He and Xe (J. Chem. Phys. 79:10, 5206–5207 (1983))

J.W. Dreher and E.D. Feigelson, Rings and Wiggles in Hercules A (Nature Vol. 308, No. 5954, pp. 43–45, March 1984)

J.W. Dreher and W.J. Welch, VLA Observations of MWC349 at 15 and 23 GHz (Astron. J. 88:7, 1014–1016 (1983))

T.H. Dupree, Growth of Phase Space Density Holes (Phys. Fluids 26:9, 2460–2481 (1983))

A. Erbil, A.R. Kortan, R.J. Birgeneau, and M.S. Dresselhaus, Intercalate Structure, Melting and the Commensurate–Incommensurate Transition in Bromine–Intercalated Graphite (Phys. Rev. B 28:11, 6329–6346 (1983))

C. Espy and J.S. Lim, Effects of Additive Noise on Signal Reconstruction from Fourier Transform Phase (IEEE Trans. Vol. ASSP–31, No. 4, pp. 894–898, August 1983)

M. Florentine, Intensity Discrimination as a Function of Level and Frequency in Its Relation to High–Frequency Hearing (J. Acoust. Soc. Am. 74:5, 1375–1379 (1983))

J.J. Fratamico, P.L. Bogler, and J.H. Shapiro, Adaptive Diversity–Combining for Improved Millimeter–Wave Communication Through Rain (IEEE J. Vol. SAC–1, No. 4, pp. 686–694, September 1983)

L.S. Frishkopf and D.J. DeRosier, Mechanical Tuning of Freestanding Stereociliary Bundles and Frequency Analysis in the Alligator Lizard Cochlea (Hearing Res. 12, 393–404 (1983))

J.G. Fujimoto, S.G. Shevel, and E.P. Ippen, Femtosecond Time–Resolved Exciton in CdSe (Solid State Commun. 49:6, 605–609 (1984))

M.L. Gifford and J.J. Guinan, Jr., Effects of Crossed Olivocochlear Bundle Stimulation on Cat Auditory Nerve Fiber Responses to Tones (J. Acoust. Soc. Am. 74:1, 115–123 (1983))

S.M. Goldwasser and D.E. Troxel, Page Composition of Continuous Tone Imagery (Comput. Vision, Graphics, Image Processing 26, 30–44 (1984))

J.J. Guinan, Jr., W.B. Warr, and B.E. Norris, Differential Olivocochlear Projections from Lateral vs. Medial Zones of the Superior Olivary Complex (J. Comp. Neurol. 221, 358–370 (1983))

H.A. Haus and M.N. Islam, Synchroton Radiation of Wiggled Electron Beam in Rectangular Waveguide (J. Appl. Phys. 54:9, 4784–4793 (1983))

H.A. Haus and Y. Yamamoto, Quantum Noise of an Injection–Locked Laser Oscillator (Phys. Rev. A 29:3, 1261–1274 (1984))

R. Häusler, S. Colburn, and E. Marr, Sound Localization in Subjects with Impaired Hearing (Acta Oto–Laryngol., Supplement 400, pp. 1–62(1983))

A.M. Hawryluk, H.I. Smith, and D.J. Ehrlich, Deep–UV Spatial–Frequency Doubling by Combining

Multilayer Mirrors with Diffraction Gratings (J. Vac. Sci. Technol. B1(4), 1200–1203 (1983))

D.D. Hinshelwood, Cathode Plasma Formation in Pulsed High Current Vacuum Diodes (IEEE Trans. Vol. PS–11, No. 3, pp. 188–196, September 1983)

T. Holton and T.F. Weiss, Receptor Potentials of Lizard Cochlear Hair Cells with Free–Standing Stereocilia in Response to Tones (J. Physiol. 345, 205–240 (1983))

T. Holton and T.F. Weiss, Frequency Selectivity of Hair Cells and Nerve Fibers in the Alligator Lizard Cochlea (J. Physiol. 345, 241–260 (1983))

C.M. Horwitz, Radio Frequency Sputtering — The Significance of Power Input (J. Vac. Sci. Technol. A 1:4, 1795–1800 (1983))

B. Howland, New Test Patterns for Camera Lens Evaluation (Appl. Opt. 22:12, 1792–1793 (1983))

Y.Q. Jin and J.A. Kong, Passive and Active Remote Sensing of Atmospheric Precipitation (Appl. Optics 22:17, 2535–2545 (1983))

Y.Q. Jin and J.A. Kong, Strong Fluctuation Theory for Electromagnetic Wave Scattering by a Layer of Random Discrete Scatterers (J. Appl. Phys. 55:5, 1364–1369 (1984))

M.S. Kaplan, B.G. Szaro, and T.F. Weiss, Components of Cochlear Electric Responses in the Alligator Lizard (Hearing Res. 12, 323–351 (1983))

M. Kardar, Crossover to Equivalent–Neighbor Multicritical Behavior in Arbitrary Dimensions (Phys. Rev. B 28:1, 244–246 (1983))

M. Kaufman and D. Andelman, Critical Amplitude of the Potts Model: Zeroes and Divergences (Phys. Rev. B 29:7, 4010–4016 (1984))

E.M. Keithley and M.L. Feldman, The Spiral Ganglion and Hair Cells of Bronx Waltzer Mice (Hearing Res. 12, 381–391 (1983))

A.R. Kortan, H. von Känel, R.J. Birgeneau, and J.D. Litster, Nematic—Smectic A—Reentrant Nematic Transitions in 80CB:60CB Mixtures (J. Physique 45:3, 529–538 (1984))

M. Kotlarchyk and S–H. Chen, Analysis of Small Angle Neutron Scattering Spectra from Polydisperse Interacting Colloids (J. Chem. Phys. 79:5, 2461–2469 (1983))

A.L. Kurkjian and S–K. Chang, Arrays of Synthetic Acoustic Well Logging Waveforms: Computation and Source Design (IEEE Trans. Vol. ASSP–31, No. 4, pp. 946–955, August 1983)

M. Kuznetsov and H.A. Haus, Radiation Loss in Dielectric Waveguide Structures by the Volume Current Method (IEEE J. Vol. QE–19, No. 10, pp. 1505–1514, October 1983)

A. Lattes, H.A. Haus, F.J. Leonberger, and E.P. Ippen, An Ultrafast All–Optical Gate (IEEE J. Vol. QE–19, No. 11, pp. 1718–1723, November 1983)

C.R. Lawrence, D.P. Schneider, M. Schmidt, C.L. Bennett, J.N. Hewitt, B.F. Burke, E.L. Turner, and

J.E. Gunn, Discovery of a New Gravitational Lens System (Science 223, 46–49 (1984))

D.H. Lee, R.G. Caflisch, J.D. Joannopoulos, and F.Y. Wu, Antiferromagnetic Classical XY Model: A Mean-Field Analysis (Phys. Rev. B 29:5, 2680–2684 (1984))

D.H. Lee and J.D. Joannopoulos, Renormalization Scheme for the Transfer-Matrix Method and the Surfaces of Wurtzite ZnO (Phys. Rev. B 24:12, 6899–6907 (1981))

H.J. Lezec, E.H. Anderson, and H.I. Smith, An Improved Technique for Resist-Profile Control in Holographic Lithography (J. Vac. Sci. Technol. B 1:4, 1204–1206 (1983))

J.D. Litster, C.W. Garland, K.J. Lushington, and R. Schaetzing, Experimental Studies of Liquid Crystal Phase Transitions (Mol. Cryst. Liq. Cryst. 63, 145–156 (1981))

R.E. Meyer, G.A. Sanders, and S. Ezekiel, Observation of Spatial Variations in the Resonance Frequency of an Optical Resonator (J. Opt. Soc. Am. 73:7, 939–942 (1983))

L.A. Molter-Orr, H.A. Haus, and F.J. Leonberger, 20 GHz Optical Waveguide Sampler (IEEE J. Vol. QE–19, No. 12, pp. 1877–1883, December 1983)

D.R. Mook, An Algorithm for the Numerical Evaluation of the Hankel and Abel Transforms (IEEE Trans. Vol. ASSP–31, No. 4, pp. 979–985, August 1983)

F.R. Morgenthaler, Magnetostatic Surface Modes in Nonuniform Thin Films with In-Plane Bias Fields (J. Appl. Phys. 52:3, 2267–2269 (1981))

F.R. Morgenthaler, Nondispersive Magnetostatic Forward Volume Waves Under Fields Gradient Control (J. Appl. Phys. 53:3, 2652–2654 (1982))

S.H. Nawab, T.F. Quatieri, and J.S. Lim, Signal Reconstruction from Short-Time Fourier Transform Magnitude (IEEE Trans. Vol. ASSP–31, No. 4, pp. 986–998, August 1983)

B.M. Ocko, A.R. Kortan, R.J. Birgeneau, and J.W. Goodby, A High Resolution X-Ray Scattering Study of the Phases and Phase Transitions in N-(4–n-butyloxybenzylidene)-4–n-heptylaniline (40.7) (J. Physique 45:1, 113–128 (1984))

A.V. Oppenheim, J.S. Lim, and S.R. Curtis, Signal Synthesis and Reconstruction from Partial Fourier-Domain Information (J. Opt. Soc. Am. 73:11, 1413–1420 (1983))

D. O'Shaughnessy and J. Allen, Linguistic Modality Effects on Fundamental Frequency in Speech (J. Acoust Soc. Am. 74:4, 1155–1171 (1983))

P.J. Price and A.G. Levitt, The Relative Roles of Syntax and Prosody in the Perception of the /š/–/č/ Distinction (Language and Speech Vol. 26, Part 3, pp. 291–304 (1983))

T.F. Quatieri, S.H. Nawab, and J.S. Lim, Frequency Sampling of the Short-Time Fourier-Transform Magnitude for Signal Reconstruction (J. Opt. Soc. Am. 73:11, 1523–1526 (1983))

C.M. Reed, B.L. Hicks, L.D. Braida, and N.I. Durlach, Discrimination of Speech Processed by Lowpass Filtering and Pitch-Invariant Frequency Lowering (J. Acoust. Soc. Am. 74:2, 409–419 (1983))

H.C. Reeve III and J.S. Lim, Reduction of Blocking Effects in Image Coding (Optical Eng. 23:1, 34–37 (1984))

J.J. Rosowski, W.T. Peake, and J.R. White, Cochlear Nonlinearities Inferred from Two-Tone Distortion Product in the Ear Canal of the Alligator Lizard (Hearing Res. 13, 141–158 (1984))

J. Rubinstein, P. Penfield, Jr., and M.A. Horowitz, Signal Delay in RC Tree Network (IEEE Trans. Vol. CAD-2, No. 3, pp. 202–211, July 1983)

S. Sachdev, Atom in a Damped Cavity (Phys. Rev. A 29:5, 2627–2633 (1984))

K.L. Saenger, N. Smith, S.L. Dexheimer, C. Engelke, and D.E. Pritchard, Role of Initial Rotation on Vibrationally Inelastic Collisions: Enhancement and Specificity in Level to Level Rate Constants for $Li_2^* + Xe$ (J. Chem. Phys. 79:8, 4076–4077 (1983))

A. Sezginer and J.A. Kong, Physical Optics Approach for Scattering by Thin Helical Wires (Radio Sci. 18:5, 639–649 (1983))

A. Sezginer, S.L. Chuang, and J.A. Kong, Modal Approach to Scattering of Electromagnetic Waves by a Conducting Tape Helix (IEEE Trans. Vol. AP-31, No. 5, pp. 732–739, September 1983)

R.E. Shefer, Y.Z. Yin, and G. Bekefi, Velocity Diagnostics of Mildly Relativistic, High Current Electron Beams (J. Appl. Phys. 54:11, 6154–6159 (1983))

R.A. Siegel and H.S. Colburn, Internal and External Noise in Binaural Detection (Hearing Res. 11, 117–123 (1983))

H.I. Smith, M.W. Geis, C.V. Thompson, and H.A. Atwater, Silicon-on-Insulator by Graphoepitaxy and Zone-Melting Recrystallization of Patterned Films (J. Cryst. Growth 63, 527–546 (1983))

H.I. Smith, C.V. Thompson, and H.A. Atwater, Graphoepitaxy and Zone-Melting Recrystallization of Patterned Films (J. Cryst. Growth 65:1–3, 337–338 (1983))

H.I. Smith, C.V. Thompson, M.W. Geis, R.A. Lemons, and M.A. Bosch, The Mechanism of Orientation in Si Graphoepitaxy by Laser or Strip-Heater Recrystallization (J. Electrochem. Soc. 130:10, 2050–2053 (1983))

V. Stefan and A. Bers, Parametric Absorption in Electron Cyclotron Resonance Heating of Tokamak Plasmas (Phys. Fluids 27:1, 175–183 (1984))

D.J. Tetreault, Growth Rate of the Clump Instability (Phys. Fluids 26:11, 3247–3261 (1983))

K. Theilhaber, Non-Linear Coupling to Lower-Hybrid Waves in a Tokamak Plasma (Nucl. Fusion 22:3, 363–381 (1982))

L. Tsang and J.A. Kong, Scattering of Electromagnetic Waves from a Half Space of Densely Distributed Dielectric Scatterers (Radio Sci. 18:6, 1260–1272 (1983))

L. Tsang, J.A. Kong, and R.T. Shin, Radiative Transfer Theory for Active Remote Sensing of a Layer of Nonspherical Particles (Radio Sci. 19:2, 629–642 (1984))

P.L. Van Hove, M.H. Hayes, J.S. Lim, and A.V. Oppenheim, Signal Reconstruction from Signed Fourier Transform Amplitude (IEEE Trans. Vol. ASSP-31, No. 5, pp. 1286–1293, October 1983)

H. von Känel and J.D. Litster, Light-Scattering Studies on the Single-Layer Smectic p-Butoxybenzilidene p-Octylaniline (Phys. Rev. A 23:6, 3251–3254 (1981))

R. Walkup, A. Migdall, and D.E. Pritchard, Inelastic Collisions of Virtually Excited Atoms (Phys. Rev. A 29:5, 2651–2655 (1984))

R. Walkup, B. Stewart, and D.E. Pritchard, Collisional Line Broadening Due to van der Waals Potentials (Phys. Rev. A 29:1, 169–173 (1984))

A.M. Weiner, Effect of Group Velocity Mismatch on the Measurement of the Ultrashort Optical Pulses via Second Harmonic Generation (IEEE J. Vol. QE-19, No. 8, pp. 1276–1283, August 1983)

A.M. Weiner, Erratum: Effect of Group Velocity Mismatch on the Measurement of the Ultrashort Optical Pulses via Second Harmonic Generation [IEEE J. Vol. QE-19, No. 8, p. 1276 (1983)] (IEEE J. Vol. QE-20, No. 4, p. 499, April 1984)

T.F. Weiss, Relation of Receptor Potentials of Cochlear Hair Cells to Spike Discharges of Cochlear Neurons (Ann. Rev. Physiol. 46, 247–259 (1984))

J.L. Wyatt, Jr. and L.O. Chua, Nonlinear Resistive Maximum Power Theorem, with Solar Cell Application (IEEE Trans. Vol. CAS-30, No. 11, pp. 824–828, November 1983)

Y.Z. Yin and G. Bekefi, Dispersion Characteristics of a Free Electron Laser with a Linearly Polarized Wiggler and Axial Guide Field (J. Appl. Phys. 55:1, 33–42 (1984))

J. Yorsz, S.G. Shevel, and E.P. Ippen, Optically Pumped $Zn_xCd_{1-x}S$ Platelet Lasers (Optics Comm. 48:2, 139–142 (1983))

28.3 Journal Papers Accepted for Publication

A. Bers, RF Heating and Current Generation — An Overview and Perspective of This Special Issue (IEEE Trans. (Plasma Sci.))

S.L. Chuang and J.A. Kong, Enhancement of Smith-Purcell Radiation from a Grating Surface with Plasmon Excitation (J. Opt. Soc. Am.)

J.G. Fujimoto and T.K. Yee, Influence of Dephasing Relaxation on the Transient Properties of Parametric Four-Wave Mixing (Appl. Phys. B)

D.W. Griffin and J.S. Lim, Signal Estimation from Modified Short-Time Fourier Transform (IEEE Trans. (ASSP))

R. Goldstein, On the Theory of Lower Critical Solution Points in Hydrogen-Bonded Mixtures (J. Chem.

Phys.)

T.M. Habashy and J.A. Kong, Coupling Between Two Circular Microstrip Disk Resonators (Electromagnetics)

M.N. Islam, H.A. Haus, and J. Melngailis, Bulk Radiation by Surface Acoustic Waves Propagating Under a Grating (IEEE Trans (SU))

J.M. Jackson, J.T. Armstrong, and A.H. Barrett, HNCO in Molecular Clouds (Astrophys. J.)

C.J. Keavney and H.I. Smith, A 3.8m Period Sawtooth Grating in InP by Anisotropic Hetching (J. Electrochem. Soc.)

J.A. Kong, S.L. Lin, and S.L. Chuang, Microwave Thermal Emission from Periodic Surfaces (IEEE Trans. (GR))

P. Kumar, R.S. Bondurant, and J.H. Shapiro, Fluctuations in the Phase–Conjugate Signal Generated via Degenerate Four–Wave Mixing (Optics Comm.)

J.K. Lee and J.A. Kong, Dyadic Green's Functions for Layered Anisotropic Medium (Electromagnetics)

W.P. Moskowitz, B. Stewart, R.M. Bilotta, J.L. Kinsey, and D.E. Pritchard, Velocity Dependence of Rotational Rainbow Structure in Na_2–Ar (J. Chem. Phys.)

P.J. Price and H.J. Simon, Perception of Temporal Differences in Speech by Normal–Hearing Adults: Effects of Age and Intensity (J. Acoust. Soc. Am.)

T.P. Scott, N. Smith, and D.E. Pritchard, Application of Fitting Laws to Rotationally Inelastic Rate Constants: $Li_2^*(A'\Sigma)$ + Ne, Ar, Xe (J. Chem. Phys.)

J.H. Shapiro and S.S. Wagner, Phase and Amplitude Uncertainties in Heterodyne Detection (IEEE J. (QE))

R.T. Shin and J.A. Kong, Scattering of Electromagnetic Waves from a Randomly Perturbed Quasi–Periodic Surface (J. Appl. Phys.)

N. Smith, T.P. Scott, an D.E. Pritchard, Velocity Dependence of Rotationally Inelastic Collisions: $Li_2^*(A'\Sigma)$ + Ne, Ar, Xe (J. Chem. Phys.)

J.H. Stathis and M.A. Kastner, Vacuum–Ultraviolet Generation of Luminescence and Absorption Centres in a–SiO_2 (Philos. Mag.)

J.H. Stathis and M.A. Kastner, Photoinduced Paramagnetic Defects in Amorphous Silicon Dioxide (Phys. Rev. B)

28.4 Letters to the Editor Published

E.H. Anderson, C.M. Horwitz, and H.I. Smith, Holographic Lithography with Thick Photoresist (Appl. Phys. Lett. 43:9, 874–875 (1983))

H.A. Atwater, C.V. Thompson, H.I. Smith, and M.W. Geis, Orientation Filtering by Growth-Velocity Competition in Zone-Melting Recrystallization of Silicon on SiO_2 (Appl. Phys. Lett. 43:12, 1126–1128 (1983))

H.A. Atwater, H.I. Smith, C.V. Thompson, and M.W. Geis, Zone Melting Recrystallization of Thick Silicon on Insulator Films (Mater. Lett. 2:4A, 269–273 (1984))

Y. Bar-Yam and J.D. Joannopoulos, The Barrier to Migration of the Silicon Self-Interstitial (Phys. Rev. Lett. 52:13, 1129–1132 (1984))

G. Bekefi, R.E. Shefer, and W.W. Destler, Millimeter Wave Emission from a Rotating Electron Ring in Rippled Magnetic Field (Appl. Phys. Lett. 44:3, 280–282 (1984))

D. Bendedouch and S-H. Chen, Effect of an Attractive Potential on the Interparticle Structure of Ionic Micelles at High Salt Concentration (J. Phys. Chem. (Letter) 88:4, 648–652 (1984))

J. Collett, L.B. Sorensen, P.S. Pershan, J.D. Litster, R.J. Birgeneau, and J. Als-Nielsen, Synchrotron X-Ray Study of Novel Crystalline-B Phase in Heptyloxybenzylidene-Heptylaniline (70.7) (Phys. Rev. Lett. 49:8, 553–556 (1982))

B. Coppi, F. Pegoraro, and J.J. Ramos, Instability of Fusing Plasmas and Spin-Depolarization Processes (Phys. Rev. Lett. 51:10, 892–895 (1983))

A. Fuchs, D. Bebelaar, and M.M. Salour, Optically Pumped cw Semiconductor Ring Laser (Appl. Phys. Lett. 43:1, 32–34 (1983))

K.J. Gabriel, Comparison of Three Correlation Coefficient Estimators for Gaussian Stationary Processes (IEEE Trans. (Correspondence) Vol. ASSP-31, No. 4, pp. 1023–1025, August 1983)

R.G. Hulet and D. Kleppner, Rydberg Atoms in "Circular" States (Phys. Rev. Lett. 51:16, 1430–1433 (1983))

J. Ihm, D.H. Lee, J.D. Joannopoulos, and J.J. Xiong, Structural Phase Diagrams for the Surface of a Solid: A Total-Energy, Renormalization-Group Approach (Phys. Rev. Lett. 51:20, 1872–1875 (1983))

M. Kaufman and K.K. Mon, Realizable Renormalization Group and Finite-Size Scaling (Phys. Rev. B (Brief Reports) 29:3, 1451–1453 (1984))

A.R. Kortan, H. von Känel, R.J. Birgeneau, and J.D. Litster, High-Resolution X-Ray Scattering Study of the Nematic-Smectic A-Reentrant Nematic Transitions in 80CB/60CB Mixtures (Phys. Rev. Lett. 47:17, 1206–1209 (1981))

R.F. Kwasnick, M.A. Kastner, J. Melngailis, and P.A. Lee, Nonmonotonic Variations of the

Conductance with Electron Density in ~70-nm-Wide Inversion Layers (Phys. Rev. Lett. 52:3, 224-227 (1984))

M. Kuznetsov, Expressions for the Coupling Coefficient of Rectangular-Waveguide Directional Coupler (Optics Lett. 8:9, 499-501 (1983))

C.R. Lawrence, C.L. Bennett, J.N. Hewitt, and B.F. Burke, 5 GHz Structure and Optical Identification of Weak Extragalactic Radio Source (Astrophys. J. (Letters) 278, L95-L98 (1984))

D.H. Lee, J.D. Joannopoulos, J.W. Negele, and D.P. Landau, Discrete-Symmetry Breaking and Novel Critical Phenomena in an Antiferromagnetic Planar (XY) Model in Two Dimensions (Phys. Rev. Lett. 52:6, 433-436 (1984)

R.E. Meyer, S. Ezekiel, D.W. Stowe, and V.J. Tekippe, Passive Fiber Optic Ring Resonator for Rotation Sensing (Optics Lett. 8:12, 644-646 (1983))

A.L. Migdall, R.E. Walkup, and D.E. Pritchard, A Search for a Radiative Transition in an Atom-Molecule System (Chem. Phys. Lett. 103:2, 138-142 (1983))

P.E. Moskowitz, P.L. Gould, S.R. Atlas, and D.E. Pritchard, Diffraction of an Atomic Beam by Standing-Wave Radiation (Phys. Rev.Lett. 51:5, 370-373 (1983))

B.M. Ocko, R.J. Birgeneau, J.D. Litster, and M.E. Neubert, Critical and Tricritical Behavior at the Nematic to Smectic A Transition (Phys. Rev. Lett. 52:3, 208-211 (1984))

D.E. Pritchard, Coding Neutral Atoms in a Magnetic Trap for Precision Spectroscopy (Phys. Rev. Lett. 51:15, 1336-1339 (1983))

P.W. Stephens and J.G. King, Experimental Investigation of Small Helium Clusters: Magic Numbers and the Onset of Condensation (Phys. Rev. Lett. 51:17, 1538-1541 (1983))

C.V. Thompson and H.I. Smith, Surface-Energy-Driven Secondary Grain Growth in Ultrathin (<100 nm) Films of Silicon (Appl. Phys. Lett. 44:6, 603-605 (1984))

A.M. Weiner and E.P. Ippen, Novel Transient Scattering Technique for Femtosecond Dephasing Measurements (Optics Lett. 9:2, 53-55 (1984))

J.M. Wiesenfeld, L.F. Mollenauer, and E.P. Ippen, Ultrafast Configurational Relaxation of Optically Excited Color Centers (Phys. Rev. Lett. 47:23, 1668-1671 (1981))

S.Y. Yuen, Degenerate Four-Wave Mixing Due to Intervalance Band Transition in p-Type Mercury Cadmium Telluride (Appl. Phys. Lett. 43:5, 479-481 (1983))

S.Y. Yuen, Fast Relaxing Absorbtive Nonlinear Refraction in Superlattices (Appl. Phys. Lett. 43:9, 813-815 (1983))

28.5 Letters to the Editor Accepted for Publication

J.G. Fujimoto, A.M. Weiner, and E.P. Ippen, Generation and Measurement of Optical Pulses as Short as 16 Femtpseconds (Appl. Phys. Lett.)

H.A. Haus, L. Molter-Orr, and F.J. Leonberger, A Multiple Waveguide Lens (Appl. Phys. Lett.)

M. Kaufman, Duality and Potts Critical Amplitudes on a Class of Hierarchical Lattices (Phys. Rev. B (Brief Reports))

E. Wintner and E.P. Ippen, Nonlilnear Carrier Dynamics in $Ga_xIn_{1-x}As_yP_{1-y}$ Compounds (Appl. Phys. Lett.)

28.6 Special Publications

G. Bekefi, R.E. Shefer, and B.D. Nevins, Radiation Measurements from a Rippled-Field Magnetron (Crossed-Field FEL), in the Proceedings of the 1982 International Conference on Lasers, New Orleans, Louisiana, December 13–17, 1982, pp. 136–148.

A. Bers, Space-Time Evolution of Plasma Instabilities–Absolute and Convective, Chapter 3.2, in M.N. Rosenbluth and R. Z. Sagdeev (Eds.), Handbook of Plasma Physics, Vol. 1: Basic Plasma Physics I (North-Holland Publishing Company, Amsterdam, The Netherlands, 1983), pp. 451–517.

L.D. Braida, N.I. Durlach, S.V. De Gennaro, P.M. Peterson, and D.K. Bustamante, Review of Recent Research on Multiband Amplitude Compression for the Hearing Impaired, in G.A. Studebaker and F.H. Bess (Eds.), The Vanderbilt Hearing-Aid Report (Monographs in Contemporary Audiology, Pennsylvania, 1982), pp. 133–140.

E.P. Ippen, Picosecond Pulse Generation with Diode Lasers, in Picosecond Phenomena II, Springer Series in Chemical Physics, Vol. 14 (Springer Verlag Publisher, 1980), pp. 21–25.

J.S. Lim, Signal Processing for Speech Enhancement, in G.A. Studebaker and F.H. Bess (Eds.), The Vanderbilt Hearing-Aid Report (Monographs in Contemporary Audiology, Pennsylvania, 1982), pp. 124–129.

B. Scharf and M. Florentine, Psychoacoustics of Elementary Sounds, in G.A. Studebaker and F.H. Bess (Eds.), The Vanderbilt Hearing-Aid Report (Monographs in Contemporary Audiology, Pennsylvania, 1982), pp. 3–15.

K.N. Stevens, Acoustic Properties Used for the Identification of Speech Sound, in Proceedings Cochlear Prostheses: An International Symposium (New York Academy of Science, New York, 1983), pp. 2–17.

29. Personnel

Jonathan Allen, Director
Robert J. Birgeneau, Associate Director

Professors

Allen, Jonathan
Allis, William P.*
Baggeroer, Arthur B.
Barrett, Alan H.
Bekefi, George
Bers, Abraham
Birgeneau, Robert J.
Bose, Amar G.
Braida, Louis D.
Bresnan, Joan W.
Burke, Bernard F.
Chen, Sow-Hsin
Chomsky, A. Noam
Coppi, Bruno
Dupree, Thomas H.
Edgerton, Harold E.*
Ezekiel, Shaoul
Fodor, Jerry A.
Fonstad, Clifton G.
French, Anthony P.
Frishkopf, Lawrence S.
Gyftopoulos, Elias P.
Hale, Kenneth L.
Halle, Morris
Harris, James W.
Harvey, George G.*
Haus, Hermann A.
Ippen, Erich P.
Jenkins, Michael+
Kennedy, Robert S.
Keyser, Samuel J.
Khyl, Robert L.*
King, John G.
Kiparsky, R. Paul V.
Kleppner, Daniel
Kong, Jin Au
Lee, Francis F.
Lee, Patrick A.
Lettvin, Jerome Y.
Lidsky, Lawrence M.
Litster, James D.
McCune, James E.
Morgenthaler, Frederic R.
Oppenheim, Alan V.
Peake, William T.
Penfield, Paul, Jr.
Pomorska, Krystyna
Porkolab, Miklos
Pritchard, David E.
Schreiber, William F.
Searle, Campbell L.
Siebert, William M.
Smith, Henry I.
Smullin, Louis D.
Staelin, David H.
Stevens, Kenneth N.
Strandberg, Malcolm W.P.
Weiss, Thomas F.
Wolff, Peter A.
Zimmerman, Henry J.*

Associate Professors

Benton, Stephen A.
Berker, A. Nihat
Joannopoulos, John D.
Kastner, Marc A.
Lim, Jae S.
Shapiro, Jeffrey H.
Troxel, Donald E.

Assistant Professors

Ceyer, Sylvia T.
Dreher, John W.
Glasser, Lance A.
Lang, Jeffrey H.
Musicus, Bruce R.
Nelson, Keith A.
Thompson, Carl V., II
Wyatt, John L., Jr.
Zue, Victor W.

**Emeritus*
+ *Visiting*

Senior Research Scientists

Durlach, Nathaniel I.
Kamentsky, Louis A.
Klatt, Dennis H.
Rediker, Robert H.

Principal Research Scientists and Associates

Colburn, H. Steven
Melngailis, John
Perkell, Joseph S.

Postdoctoral Fellows

Brown, M. Christian
Eatock, Ruth Anne[1]
Furst, Miriam[2]
Gardner, Jill
Keithley, Elizabeth M.[3]
Kobler, James B.
Koehnke, Janet
Larkey, Leah S.[3]
MacMillan, Neil[3]
Maxwell, Edith M.[3]
Price, Patti Jo[3]
Wintner, Ernst[4]

Research Staff

Barrett, John W.
Barrows, Francis W.
Berman, Robert H.
Bhattacharjee, Tushar
Bilotta, Robert
Bonoli, Paul T.
Boutros-Ghali, Teymour
Church, Kenneth W.
Cline, Richard W.
Cohen, Marc H.
Corteselli, Stephen
Crew, Geoffrey B.
Delhorne, Lorraine A.
Eddington, Donald
Englade, Ronald C.
Farrar, Catherine L.
Fisher, Alan S.
Fitzgerald, Edward W.
Freeman, Dennis M.
Gabriel, Kaigham J.
Gerver, Michael
Guinan, John J., Jr.
Hale, Roger L.
Hizanidis, Kyriakos
Houtsma, Adrian J.M.
Hume, Christopher
Irby, James H.
Jagannath, Chirravuri
Jakimik, Joseph A.
Jarrell, Joseph A.
Kawasaki, Haruko
Kiang, Nelson Y.S.
Kierstead, John D.
Kortan, Ahmet R.
Krapchev, Vladimir B.
Kupferberg, Lenn C.
Lee, Dung-Hai Tom
Lo, Chi Cheung
Luckhardt, Stanley C.
Mastovsky, Ivan
McCrosky, Carl
McIlrath, Michael B.
Mook, Douglas R.
Morey, Kenneth A.
Papa, D. Cosmo
Plotkin, George M.
Rabinowitz, William M.
Ramos, Jesus
Reed, Charlotte M.
Rosenkranz, Philip W.
Rudy, Stephen
Russell, Roy P.
Saenger, Katherine L.
Shao, Michael
Sharky, Nazih N.
Shattuck-Hufnagel, Stefanie
Shefer, Ruth E.
Shipman, David W.
Smith, Neil
Spencer, William P.
Stone, Alfred D.
Sugiyama, Linda E.
Sutton, D. Mark
Tetreault, David J.
Walker, Russell H.
Youngdale, Eric P.
Yuen, Sunny Y.C.
Zurek, Patrick M.

1. Canadian Government Fellow
2. Bantrell Fellow
3. NIH Trainee
4. Max Kade Foundation Fellow

Visiting Scientists and Guests

Ahmad-Bitar, Riyad
Allen, Gregory H.
Bertin, Guiseppe
Bhattacharje, Gopa
Bradley, Dianne C.
Brown, Fielding
Carrell, Thomas
Chen, Chih-Fan
Chen, Dong-Pei
Chew, Weng-Cho
DeRosier, David T.
De Silvestri, Sandro
Detragiache, Paolo
Ducas, Theodore W.
Florentine, Mary S.
Fuchs, Adrian
Gabrielsen, Geir W.
Geiger, Gad
Gu, Qizheng
Habashy, Tarek
Hartemann, Frederick
Hawryluk, Andrew M.
Jesteadt, Walt
Jhaveri, Sonal
Kanbe, Hiroshi
Kanwisher, John W.
Kawakami, Shojiro
Kayoun, Pierre H.
Koizumi, Takuya
Kumar, Prem
Landahl, Karen
Li, Ren-Jun
Ligare, Martin
Liu, Hua-Khuang
Lyrra, A. Marjatta
Michel, Jean C.
Mills, Allen W.
Mollow, Benjamin
More, Trenchard
Pardo, José M.M.
Perlman, David M.
Porcelli, Francesca
Qiding, Du
Read, Michael E.
Rosenthal, Stanley J.
Rosowski, John J.
Saarelma, Hannu J.
Shapira, Ruth
Shevel, Sergey G.
Wang, Hong-Ming
Wang, Hu-Zhuang
Wang, Yi-Ming
Watanabe, Takao
Welte, Roland
Wiesner, Stephen
Xu, Xi Ru
Xue, Ming-Lun
Yamamoto, Yoshihisa
Yu, Chongzhi
Yin, Yuan-Zhao

Research Affiliates

Barlow, John S.
Boduch, Raymond
Brown, Robert M.
Curby, Mark L.
Danly, Martha
Dowdy, Leonard C.
Ferrier, Linda J.
Grosjean, François
Hawkins, C. Sarah
Hillman, Robert E.
Holmberg, Eva B.
Huggins, Allan W.F.
Khan, Malik
Larrabee, Joanne W.
Locke, John L.
Lyberg, Bertil
Makhoul, John I.
Menn, Lise
Menyuk, Paula
Miller, Joanne L.
Picard, Leonard
Pollack, Robert A.
Ram-Mohan, L. Ramdas
Schultz, Martin C.
Stefanov-Wagner, Frank J.
Steffens, David A.
Vaidyanathan, A. Ganesh
Wacks, Kenneth P.

Research Assistants

Ali, Ali D.
Anderson, Erik H.
Armstrong, John T.
Armstrong, Robert C.
Atwater, Harry A.
Bain, Isaac
Bamji, Cyrus
Bennett, Charles L.
Bernstein, Jeffrey G.
Bickley, Corine A.
Bondurant, Roy S.
Borgeaud, Maurice
Brewer, Lawrence R.
Briançon, Alain C.
Cantarutti, Paolo
Chan, David A.
Chanty, Jean-Marc
Chou, Yu

Research Assistants (continued)

Clemens, David T.
Colavita, M. Mark
Dagli, Nadir
Dana, Stephane S.
Dexheimer, Susan
Dhawan, Vivek
Dowla, Farid U.
Dynes, Scott B.C.
Flanagan, Robert
Fortino, Ronald
Fujimoto, James G.
Gaal, Imre
Gamble, Edward, B., Jr.
Garber, Edward M.
Garnavich, Peter M.
Gasiewski, Albin J.
Ghavamishahidi, Ghavam
Gifford, Margaret L.
Goldhor, Richard S.
Gould, Phillip L.
Griffin, Daniel W.
Hakimi, Farhad
Harris, John
Harrison, William A.
Hauck, Charles
Hegi, Larry G.
Hemmer, Philip R.
Hewitt, Jacqueline N.
Hinman, Brian L.
Hinshelwood, David
Horowitz, David M.
Hulet, Randall G.
Isaacs, Eric D.
Islam, Mohammed N.[1]
Ito, Yoshiko
Jackson, James M.
Jacobs, Kenneth D.
Kash, Michael M.
Keavney, Christopher J.
Kiang, Jean-Fu
Kim, Sei-Hee
Kirkpatrick, Douglas A.
Knowlton, Stephen F.
Krause, Edward A.
Krystal, Andrew D.
Kuznetsov, Mark
Kwasnick, Robert F.
Larson, Brent D.
Lawrence, Charles R.
Lee, Chong U.
Lee, Jay Kyoon
Leotta, Daniel F.
Lin, Sching Lih
Magill, Peter D.
Mahoney, James H.
Martinez, Dennis M.
Mayberry, Matthew J.
McCormick, Steven P.
McDermott, F. Scott
Medina, Antonio
Mesite, Paula L.
Meyer, Raymond E.
Migdall, Alan L.
Milios, Evangelos E.
Mochrie, Simon G.J.
Molter-Orr, Lynne M.
Moskowitz, Philip E.
Moulton, Andrew S.
Murphy, David C.
Myers, Cory
Nathan, Krishna S.
Nguyen, Trung Tien
Pan, Davis Yen
Pang, Xiao-Dong
Pappas, Thrasyvoulos
Park, Anne H.
Peuse, Bruce W.
Pian, Donald
Plotnick, Irving
Poh, Soon Yun
Prentiss, Mara G.
Pu, Yikang
Putnam, Roger S.
Raab, Eric
Richard, Michael D.
Rohatgi, Rajeev R.
Rotman, Ruth R.
Sanders, Glen A.
Sara, Jason
Saussy, Gordon C.
Schloss, Robert P.
Scott, Thomas P.
Seiler, Larry D.
Sezginer, Abdurrahman
Shadle, Christine H.
Shih, Shih-Ming
Silletto, Karen
Skarda, Gregory M.
Song, William S.
Specht, Eliot D.
Stathis, James H.
Stein, Josephine A.
Stix, Michael
Sulecki, Joan M.E.
Tench, Robert E.
Uchanski, Rosalie M.
Van Hove, Patrick L.
Wang, John S.
Ware, Kurt M.
Warnock, James D.
Warren, Alan C.
Weisskoff, Robert
Wengrovitz, Michael S.
Whitaker, Norman A., Jr.
Williams, Brian C.
Wills, D. Scott
Wong, Albert K-S.
Wong, Chee C.
Wong, Stephen B.
Yam, Yeung
Yang, Ying-Ching
Yorsz, Jeffrey
Yun, Kenneth Yi

1. Hertz Fellow

Teaching Assistants

Allen, Janet A.
Atlas, Susan
Carney, Laurel H.
Chambers, William N.
Chu, Tom
Denton, Denise D.
Engelke, Charles W.
Hofman, William D.
Humphreys, David A.
Izraelevitz, David
Jin, Yaqiu
Kanapathipillai, M.
Karl, William C.
Mizumoto, Chris T.
Ocko, Benjamin M.
Pachtman, Arnold
Park, Dongwook
Peterseon, Patrick M.
Reid, Jean
Rohlicek, Robin J.
Summers, John D.
Sundaram, Ramakrishnan
Szabo, Bernard I.
Teweik, Ahmed H.
Towe, Elias D.
Wagner, Stuart S.
White, Jeffrey R.
Wroclawski, John T.

Graduate Students

Aeppli, Gabriel
Allard, Terry T.
Allen, Barry R.
Anderson, James C.
Aoki, Chieko
Aull, Ann Marie[1]
Bagnoto, Vanderlei
Bar-Yam, Yaneer
Bassett, Paul D.[2]
Benson, Priscilla J.
Boebinger, Gregory S.[3]
Bordley, Thomas E.
Bristol, Norman, Jr.[4]
Bustamante, Diane K.[5]
Carley, David[6]
Cassereau, Philippe
Chan, Philip[7]
Chao, Yao-Ming
Chen, Chih-Yung
Chen, Francine R.[1]
Chiang, Wei-Chung
Curtis, Susan R.[4]
Cyphers, David S.[1]
Deadrick, Douglas
DiFilippo, David[8]
Dove, Webster P.[9]
Duckworth, Gregory L.
Espy, Carol Y.
Fajans, Joel[3]
Francis, Gregory E.
Fujimura, Akira
Gabriel, M. Christina[4]
Garcia, Armando
Garner, Richard C.
Gentile, Thomas R.
Glaser, Michelle J.[10]
Glass, James P.[8]
Hamilton, Greg D.[4]
Hamza, Abdelhaq M.[11]
Harten, Leo P.
Harton, Sara M.A.[12]
Heron, Courtney D.[13]
Howland, Bradford
Hsu, Stephen C.[14]
Huang, Caroline
Hughey, Barbara J.[15]
Huttenlocher, Daniel[1]
Isnardi, Michael[4]
Jeong, Hong[16]
Joshi, Kiran Raj
Kobota, Ichiro
Kunoff, Estelle[17]
Lamel, Lori F.[1]
Leung, Hong Chung[1]
Lin, Chen-Shi F.
Livingston, Jay N.
MacDonald, Heather
Maeda, Mari
Magnus, Margaret H.

1. SDF Fellow
2. MIT Fellowship
3. Hertz Fellow
4. Bell Lboratories Fellow
5. NIH Trainee
6. HST Fellow
7. Singapore Government Fellow
8. Canadian Government Fellow
9. Amoco Fellow
10. Hughes Aircraft Fellow
11. Algerian Scholarship
12. Lincoln Laboratories Fellow
13. GEM Fellow
14. NSF Fellow
15. MIT Karl T. Compton Fellow
16. Korean Government Scholarship
17. IBM Fellow

Graduate Students (continued)

Malvar, Henrique S.[1]
Mark, Martin
Marroquin, Jose Luis[2]
Marshall, Shelley
Martinelli, Julio J.[2]
Martinez-Miranda, Luz[3]
Matson, Mark D.
Mauel, Michael E.
McCue, Michael P.
McLeod, Kenneth J.
Melcher, Jennifer
Mesa, Osvaldo A.[4]
Moser, James R.[3]
Moskowitz, Warren E.
Ocenasek, Josef[4]
Paulik, Mark J.[5]
Paulos, John J.
Pineda, Juan[6]
Ponikvar, Donald R.[7]
Posen, Miles P.
Prasanna, G.N.S.
Pratt, Gill
Propp, Michael
Randolph, Mark[4]
Rappaport, Carey M.
Robinson, Andrew L.[8]
Rose, Christopher
Saxberg, Bror V.H.[9]
Schulert, Andrew J.[3]
Schurr, Thierry M.
Sekiguchi, Hiroshi [10]
Seneff, Stephanie
Shapiro, Philip D.
Shin, Robert R.I.
Sia, Eng-Beng
Stautner, John P.
Stewart, Brian A.
Swanson, Eric A.[8]
Teich, Jonathan M.[6]
Tan, Han-Ngee
Tran, Hai Van
Ulichnev, Robert
Urbaniak, Walter
Vachon, Guy
Velez, Ricardo E.[2]
Voldman, Steven H.
Waissman, Roberto S.[12]
Wang, David L.[13]
Weiner, Andrew M.[14]
Welsh, George R.
Williams, Douglas D.
Williams, Gegory E.
Wilson, Robert J.
Zarinetchi, Farhad[9,15]
Zayhowski, John J.[14]
Zukowski, Charles A.

Undergraduate Students

Ahern, Lance J.
Alkhairy, Ashraf
Ames, Michael
Ataki, Patrick R.
Babalitis, Panagiotis A.
Bacon, Stephanos
Bade, Edward R.
Baraniuk, Steven P.
Bavly, Eric M.
Bonney, Laura A.
Bounds, Jeffrey K.
Chavez-Pirson, Arturo
Chen, Thomas M.
Chiang, Carol J.
Cohen, Alan I.
Corcoran, Christopher
Dale, George
Damle, Ratnadeep
DeRozairo, Andrew M.
Detlefs, William F.
Dippert, Jonathan I.
Dixon, Stephen K.
Downs, Maralene M.
Drogaris, Anthony N.
Duffey, Thomas P.
Duncan, Ronald B.
Eberman, Brian
Ericson, Daniel W.
Felshin, Susan L.
Ferguson, Sarah
Foss, Kristin K.
Fox, Brent
Ghosh, Biswa R.
Giambalvo, Corrado
Hagemeister, Mark
Hakkarainen, J. Mikko
Hosein, Patrick A.
Hughes, Duncan F.
Jain, Manoj
Jain, Sudhanshu K.

1. Brazilian Government Fellow
2. Mexican Government Fellow
3. NSF Fellow
4. Bell Laboratories Fellow
5. General Motors Fellow
6. IBM Fellow
7. Hertz Fellow
8. DEC Fellow
9. MIT Fellow
10. Toshiba Fellow
11. NIH Trainee
12. National Research Council of Brazil
13. Hughes Aircraft Fellow
14. Fannie Hertz Foundation Fellow
15. Richard D. DuPont Fellow

Undergraduate Students (continued)

Kassell, Robert
Kim, Richard Y.
Klotz, Sharon
Kositsky, Joel
Lambert, Katherine H.
Lambrou, John
Lane, Daniel R.
Larky, Steven P.
Lauritzen, Niels
Lee, Hojohn
Levine, Eric C.
Lezec, Henri J.
Lin, Daniel
Liu, Shih-Chii
Long, Frederick H.
Lorenz, Natalie M.
Loughridge, Michael F.
Lui, Yuk
Lyon, David J.
Mannion, Brian
Mars, Mark E.
Matter, Michael C.
McCrae, Jack E., Jr.
Mellis, Adam G.
Mok, Chee Kong
Mutz, Andrew
Nevins, Bryan D.
Nilsson, Karin E.
Nir, Ishai
Nykolak, Gerald
Osler, Andrew
Paczuski, Maya
Pandava, Krishna A.
Pavlenkov, Victor
Pearsall, C. Robert, II
Pemberton, Joseph C.
Plonty, Karen E.
Quattrociocchi, Stephen W.
Raman, Shankar
Schaefer, Robert J.
Schenck, Jeffrey L.
Sherdin, Steven M.
Schnitzler, Raymond A.
Sherloch, Thomas
Sherman, Derin
Sheu, Eric V.
Sleeper, Lionel J.
Smoot, Peter
Spacek, Petr W.
Stanzel, Robert P.
Steinbeck, John W.
Summa, Deborah
Sybertz, Maureen
Tamur, Alfredo
Teachy, Robert D.
Thayer, Jeffrey S.
Tiao, Julie
Tien, Ben Tze
Tsai, John C-H.
Tulintseff, Ann N.
Virany, Leslie
Visser, Susan A.
Wan, Pong-Liang
Weidman, Daniel J.
Wilson, Dave M.
Winkelman, John R.
Wittman, Susan J.
Wong, Gerald G.
Wong, Ha-Fong
Wong, Raymond W.
Wu, Linna
Yamaguchi, Kogi
Yeh, Huoy-Ming
Yew, Pearl C.C.
Zabor, William C.
Zimmerman, Karl
Zion, David

Administrative Staff

Bella, Charles J.
Duffy, Donald F.
Keyes, Richard V., Jr.
Lauricella, Virginia R.
Maguire, Lawrence E.
Moore, Janet E.
Peck, John S.
Sincuk, Joseph, Jr.

Support Personnel

Aelerud, Robert W.
Budd, Holly N.
Cabral, Manuel, Jr.
Cairns, Kathleen E.
Carter, James M.
Chambers, Virginia N.
Clements, Donald A.
Cook, John F.
DeBilio, Peter
Demakos, Steven
Doucette, Wilfred F.
Dove, Monica Edelman
Duffy, Cheryl A.
Evans, Thomas M.
Foster, Stella J.
Gale, Donna L.
Garalis, Thalia
Gelinas, Andrea L.
Griswold, Marsden P.
Hall, Kyra M.
Johnson, Rebecca F.
Kaloyanides, Venetia
Kopf, Cynthia Y.
Lavalle, Edward R.

Support Personnel (continued)

Leach, George H.
Ledgister, Enid I.
Levy, David S.
Lewis, Ionia D.
Lorusso, Catherine
Lydon, Catharine A.
McCue, Kathleen M.
McDonald, Margaret M.
McDonnell, Russell A.
McKinnon, Rita C.
Mitchell, Joseph E.
Nazeley, Elisa
Nelson, Susan
Nelson, Sylvia A.
Nickerson, John C.
North, Donald K.
O'Keefe, Patrick M.
Poynor, Charles A.
Scalleri, Mary S.
Scivally, Bonnie
Smith, Clare F.
Sobel, Judith H.
Southwick, Marie L.
Stram, Henry
Sullivan, Eve O.
Taylor, David M.
Taylor, Vicky-Lynn
Vandermolen, Phyllis
Vine, Brent H.
Vitale, Peter
Williams, Arbella P.C.

30. Research Support Index

U.S. Department of Energy	
Contract DE-AC02-78-ET-51013	101, 110, 116
Contract DE-AC02-82-ER-13019	88
U.S. Navy - Office of Naval Research	
Contract N00014-77-C-0266	132
Contract N00014-79-C-0183	9
Contract N00014-79-C-0908	85, 87, 88
Contract N00014-80-C-0941	123
Contract N00014-81-K-0662	121
Contract N00014-81-K-0742	132, 133, 134, 135, 137, 138, 139, 140, 141, 142, 144, 145
Contract N00014-82-K-0727	147
Contract N00014-83-K-0258	78
Contract N00014-83-K-2024	95
Contract N00014-84-K-0073	89
Whitaker Health Sciences Fund	1

Index

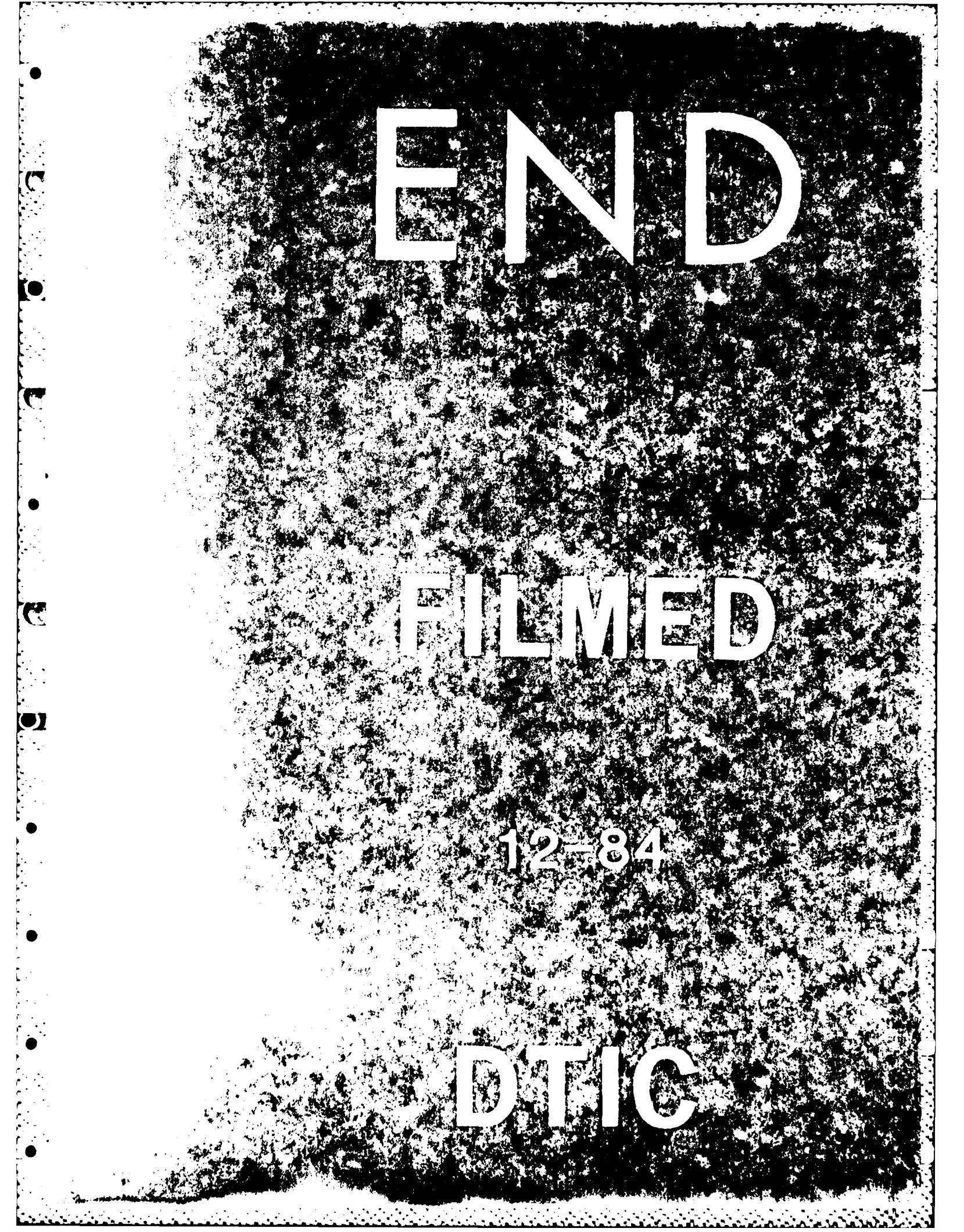
END
FILMED
12-84
DTIC